

https://dspace.org/

Modelling the impact of land cover and forestry change on the hydrological characteristics of the two streams sub-catchment, Natal Midlands

Duncan, Gabriella Elisabeth

2019

https://hdl.handle.net/10539/27277

Duncan, Gabriella Elisabeth (2019) Modelling the impact of land cover and forestry change on the hydrological characteristics of the two streams sub-catchment, Natal Midlands, University of the Witwatersrand, Johannesburg, <http://hdl.handle.net/10539/27277>

Downloaded from a DSpace repository. https://dspace.org/

Modelling the impact of land cover and forestry change on the hydrological characteristics of the Two Streams sub-catchment, Natal Midlands



Gabriella Elisabeth Duncan

562123

Supervisors: Prof. Trevor Hill, Prof. Christopher Curtis and Dr. Jennifer Fitchett

Declaration

I declare that this Dissertation is my own, unaided work. It is being submitted for the Master of Science within the School of Geography, Archaeology and Environmental Science at the University of the Witwatersrand, Johannesburg under the supervision of Prof. C. Curtis, Prof. Trevor Hill and Dr. Jennifer Fitchett.

This declaration is to certify that the work reported in the Master of Science dissertation is my own original and unaided work, unless where specific acknowledgment has been made, and has not been submitted in part or in whole to any other university or for any other degree.



Gabriella Duncan

Student number: 562123

Date: 6 February 2019

Abstract

Understanding of the impacts of land cover and the changes thereof on water resources is essential in improving management practices and protecting water resources, particularly in water scarce countries such as South Africa. To determine the impacts of land cover and land cover change on hydrological processes, a small sub-catchment in the KwaZulu-Natal Midlands was modelled. The Two Streams sub-catchment was modelled for both a current (2007 – 2016) and future (2019 – 2028) scenario using MIKE SHE deterministic hydrological modelling software. The aims of the study were to: 1) Assess the ability for MIKE SHE software to model the hydrological cycle of the Two Streams sub-catchment, based on the current scenario set-up. 2) Assess and compare modelled hydrological outputs and characteristics of the dominant land cover types present within the (current scenario) Two Streams sub-catchment: sugarcane (*Saccharum officinarum*), black wattle (*Acacia mearnsii*) and riparian vegetation. 3) Determine the impact that a change in plantation forestry from black wattle (*A. mearnsii*) to *Eucalyptus dunnii* will have on the hydrological characteristics and hydrological cycle of the Two Streams sub-catchment, using MIKE SHE modeling software (future scenario). Results indicated that the MIKE SHE model was effective at modelling the Two Streams study site. The black wattle plantation was found to use more water through evapotranspiration and experience greater loss in subsurface water supplies in relation to sugarcane and riparian vegetation. In comparing the hydrological characteristics of black wattle and *E. dunnii* forestry plantations, *E. dunnii* was the greater water user and experienced greatest reduction in subsurface storage. Before the MIKE SHE model can be used for further modelling on-site, the limitations identified, including those pertaining to the subsurface hydrological characteristics, limited LAI data and limited *E. dunnii* research, need to be addressed and overcome.

Keywords: MIKE SHE, LUCC, hydrological, modelling, Two Streams

Acknowledgements

To my supervisor and co-supervisors, Prof. Trevor Hill, Prof. Christopher Curtis and Dr. Jennifer Fitchett, I thank you for the assistance provided throughout, and the time dedicated to reading, advising and editing the multiple drafts of my thesis. I thank you too for your patience, dedication and the effort expended in ensuring I produced the best work I could.

Thanks to the National Research Foundation (NRF) for their financial support for this MSc. All of my university fees were paid through their generous contribution to my project. In addition SARAO personnel must also be given thanks, in particular to Alice Pienaar-Marais and Tracy Cheetham for their support and encouragement throughout this process and for the time they allowed for me to complete my MSc, as this thesis was written on a part-time basis.

This research formed part of a project initiated, managed and funded by the Water Research Commission (WRC project No Project: K5/2402: Assessing the impact of erosion and sediment yield from different land uses in farming and forestry systems and their effect on water resources in selected catchments of South Africa). As such thanks must be paid to the WRC for support of this project and for financial compensation made for a fieldtrip and travel costs expended for this research. In addition, I would like to acknowledge and thank the following organizations, institutions and individuals:

- Dr. Jennifer Fitchett for coming on board as a co-supervisor after the first year of the project, for her invaluable support and in particular her assistance with climatic datasets.
- Jason Hallowes and Bruce Eady at DHI South Africa for software support and a particular thank you to Bruce Eady for his help in understanding the MIKE SHE model.
- Mondi for allowing research to be conducted within one of their commercial forests.
- Mr Vivek Naiken and Dr. Alistair Clulow of UKZN for data support and special thanks to Dr. Alistair Clulow for support in data interpretation, clarification and explanation.
- Bruce Scott-Shaw and Brice Gijsbertsen for Geographic Information System (GIS) support.

- The Geography Discipline at the University of KwaZulu-Natal (Pietermaritzburg Campus), the Geography Department and the School of Animal, Plants and Environmental Sciences at the University of the Witwatersrand for the use of their equipment.
- The South African Weather Service for the meteorological data provided for the project.
- To Prof. Trevor Hill for coordinating and assisting with travel arrangements and all persons who assisted in fieldwork and site visits, in particular Matthew Dickey and Dr. Khatab Mohamed Abdalla.

Last, but not least, thank you to all my family and friends for their continual support and encouragement throughout my research.

Table of Contents

Declaration ..... **i**
Abstract ..... **ii**
Acknowledgements ..... **iii**
List of Figures ..... **ix**
List of Tables ..... **xviii**
List of Equations ..... **xxiv**
Abbreviations and Acronyms ..... **xxvi**
Chapter One Introduction **1**
1.1 Introduction 1
1.2 Research Aims and Objectives 4
Chapter Two Literature Review **8**
2.1 Introduction 8
2.2 Hydrology and the hydrological cycle 8
2.3 Hydrological modelling 10
2.3.1 Empirical models 12
2.3.2 Conceptual models 12
2.3.3 Physically-based models 12
2.3.4 Comparing lumped and distributed hydrological models 13
2.4 Types of hydrological models 14
2.4.1 The Soil and Water Assessment Tool (SWAT) model 14
2.4.2 The agrohydrological ACRU model 16
2.4.3 The Hydrologiska Byrans Vattenavdelning (HBV) model 16
2.4.4 TOPMODEL (TOPography based hydrological MODEL) 17
2.4.5 The Variable Infiltration Capacity (VIC) model 17
2.4.6 The Agricultural Policy/Environmental eXtender (APEX) model 18
2.4.7 The SPAtial and Time Series Information Modeling (SPATSIM) model 19
2.5 Hydrological model employed for this study 19
2.5.1 Comparing MIKE SHE to other hydrological models 22
2.6 Advances in Remote Sensing (RS) and Geographic Information Systems (GIS) 25
2.7 Water Balance 26
2.7.1 Precipitation (P) 27
2.7.2 Evapotranspiration (ET) 27
2.7.3 Surface runoff and streamflow (Q) 28
2.7.4 Recharge (R) 29

2.7.5 Change in soil water storage (ΔS) 30
2.8 Land use and/or land cover change (LUCC) and hydrology 30
2.8.1 Sugarcane plantation 34
2.8.2 Plantation forestry 35
2.9 Scaling in land use and/or land cover (LULC) and hydrology studies 42
2.10 Conclusion 43
Chapter Three Study site 45
3.1 Introduction 45
3.2 Study site description 45
3.3 Research history at the Two Streams study site 48
3.3.1 Research instrumentation 49
3.3.2 Hydrological modeling 49
3.4 Summary 51
Chapter Four Methods 53
4.1 Introduction 53
4.2 MIKE SHE modelling of the Two Streams sub-catchment 53
4.3 MIKE SHE model set-up – current scenario 56
4.3.1 Simulation specification module 59
4.3.2 Model domain and grid module 60
4.3.3 Topography module 61
4.3.4 Climate module 62
4.3.5 Land use module 65
4.3.6 Overland flow module 72
4.3.7 Rivers and lakes module 74
4.3.8 Unsaturated flow module 78
4.3.9 Saturated groundwater flow module 81
4.4 Calibration and validation of the MIKE SHE current scenario model 84
4.4.1 Storing of results module 85
4.4.2 MIKE SHE current scenario model run 86
4.4.3 MIKE SHE current scenario model alterations 87
4.5 MIKE SHE model set-up – future scenario 87
4.5.1 Simulation specification module 87
4.5.2 Modules kept constant for the future scenario 88
4.5.3 Climate module 88
4.5.4 Land use module 88
4.5.5 Rivers and lakes module 89

4.6 Analysis of the MIKE SHE scenario results 90
4.6.1 Time series outputs 90
4.6.2 Statistical analysis 90
4.7 Summary 91
Chapter Five MIKE SHE model input characteristics, calibration and validation 92
5.1 Introduction 92
5.2 Biophysical characteristics of the site 92
5.3 Fieldwork findings 96
5.4 MIKE SHE pre– calibration and validation model outputs 99
5.4.1 Comparing modelled outputs to observed records. 99
5.4.2 Initial MIKE SHE water balance summary 102
5.4.3 Correcting the MIKE SHE river component 104
5.4.4 Alterations to the model simulation run time 106
5.5 MIKE SHE current scenario model refinement results 106
5.5.1 Calibrated model water balance summary 112
5.6 Discussion 113
5.6.1 Soil characteristics of the Two Streams sub-catchment 114
5.6.2 Model uncertainty 116
5.6.3 Leaf Area Index (LAI) 117
5.6.4 Model calibration and validation 120
5.6.5 The benefits and limitations of the MIKE SHE model for the Two Streams study site. 124
5.6.6 Future areas of research 126
5.7 Conclusion 127
Chapter Six Comparing the MIKE SHE current scenario vegetation class model outputs 128
6.1 Introduction 128
6.2 Evapotranspiration 128
6.3 Evapotranspiration components 132
6.4 Canopy interception storage (CIS) 139
6.5 Depth of overland flow 144
6.6 Infiltration to the unsaturated zone (I_{UZ}) 149
6.7 Recharge to the saturated zone 154
6.8 Correlation and comparison of the vegetation class hydrological outputs 157
6.9 Discussion 159
6.9.1 Evapotranspiration 159
6.9.2 Limitations in the model inputs governing evapotranspiration components and canopy interception 160

6.9.3 Runoff and infiltration 164
6.9.4 Groundwater recharge 166
6.9.5 The riparian zone 168
6.9.6 Sub-catchment heterogeneity 169
6.10 Conclusion 170
Chapter Seven Impact of a change in plantation forestry on hydrological characteristics of the Two Streams sub-catchment 172
7.1 Introduction 172
7.2 Comparison and correlation of totaled model outputs 173
7.3 Annual differences in hydrological outputs 175
7.4 Comparison of daily modelled outputs 179
7.5 Monthly and seasonal comparisons of the hydrological outputs 185
7.6 Comparing the water balances of the two plantation types 188
7.7 Discussion 190
7.7.1 Comparing the water use and invasive nature of *A. mearnsii* and *E. dunnii* 190
7.7.2 Contributing to the understanding of genus exchange 193
7.7.3 Transpiration and soil evaporation 194
7.7.4 Hydrological processes and capacity thresholds 195
7.7.5 Limitations in research 198
7.8 Conclusion 200
Chapter Eight Conclusion 201
8.1 Summary of study findings 201
8.2 Future research 204
8.3 Conclusion 205
References 207
Appendices 243
Appendix A: MIKE SHE scenario (current and future) set-ups 243
Appendix B: Catchment delineation 256
Appendix C: Penman-Monteith equation 264
Appendix D: Vegetation inputs for the land use module in MIKE SHE 275
Appendix E: MIKE SHE rivers and lakes module and related software connections. 277
Appendix F: van Genuchten soil water retention curves (SWRC) 283
Appendix G: Determining MIKE SHE model error specific to model component 287
Appendix H: Determination of time series data distribution 289

List of Figures

Figure 2.1: Depiction of the hydrological cycle (Hendriks, 2010)……....10

Figure 2.2: Hydrological processes simulated by MIKE SHE (Graham and Butts, 2005)……....20

Figure 3.1: Locality of the Two Streams catchment in the KwaZulu-Natal midlands……..……46

Figure 3.2: The Two Streams catchment, in which the study site of this project falls…….....48

Figure 4.1: The Two Streams sub-catchment...…….……54

Figure 4.2: Flow chart for the MIKE SHE, current scenario, model set-up……..……57

Figure 4.3: Conceptualisation of the MIKE SHE (and related MIKE 11) software. Illustrating the processes that can be modelled (black bulleted points) and the specific processes modelled in this study (red bulleted points). The interconnected nature of the MIKE SHE processes and how water moves through the system is shown by blue directional arrows……58

Figure 4.4: Screen display of the hydrological cycle components selected for the MIKE SHE current scenario and the method options chosen for the overland flow, unsaturated flow and saturated flow modules…….……..59

Figure 4.5: Screen display of the default time step control settings used for the MIKE SHE current scenario set-up…….……60

Figure 4.6: The Two Streams catchment boundary and sub-catchment (study site) boundaries delineated through Arc-Hydro tools in ArcGIS 10.3 software……61

Figure 4.7: 5m Digital Elevation Model (DEM) showing the Two Streams site topography, based on 5m and 10m contours and spot heights……..……..62

Figure 4.8: Correlation between the FAO Automatic Weather Station (AWS) daily rainfall (mm) record and the mast Automatic Weather Station (AWS) daily rainfall (mm) record…….....…….....64

Figure 4.9: Correlation between the combined Automatic Weather Station (AWS) daily rainfall (mm) record for the Two Streams study site and the South African Weather Services' Greytown weather stations daily rainfall (mm) record……...……..…64

Figure 4.10: Land cover map of the Two Streams catchment and sub-catchments, generated using the Ezemvelo KwaZulu-Natal Wildlife (EKZNW) land use and/or land cover shapefile for the area……...66

Figure 4.11: The LAI-2200 Plant Canopy Analyzer used to measure the average Leaf Area Index (LAI) for the riparian vegetation……...……..71

Figure 4.12: Example of view caps used by the LAI-2250 optical sensor (LAI-2200 Plant Canopy Analyser, 2012)……..……..72

Figure 4.13: Flow chart showing the link between MIKE Hydro, MIKE 11 and MIKE SHE software……..……..74

Figure 4.14: The V-notch weir located along the river of the Two Streams larger sub-catchments (Everson *et al*., 2014)……...75

Figure 4.15: Model screen display showing the locations of the cross-sections generated along the length of the Two Streams stream. The stream is mapped on a geo-reference grid (m). The red boxes indicate where cross-sections were generated and the black lines perpendicular to the stream indicate the length and angle the cross-sections were captured at. The blue boxes indicate the start and end chainage points of the river…….……....77

Figure 4.16: Available selection options in the unsaturated zone and the options selected for this study……..……...79

Figure 4.17: Soil map showing the soil forms of the Two Streams sub-catchment (Kuenene, 2013)...79

Figure 4.18: Initial water table depth of the Two Streams catchment and sub-catchments for the 11th of October 2007 (the closest date to the start of the simulation – the 14th of February 2007)…….…...83

Figure 5.1: Daily and annual rainfall (mm) records extending from the 14th of February 2007 – 2nd of October 2016, for the Two Streams study site……..…….....93

Figure 5.2: Daily reference evapotranspiration (mm) for the Two Streams study site, extending from the 14th of February 2007 – 2nd of October 2016, based on the Penman-Monteith method..…..94

Figure 5.3: Scatter plot of the relationship between the Leaf Area Index (LAI) values calculated from the SPOT imagery and the LAI measures from the LAI-2200 Plant Canopy Analyzer…….....99

Figure 5.4: The observed and modelled actual evapotranspiration records, extending from 01 October 2011 – 25 October 2013, for the Two Streams sub-catchment (29°12'19.2''S; 30°39'1.3''E)…….100

Figure 5.5: Accumulated actual evapotranspiration (mm) records (both observed and modelled) for the period 01 October 2011 – 25 October 2013……...…….100

Figure 5.6: Scatter plot comparing the observed and modelled evapotranspiration (mm) rates between 01 October 2011 – 25 October 2013. A 1:1 line is included for comparison (red)……..…....101

Figure 5.7: Modelled and observed streamflow records for the Two Streams sub-catchment, extending from 14 February 2007 – 09 December 2013……..……..102

Figure 5.8: MIKE SHE accumulated water balance diagram showing the normalized flows (mm) within the modelled area over the simulated period (14 February 2007 – 02 October 2016) for the MIKE SHE current scenario (pre-validation) run……...….103

Figure 5.9: Model screen display of the river bank level minus ground level map produced in the processed data section of the MIKE SHE simulation……..……..104

Figure 5.10: Model screen display showing the locations of the new cross-sections generated along the length of the Two Streams stream. The x- and y-axis represent the MIKE SHE geographically positioned grid (m). The red boxes indicate where cross-sections were generated and the black lines perpendicular to the stream indicate the length and angle the cross-sections were captured at. The blue boxes indicate the start and end chainage points of the river…….105

Figure 5.11: Model screen display of the river bank level minus ground level map produced in the processed data section of the MIKE SHE simulation once the cross-sections were altered……106

Figure 5.12: Modelled and observed streamflow records, following model calibration, for the period 14 February 2007 – 09 December 2013...…….107

Figure 5.13: Accumulated streamflow records (mm), both observed and modelled, for the period 14 February 2007 – 09 December 2013...…….....108

Figure 5.14: Scatter plot of the relationship between the observed and modelled streamflow records ($m^3.s^{-1}$) for the Two Streams sub-catchment, over the period 14 February 2007 – 09 December 2013. 1:1 line included as well for comparison (red)……109

Figure 5.15: MIKE SHE validated total water balance diagram showing the normalized flows (mm) within the modelled area over the entire simulated period (14 February 2007 – 02 October 2016)……..113

Figure 5.16: Soil textural class pyramid, developed by the United States Department of Agriculture (USDA), to define soil textural classes based on percentage sand, silt and clay (Soil Survey Division Staff, 1993)……..…….....116

Figure 5.17: Photographs taken during fieldtrips showing the heterogeneity of the species composition of the Two Streams sub-catchment riparian zone……..……118

Figure 5.18: The normalized difference vegetation indices (NDVIs) generated from the SPOT satellite imagery attained for the Two Streams site showing the effect of low resolution on the data. (a) 20m resolution – image taken on 19 January 2011; (b) 10m resolution – image taken on 01 February 2007; (c) 10m resolution – image taken on 31 July 2012……..119

Figure 6.1: Daily and annual evapotranspiration outputs for the [a] sugarcane, [b] riparian and [c] black wattle vegetation classes, modelled over the total simulation period (14 February 2007 – 02 October 2016). In addition, the sugarcane harvest dates are indicated in [a] with red lines……131

Figure 6.2: Averaged monthly evapotranspiration for the sugarcane, riparian and black wattle vegetation classes for the total simulated period (14 February 2007 – 02 October 2016). The averages exclude the incomplete months of February 2007 and October 2016……....132

Figure 6.3: Daily transpiration, soil evaporation, evaporation from interception and evaporation from ponded water (separate vertical axis) outputs, for the [a] sugarcane, [b] riparian, and [c] black wattle vegetation classes……...…….……136

Figure 6.4: Annual rates of [a] transpiration, [b] soil evaporation, [c] evaporation from interception and [d] evaporation from ponded water for the sugarcane, riparian and black wattle vegetation

classes over the total simulated period (14 February 2007 – 02 October 2016). In addition, the sugarcane harvest dates are indicated in each graph with red lines.....138

Figure 6.5: Daily and annual canopy interception storage outputs for the [a] sugarcane, [b] riparian and [c] black wattle vegetation classes, modelled over the total simulation period (14 February 2007 – 02 October 2016)……..…….141

Figure 6.6: Averaged monthly canopy interception storage for the sugarcane, riparian and black wattle vegetation classes for the total simulated period (14 February 2007 – 02 October 2016). The averages exclude February 2007 and October 2016…….…….142

Figure 6.7: Scatter plots showing the relationship between monthly [a] evapotranspiration, [b] transpiration, and [c] canopy interception and monthly Leaf Area Index (LAI) for the black wattle vegetation class over the period February 2007 – October 2013……...…..…143

Figure 6.8: Daily and annual depth of overland flow outputs for the [a] sugarcane, [b] riparian and [c] black wattle vegetation classes, modelled over the total simulation period (14 February 2007 – 02 October 2016)……...……..……..146

Figure 6.9: Daily rainfall (mm) and temperature (˚C) measures for January 2015, for the Two Streams study site……..……..…….147

Figure 6.10: Daily average infiltration (mm) and average evapotranspiration (mm) measures for January 2015, for the Two Streams study site ….....…….148

Figure 6.11: Model screen display of the spatially explicit depth of overland flow values for the 28th of January 2015, for the Two Streams study site……..……149

Figure 6.12: Daily and annual infiltration outputs for the [a] sugarcane, [b] riparian and [c] black wattle vegetation classes, modelled over the total simulation period (14 February 2007 – 02 October 2016)……152

Figure 6.13: Monthly infiltration rates of the sugarcane, riparian and black wattle vegetation classes for the total simulated period (14 February 2007 – 02 October 2016). The averages exclude February 2007 and October 2016……...……..…….153

Figure 6.14: Daily and annual groundwater recharge outputs for the [a] sugarcane, [b] riparian and [c] black wattle vegetation classes, modelled over the total simulation period (14 February 2007 – 02 October 2016)……..……..156

Figure 6.15: Monthly groundwater recharge rates of the sugarcane, riparian and black wattle vegetation classes for the total simulated period (14 February 2007 – 02 October 2016). The averages exclude February 2007 and October 2016……...……..…….157

Figure 6.16: Diagram showing the nature of a deep, *E. marginata*, rooting system (Kimber, 1974)…….163

Figure 7.1: Differences between the [a] evapotranspiration, [b] transpiration, [c] soil evaporation, [d] evaporation from ponded water, [e] and evaporation from interception rates of the *E. dunnii* and *A. mearnsii* plantation species (*E. dunnii* minus *A. mearnsii*). For rates > 0 *E. dunnii* rates exceed *A. mearnsii* rates, while rates < 0 *A. mearnsii* exceeded *E. dunnii*…….……...176

Figure 7.2: Modelled Leaf Area Index (LAI) and Rooting Depth (RD) of *A. mearnsii* and *E. dunnii*..……..…….177

Figure 7.3: Differences between the [a] canopy interception storage, [b] depth of overland flow, [c] infiltration, and [d] groundwater recharge rates of the *E. dunnii* and *A. mearnsii* plantation species (*E. dunnii* minus *A. mearnsii*). For rates > 0 *E. dunnii* rates exceed *A. mearnsii* rates, while rates < 0 *A. mearnsii* exceeded *E. dunnii*.……..…….…….178

Figure 7.4: Accumulated daily [a] evapotranspiration, [b] transpiration, [c] soil evaporation, [d] evaporation from ponded water, [e] evaporation from interception rates of the *A. mearnsii* and *E. dunnii* plantation species…….....……...181

Figure 7.5: Accumulated daily [a] canopy interception storage, [b] depth of overland flow, [c] infiltration, and [d] groundwater recharge rates of the *A. mearnsii* and *E. dunnii* plantation species……..……..183

Figure 7.6: Averaged monthly evapotranspiration totals for the *A. mearnsii* and *E. dunnii* plantation types for the total simulated periods..……..……..…185

Figure 7.7: Averaged monthly [a] canopy interception storage, [b] depth of overland flow, [c] infiltration, and [d] groundwater recharge rates for the *A. mearnsii* and *E. dunnii* plantation types for the total simulated period……...188

Figure B.1: The original Two Streams catchment delineated for previous WRC reports (Everson *et al*., 2006, 2014; Clulow *et al*., 2011)……..…….256

Figure B.2: Steps taken in delineating the Two Streams catchment and sub-catchments using ArcHydro in ArcGIS 10.3……..……257

Figure B.3: Flow direction output from the Arc Hydro Terrain preprocessing step……...258

Figure B.4: Flow accumulation output from the Arc Hydro Terrain preprocessing step……258

Figure B.5: Stream definition output from the Arc Hydro Terrain preprocessing step……...259

Figure B.6: Stream segmentation output from the Arc Hydro Terrain preprocessing step…….260

Figure B.7: Catchment grid delineation output from the Arc Hydro Terrain preprocessing step…...260

Figure B.8: Catchment polygon processing output from the Arc Hydro Terrain preprocessing step…….261

Figure B.9: Drainage line processing output from the Arc Hydro Terrain preprocessing step……...261

Figure B.10: Adjoint catchment processing output from the Arc Hydro Terrain preprocessing step……..…...262

Figure B.11: Batch watershed delineation output from the Arc Hydro Terrain preprocessing step…….....263

Figure B.12: Batch sub-watershed delineation output from the Arc Hydro Terrain preprocessing step……..…...263

Figure C.1: Correlation between the FAO Automatic Weather Station daily maximum temperature (°C) record and the mast Automatic Weather station daily maximum temperature (°C) record…….264

Figure C.2: Correlation between the combined Automatic Weather Station daily maximum temperature (°C) record for the Two Streams site and the South African Weather Services' Greytown weather stations daily maximum temperature (°C) record…….……..265

Figure C.3: Daily maximum temperature (˚C) record extending from 14 February 2007 – 02 October 2016 for the Two Streams study site…….……....265

Figure C.4: Correlation between the FAO Automatic Weather Station daily minimum temperature (°C) record and the mast Automatic Weather station daily minimum temperature (°C) record…….266

Figure C.5: Correlation between the combined Automatic Weather Station daily minimum temperature (°C) record for the Two Streams site and the South African Weather Services' Greytown weather stations daily minimum temperature (°C) record……....266

Figure C.6: Daily minimum temperature (˚C) record extending from 14 February 2007 – 02 October 2016 for the Two Streams study site…….……267

Figure C.7: Correlation between the FAO Automatic Weather Station daily average temperature (°C) record and the mast Automatic Weather station daily average temperature (°C) record…….…267

Figure C.8: Correlation between the combined Automatic Weather Station daily average temperature (°C) record for the Two Streams site and the South African Weather Services' Greytown weather stations daily average temperature (°C) record……268

Figure C.9: Daily average temperature (˚C) record extending from 14 February 2007 – 02 October 2016 for the Two Streams study site……...……..268

Figure C.10: Correlation between the FAO Automatic Weather Station daily wind speed ($m.s^{-1}$) record and the mast Automatic Weather Station daily wind speed ($m.s^{-1}$) record……..…..269

Figure C.11: Correlation between the combined Automatic Weather Station daily wind speed ($m.s^{-1}$) record for the Two Streams site and the South African Weather Services' Greytown weather stations daily wind speed ($m.s^{-1}$) record……..……...……..270

Figure C.12: Daily wind speed ($m.s^{-1}$) record extending from 14 February 2007 – 02 October 2016 for the Two Streams study site……..……..270

Figure C.13: Correlation between the South African Weather Services' Greytown weather stations daily average relative humidity (%) record and the FAO Automatic Weather Station daily relative humidity (%) record averaged for the Two Streams site…….…….271

Figure C.14: Daily average relative humidity (%) record extending from 14 February 2007 – 02 October 2016 for the Two Streams study site……..……..271

Figure C.15: Correlation between the FAO Automatic Weather Station solar radiation ($MJ.m^{-2}.day^{-1}$) record and the mast Automatic Weather station daily net radiation ($MJ.m^{-2}.day^{-1}$) record……272

Figure C.16: Daily solar radiation ($MJ.m^{-2}.day^{-1}$) record extending from 14 February 2007 – 02 October 2016 for the Two Streams study site, with gaps identified in red……...…273

Figure C.17: Daily solar radiation ($MJ.m^{-2}.day^{-1}$) record extending from 14 February 2007 – 02 October 2016 for the Two Streams study site……...……273

Figure E.1: Flow chart for MIKE 11 model set-up……..277

Figure E.2: Model screenshot showing the locations of cross-sections generated along the length of the Two Streams stream……..……...281

Figure H.1: Frequency histograms for the evapotranspiration records of the three current scenario vegetation classes and the future scenario *E. dunnii* vegetation class……...289

Figure H.2: Frequency histograms of the canopy interception storage records of the three current scenario vegetation classes and the future scenario *E. dunnii* vegetation class…….290

Figure H.3: Frequency histograms of the depth of overland flow records of the three current scenario vegetation classes and the future scenario *E. dunnii* vegetation class…….....…...291

Figure H.4: Frequency histograms of the infiltration records of the three current scenario vegetation classes and the future scenario *E. dunnii* vegetation class…….292

Figure H.5: Frequency histograms of the groundwater recharge records of the three current scenario vegetation classes and the future scenario *E. dunnii* vegetation class……...293

List of Tables

Table 4.1: MIKE SHE file formats……54

Table 4.2: The file formats used for the different data inputs (derived from external sources) as required by the MIKE SHE simulation modules…….……55

Table 4.3: Coordinates of the locations of the Automatic Weather Station's (AWSs) used in this study….……..……..…62

Table 4.4: Sugarcane harvest periods that fall within the current scenario study period considered…68

Table 4.5: Information on the SPOT satellite imagery acquired from the South African National Space Agency (SANSA)……..……..69

Table 4.6: Branch properties of the Two Streams stream……..76

Table 4.7: Soil hydraulic characteristics of the soil horizons of the Two Streams sub-catchment (Kuenene, 2013).…….80

Table 4.8: Leaf Area Index (LAI) and Rooting Depth (RD) values used for *E. dunnii* in the MIKE SHE, future scenario, *land use module*……..…….....89

Table 5.1: Elevation characteristics of the black wattle, riparian and sugarcane vegetation classes….93

Table 5.2: The soil types of the Two Streams sub-catchment and the soil type coverage extents (ha) in relation to the total area and to the individual vegetation class areas…….……95

Table 5.3: The soil types of the Two Streams sub-catchment, indicating the horizons, textural classes and slope characteristics of each soil type……..……..……...96

Table 5.4: Leaf Area Index (LAI) measures for the riparian vegetation class, measured using the LAI-2200 Plant Canopy Analyzer……..…….97

Table 5.5: Leaf Area Index (LAI) calculated for the riparian vegetation class, using ArcGIS 10.3 software and SPOT imagery……...……..98

Table 5.6: Water balance errors of the MIKE SHE current scenario model……...103

Table 5.7: Monthly streamflow records showing the greatest similarity between the observed and modelled records – over days when rainfall was detected by the model……...110

Table 5.8: Monthly streamflow records showing the greatest difference between the observed and modelled records over days when rainfall was detected by the model……..….110

Table 5.9: How well or poorly represented the largest rainfall events were in the modelled streamflow record……..……...111

Table 5.10: The water balance errors of the calibrated MIKE SHE current scenario model…….....113

Table 5.11: Comparing the unsaturated hydraulic conductivities of the Kuenene (2013), to those of the UNSODA database (Leij *et al*., 1994)……..……..116

Table 6.1: The accumulated total, summer and winter evapotranspiration rates for the sugarcane, riparian and black wattle vegetation classes……..……129

Table 6.2: Statistical significance of the evapotranspiration outputs of the sugarcane, riparian and black wattle vegetation classes, compared using the Kruskal Wallis test by ranks and the two-sample Wilcoxon's signed rank non-parametric tests……..……..130

Table 6.3: Totals of each evaporation component including overall simulated total and seasonal totals for the summer and winter season……..……133

Table 6.4: Statistical significance of the total and seasonal transpiration, soil evaporation, evaporation from interception and evaporation from ponded water outputs of the sugarcane, riparian and black wattle vegetation classes, compared using the Kruskal Wallis test by ranks and the two-sample Wilcoxon's signed ranks non-parametric tests……..…….134

Table 6.5: Accumulated total, summer and winter canopy interception storage rates for the sugarcane, riparian and black wattle vegetation classes, captured over the simulation period (14 February 2007 – 02 October 2016)…….…….…….....139

Table 6.6: Statistical significance of the total and seasonal canopy interception storage outputs of the sugarcane, riparian and black wattle vegetation classes, compared using the Kruskal Wallis test by ranks and the two-sample Wilcoxon's signed ranks non-parametric tests…….…...140

Table 6.7: Accumulated total, summer and winter depth of overland flow values for the sugarcane, riparian and black wattle vegetation classes, captured over the simulation period (14 February 2007 – 02 October 2016)…….…….…….144

Table 6.8: Statistical significance of the total and seasonal depth of overland flow outputs of the sugarcane, riparian and black wattle vegetation classes, compared using the Kruskal Wallis test by ranks and the two-sample Wilcoxon's signed ranks non-parametric tests……....145

Table 6.9: Daily depth of overland flow values for the 28th of January 2015 for the sugarcane, riparian and black wattle vegetation classes…….……..……145

Table 6.10: Pearson's correlation coefficients based on the linear correlation between the annual depth of overland flow and infiltration rates and the annual depth of overland flow and evaporation from ponded water rates for the three vegetation classes: sugarcane, riparian and black wattle…….…....149

Table 6.11: Accumulated total, summer and winter infiltration rates for the sugarcane, riparian and black wattle vegetation classes, captured over the simulation period (14 February 2007 – 02 October 2016)…….....……150

Table 6.12: Statistical significance of the total and seasonal infiltration outputs of the sugarcane, riparian and black wattle vegetation classes, compared using the Kruskal Wallis test by ranks and the two-sample Wilcoxon's signed ranks non-parametric tests…….……150

Table 6.13: Total infiltration rates of the different soil types of the Two Streams sub-catchment.…153

Table 6.14: Statistical significance of the daily infiltration rates of the different soil types that fall within the Two Streams sub-catchment, compared using two-sample Wilcoxon's signed ranks non-parametric tests.....……154

Table 6.15: Accumulated total, summer and winter groundwater recharge rates for the sugarcane, riparian and black wattle vegetation classes, captured over the simulation period (14 February 2007 – 02 October 2016)…….....……...155

Table 6.16: Statistical significance of the total and seasonal groundwater recharge outputs of the sugarcane, riparian and black wattle vegetation classes, compared using the Kruskal Wallis test by ranks and the two-sample Wilcoxon's signed ranks non-parametric tests……155

Table 6.17: Pearson's correlation coefficients based on linear correlation between the vegetation class outputs of the different hydrological components, considered for this study.....……..158

Table 6.18: Pearson's correlation coefficients based on linear correlation between the hydrological components of the sugarcane, riparian and black wattle vegetation classes and the rainfall record of the Two Streams sub-catchment……...…….159

Table 7.1: The accumulated totals (overall simulated total and seasonal totals) for evapotranspiration and the evapotranspiration components: transpiration, soil evaporation, evaporation from interception and evaporation from ponded water, for the *A. mearnsii* and *E. dunnii* plantation species……..……..173

Table 7.2: The accumulated totals (overall simulated total and seasonal totals) for the canopy interception storage, depth of overland flow, infiltration and groundwater recharge outputs, for the *A. mearnsii* and *E. dunnii* plantation types……...……...……175

Table 7.3: Correlation results (Pearson's correlation coefficients) of the daily hydrological components of the *A. mearnsii* and *E. dunnii* vegetation classes….……..…...179

Table 7.4: Statistical significance of the daily hydrological component outputs of the *A. mearnsii* and *E. dunnii* plantation types compared using the two-sample Wilcoxon's signed rank non-parametric test……....180

Table 7.5: Pearson's correlation coefficients based on linear correlation between each annual hydrological output and annual rainfall……..……...184

Table 7.6: Pearson's correlation coefficients based on linear correlation across the outputs of: evaporation from ponded water and depth of overland flow, evaporation from interception and canopy interception storage, and soil evaporation and infiltration for the *A. mearnsii* and *E. dunnii* plantation types……...……..……..184

Table 7.7: Percentage composition (transpiration, soil evaporation, evaporation from interception and evaporation from ponded water) of the monthly *A. mearnsii* evapotranspiration rates……....186

Table 7.8: Percentage composition (transpiration, soil evaporation, evaporation from interception and evaporation from ponded water) of the monthly *E. dunnii* evapotranspiration rates…....….187

Table 7.9: Summary of the water balance component rates and errors for the *A. mearnsii* and *E. dunnii* plantation types……...……...……...……..189

Table A.1: MIKE SHE input data for the simulation specification module……...243

Table A.2: MIKE SHE input data for the model domain and grid module…….....244

Table A.3: MIKE SHE input data for the topography module…….…...245

Table A.4: MIKE SHE input data for the climate module…….....245

Table A.5: MIKE SHE input data for the land use module…….....246

Table A.6: MIKE SHE input data for the vegetation development of the vegetation property file, for the sugarcane (*S. officinarum*) and black wattle (*A. mearnsii*) vegetation classes….....247

Table A.7: MIKE SHE input data for the rivers and lakes module…….....248

Table A.8: MIKE SHE input data for the overland flow module……..…..251

Table A.9: MIKE SHE input data for the unsaturated flow module…….....251

Table A.10: MIKE SHE input data for the soil profiles for the seven soil types considered……..252

Table A.11: MIKE SHE input data for the saturated zone module…….....254

Table A.12: MIKE SHE input data for the storing of results module…….255

Table D.1: Black wattle vegetation property file (.etv) input data for the period 14 February 2007 – 12 October 2013…….…….…...275

Table D.2: Normalized Difference Vegetation Index (NDVI) values extracted at fifteen random point locations within the riparian vegetation class of five NDVI images generated from SPOT imagery…….…….276

Table D.3: Leaf Area Index (LAI) values calculated for each Normalized Difference Vegetation Index (NDVI) value extracted from the NDVI images generated from SPOT imagery……..276

Table E.1: The branch properties defined in the river network section of a MIKE Hydro research (DHI software, 2012)…….…….278

Table F.1: Soil water retention curves (SWRC) for the Kuenene (2013) soil (used in this study) and the generic UNSODA soils (Leij *et al*., 1996) based on the soil textural classes and soil horizons defined by Kuenene (2013). The SWRCs indicate field capacity (green line), wilting point (red line) and plant available water (moisture content at field capacity minus moisture content at wilting point)…….…….283

Table G.1: Water balance components and processes involved in the calculation of water balance error (DHI software, 2012)……..……..287

List of Equations

Equation 2.1: Water balance model (Thornthwaite and Mather, 1957)

$$P = ET + Q + R + \Delta S$$

Equation 4.1: The FAO Penman-Monteith equation (Allen *et al*., 1998)

$$ET_{ref} = \frac{0.408\Delta(R_n - G) + \gamma \frac{900}{T + 273} u_2 (e_s - e_a)}{\Delta + \gamma(1 + 0.34u_2)}$$

Equation 4.2: Calculation of crop reference evapotranspiration (ET_C; DHI software, 2012).

$$ET_C = ET_{Ref} \times K_c$$

Equation 4.3: The Normalized Difference Vegetation Index (NDVI) equation

$$NDVI = \frac{NIR - red}{NIR + red}$$

Equation 4.4: Relationship between Leaf Area Index (LAI) and the Soil-adjusted Vegetation index (SAVI)

$$LAI = \frac{-\ln (SAVI + 0.371)}{0.48}$$

Equation 4.5: The Soil-adjusted Vegetation index (SAVI) equation

$$SAVI = \frac{(1 + L)(NIR - red)}{NIR + red + L}$$

Equation 4.6: Van Genuchten soil water retention curve function (DHI software, 2012)

$$\theta(h) = \left[(\theta_s - \theta_r)\left(\frac{1}{1 + (\alpha h)^n}\right)^m\right] + \theta_r$$

Equation 4.7: Brooks and Corey model for soil hydraulic conductivity (DHI software, 2012)

$$K(\theta) = K_{sat}\left(\frac{\theta - \theta_r}{\theta_s - \theta_r}\right)^N$$

Equation C.1: Average daily wind speed ($m.s^{-1}$) measured at 2 m above ground level (Zotarelli *et al*., 2015)

$$u_2 = u_h \frac{4.87}{\ln(67.8h - 5.42)}$$

Equation C.2: The relationship determined between the FAO Automatic Weather Station's solar radiation ($MJ/m^2/day$) record and the mast Automatic Weather Station's daily net radiation ($MJ.m^{-2}.day^{-1}$) record.

$$y = 0.9627x + 5.0972$$

Abbreviations and Acronyms

ACRU	-	Agricultural Catchments Research Unit
APEX	-	Agricultural Policy/Environmental eXtender
AWS	-	Automatic Weather Station
CI	-	Canopy Interception
CIS	-	Canopy Interception Storage
DAFF	-	Department of Agriculture, Forestry and Fisheries
DEM	-	Digital Elevation Model
DHI	-	Danish Hydrological Institute
DHSVM	-	Distributed Hydrology Soil Vegetation Model
E_i	-	Evaporation from Interception
E_p	-	Evaporation from Ponded Water
E_s	-	Soil Evaporation
ET	-	Evapotranspiration
E_t	-	Transpiration
ET_A	-	Actual Evapotranspiration
ET_C	-	Crop Reference Evapotranspiration
ET_{Ref}	-	Reference Evapotranspiration
FAO	-	Food and Agricultural Organization
GIS	-	Geographic Information System
GR	-	Groundwater Recharge
HBV	-	Hydrologiska Byrans Vattenavdelning
HRU	-	Hydrological Response Unit
I_{UZ}	-	Infiltration
K_c	-	Crop Coefficient
LAI	-	Leaf Area Index
LUCC	-	Land Use and/or Land Cover Change
LULC	-	Land Use and/or Land Cover

NDVI	-	Normalized Difference Vegetation Index
OL	-	Overland Flow
PRMS	-	Precipitation Runoff *Modelling* System
RD	-	Rooting Depth
RS	-	Remote Sensing
SAVI	-	Soil-adjusted Vegetation Index
SAWS	-	South African Weather Service
SHE	-	Systeme Hydrologique European
SWAT	-	Soil and Water Assessment Tool
SWRC	-	Soil Water Retention Curve
SZ	-	Saturated Zone
TOPMODEL	-	TOPography based hydrological MODEL
UZ	-	Unsaturated Zone
VIC	-	Variable Infiltration Capacity
WAVES	-	Water, Vegetation, Energy, Solute Model
WRC	-	Water Research Commission

Chapter One

Introduction

1.1 Introduction

Understanding of the impacts of land use and/or land cover (from here on referred to as LULC) on water resources is essential in improving management practices and protecting these resources (Toohey *et al*., 2018). The impacts of LULC and the change thereof (from here on referred to as LUCC) have been investigated worldwide at a range of scales (Lambin *et al*., 2003; Warburton *et al*., 2012; Isik *et al*., 2013; Payn *et al*., 2015; Zhang *et al*., 2017; Zhang *et al*., 2018). However, quantifying these impacts is still a challenging problem in hydrology (da Silva *et al*., 2018) as hydrological processes are nonlinear, complex, dynamic, and depend on numerous factors and system feedback responses (Lambin *et al*., 2003; Devi *et al*., 2015).

The impacts pertaining to LULC and LUCC on water resources are particularly problematic in areas where water resources are already under pressure and/or where further growth is progressively constrained by water availability (Dye and Versfeld, 2007). These vulnerable areas are more at risk and less likely to recover from detrimental LUCC (Ashton *et al*., 2008). South Africa is one such area, where LUCC has a detrimental impact on the already scarce water resources. A study by Bosch (1979), undertaken in South Africa, indicated an 82% reduction in streamflow in the KwaZulu-Natal Drakensburg 20 years after the conversion of grassland into pine plantations, whilst van Wyk (1987) found a 55% reduction in streamflow in the Western Cape, South Africa 23 years after planting pines in previous fynbos planted land.

For thousands of years humans have altered LULC patterns and brought about LUCC with little to no consideration of the long-termed impacts on hydrology (Ojima *et al*., 1994; Legesse *et al*., 2003; Farley *et al*., 2005; Toohey *et al*., 2018). The impacts that pertain to LUCC relate to: the conversion of land, the modification of land and/or the maintenance of land (Lambin *et al*., 2001). While

conversion considers the complete change from one land cover to another (e.g. forestry to grassland), modification considers alterations in land use or land cover attributes (e.g. harvesting) and maintenance considers activities used in ensuring land use or land cover activity is sustained or improved (e.g. irrigation, pesticide application; Turner *et al*., 1994).

In general, anthropogenic causes of LUCC are more problematic than natural causes as they occur at more rapid rates (DeFries and Eshleman, 2004), such as agriculture, farming, and commercial forestry. Such LULC activities have a number of knock-on effects and have modified landscapes, altered plant and animal communities, degraded water quality and soil fertility, reduced biotic diversity, altered hydrological flows and introduced exotic species (Turner *et al*., 1994; Lambin *et al*., 2001). Soil erosion is one such problem, where changes in land use and climate are major external agents of water erosion (Le Roux *et al*., 2007). In South Africa, more than 70% of the land is affected by varying intensities of soil erosion (Le Roux *et al*., 2007), which not only affects soil quality but is coupled with serious off-site impacts related to increased movement of sediment and delivery to water systems (Le Roux, 2012).

Research on the impact of LUCC on hydrological processes has considered the various hydrological components that make-up a system, both surface and sub-surface components: precipitation, canopy interception (CI), evapotranspiration (ET), soil moisture, infiltration (I_{UZ}), streamflow and surface runoff and groundwater recharge (GR; Fohrer *et al*., 2001; DeFries and Eshleman, 2004; Warburton *et al*., 2012; Hasenmueller and Criss, 2013; Isik *et al*., 2013; Zhang *et al*., 2018). The need to integrate all of these processes in a holistic manner has seen the development of a range of hydrological models, capable of modelling multiple interconnected processes at varying spatial and temporal scales, thereby capturing the holistic system behaviour or response.

Modelling is useful for understanding both the current situation at multiple scales and for predicting future scenarios (Merritt *et al*., 2003). Hydrological models have been widely used to explain and predict complex behaviours associated with the management of environmental systems and the

impacts pertaining to LULC and LUCC (Bergström and Graham, 1998; Isik *et al*., 2013; Devi *et al*., 2015; Ma *et al*., 2016; Singh *et al*., 2017; Sonnenborg *et al*., 2017; Zhang *et al*., 2018). Technological improvements in computing capabilities and knowledge advancements in the field of hydrology and hydrological processes have brought about the revision and advancement in many of the current suite of hydrological models (Singh *et al*., 2017). Improvements in modelling capabilities seen today can be attributed to the incorporation of Geographic Information Systems (GIS) and satellite Remote Sensing (RS) technologies (Gangodagamage, 2001; Xu *et al*., 2001), improving on spatial and temporal modelling capabilities by allowing for larger areas to be investigated over shorter time periods and at reduced costs (Xu *et al*., 2001). Geographic Information Systems (GIS) and RS allow for temporal variations to be visualized over varying time periods depending on modelling requirements (e.g. daily, monthly, seasonally and annually; Sui and Maggio, 1999; Xu *et al*., 2001). The improvements in hydrological models enable models to process high resolution data at fast rates allowing for more thorough testing of hydrological concepts (DeFries and Eshleman, 2004).

The variety of hydrological models that exist (Merritt *et al*., 2003) differ in terms of complexity, processes considered, and the data required for calibration, validation and use (Merritt *et al*., 2003; Devi *et al*., 2015). Examples of hydrological models include: physically-based fully distributed models such as the Distributed Hydrology Soil Vegetation Model (DHSVM) and the Systeme Hydrologique European (MIKE SHE) model, physically-based semi-distributed models such as the Soil and Water Assessment Tool (SWAT) and the Precipitation Runoff Modelling System (PRMS), and conceptual lumped models such as The North American Mesoscale Forecast System (Isik *et al*., 2013). Hydrological models are essential for studying hydrological processes and their responses to both natural and anthropogenic factors and play a central role in the development of water management strategies (da Silva *et al*., 2018).

To investigate the impact that different LULC types have on hydrological processes, a small research sub-catchment in KwaZulu-Natal was chosen, falling within the larger Two Streams catchment. The Two Streams catchment is one of the few remaining small catchment research areas in South Africa,

with experiments on-site having been conducted since the late 1990s (Everson *et al.*, 2006, 2014; Clulow *et al.*, 2011). At the start of the study, the Two Streams sub-catchment comprised of three main land cover classes: black wattle (*A. mearnsii*) forestry plantation, sugarcane (*S. officinarum)* plantation and riparian vegetation. By the end of the study the black wattle plantation had been cleared with the intention of Mondi planting *E. dunnii*. Given that the site has been used as a hydrological research catchment for a number of years it provided a unique opportunity to model hydrological processes relative to various LULC classes and under a LUCC scenario.

The Two Streams sub-catchment has a plethora of hydrological data collected over years of research (Everson *et al.*, 2006, 2014; Clulow *et al*., 2011) which facilitates the use of a more complicated physically-based modelling software. For this study the deterministic, physically-based hydrological model MIKE SHE was used to model the Two Streams sub-catchment. MIKE SHE is a very flexible model allowing physically-based concepts to be considered where sufficient data exist and for more conceptual approaches to be taken where data is limited (Graham and Butts, 2005). MIKE SHE connects to external software (MIKE 11) to model stream flow and allows for the incorporation of GIS derived spatial datasets to improve spatial consideration in modelling (DHI software, 2012).

1.2 Research Aims and Objectives

South Africa is a water scarce country (Claasen, 2010), and, all effort to reduce water use and prevent degradation of water resources should be taken. These factors of degraded water quality and reduced water quantity all arise as a consequence of LUCC and by understanding catchment hydrological processes one is able to improve water resource management in an area subject to LUCC (Forrester *et al*., 2011; Toohey *et al*., 2018). Modelling and the use of GIS and RS techniques in such circumstances allow for the consideration of multiple spatial and temporal factors (Gangodagamage, 2001; Xu *et al*., 2001). These techniques can be beneficial particularly in data rich environments such as the Two Streams sub-catchment.

This project forms part of a larger project that is being managed and funded by the Water Research Commission (WRC) – WRC project No K5/2402: "Assessing the impact of erosion and sediment yield from different land uses in farming and forestry systems and their effect on water resources in selected catchments of South Africa." Developing a holistic hydrological model set-up for the Two Streams sub-catchment based on the hydrological data available for the site will allow future research, once longer term soil erosion and sediment yield data are available, to investigate the impacts of soil erosion on water resources.

This dissertation aims to:

1. Assess the ability for MIKE SHE software to model the hydrological cycle of the Two Streams sub-catchment and evaluate the model against measured data recorded in the past.
2. Assess and compare modelled hydrological outputs and characteristics of the dominant land cover types present within the Two Streams sub-catchment: sugarcane (*S. officinarum*) plantation, black wattle (*A. mearnsii*) plantation and riparian vegetation.
3. Determine the impact that a change in plantation forestry from *A. mearnsii* to *E. dunnii* will have on the hydrological characteristics and hydrological cycle of the Two Streams sub-catchment, using MIKE SHE modeling software.

The research aims are addressed in three parts; the first documents the set-up, calibration and validation of a MIKE SHE model that represents the current scenario of the Two Streams sub-catchment, where the dominant vegetation types comprise black wattle plantation, sugarcane plantation and natural riparian vegetation. The second employs the calibrated MIKE SHE model of the current scenario to generate hydrological outputs for the three dominant vegetation classes and compares these outputs across the different classes. The third develops the set-up of a MIKE SHE model that predicts the future scenario of the sub-catchment, i.e. where black wattle plantation forestry is replaced with *E. dunnii*, and compares the *E. dunnii* hydrological outputs to those of the black wattle class to observe the differences in hydrology with land cover change.

The objectives of this dissertation are as follows:

- Populate the MIKE SHE current (*A. mearnsii* plantation) and future (*E. dunnii* plantation) models with appropriate datasets, by identifying, sourcing, collecting, gathering, measuring and generating required inputs.
- Calibrate and validate the MIKE SHE set-up to determine how accurately the current scenario modelled the observed sub-catchment hydrology.
- Simulate the water movement and water balance of the Two Streams sub-catchment for the current scenario.
- Simulate the water movement and water balance of the Two Streams sub-catchment for the future scenario.
- Draw conclusions on the hydrological impacts pertaining to the different land cover types and land cover change, taking into consideration spatial and temporal variations.

This thesis comprises eight chapters (inclusive of this introduction chapter). Chapter two is the literature review. The methods have been separated into two chapters with chapter three detailing the study site and chapter four the methods. This was done as the method chapter is very descriptive of the model set-up process and would be too lengthy if incorporated with the study site description. The results and discussion are separated into three chapters; where chapter five deals predominantly with the model calibration and validation process, chapter six compares the model outputs of the sugarcane, riparian and black wattle classes, and chapter seven compares the black wattle model outputs of the current scenario to the *E. dunnii* outputs of the future scenario. Chapter eight is the conclusion. Most of the model inputs are considered in chapter four methods including some of the inputs that were generated during this study (i.e. they are technically results) and some are considered under the biophysical characteristics of the site under chapter five. The reason for the inclusion of some results in the method chapter was for ease of understanding, as some of the inputs are required for subsequent processes to occur and the description thereof was easier if those input 'results' were included. The results sections focus more on the model outputs than the model inputs, except chapter

five which considers both. The discussion sections focus on addressing both the model outputs findings and the inputs, particularly where uncertainties or limitations exist. The appendices comprise 60 pages.

Chapter Two

Literature Review

2.1 Introduction

The literature review explores relevant research to this dissertation focussing on hydrology related themes of the hydrological cycle, hydrological models and modelling approaches and the water balance calculation, followed by considerations of the impact of LULC and LUCC on hydrology, specifically focussing on the impacts of forestry and sugarcane plantations on water quantity, and on issues of scaling in LULC studies. The literature reviewed is used to motivate for the use of the MIKE SHE modelling software for this dissertation.

2.2 Hydrology and the hydrological cycle

Hydrology is concerned with the quantity, supply, movement and allocation of water, and how water reacts and interacts with both the living and non-living environment (Hendriks, 2010). Over time the purpose and focus of hydrology related research has evolved from focussing on flood prediction to focussing on comprehensive water resource management (Ma *et al*., 2016). Advancements in hydrological research have primarily been driven by technological advancements that have allowed for improved understanding of detailed hydrological processes of the hydrological cycle (Moradkhani and Sorooshian, 2008).

The hydrological cycle (Figure 2.1) is the central concept in hydrology and involves many complex interactions (Music and Caya, 2007; Hendriks, 2010). Within the hydrological cycle, water exists in different phases and can be grouped into different types, namely: atmospheric water, surface water, soil water, and groundwater (Hendriks, 2010). Atmospheric water exists predominantly in a gaseous form, whilst water on the surface occurs either in a liquid or solid state, and is stored in terrestrial water bodies including rivers, lakes and dams (Hagemann *et al*., 2006). Subsurface water is separated between the unsaturated (UZ) and the saturated zone (SZ; Mimikou *et al*., 2016). The SZ, where

groundwater occurs, is located below the water table, whilst the UZ, where soil water is found, occurs below the ground, but above the water table (Hendriks, 2010). At a global scale, water cycling differs both over space and time. Spatially, different areas experience a surplus of water while others a deficit (Trenberth *et al*., 2003; Eggert *et al*., 2015). Temporally, water at different cycle stages is cycled at different rates (Eggert *et al*., 2015), for example, water in the SZ is cycled at a much slower rate that water in shallow surface water bodies (Graham and Butts, 2005).

The hydrological cycle is driven by precipitation and energy inputs, with energy supplied primarily through solar radiation (Trenberth *et al*., 2006). Solar radiation brings about ET. Once water evaporates it is converted into atmospheric water vapour and if atmospheric conditions are conducive, condensation will occur and clouds will form leading to precipitation in many possible forms including snow, rainfall and hail (Trenberth *et al*., 2006; Hendriks, 2010). Precipitation falling to the land induces a number of processes: water can be trapped by vegetation from where canopy evaporation can occur, water can infiltrate into the soil and recharge groundwater, and water can discharge into terrestrial water bodies (Trenberth *et al*., 2006; Hendriks, 2010). Although this simplistic notion of water movement provides a sound basis of understanding hydrology, there are a range of more complex processes that occur, both above and below the ground surface, as a result of the interaction of water with vegetation, topography, soil and geology (Zhang *et al*., 1999). All of these factors are integrative in determining the movement, distribution and storage of water (Trenberth *et al*., 2006).

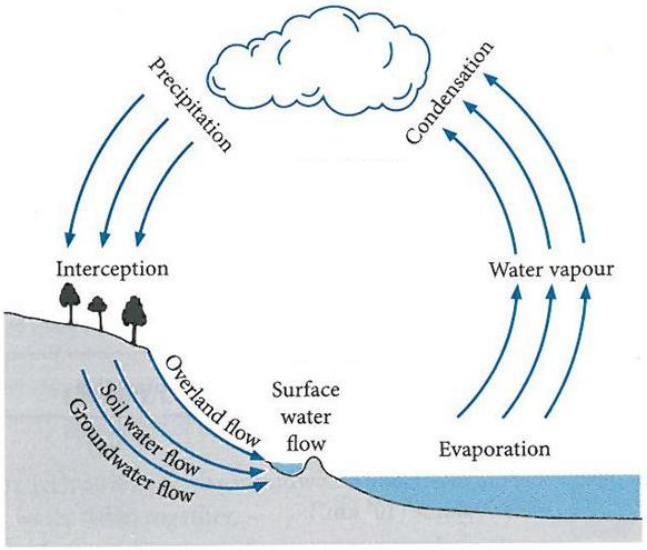

Figure 2.1: Depiction of the hydrological cycle (Hendriks, 2010).

The hydrological cycle is crucial for life on Earth and having an accurate representation of the exchanges of water between the atmosphere, the land surface and subsurface is necessary for improved awareness and water management (Hagemann *et al*., 2006; Devi *et al*., 2015). Hydrological modelling provides a means to investigate hydrological processes and the hydrological cycle in a holistic manner.

2.3 Hydrological modelling

Many hydrological models have been developed, each with their own objectives and capabilities (Merritt *et al*., 2003; Aksoy and Kavass 2005; Gassman *et al*., 2010; Devi *et al*., 2015). For example, the SWAT was developed to examine and predict the movement of water and sediment, and was tailored to model agriculture production and chemical circulation related to agriculture (Devi *et al*., 2015); whilst the PRMS was developed to assess impacts of precipitation, climate and land use on catchment response (Legesse *et al*., 2003).

The primary purposes of a hydrological model are to understand hydrological processes and the implications of making certain assumptions regarding the nature of the real world hydrological

system, and to predict hydrological system behaviour (Moradkhani and Sorooshian, 2009**;** Devi *et al*., 2015). Hydrological models are used to provide predictions of different factors such as climate and climate change (Legesse *et al*., 2003; Teutschbein and Seibert, 2010, 2012; Pohl *et al*., 2017; Zhang *et al*., 2018) and LULC and LUCC (Zhang *et al*., 1999; Xu and Singh, 2004; Siriwardena *et al*., 2006; Vanclay, 2009; Warburton *et al*., 2012; Isik *et al*., 2013; da Silva *et al*., 2018; Toohey *et al*., 2018). Each hydrological model has its own unique characteristics and considers its own inputs, depending on the purpose of the model and the detail at which hydrological processes are investigated (Merritt *et al*., 2003). The ability for hydrological models to run predictive scenarios of change is one of the most useful abilities of modelling as an analytical tool (Devi *et al*., 2015). The ability to explore and model hydrological processes of historical scenarios and also extrapolate future hydrological happenings makes modelling a valuable tool in change analysis (Miller *et al*., 2002).

The model input requirements depend on the processes considered by the model, the complexity at which processes are considered, the scaling capabilities of the modelling software and the model use or user requirements (Moradkhani and Sorooshian, 2009; Devi *et al*., 2015). In general, there is no best fit hydrological model for all applications (Merritt *et al*., 2003). Choosing the most appropriate model will depend on what the model will be used for (Merritt *et al*., 2003; Aksoy and Kavass, 2005). Each model has its own advantages and limitations, and some require high detail information, which is on occasion not easily available or not economically feasible (Merritt *et al*., 2003). Detailed reviews of catchment modelling have been provided by Merritt *et al.* (2003), Aksoy and Kavass (2005), and Devi *et al.* (2015).

Models can be categorised to facilitate understanding of model capabilities, and can be broadly classified into three groups: empirical, conceptual and physically-based (Legesse *et al*., 2003; Merritt *et al.*, 2003; Devi *et al*., 2015), but can also be categorised based on spatial or temporal capabilities. Spatially, models can be distinguished as lumped, semi-distributed or distributed (Merritt *et al.*, 2003; Aksoy and Kavass, 2005; Devi *et al*., 2015) and temporally as static and dynamic (Merritt *et al*., 2003; Devi *et al*., 2015), where static models exclude time whilst dynamic models include time.

Temporally, models can be classified as event based and continuous, where event based produces outputs only for specific time periods while continuous produces continuous outputs (Merritt *et al*., 2003; Devi *et al*., 2015). The different model categories are elaborated on further in the coming paragraphs.

2.3.1 Empirical models

Empirical models provide a simplistic, homogeneous representation of the environment, relying on empirically derived fits of observed data (Merritt *et al*., 2003; Devi *et al*., 2015), and generally run on minimal, coarsely measured inputs (Merritt *et al*., 2003; Aksoy and Kavass, 2005). Empirical models are used to relate the input and output variables using transformation functions and, as such, they do not consider the features, processes or the governing physical principles of processes involved in hydrological systems (Legesse *et al*., 2003; Devi *et al*., 2015).

2.3.2 Conceptual models

Conceptual models describe the hydrological processes of a number of interconnected components representing the physical elements of a catchment (Merritt *et al*., 2003; Devi *et al*., 2015). Conceptual models can be considered as semi-empirical as they rely on observed field data. However, they also rely on calibration to assess model parameters (Devi *et al*., 2015). For the calibration of conceptual models, large amounts of meteorological and hydrological data are required (Devi *et al*., 2015). Examples of conceptual models include the Hydrologiska Byrans Vattenavdelning (HBV) model (Bergström, 1992; Devi *et al*., 2015),the TOPography based hydrological MODEL (TOPMODEL; Beven *et al*., 1995; Beven, 1997), the Identification of unit Hydrographs and Component flows from Rainfall, Evapotranspiration and Streamflow (IHACRES) model (Dye and Croke, 2003) and the Agrohydrological (ACRU) model (Schulze, 1995).

2.3.3 Physically-based models

Physically-based models are used to describe the ideal mathematical representation of the real world (Devi *et al*., 2015). They include the principles of physical processes that are measurable and are

functions of both time and space (Legesse *et al*., 2003). Physically-based models quantify outputs based on a large number of physically-based input parameters. Unlike conceptual models, physically-based models do not require extensive data for calibration (Merritt *et al*., 2003; Devi *et al*., 2015; Ma *et al*., 2016). Physically-based models can overcome many problems of empirical and conceptual models due to their physical interpretation and increased complexity at which hydrological processes are considered (Merritt *et al*., 2003). Physically-based models can be more precise, provided that there is sufficient available input data, as they aim to reduce the bias between the modelled processes and observations made (Devi *et al*., 2015). Examples of a physically based hydrological model include the DHSVM (Isik *et al*., 2013) and MIKE SHE model (Graham and Butts, 2005) – MIKE SHE is discussed further under section 2.4.2.

2.3.4 Comparing lumped and distributed hydrological models

Differences in spatial consideration in modelling distinguish lumped from distributed hydrological models (Merritt *et al.*, 2003; Aksoy and Kavass, 2005; Devi *et al*., 2015). Lumped models consider an entire area as a single unit, thereby disregarding spatial variability in the components and the natural heterogeneous nature of the system (Aksoy and Kavass, 2005; Moradkhani and Sorooshian, 2009). Distributed models, on the other hand, explicitly represent spatial variability of hydrological components, such as: topography, LULC, soil, precipitation and ET, and system heterogeneity (Legesse *et al*., 2003; Merritt *et al*., 2003; Moradkhani and Sorooshian, 2009). Hence in the selection of a model there are trade-offs to consider in terms of data availability, time constraints and computing capabilities.

In the range of hydrological models, models differ in their consideration of spatial scale and physics considerations, for example the Kinematic Runoff and Erosion (KINEROS) *model,* the Institute of Hydrology Distributed (IHDM) model and the MIKE SHE model are all physically-based fully distributed models while the SWAT and the PRMS are physically-based semi-distributed models and the North American Mesoscale Forecast System (NAM) is a conceptual lumped model (Isik *et al*., 2013). Over time the different modelling categories have evolved from the initial creation of

simplistic empirical approaches, to lumped parameter models, to spatially distributed models (DeFries and Eshleman, 2004).

With ever increasing consequences of human impacts, it is becoming increasingly important to account for change, interactions and feedback mechanisms at play in hydrological systems (Ma *et al*., 2016). Thus, there is a shift toward distributed hydrological modelling due to both social need and technological advancements in computing (Ma *et al*., 2016). Physically-based, distributed models have important applications in interpreting and predicting the effects of LUCC and climate variability as they are able to relate model parameters directly to physically observable land surface characteristics (Legesse *et al*., 2003). Although there is a shift toward distributed hydrological modelling over lumped models, there are concerns with regards to these complex distributed models. One of the main sources of uncertainty and concern surrounds the estimation of the number of parameters within distributed models, as due to the large amount of input requirements not all parameters can be measured and some will need to be estimated causing a degree of uncertainty in the model (Moradkhani and Sorooshian, 2009; Ma *et al*., 2016).

2.4 Types of hydrological models

In general, hydrological models are the widely employed tools for investigating hydrological processes and assisting in water management (Devi *et al*., 2015). However, there will always be a degree of uncertainty in model projections as all models are abstractions, simplifications and interpretations of reality and not reality themselves (Ma *et al*., 2016). Some examples of hydrological models are described below.

2.4.1 The Soil and Water Assessment Tool (SWAT) model

The SWAT model is a physically-based, continuous daily time step model developed to simulate long-term impacts of land and water management and agricultural practices (Govender and Everson, 2005). The physical processes simulated in a catchment by the SWAT model can be grouped into

upland and channel processes (Govender and Everson, 2005). The model components include: climate, surface runoff, ET, crop growth, irrigation, and nutrient and pesticide inputs (Arheimer and Olsson, 2003).

The model can simulate a catchment in both a lumped or distributed approach, by automatically delineating the catchment either into sub-catchments or grid cells based on a digital elevation model (DEM; Govender and Everson, 2005). By delineating into sub-catchments the model is based on semi-distribution. During this process, a catchment is first sub-divided into sub-catchments according to the terrain and river channels, and then into multiple hydrological response units (HRUs) based on the soil and LULC types within the sub-catchments (Devi *et al*., 2015). A HRU is a fundamental homogeneous spatial unit upon which SWAT simulates the water balance (Xu *et al*., 2009). The use of sub-catchments in a simulation is useful in differentiating between the impacts of various land uses and soils on the hydrology of a catchment (Govender and Everson, 2005).

The SWAT model is advantageous due to its availability and user-friendliness (Xu *et al*., 2009). The SWAT model has been developed with an ArcView GIS interface (Easton *et al*., 2010), allowing for improved spatial analysis and visualization together with increased model flexibility (Govender and Everson, 2005). ArcGIS provides a platform to incorporate soil input maps, DEMs and LULC maps required in a SWAT model (Easton *et al*., 2010). The SWAT model is computationally capable of modelling small and large sub-catchments or catchments within reasonable times (Govender and Everson, 2005). The SWAT model has been widely used, and applied worldwide, for a number of water quantity and water quality issues (Govender and Everson, 2005; Xu *et al*., 2009; Oeurng *et al*., 2010). Within South Africa, SWAT has been applied to model effect of land use change on hydrology of the catchment (Govender and Everson, 2005).

2.4.2 The agrohydrological ACRU model

The ACRU model is an agrohydrological model developed by the Agricultural Catchments Research Unit of the School of Bio-resources Engineering and Environmental Hydrology at the University of KwaZulu-Natal in Pietermaritzburg South Africa (Schulze, 1995). It is a similar model to the SWAT model in that it uses hydrological responses units to simulate catchment hydrology (Aduah *et al*., 2017). It is a deterministic, daily time step, physical-conceptual, and integrated multipurpose modelling system (Schulze, 1995). It can operate as a point or lumped model for small catchments and as a distributed model for large catchments (Jewitt and Schulze, 1999). The ACRU model has been widely used for modeling eco-hydrological impacts or implications in South Africa and the surrounding regions (Mugabe *et al*., 2011; Warburton *et al*., 2012). For example, ACRU has been used to assess the hydrological impacts resulting from land use change in three South African catchments (Warburton *et al*., 2012).

2.4.3 The Hydrologiska Byrans Vattenavdelning (HBV) model

The HBV model is a semi-distributed conceptual model (Bergström, 1992). It was designed to consider what were deemed by Bergström (1992) as the most significant components of the runoff generating processes, and thus the HBV model avoided complexities by only focusing on certain hydrological components. The model divides the modelled catchment area into sub-catchments or primary hydrological units that are then further classified based on elevation and land use (Lindström *et al*., 1997). The HBV model consists of three main components: snow accumulation and snowmelt, soil moisture and river routing (Bergström, 1992).

The HBV model is primarily used in Scandinavian countries, but has been used globally under a range of varying conditions such as in Zimbabwe, India and Colombia (Lindstrom *et al*., 1997). The HBV model was used to simulate land use scenarios in Costa Rica where land use change was found to have relatively little effect on the overall mean annual water yield (< 3%; Birkel *et al*., 2012). However, streamflow dynamics were found to be sensitive in frequency, timing and magnitude of discharge extremes (Birkel *et al*., 2012). Originally the HBV model was developed at the Swedish

Meteorological and Hydrological Institute (SMHI) for runoff simulation and hydrological forecasting (Bergström, 1992); however the scope of applications has increased with the model undergoing multiple revisions since inception (Lindstrom *et al*., 1997). However, even with revisions, the model philosophy has remained the same, which is that the model complexity and data demand must not be in conflict with the operational requirements (Bergström, 1992). Today many versions of the HBV model exist and new codes are constantly being developed by different research groups (Scheepers *et al*., 2018).

2.4.4 TOPMODEL (TOPography based hydrological MODEL)

The topography based hydrological model (TOPMODEL) provides a user-friendly model structure that makes use of digital terrain model (DTM) data to model runoff (Beven, 1997). The TOPMODEL differs from the previous hydrological models discussed in that it does not comprise of a single model structure that is generally applicable, but rather comprises a set of conceptual tools that can be used to simulate hydrological processes (Beven *et al*., 1995). The two main factors considered by TOPMODEL in modelling hydrology are catchment topography and soil transmissivity (Beven, 1997). The main aim of the model is to spatially determine the water table depth of the modelled area (Devi *et al*., 2015) and thereby TOPMODEL is capable of capturing the dynamics of surface or subsurface areas (Beven *et al*., 1995). Due to advancements in RS and GIS, topographic data are more readily available and at higher resolutions, making the TOPMODEL popular and widely implemented (Devi *et al*., 2015). TOPMODEL has been used to investigate the role of topographic factors in the invasion of hillslopes by *Pteronia incana*, in Eastern Cape, South Africa (Kakembo *et al*., 2007). The study found the occurrence of *P. incana* to be strongly influenced by slope angle and aspect and that the combined influence of slope gradient, aspect, and land use promoted the invasion (Kakembo *et al*., 2007).

2.4.5 The Variable Infiltration Capacity (VIC) model

The Variable Infiltration Capacity (VIC) model is a semi-distributed macroscale hydrological model that represents surface and subsurface hydrological processes on spatially distributed grid cells

(Demaria *et al*., 2007; Devi *et al*., 2015). The VIC model uses energy and water balance equations (Demaria *et al*., 2007) and has been extensively used in studies on water resources management, land-atmosphere interactions, and climate change. (Xu and Singh, 2004**)**. The key characteristics of the VIC model are the representation of heterogeneous vegetation, multiple soil layers with individual I_{UZ} measures, and non-linear base flow (Nijssen *et al*., 2001). The VIC model consists of three layers; the top layer which allows for quick soil evaporation (E_s), the middle layer represents the dynamic response of soil to rainfall events and the lower layer is used to characterise behaviour of soil moisture (Devi *et al*., 2015). The VIC model is advantageous in considering the dynamic nature of surface and ground water interactions and at modelling the ground water table (Devi *et al*., 2015). The VIC model can be applied to a range of conditions globally, for example Nijssen *et al*. (2001) used the VIC model to provide a global estimate of soil moisture over the period 1980 – 1993. The study found that in comparison to observational datasets the components of the global and continental water balance are similar to those in previously produced datasets, although runoff was found to be lower than observed as was mean modelled soil moisture (Nijssen *et al*., 2001).

2.4.6 The Agricultural Policy/Environmental eXtender (APEX) model

The Agricultural Policy/Environmental eXtender (APEX) model is a flexible and dynamic model capable of simulating a wide range of management practices, cropping systems, and other land use across a broad range of agricultural landscapes (Gassman *et al*., 2010; Wang *et al*., 2012). The model was developed for the evaluation of land management strategies by considering sustainability, erosion, water supply and water quality, soil quality, plant competition, weather conditions and pests (Williams *et al*., 2015). The APEX model is an advancement on its predecessor, the Erosion/Productivity Impact Calculator (EPIC) model (Wang *et al*., 2012), as APEX can be used at a range of spatial scales and soil types (Williams *et al*., 2015). The APEX functions on a daily time step and can perform long term continuous simulations or can be used for simulating the impacts of different short-term management practices (Gassman *et al*., 2010).

2.4.7 The SPAtial and Time Series Information Modeling (SPATSIM) model

The SPAtial and Time Series Information Modeling (SPATSIM) model was developed by the Institute for Water Research (IWR) at Rhodes University, South Africa (Hughes, 2005). It was designed as a database, data analysis and modelling system, specifically for hydrological and water resource applications (Hughes, 2002). SPATSIM is a semi-distributed model capable of modelling individual sub-catchments with their own parameter sets and input data (Hughes, 2002). One of the primary motivations for the development of this model was to integrate many of the ecological Reserve determination methods into a single integrated software package, however outside of this core purpose it can be used for a variety of other water resource assessment applications (Hughes, 2005). SPATSIM is beneficial in that it contains an integrated database management system that uses GIS shapefiles for data access.

SPATSIM comprises a number of utilities, but also has access to external, additional utilities and integrates easily with other water resource estimation models (Clark *et al*., 2012). As such the model is flexible and dynamic in development and design and can respond more rapidly to advancements in technology or research than more conservative models (Hughes, 2005; Clark *et al*., 2012). Since inception SPATSIM has undergone multiple iterations and is now referred to as SPATSIM-HDSF (Clark *et al*., 2012). The improvements to the original SPATSIM model that gave rise to SPATSIM-HDSF include changes to the database structure, changes and enhancements to the main user interface, enhancements to the internal GIS functionality, improvements in time series analysis tools and improvements in GIS functionality (Clark *et al*., 2012).

2.5 Hydrological model employed for this study

The plethora of information available on the Two Streams sub-catchment allows for the employment of a more complicated, physics based modelling system, capable of incorporating large quantities of measured data over varying spatial and temporal scales. This is as opposed to using a more simplistic modelling approach that is limited by data availability. The Systeme Hydrologique European (MIKE

SHE) model is one such modelling software. This study will employ MIKE SHE and evaluate its performance for use in modelling the Two Streams sub-catchment.

MIKE SHE is a physically-based distributed hydrological model developed to integrate the simulation of both surface water and groundwater flow and transport processes in a fully coupled modelling environment (Hughes and Liu, 2008). MIKE SHE is globally recognized and has been implemented in numerous water related research projects at a range of spatial scales from 1 – 1,000 km² (Bathurst, 1986; Wicks and Bathurst, 1996; Christiaens and Feyen, 2001; Hughes and Liu, 2008; Zhang *et al*., 2008; Ma *et al*., 2016; Sonnenborg *et al*., 2017). MIKE SHE modelling software covers all the major processes of the hydrological cycle (Figure 2.2) and the interactions between the processes: precipitation, ET, overland flow (OL), unsaturated flow, saturated flow and channel flow (Graham and Butts, 2005) and is capable of simulating water quality (Butts *et al*., 2005).

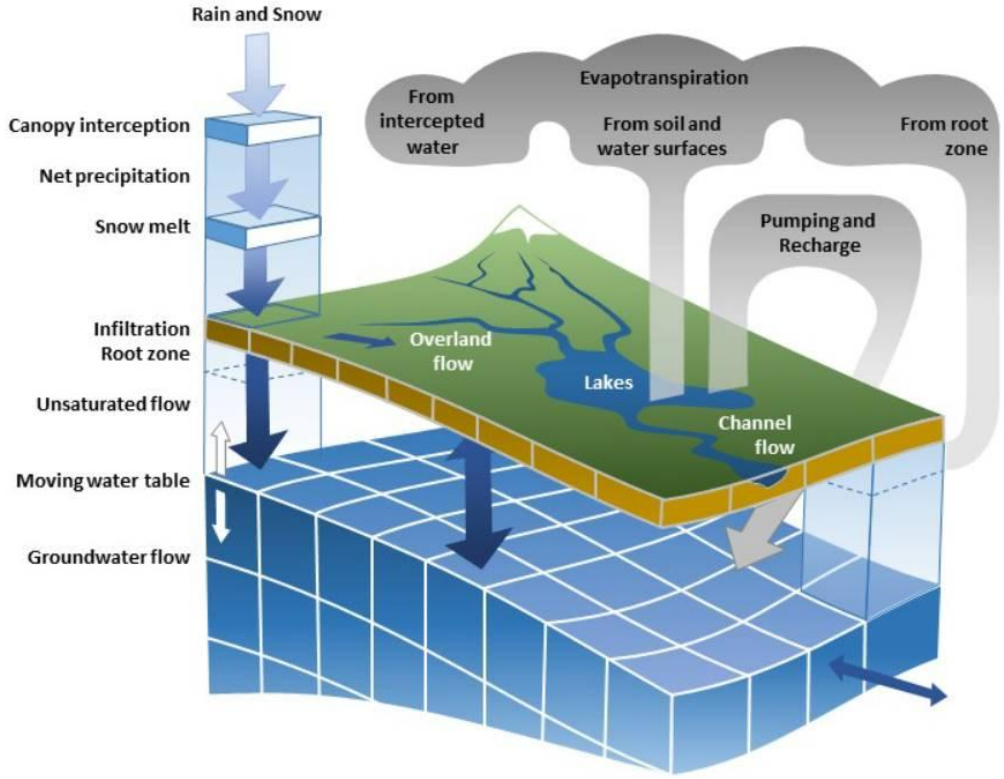

Figure 2.2: Hydrological processes simulated by MIKE SHE (Graham and Butts, 2005).

MIKE SHE software is flexible to selection preferences and data availability enabling the user to select from a number of different modelling options when modelling different processes and allowing for flexibility in spatial and temporal analysis (Graham and Butts, 2005). Temporally, the model allows the user to define the simulation and run time of each process enabling different processes to run at different time intervals or speeds, simulating more realistic representations of hydrological processes and the hydrological cycle (Graham and Butt, 2005; DHI Software, 2012). For example, movement of groundwater in the SZ is slower than the movement of water in the unsaturated or OL regions (DHI Software, 2012).

Not all hydrological processes can be calculated directly in MIKE SHE and are calculated through additional software that is then linked to the MIKE SHE framework, such as channel flow. MIKE SHE uses MIKE 11 to simulate channel flow (Graham and Butts, 2005). This allows for the modelling of complex channel networks, lakes and reservoirs and river structures for example gates, sluices and weirs (Graham and Butts, 2005). Separate software is used to allow for a more accurate representation of the river structures and their processes of operation (Butts *et al*., 2005).

Many studies have employed MIKE SHE modelling, such as Zhang *et al*. (2008), who used MIKE SHE to quantify the response in hydrology with changes in LULC and climate for the Loess Plateau in Northwestern China. Through calibration and validation, the study found that the model could capture the dominant runoff process of the small watershed and that the model was useful for understanding the rainfall-runoff mechanisms (Zhang *et al*., 2008). However, more measured data with higher temporal resolution are needed to further test the model for regional applications (Zhang *et al*., 2008). Another study by Im *et al*. (2009) considered the impact a change from non-urban to urban land use, in the Gyeongecheon watershed, South Korea, would have on catchment hydrology. The study successfully showed that between 1980 – 1990 there was a 10% increase in runoff, followed by a further 15% increase between 1990 – 2000 (Im *et al.*, 2009). Results further showed that over the studied years (1980 – 2000) ET declined by 18mm (Im *et al.*, 2009). This study

supported previous views on urbanization increasing surface runoff and decreasing ET (Im *et al.*, 2009).

In South Africa, Prucha *et al*. (2016) developed a MIKE SHE/MIKE 11 model for the Mokolo River Basin flow system, in the Limpopo Province. The aim of the study was to simulate key hydraulic and hydrologic outputs that would then be used as inputs to the Downstream Response to Imposed Flow Transformation for Arid Rivers (DRIFT-ARID) decision support system (DSS; Prucha *et al*., 2016). A key limitation in the development of the MIKE SHE/MIKE 11 model was the lack of data for calibration (Prucha *et al*., 2016). The climatic data record used to calibrate the daily discharge record was effective at calibrating the model to seasonal and post-climatic event stream discharge response characteristics. However, it was not able to calibrate the model to individual events given that no sub-daily climate data was available for calibration (Prucha *et al*., 2016). In addition, there was a lack of basic subsurface hydrogeologic characterisation and limitations on groundwater level data that limited the ability to calibrate the groundwater flow model and baseflow response of the model. However despite these limitations the MIKE SHE/MIKE11 model outputs were still used as inputs into DRIFT-ARID (Prucha *et al*., 2016). This study was effective in showing the high data requirements of the MIKE SHE/MIKE11 model not just for input but also for calibration. However given the physical nature of the model, calibration is less necessary than if the model where more conceptually or empirically based (Abbott *et al*., 1986; Merritt *et al*., 2003; Devi *et al*., 2015).

2.5.1 Comparing MIKE SHE to other hydrological models

Numerous studies have been conducted comparing the modelling capabilities of MIKE SHE to other hydrological models (Merritt *et al.*, 2003; El-Nasr *et al*., 2005; Golmohammadi *et al*., 2014; Devi *et al*., 2015). Golmohammadi *et al*. (2014) evaluated MIKE SHE, SWAT and APEX to model the Canagagigue Watershed in Ontario, Canada. The mean daily and monthly flow was modelled and found to be best simulated by MIKE SHE, during both the calibration and validation periods

(Golmohammadi *et al*., 2014). Moreover, MIKE SHE was able to predict streamflow variation better than the other models (Golmohammadi *et al*., 2014).

Devi *et al*. (2015) reviewed five hydrological models: HBV, VIC, SWAT, MIKE SHE and TOPMODEL, and suggested that VIC performed well in moist areas and could be well employed for use in water management of agricultural lands (Devi *et al*., 2015). MIKE SHE performed best in smaller catchments due to the large data requirements and physical parameters of the model and SWAT performed well with minimal calibration (Devi *et al*., 2015). El-Nasr *et al*. (2005) compared the performance of MIKE SHE and SWAT to examine whether both models were equally able to describe the different phases in the hydrological cycle of the Jeker river basin, Belgium (El-Nasr *et al*., 2005). The analysis showed both to well simulate the hydrology of the catchment. However, based on the calibration results MIKE SHE was found to model the overall variation of the river better than SWAT (El-Nasr *et al*., 2005).

Comparing the physically-based MIKE SHE model to the semi-distributed SWAT model, Ma *et al*. (2016) found MIKE SHE to be a better model choice. The study found MIKE SHE to better express spatial heterogeneity and describe the complete hydrological system due to the integration of the surface and subsurface processes (Ma *et al*., 2016). The SWAT model makes use of the HRU as its modelling computational unit, whilst MIKE SHE relies on a grid unit as its computational unit (Arnold *et al.*, 2012). Using a grid cell allows for improved expression of hydrological processes between consecutive units, whilst in each HRU, processes are isolated and individual (Ma *et al*., 2016).

Comparing MIKE SHE to other non-physically-based models, MIKE SHE has some limitations. As with all physically-based models, large amounts of data are required to operate the MIKE SHE model and this can be expensive to attain (Graham and Butts, 2005). A further limitation is that physics based models require a long execution time to run the complex processes, and MIKE SHE models may be over complicated by the user (Butts *et al.*, 2005; Graham and Butts, 2005). Despite these

limitations, MIKE SHE is able to explore the mechanisms of hydrological processes in response to the environment, rather than simply pursuing the improvement of the fit between simulation and observation, as many conceptual or empirical models attempt (Ma *et al*., 2016).

MIKE SHEs integrated modelling approach (Graham and Butts, 2005) coupled with the ability to model dynamic hydrological processes such as: LUCC, wetland management, groundwater extraction, irrigation-drainage and climate change enable MIKE SHE to achieve objectives not well met by conceptual models (Ma *et al*., 2016). A further desirable feature of the MIKE SHE model design and use is flexibility. In general, the modelling system employed should be able to match the sophistication of the solution with the project requirements and the availability of data (Abbott *et al*., 1986). Thus, depending on the situation, complex solutions are not always required, and in MIKE SHE the flexible user interface allows for choices in modelling methodology to cater for varying degrees of complexity or physical consideration and data availability. The physical processes considered and the flexibility attributes to MIKE SHE are well suited for predicting hydrological change as they account for the inclusion of vegetation responses to inter-annual variability of climate and water availability (Troch *et al*., 2009).

MIKE SHE provides a good expression of the heterogeneity of natural properties and a detailed description of physical hydrological processes (Ma *et al*., 2016). It is a globally recognized modelling software and has been implemented in numerous water related studies for a variety of applications (Bathurst, 1986; Wicks and Bathurst, 1996; Christiaens and Feyen, 2001; Hughes and Liu, 2008; Zhang *et al*., 2008; Ma *et al*., 2016; Sonnenborg *et al*., 2017), such as water resource management and hydrological prediction under LUCC and climate change (Ma *et al*., 2016).

2.6 Advances in Remote Sensing (RS) and Geographic Information Systems (GIS)

Technological improvements in computing capabilities and knowledge advancements in the field of hydrology and hydrological processes have brought about the revision and advancements of many of the current hydrological models (Lindstrom *et al*., 1997; Govender and Everson, 2005; Devi *et al*., 2015). These advancements have brought about an improvement in modelling of physically-based processes, processing times, model flexibility, and user friendliness (Merritt *et al.*, 2003; Govender and Everson, 2005; Easton *et al*., 2010; Devi *et al*., 2015). The limitation with the rapid advancements in hydrological modelling is that practically these advancements have not been mirrored in field study observations and data collection procedures and as such there is a disconnect between the large model input requirements and on-the-ground point data collection capabilities (McGuire *et al*., 2005; Singh *et al*., 2017). In addition, the economic impracticalities and time constraints related to data acquisition can limit model usage (Abbott *et al*., 1986).

To address scaling issues in hydrological modelling many models have developed a GIS interface allowing for the incorporation of RS and GIS derived data into the modelling environment. Up until the early 1980s the fields of GIS and hydrological modelling had been developing in isolation of one another (Sui and Maggio, 1999), despite the fact that GIS and hydrological modelling are closely connected (Jain and Singh, 2003).

The hydrological system in most areas is quite complex and to have a sound understanding of these systems, rational analysis of all the influencing factors needs to be performed (Jain and Singh, 2003). For this purpose, large volumes of data from various sources are required, and RS is useful for generating such datasets (Gangodagamage, 2001; Easton *et al*., 2010; Khalil, 2017) whilst GIS provides a platform to manage, integrate, visualize, edit, manipulate, store and analyze such spatial datasets (Xu *et al*., 2001; Khalil, 2017).

Remote sensing (RS) and GIS can be integrated, as RS data are a major source of spatial information in GIS analysis and GIS data can be used to support RS data and for the interpolation therefore (Khalil, 2017). Advancements in GIS and RS allow for: widespread coverage at high resolution, large areas to be investigated over short time periods and at reduced costs, and improved spatial assessment and analysis (De Roo, 1996; Easton *et al*., 2010).

2.7 Water Balance

In hydrological research, and for water management, knowledge of the amount of water and change in water storage in a system is critical. Thus, tools for such application are of importance, such as the water balance equation which is the central equation used in studying hydrological processes (Hendriks, 2010). Overall, hydrological models account for, or allow for, the calculation of a water balance as part of the simulation run (Singh *et al*., 2017). The water balance provides a framework for studying the hydrological behaviour of an area and for identifying changes in the hydrological components as a result of hydrological processes (Hendriks, 2010). The components considered in the water balance equation, can be extensive or they can be an amalgamation to simplify the process (Harlow, 2018). Ultimately the water balance concept is used to determine whether all water inflows into the system are equal, or balance out, the water outflows. Water balance calculations incorporate both reservoirs and fluxes (DHI software, 2012). The water balance method was first used by Thornthwaite and Mather (1957; Equation 2.1). Since its introduction the equation has undergone alterations and revisions to improve performance and refine parameters (Harlow, 2018), however the simplistic notion originally developed by Thornthwaite and Mather (1957) still holds true (Zhang *et al*., 1999). For water management purposes, the water balance is an important tool for estimating water management effects such as those related to LUCC and climate change (Hendriks, 2010).

$$P = ET + Q + R + \Delta S$$

Equation 2.1: Water balance model (Thornthwaite and Mather, 1957).

Where P is precipitation, ET is evapotranspiration, Q is surface runoff (streamflow), R is groundwater recharge and ΔS is the change in soil water storage.

2.7.1 Precipitation (P)

Precipitation is the largest water inflow into an area and comprises all atmospheric water entering the system inclusive of both liquid (rainfall) and solid (snow or hail) water particles (Hendriks, 2010). Precipitation is both spatially and temporally variable (Pohl *et al*., 2017). In hydrological modelling and water balance calculations rainfall and snow are dominant precipitation measures (Bergström, 1992; DHI software, 2012). Less conventional precipitation measures, including fog and other horizontal precipitation, are not commonly measured with conventional rain gauge instruments, and are often not included in hydrological modelling and water balance calculations (Scholl *et al*., 2010).

2.7.2 Evapotranspiration (ET)

Evaporation is the change of water in a liquid or solid state into water vapour and involves the movement of water into the atmosphere (Hendriks, 2010). Transpiration (E_t) accounts for the movement of water within a plant and the conversion of, and/or loss of, water in the form of water vapour through the stomata in plant leaves (Hasenmueller and Criss, 2013). Evapotranspiration (ET) is the combination of all evaporation and E_t from an area and can be sub-divided into different components including: evaporation from soil, evaporation from intercepted storage, E_t, and evaporation from surface ponded water (Savenije 2004; Hendriks, 2010).

Outside of precipitation, ET is typically the largest component of many ecosystem water balances (Zhang *et al*., 2001). Globally, approximately 57% of all precipitation on land evaporates or transpires and in warm, dry climates this value increases up to approximately 96% (Hendriks, 2010). Evapotranspiration (ET) thus constitutes an important component of the hydrological cycle and water balance (Hasenmueller and Criss, 2013; Zou *et al*., 2017). The average ET in South Africa, recorded over the period 2000 – 2012, was estimated to be 303mm.a^{-1} (Jovanovic *et al*., 2015). This amount comprised mostly of E_t (53%) and of E_s (39%; Jovanovic *et al*., 2015).The average rainfall in South

Africa amounts to approximately 450mm.a^{-1} (Jovanovic *et al.*, 2015). Thus ET accounts for approximately 67% of rainfall over South Africa. There exist different types of ET: potential, actual (ET_A) and reference (ET_{Ref}; Hendriks, 2010). Potential evapotranspiration is the maximum ET rate (mm.day^{-1}) that can occur, whilst ET_A is the amount (mm.day^{-1}) that occurs under the existing environmental conditions of an area (Hendriks, 2010). The ET_{Ref} is the potential ET rate (mm.day^{-1}) of an idealized grass crop that serves as a reference value for other crops (Hendriks, 2010; Zotarelli *et al*., 2015).

Evapotranspiration (ET) is difficult to directly measure and the issues that surround calculation accuracy are generally related to the calculation techniques used (Zotarelli *et al*., 2015). Generally, conventional methods of lumping ET measures (all evaporation and E_t are lumped together) tend to underestimate ET. For example, Gwate *et al*. (2018) compared the performance of two Penman-Monteith ET models in accurately modelling ET in South Africa. The study found the Penman-Monteith-Leuning (PML) model performed better than the Penman-Monteith-Palmer (PMP) model, as the former incorporates both E_t and E_s, whilst the later only incorporates E_t (Gwate *et al*., 2018) Evaporation from interception (E_i) is often under-represented and this is a concern given that E_i contributes a considerable proportion of total ET (Savenije, 2004). For example, Calder (1990) explored E_i, in upland forest catchments in the United Kingdom, and found that E_i amounts to 35% in areas receiving 1000 mm of rainfall per annum and up to between 40 – 50% in areas receiving between 500 – 600mm of rainfall per annum. A further concern with the estimation of ET is spatial heterogeneity. Evapotranspiration (ET) is spatially affected by land cover (vegetation type), soil hydraulic properties and subsurface storage of moisture (Zhang *et al*., 1999). Within plant communities, the type, structure, abundance and geographic location of the vegetation can have significant impacts on the rate of ET (Zhang *et al*., 1999; van Dijk and Keenan, 2008).

2.7.3 Surface runoff and streamflow (Q)

Surface runoff and streamflow originate when the capacity for the land surface to store water is overcome. This occurs once I_{UZ}, evaporation and interception have all taken place (Hendriks, 2010).

Water will flow as OL or surface runoff once both CI capacity and surface storage capacity have been reached (Hendriks, 2010). Surface runoff will generally show good correlation with annual rainfall, particularly in areas with winter dominant rainfall (Zhang *et al*., 1999). When surface runoff makes its way into streams, rivers or other terrestrial water bodies it becomes known as streamflow (Hendriks, 2010). Streamflow is an important aspect of the water balance and the water cycle as streams are a major source of freshwater for humans, animals, plants and the natural ecosystem (Oyebode, 2014). Thus, prediction of streamflow, both in the short- and, long-term, are critically important forming the basis upon which water managers, consumers, policy makers and other stakeholders put in place plans and adaptive strategies for the allocation and control of water resources (Oyebode, 2014).

2.7.4 Recharge (R)

Recharge is the amount of infiltrated water that leaves the bottom of the soil zone and becomes part of the saturated groundwater zone (Zhang *et al*., 1999; Harlow, 2018). The calculation of recharge is dependent on many physical factors including: LULC, climate, geology, snowmelt and soil type (Jyrkama and Sykes, 2007; Harlow, 2018), all of which impact on the determination of recharge rates and thus recharge rates are highly variable, ranging from less than 10 mm to multiple metres per year (Harlow, 2018). Determination of GR is important for developing and monitoring groundwater management strategies and for determining the impacts of climate change and urbanization on groundwater aquifers (Jyrkama and Sykes, 2007). This is particularly important in areas where the underlying aquifers are vulnerable to abstraction, contamination or exploitation (Jyrkama and Sykes, 2007).

Extensive research into GR has been undertaken in Western and south-eastern Australia, as summarised by Scott and Le Maitre (1998). The summary showed that with a change in vegetation coverage from Banksia shrubland to *Pinus radiata* plantation that recharge as a percentage of rainfall declined from 25 – 7%. Similarly with a change in vegetation from native grassland to *P. radiata* there was a decline in GR from 63 – 0 mm (Scott and Le Maitre, 1998). Numerous studies into groundwater recharge have also been undertaken in South Africa (Scott and Le Maitre, 1998). In a

study by Kok (1976) a wattle plantation in Pietermaritzburg was found to have a groundwater recharge of approximately 7%. This is lower than that expected for the area (approximately 10%) due to the exchange of native vegetation for wattle plantation (Kok, 1976).

2.7.5 Change in soil water storage (ΔS)

A significant percentage of precipitation infiltrates to become stored soil water (Hendriks, 2010). The soil water storage is the total amount of water stored in the soil within the rooting zone of plants (Reichardt *et al*., 2013). Soil water, in the hydrological cycle, is dynamic, being either returned to the atmosphere by plant E_t and evaporation or moving into lower levels to become groundwater (through recharge; Saxton and Rawls, 2006). Understanding the characteristics of the soil properties is necessary to determining soil water storage and the change thereof. This is emphasised by Yates *et al.* (1989), who explain that an understanding of the basic soil hydraulic properties (particularly unsaturated hydraulic conductivity) is essential in accurately determining, flow, water movement and water storage potential.

2.8 Land use and/or land cover change (LUCC) and hydrology

The hydrological components that collectively determine the hydrological response of an area are both spatially and temporally heterogeneous. These components are dependent on, and are determined by, a range of characteristics including topography, soil, geology and LULC (Isik *et al*., 2013). Spatially, all of these characteristics differ, thus creating a unique spatially heterogeneous hydrological response. Temporally, LULC readily undergo changes, while geology, topography and soil types generally tend to remain the same over time, or changes to these aspects may be dependent on LUCC (Zhang *et al*., 1999). For example, Vanclay (2009) explained how plantation establishment involves actively modifying the soil to improve I_{UZ} and reduce runoff and these changes affect site hydrology including base flow and channel flow. Similarly, Zhang *et al*. (2018) found LUCC to indirectly modify soil layers.

The causes of LUCC are complex and can result from both natural and anthropogenic activities (Lambin *et al*., 2001, 2003; DeFries and Eshleman, 2004). Naturally, LUCC can be driven by climatic related changes or natural disaster (Lambin *et al*., 2003; Shi *et al*., 2007), while anthropogenically, LUCC can be driven by increased need for natural resources for: food, fuel, fibre, building materials, and by human settlement expansion (Lambin *et al*., 2003 DeFries and Eshleman, 2004). These anthropogenic drivers lead to activities such as the establishment or expansion of agricultural practices, urbanisation, plantation forestry and afforestation (Isik *et al*., 2013). A study by Gyamfi *et al*. (2016) investigated the hydrological impacts of LUCC on the Olifants catchment in South Africa. The results revealed that from 2000 – 2013 there was a 31.6% decrease in savanna, a 20.1% increase in agriculture lands, 10.5% increase in urban areas and a 0.7% increase in forest, which led to a 46.97% increase in surface runoff generation (Gyamfi *et al*., 2016). Furthermore, the study revealed that urbanisation was the greatest contributor to increases in surface runoff generation, water yield and ET (Gyamfi *et al*., 2016).

Land cover is defined by the biophysical condition of the Earth's land surface and the immediate subsurface, including biota, soil, topography, surface water, groundwater and anthropogenic structures (Lambin *et al*., 2003; Warburton *et al*., 2012; da Silva *et al*., 2018). Those human activities that are related to the soil are called land use (da Silva *et al*., 2018). Land cover is described in terms of broad categories such as grassland, cropland, natural or plantation forestry and human settlements (Warburton *et al*., 2012). Land use and/or land cover (LULC), and LUCC, impact on hydrological components and processes, including: CI, I_{UZ}, ET, surface runoff, streamflow (Fohrer *et al*., 2001; DeFries and Eshleman, 2004; Hasenmueller and Criss, 2013; Zhang *et al*., 2018) and GR (DeFries and Eshleman, 2004; Warburton *et al*., 2012; Isik *et al*., 2013). Land use and/or land cover change (LUCC) impacts on soil hydrological characteristics such as preferential flow paths, saturated hydraulic conductivity (Ksat), macropore connectivity, root mass and water retention (Christiaens and Feyen, 2001; Toohey *et al*., 2018).

The impact LUCC has on catchment hydrology is dependent on a number of factors, including the degree of modification, conversion and/or maintenance of the natural landscape, the intensity of the changes, and the location of the LUCC within an area (Warburton *et al*., 2012). The interactions between water and LUCC, within an area, vary spatially, as water fluxes within a system move both vertically (e.g. ET) and laterally (e.g. through soils, aquifers and rivers; Warburton *et al*., 2012). For example, the impact of LUCC on groundwater recharge was investigated in the upper Berg catchment, Western Cape, South Africa (Albhaisi *et al*., 2013). It was found that with the clearing of alien hill slope vegetation upstream of the Berg River Dam that there was an approximate 8% per annum increase in groundwater recharge over the 21 year (1984 – 2004) period investigated *(*Albhaisi *et al*., 2013).

The positioning of LULC in a landscape is important in modulating the effects of scale in the system (Blöschl *et al*., 2007). This was shown by Toohey *et al*. (2018), who considered nested catchments where sugarcane land cover was nested within a forested catchment. The study observed that the forest site was able to re-infiltrate sugarcane runoff. A conclusion drawn was that woody based LULC positioned below runoff prone LULCs can assist in mitigating both flooding and reduction of GR (Toohey *et al*., 2018). Similarly, the location and spatial design of tree plantings can influence streamflow generation (van Dijk and Keenan, 2008). A study by Vertessy *et al*. (2003) suggested that as the location of tree plantations has an influence on streamflow, planting trees on upper slopes can have less of an impact on streamflow than planting on lower slopes, in particular in water-stressed landscapes.

Zoning of plantations away from streams and drainage lines is common practice in many countries and it is believed to reduce the overall impact of trees on water resources (Richardson *et al*., 2012). A study conducted in the Western Cape, South Africa, by Dzikiti *et al*. (2013), found that pine (*Pinus pinaster* and *Pinus halepensis*) stands growing in riparian zones use at least 36% more water than those growing in non-riparian areas. Riparian zones form the ecological boundary (ecotone) between terrestrial and aquatic ecosystems and are important for regulating the movement of water, solutes and

other materials through the catchment (Burt *et al*., 2002). Riparian zones play an important role in moderating the effects of upland land management activities through nutrient sequestration, filtering of sediment and other materials, and changing water uptake (Clinton, 2011). Given their topographic location and sedimentary structure, most riparian zones are characterised by high water tables (Burt *et al*., 2002), and thus have historically provided a favourable environment for forestry plantation establishment (Richardson *et al*., 2012). The general characteristics of riparian zones often include anoxic conditions, high organic matter content and low hydraulic conductivity (Jencso *et al*., 2009).

Changes to LULC alter the dominant vegetation communities in an area and impact upon the hydrological response of that area (Legesse *et al*., 2003; De Fries and Eshleman, 2004; Warburton *et al*., 2012). For example, comparing grassland to forested land (native or plantation forestry), forests tend to have higher rates of ET than grassland, resulting in lower rates of surface runoff and streamflow (Scott *et al*., 1998; Vertessy, 2001; Zhang *et al*., 2001; Everson *et al*., 2011). In a Study by Everson *et al*. (2011) it was found that measurements of ET_A from different vegetation types showed that annual water use is strongly related to the proportion of the year in which a dense canopy of transpiring leaves is maintained. Therefore, evergreen vegetation such as plantation forests of alien tree species exhibit a relatively high annual ET_A when compared to grasslands and deciduous trees of a seasonal nature that only maintain their transpiring canopy during the warmer summer months (Everson *et al*., 2011).

Water scarcity is an important issue that needs to be addressed by taking precautions in highly water-demanding activities such as commercial forestry and agricultural plantations (Dye and Versfeld, 2007). Plantations are typically mono-cropped areas of homogeneous vegetation coverage, comprising perennial crops, that require quick, well-timed initial processing and for which there is an export market (Hartemink, 2005). The term plantation is also used in forestry: timber plantations, plantation forests or forest plantations. Commercial forests (forest plantations) are man-made and are artificially cultivated through planting or sowing (Hartemink, 2005). Some of the concerns of mono-cropped and rotation plantations include: the export and depletion of nutrients (particularly nitrogen

and phosphorus), depletion of soil organic matter, soil erosion and soil compaction, reduced biodiversity and pest or disease outbreaks (Bauhus *et al*., 2004).

2.8.1 Sugarcane plantation

Sugarcane is an important plantation crop with the extent of plantation increasing considerably in recent decades (Hartemink, 2005). Sugarcane growth is favoured in tropical and subtropical regions of the world (da Silva *et al*., 2013), with Brazil currently the country contributing the most to global sugarcane production, producing approximately 39% of the global production as of 2012 (Cabral *et al*., 2012; Jorrat *et al*., 2018; Silalertruksa and Gheewala, 2018). As of 2012, sugarcane production accounted for approximately 29% of the total world crop production with 1.8 billion tonnes produced from more than 100 countries (Jorrat *et al*., 2018; Silalertruksa and Gheewala, 2018). Between the period 2005 – 2015 sugarcane plantation extent increased by 3% per year, to approximately 1.65Mha in 2016 (Jorrat *et al*., 2018). The increase can be attributed to improved agronomic practices (Hartemink, 2005). In South Africa the area under sugarcane production is approximately 400,000ha (Schmidt *et al*., 1998). Sugarcane is a favoured crop due to its high biomass (Silalertruksa and Gheewala 2018) and is used in a range of food and other essential products including: sugar, ethanol and bio-fuel production (Jorrat *et al*., 2018; Silalertruksa and Gheewala 2018). Among the crops used for bio-fuel production, sugarcane has one of highest renewable energy outputs and bio-energy yields (Cuadra *et al*., 2012).

Sugarcane is usually harvested 12 to 24 months after planting (Cabral *et al*., 2012). Following the first harvest, crop stubble is not removed and the new crop will re-grow from the remaining stubble (this is known as a ratoon crop). Generally, a sugarcane crop can be harvested up to six times (i.e. six ratoons) before the decline in yield is uneconomical and the crop needs to be replanted (Cabral *et al*., 2012; Cuadra *et al*., 2012).

Sugarcane growth, and the expansion of sugarcane cultivation, can have a range of environmental impacts on land, water and the atmosphere, such as through green house gas emissions (Silalertruksa

and Gheewala, 2018). The environmental impacts, related to sugarcane production, are dependent on a number of factors including: soil condition, amount and intensity of rainfall, degree of water stress, agricultural practices in the landscape, sugarcane productivity and the phenological stage of production (da Silva *et al*., 2013; Silalertruksa and Gheewala, 2018). Generally in the early phases of sugarcane growth, less biomass results in less CI, more surface runoff, and more soil erosion (da Silva *et al*., 2013). As sugarcane growth progress, and aboveground biomass increases, so throughfall and interception patterns are altered and more water is transpired or evaporated from interception (da Silva *et al*., 2013).

Climate is one of the most significant environmental limitations on sugar-cane production and particularly water availability is the major cause of inter-annual yield variation of sugarcane growth (da Silva *et al*., 2013). In Australia and South Africa, approximately 60 and 40% of sugarcane crops, respectively, are dependent on some form of irrigation (Inman-Bamber and Smith, 2005). Water used or required by sugarcane is predominantly determined by energy exchanges at the cropped surface and internal energy gradients through the soil, vegetation and atmosphere (Inman-Bamber and Smith, 2005). Evapotranspiration (ET) from sugarcane is far (about 100 times) greater than the amount of water retained by the crop (Inman-Bamber and Smith, 2005).

2.8.2 Plantation forestry

Globally, natural forest cover is declining rapidly due to increased human expansion and agricultural practices (van Wilgen *et al*., 2012). This is of concern as forests provide a number of important ecosystem goods including paper pulp, industrial wood and fuel wood (Bruijnzeel, 2004; van Wilgen *et al*., 2012). They also provide a number of important services including: improving the biological, chemical and physical quality of soils, improving soil fertility, and improving soil I_{UZ} (Buytaert *et al*., 2007), serving as wind breakers, and reducing soil erosion, by binding and securing soil particles (Pimentel, 2006). In addition, in considering global climate change, forests provide a means for carbon sequestration (Rangan *et al*., 2010); and serve as an important tool in phytoremediation and extraction or containment of chemical or other contaminants in soil and water resources (Dye and

Weiersbye, 2010). The global decline in forests has given rise to efforts to replenish, or alleviate the impact on, these natural ecosystems through afforestation and reforestation programmes (van Dijk and Keenan, 2008). Forest plantations play a role in offsetting the pressure and negative impacts on natural forests (Payn *et al*., 2015). To meet future demands and to supply all of the world's timber and fibre and offset the impacts of deforestation on wood supply, a 2.4% increase in global forestry plantations would be required (WWF and IIASA, 2012).

Despite the positive attributes and demand on forestry, there are many negative environmental aspects hindering plantation establishment such as: the introduction of exotic species (Versfeld *et al*., 1998; van Wilgen *et al*., 2001; Le Maitre *et al*., 2002), excessive water use (Bruijnzeel, 2004; Dye and Versfeld, 2007; van Dijk and Keenan, 2008; Forrester *et al*., 2011; Warburton *et al*., 2012; Payn *et al*,, 2015), and reduced dilution of water pollutants leading to reduced water quality (Van der Walt *et al*., 2004; Chamier *et al*., 2012). Plantation forestry favours the selection of exotic species for their competitive growth advantages over indigenous species, such as fast growth rate, high productivity and high biomass (Versfeld *et al*., 1998; van Wilgen *et al*., 2001; Le Maitre *et al*., 2002; Chamier *et al.*, 2012). Alien invasive species are non-indigenous and able to survive, reproduce and spread at rapid rates across the landscape (van Wilgen *et al*., 2001). This is problematic as most of the impacts associated with the spread of invasive species from plantations are negative (Le Maitre *et al*., 2002), detrimentally affecting the invaded system (Van der Walt *et al*., 2004) and threatening the integrity of ecosystems. They change ecosystem structure, function and composition affecting conservation initiatives, biodiversity, delivery of ecosystem services (van Wilgen *et al*., 2012) and alter fire regimes (Chamier *et al.*, 2012). Eucalypts, acacias and pines are among the most widely planted exotic tree genera globally (Bauhus *et al*., 2000).

Plantation forests and their successive establishment are detrimental to water quantity (Vertessy, 2001). There is a plethora of literature on the impacts of forestry plantation on water quantity (Calder *et al*., 1997; Bruijnzeel, 2004; Siriwardena *et al*., 2006; Dye and Versfeld, 2007; van Dijk and Keenan, 2008; Vanclay, 2009; Forrester *et al*., 2011; Warburton *et al*., 2012; Payn *et al,*, 2015; Zhang

et al., 2017; da Silva *et al*., 2018). A general conclusion is that forestry removal increases runoff and streamflow, and plantation establishment decreases runoff and streamflow (Bruijnzeel, 2004; Zhang *et al*., 2017). In a study by Sahin and Hall (1996), it was found that for every 10% increase in forest cover, annual water yield decreased by between 20 – 25mm in coniferous forest, and by between 17 – 19mm in deciduous forest cover. Another study showing the impact of forestry on water use was conducted by Calder *et al*. (1997), who found the water use of forest (*Eucalyptus* sp.) to be approximately twice that of a commonly grown annual agricultural crop (*Eleusine coracana*). However, despite the extensive literature on this topic, there is still controversy around the hydrological impacts of forest plantations, due to the numerous interconnected site specific conditions that impact on the hydrological process, that lead to different responses to forest plantation establishment, and as such there is still much needed research on the spatial and temporal patterns of tree water use (Dye *et al*., 2004).

In South Africa plantation forests tend to have higher rates of ET than native vegetation as these plantations are evergreen, deep-rooted, and maintain a relatively high green leaf area index over the entire year. Whilst the natural vegetation that plantation forestry replaces comprises mostly of seasonally dormant grasslands or fynbos shrublands which greatly limits their evapotranspiration over the dry season (Dye and Versfeld, 2007). Annual ET from natural vegetation prior to replacement by plantation forestry ranges from 700 – 900mm, whilst ET from forest plantations ranges from approximately 1100 – 1200mm (Dye and Versfeld, 2007). According to Bosch (1979), the differences in ET between natural pre- forestry plantation vegetation and forestry plantation is largely a result of seasonal differences in green leaf area.

In a study conducted in Australia (Vertessy, 2001), pine plantations were found to have higher ET rates than indigenous eucalypt forests and cause a greater decrease in annual runoff. Mean annual runoff was reduced by up to 165mm under eucalypt forest and up to 210mm under pine plantations (Vertessy, 2001). The converse was found to be true in South Africa, where data indicated that ET rates from eucalypt plantations almost always exceeded those from pines (Scott and Smith 1997).

Another study conducted by Versfeld *et al*. (1998) found acacia species to be the most pervasive invader in South Africa in terms of water use, accounting for approximately 30% of the total invader water use – the species of particular concern for water resources were *A. mearnsii* and *A. dealbata*. In terms of water use, *Acacia* spp. were followed by *Eucalyptus* spp. and *Pinus* spp. both of which accounted for less than 20% of the total invader water use in South Africa (Versfeld *et al*., 1998). Thus, different plantation species have different impacts on water resources as a result of physiological differences, differences in rooting depth (RD) or leaf area and depending on location (van Dijk and Keenan, 2008). Physiological differences in plantation canopy structure can have an influence on rainfall interception and therefore affect the entire water balance (Zhang *et al*., 1999; van Dijk and Keenan, 2008). According to van Dijk and Keenan (2008) evaporation losses from intercepted water is usually less for deciduous forests than for needle leaf forests particularly in areas receiving rainfall in winter.

The relationship between plantation forestry and water quantity is further complicated by plantation age (Farley *et al*., 2005; Rosenquist *et al*., 2010). For example, Rosenquist *et al*. (2010) found that from four plantations of common oak and Norway spruce interception rates increased considerably and water recharge declined during the first 30 – 40 years after planting. In older stands (40 – 90 years old) interception and water recharge both stabilized and water recharge started to show signs of recovery toward the pre-afforestation level (Rosenquist *et al*., 2010). This is a concern as plantation stands are generally harvested before they start to decline in growth and before water recharge declines, whilst natural forests are left to mature allowing for water recharge to stabilize (Vanclay, 2009).

Seasonally, plantation forests will have different impacts on water quantity, resulting in changes in the seasonal distribution of runoff and changes to the timing and magnitude of peak flows (Vertessy, 2001). The impacts of plantation forestry on water resources are particularly of concern in areas where water resources are already under pressure and where further growth is increasingly constrained by water availability (Dye and Versfeld, 2007; Ashton *et al*., 2008). Under such

conditions, it may not be surprising that any activity that can lead to a potential reduction in water resources is met with opposition (Ashton *et al*., 2008), such as plantation forestry. This is of particular relevance and concern for water-limited countries such as South Africa.

2.8.2.1 South African plantation forestry

South Africa receives an average annual rainfall of around 450mm, whilst the global annual average is approximately 860mm (Claassen, 2010). Together with this, the average potential evaporation rate exceeds that of the Mean Annual Precipitation (MAP) rate indicating a net deficit in water supply. These water challenges are exacerbated by high temperatures (mean temperature >17˚C; King *et al*., 2011). Commercial forestry plantations in South Africa have reduced surface runoff by approximately 1.4 billion $m^3.y^{-1}$, or 3.2% at a national scale (Gush *et al*., 2002; Le Maitre *et al*., 2002). Water is the primary resource in South Africa that will ultimately limit development and thus the efficient management and allocation of water resources is of national importance (Le Maitre *et al*., 2002).

In South Africa, natural forests cover a limited extent of the country; one of the main reasons for this is repeated fires that prevent forest species from establishing or growing beyond the 'fire-prone-zone' (Le Maitre *et al*., 2002). Natural forests cover less than 0.25% of the South African landscape (Le Maitre *et al*., 2002). This figure is slightly less than that estimated by the National Forest Inventory as indicated by the Department of Agriculture, Forestry and Fisheries (DAFF; DAFF, 2012a), estimating the extent of natural forest cover to be approximately 495666ha of South African land (approximately 0.4% of the landscape). Although these estimates differ, they both demonstrate the small contribution natural forests make to total land coverage in South Africa, which has led to the country's dependence on exotic forestry plantations to meet its timber needs (Le Maitre *et al*., 2002). Up to 2007, there has been a steady growth in the total area of forest plantation, leading to an estimated 1.5 million hectares spread over the higher-rainfall regions of the country (Dye and Versfeld, 2007). Plantation forests in South Africa are usually managed over short rotations for pulpwood or mining timber and comprise predominantly of *Pinus* species, *Eucalyptus* species, and *Acacia* spp. (du Toit *et al*., 2010; van Wilgen, 2015). *Pinus* spp. plantations cover approximately 660,000ha (van Wilgen,

2015), *Eucalyptus* spp. plantations cover approximately 540,000ha of land, of which *Eucalyptus grandis* alone covers more than 300,000ha (du Toit, 2008). *Acacia* plantation species cover approximately 100,000ha of land in South Africa (du Toit *et al*., 2010).

The first forest plantations of exotic trees were established in South Africa in 1875 (Dye and Verfeld, 2007). Shortly after establishment concerns over the effects of these forest plantations on streamflows and catchment water yields started to arise (Dye and Versfeld, 2007). These concerns were comprehensively debated during the Empire Forestry Conference, held in South Africa in 1935 (Dye and Versfeld, 2007). From this conference a decision was taken to establish a number of long-term paired catchment experiments in numerous forestry catchments throughout South Africa in order to study the impacts of plantation forestry on streamflow and catchment water yields (Scott *et al*., 2000). These initial paired catchment studies coupled with other further research into the forestry plantation impacts on catchment hydrology have provided valuable insights for plantation managers, ecologists and policy makers (Dye and Versfeld, 2007). Since the inception of these initial catchment studies, the data collected have been analysed and summarised by various researchers over the years (Bosch, 1979; Van Wyk, 1987; Scott *et al*., 2000) and the findings have led to the regulation of the expansion of the forestry industry, due to the impacts on water resources (as of 1972; Scott *et al*., 2000).

Following the 1994 democratic elections in South Africa, which brought about a shift in governance from the Apartheid regime, there came about a reform of national legislation including a change in water policy (Tewari, 2009). The new National Water Act (NWA, Act no. 36 of 1998) was adopted and introduced a shift in previous thinking (Tewari, 2009). One such shift was the classification of forestry plantation as a "Streamflow Reduction Activity" (SFRA; Scott *et al*., 2000; Dye and Versfeld, 2007). As such plantation forestry is highly regulated, requiring forestry owners to pay tariffs based on estimated water usage and to attain licenses to plant new trees for commercial forestry purposes (Kruger and Bennett, 2013). These restrictions imposed on forestry were largely driven by the outcomes of the initial paired catchment studies conducted on forestry and catchment hydrology that identified plantation forestry as a major water user (Jacobson, 2003). To date plantation forestry

is the only land use to be classified as a streamflow reduction activity and as such is a contentious issue for plantation owners, as other plantation crops have not been included (Gush *et al*., 2002; Dye and Versfeld, 2007). According to Dye and Versfeld (2007), the only other activity that could be listed as a 'Stream Flow Reduction Activity' is sugarcane, which is believed to use approximately half as much water as plantation forestry (Dye and Versfeld, 2007). In a study by Jewitt *et al*. (2009), that aimed to improve the national estimates of water use by declared and candidate SFRAs, it was found that, in the inland growing regions, sugarcane is a substantial water user and has a significant impact on available water resources. Thus, in some of the catchments explored, sugarcane could be considered for declaration as a SFRA (Jewitt *et al*., 2009).

The plantation forestry species of greatest importance in South African are pines (*Pinus* spp.), wattles (*Acacia* spp.) and gum trees (*Eucalyptus* spp.; Versfeld *et al*., 1998; van Wilgen *et al*., 2001; Le Maitre *et al*., 2002) all of which are major invaders in the country, spreading their negative impacts far beyond their respective afforested areas (Le Maitre *et al*., 2002). Invasive alien plants have reduced river flows in South Africa by approximately 6.7% (Versfeld *et al*., 1998). Görgens and van Wilgen (2004) found a reduction in the long-term mean annual runoff to range between 100 – 300mm.yr^{-1} for plantations of pine, wattle and eucalypts. Similarly, according to Dye and Jarmain (2004) annual total evaporation from indigenous grasslands and fynbos shrublands in South Africa varies over a relatively narrow range of 600 – 850mm, but once invaded by black wattle (*A. mearnsii*), the total evaporation can increase by as much as 600mm.

The KwaZulu-Natal province supports one of the largest extents of plantation forestry in South Africa, covering an area of approximately 500,000ha (as of 2011). From 2008 – 2011 this region has experienced an increase of approximately 17,000ha of plantation coverage (DAFF, 2012b). The dominant species and genera planted in KwaZulu-Natal are *Eucalyptus* spp. and *Acacia* species. More than 80% of the total wattle plantations in South Africa occur in KwaZulu-Natal. Out of all South African provinces KwaZulu-Natal has the largest number of people dependent on the forestry industry, approximately 300,000 people including both workers and dependents (DAFF, 2012b).

Since 2005/2006 KwaZulu-Natal experienced the largest increase in new afforestation while all other provinces appear to be experiencing substantial decline in new afforested land in relation to the pre 2005/2006 period (DAFF, 2012b). This is predominantly due to the small afforestation potential of South Africa, where only few provinces, KwaZulu-Natal and the Eastern Cape, have the potential to expand afforestation to new areas (DAFF, 2012b) Within KwaZulu-Natal, the Natal Midlands located between the Drakensberg and the South Coast of South Africa is a region extensively used for plantation establishment with both forestry and sugarcane prevalent (Mucina and Rutherford, 2006).

The Two Streams catchment falls within the Natal Midlands and is a key catchment in advancing the knowledge around the impacts of plantation forestry (and potentially sugarcane plantation into the future) on water. Two streams has been operating as a hydrological research catchment for decades and due to the extensive research undertaken (discussed further under section 3.3), this catchment can play a valuable role in informing policy around SFRAs and around the impact different land covers have on the hydrological components of a catchment. This study will look to compare the hydrological impact of riparian vegetation, sugarcane plantation and forestry plantations on hydrological characteristics of the site. It is expected that the hydrological impacts will not be as different between forestry and sugarcane as between forestry and riparian vegetation given that both sugarcane plantations and forestry plantations are recognised as heavy water use (Dye and Versfeld, 2007; Jewitt *et al*., 2009).

2.9 Scaling in land use and/or land cover (LULC) and hydrology studies

To understand the complexities and dynamic nature of the hydrological cycle, research tends to focus on smaller catchments, which allow for knowledge and data to be gathered at a more manageable and practicable scale of understanding and complexity and because reliable data are often only available at a smaller scale (Trenberth *et al*., 2006). Larger catchments or basins tend to have more complications preventing consistent conclusions with smaller catchments, due to the heterogeneity of variations experienced in the landscape such as variations in LULC classes, variations in vegetation phenology

and spatial and temporal variation in rainfall (Siriwardena *et al*., 2006). Modifications in LULC are easily measured at a small catchment scale, whilst at a larger catchment or basin scale it becomes difficult to differentiate the effects which individual LULC changes have on hydrological responses (Warburton *et al*., 2012). Thus, the accumulated effects of LULC on the hydrological system are most easily identified at the smaller catchment scale (Warburton *et al*., 2012). This is particularly problematic in implementing water resource management at a large catchment scale based on the extrapolation of small scale catchment findings, as these findings may be misleading (Zhang *et al*., 2017). Another concern with scale is that certain LULCs do not immediately alter the hydrological response of a catchment as there may be a time lag between the LUCC and its effect on the water balance (Blöschl *et al*., 2007).

When determining whether scale is a problem in macro-scale or meso-scale modelling one needs to consider the purpose of the modelling study, the modelling software employed and the scientific approach taken (Bergström and Graham, 1998). The expansion to macro-sized catchments in physically-based modelling is difficult due to the spatial and temporal variability in a larger catchment and the great number of data inputs required (Bergström and Graham, 1998). Conceptual models are more suited to large scale modelling given that the large catchment can be considered as an accumulation of many smaller catchments/areas, and can thus be sub-divided (Bergström and Graham, 1998).

2.10 Conclusion

Human-environmental systems are complex and adaptive and factors in these systems, such as LULC and soils, are derived from the interactions among the various components of the entire systems (Lambin *et al*., 2003). Predicting the future behaviour or state of these systems is challenging and often not possible due to the emergent and dynamic rather than predetermined nature of these systems (Lambin *et al*., 2003). However, models, although they may not provide the complete picture of reality, do provide a means of understanding the current system and predicting the future system.

Thus, such means allow for the analysis and understanding of the impacts of LULC and LUCC on the hydrological system and processes of an area and serve as a useful and, at times, critical tool for planning the management of water resources (Forrester *et al*., 2011; Toohey *et al*., 2018).

Chapter Three

Study site

3.1 Introduction

This chapter describes the study site, providing details on the climatic, soil and vegetation characteristics. This study is focused on a sub-catchment, within the larger Two Streams catchment. The name 'Two Streams' is derived from the two streams that flow through it. Even though the sub-catchment only has one of the streams flowing through it, for ease of reference the study site is still referred to as the Two Streams sub-catchment. The study site boundary for this dissertation was unknown and had to be delineated (described under section 4.3.2); as such the true extent of the sub-catchment was unknown and so the study site description makes more mention of the Two Streams catchment rather than the sub-catchment. The research history section addresses the previous WRC studies undertaken at the Two Streams site and the key findings that relate to this dissertation.

3.2 Study site description

The study site was a sub-catchment to the larger Two Streams catchment located outside of Greytown and approximately 70 km from Pietermaritzburg in the KwaZulu-Natal midlands (30.67^{o} E; 29.19^{o} S; Figure 3.1). The Two Streams catchment is situated in the Mistley-Canema Mondi forestry estate and comprises two sub-catchments (Figure 3.2). The Two Streams catchment serves as a long-term hydrological research catchment with experiments on-site having been conducted since the late 1990s (Everson *et al.*, 2006; Clulow *et al.*, 2011) and thus has provided a good opportunity to extend the understanding of hydrological processes in a commercial forestry catchment (Clulow *et al.*, 2011).

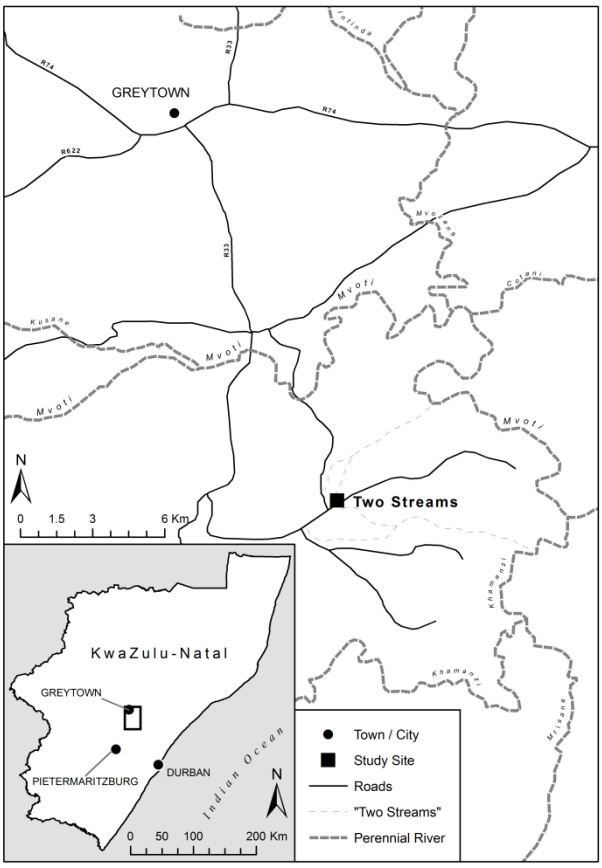

Figure 3.1: Locality of the Two Streams catchment in the KwaZulu-Natal midlands.

The Two streams sub-catchment is situated within the 'midlands mistbelt grassland' bioregion (Mucina and Rutherford, 2006) where commercial forestry is the most widespread land cover, with gum tree (*Eucalyptus* spp.), pine (*Pinus* spp.) and wattle (*Acacia* spp.) being the most common plantation species (Everson *et al*., 2006). In addition to commercial forestry, sugarcane is a prevalent commercial crop in the area grown on sites where drainage of cold air is good, ensuring that no frost or only light frost occurs (Everson *et al*., 2006). Prior to commercial forestry, the region was dominated by indigenous *Themeda triandra* grassland (Mucina and Rutherford, 2006). However, to-date only a few patches of the natural grassland remain due to the high potential of the land for agriculture and forestry and due to invasion of native 'Ngongoni' grass (*Aristida junciformis*; Everson *et al*., 2006).

The ‘midlands mistbelt grassland’ bioregion is typically associated with apedal and plinthic soil forms that are predominantly derived from the shale and sandstone of the Ecca Group (Mucina and Rutherford, 2006). The area is well suited to intensive farming systems and the agricultural potential of the soils is high, in spite of the fact that the inherent nutrient status is very low; with soils being highly leached (Mucina and Rutherford, 2006). Rainfall primarily occurs in summer with the annual rainfall ranging between 659 – 1139mm (Mucina and Rutherford, 2006), and is regarded as a high rainfall region of South Africa (rainfall > 700mm; Albaugh *et al*., 2013). However, in comparison to other areas worldwide, dominated by forestry plantations, this region is on the drier end of the spectrum (du Toit *et al*., 2010). The midlands are known to experience dense, frequent mist, which can add significantly to the amount of precipitation (Everson *et al*., 2006). The area is known to experience droughts, moderate frosts, hail and berg winds with the average number of heavy frost days ranging from 31 – 60 days per annum (Mucina and Rutherford, 2006).

The Two Streams catchment (Figure 3.2) comprises of three main land cover classes: plantation forestry, sugarcane (*S. officinarum)* plantation and riparian vegetation (comprising a mixture of indigenous and exotic species). The plantation forestry species include black wattle (*A. mearnsii*) and *Eucalyptus grandis*, with black wattle being the dominant plantation species in the catchment.

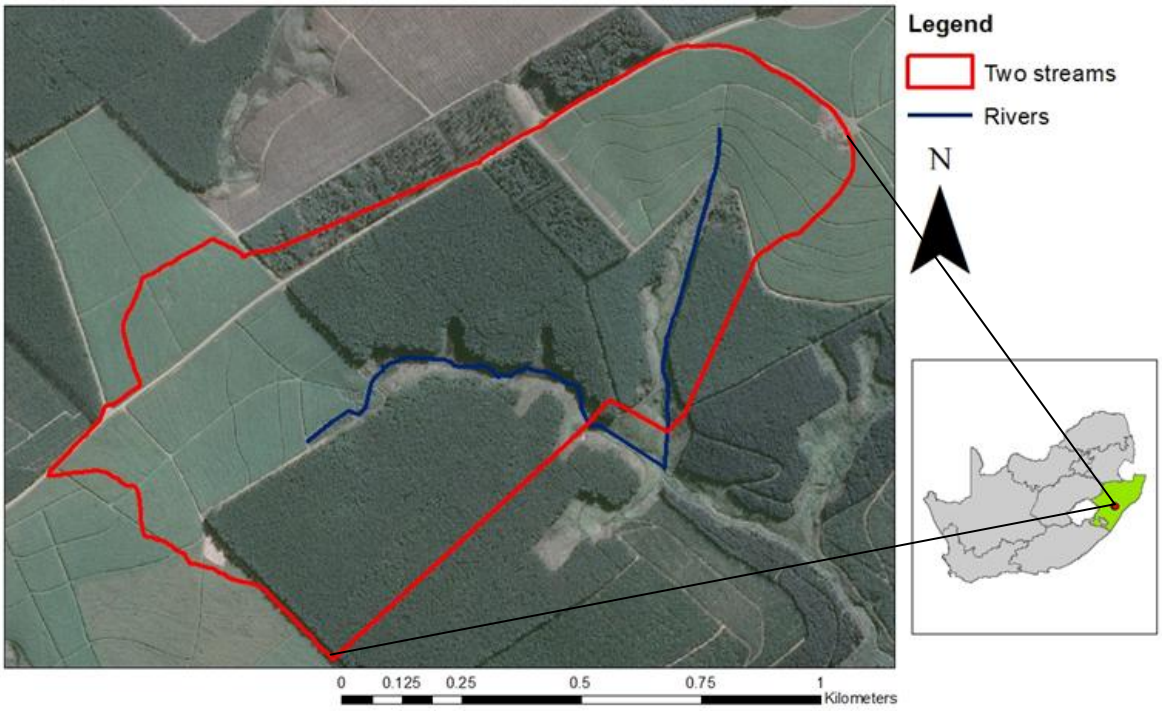

Figure 3.2: The Two Streams catchment, in which the study site of this project falls.

The black wattle (*A. mearnsii*) plantation was planted in June 2006 and harvested in February 2018. The sugarcane (*S. officinarum*) plantation is of the N48 variety and was planted in 2011. It is currently in its 3rd ratoon. The riparian vegetation comprises of a mix of species that have naturally arisen following forestry clearing from May – July 2000 (Clulow *et al*., 2011).

3.3 Research history at the Two Streams study site

The Two Streams catchment has been used as a research catchment, with research infrastructure and instrumentation being established on-site from the late 1990s (Everson *et al.*, 2006, 2014; Clulow *et al.*, 2011). Globally, there are few long-term catchment study sites, inclusive of studies focused on water balance components, such as the Two Streams catchment, and locally the site has provided a unique opportunity for long-term research on the impact of a commercial tree plantation on catchment hydrological processes (Clulow *et al.*, 2011). Previous studies at Two Streams provide a foundation from which the impacts of plantation forestry, and other land-uses, on hydrological properties could be assessed and have provided an excellent platform to extend these catchment studies. The WRC has

been instrumental in funding research within the Two Streams catchment. Important study periods include 2003 – 2006, 2006 – 2009 and 2011 – 2013 and key research achievements during these periods were considered by Everson *et al*. (2006), Clulow *et al*. (2011) and Everson *et al*. (2014) respectively. The past WRC research identified research gaps that have guided the development of this thesis.

3.3.1 Research instrumentation

Since the late 1990s, the Two Streams catchment has been extensively instrumented for hydrological research, including: a weir (established in 1999), an Automatic Weather Station (AWS) established on a 24m mast in the black wattle (*A. mearnsii*) stand (established in 2006); and runoff erosion plots in the black wattle (*A. mearnsii*) stand and sugarcane (*S. officinarum*) plantation (established between 2015 – 2016). Tensionmeters have also been used on site for a short period of time. For this study the data from the runoff plot and tensionmeter studies were not found to be of value given the short study extends, differences in research focus and shallow depths studied at. Based on the instrumentation established and the studies undertaken, a number of hydrological and related records have been captured for the site including: rainfall, ET_A, streamflow, soil and soil hydraulic properties and black wattle leaf area index (LAI).

3.3.2 Hydrological modeling

In the early 2000s (up to 2006) the University of KwaZulu-Natal, with support from The WRC and Working for Water, considered the impact that clearing riparian forestry would have on streamflow and soil water storage (Everson *et al*., 2006). As part of this WRC study, catchment scale modelling was undertaken using the SWAT and the Agrohydrological (ACRU) models. These models were used to predict the relative impacts vegetation change would have on water quantity (Everson *et al*., 2006). During this study a good initial dataset was provided (Everson *et al*., 2006). However, both the SWAT and ACRU modelling systems require a great deal of input data not all of which was available from the dataset. As a result, both models were based predominantly on assumptions (Everson *et al*.,

2006). A recommendation of this earlier study was that further monitoring be undertaken (Everson *et al*., 2006).

One of the key issues identified from this study and used to drive further research on-site was that studies, such as this one, do not estimate tree water usage (Gush *et al*. 2002). This was believed to be a result of the inability of ACRU to accurately simulate deeper soil water processes and tree root behavior (Everson *et al*., 2006). This is a significant limitation as the impact of tree water use on deeper soil water reserves can have a significant impact during times of prolonged droughts (Fohrer *et al*., 2001). This limitation impacts on the ability to quantify the impacts of trees on ground water resources (Everson *et al*., 2006).

A second WRC study (Clulow *et al*., 2011) was undertaken at Two Streams from 2006 – 2009. Part of the research was to address the recommendations made in the previous WRC study (Everson *et al*., 2006), and considered a longer term study of the impact of black wattle (*A. mearnsii*) trees on evaporation, streamflow and groundwater resources (Clulow *et al*., 2011). The aims included: providing a modelling framework for the catchment water balance to improve streamflow predictions; and extending the hydrological record of the Two Streams catchment (Clulow *et al*., 2011). For this study, the Water, Vegetation, Energy, Solute (WAVES) and revised Intermediate-Zone ACRU models were used. The Intermediate- Zone ACRU model was used to predict streamflow in the catchment (Clulow *et al*., 2011). By the time this study was undertaken, more years of hydrological data had been captured. Overall, the results for this study revealed that the WAVES values were within 20% of the actual values for 95% of the time while the ACRU model values were within 20% for only 5% of the time (Clulow *et al*., 2011). The study concluded that the ACRU model was not able to effectively simulate changes in streamflow from an afforested catchment to a fallow catchment (Clulow *et al*., 2011).

A third WRC study was undertaken at Two Streams between 2011 – 2013 (Everson *et al*., 2014). This study was very much a continuation of the previous study (Clulow *et al*., 2011), focusing on

extending and improving on hydrological records (Everson *et al*., 2014). Following the last WRC study on the Two Streams site (Everson *et al*., 2014) the following research shortfalls were identified and proposed as possible objectives for further research:

- Determining the contribution and significance of mist in the hydrological cycle of the Two Streams catchment;
- Assessing erosion risk during and after harvesting; and
- Given that the existing *A. mearnsii* stand will be replaced by gum (*E. dunnii*) trees in the (then) near future (October 2017) – continuing measurement of all the water-balance components of the catchment to determine the influence of these trees on the hydrological processes in the catchment (Everson *et al*., 2014).

Based on the research gaps identified by Everson *et al*. (2014) and the past hydrological research undertaken on-site, one of the aims of this study is to address the last research gap of predicting the impact of a change in plantation type from *A. mearnsii* to *E. dunnii* (Everson *et al*., 2014). Given the extensive hydrological research that has been undertaken, a complex physically-based hydrological model was employed – the MIKE SHE deterministic, hydrological model. The set-up of this MIKE SHE model is discussed in detail in chapter four.

3.4 Summary

This study was undertaken in the Two Streams sub-catchment situated in the Mistley-Canema Mondi forestry estate in the Seven Oaks district, approximately 70km outside of Pietermaritzburg. The study site comprised of three dominant vegetation classes: black wattle (*A. mearnsii*) plantation, sugarcane plantation (*S. officinarum*) and riparian vegetation (a mixture of species that had colonized the area since the removal of wattle plantation in 2000). The study site is one of few hydrological research areas in South Africa providing a solid research foundation for hydrological modelling and improving understanding of hydrological processes in an area dominated by forestry and agricultural plantations. Three sequential major WRC studies have been undertaken within the Two Streams catchment, thus

far. Based on the outcomes of these studies recommendations for further research were made. The latest study (undertaken between 2011 – 2013) identified a further research objective to be that once the existing *A. mearnsii* stand is replaced by gum (*E. dunnii*) trees, measurement of all the water-balance components of the catchment must continue to determine the influence of these trees on the hydrological processes in the catchment (Everson *et al*., 2014). This objective forms a fundamental part of this thesis.

Chapter Four

Methods

4.1 Introduction

This chapter details the methods employed to set-up, calibrate and validate the MIKE SHE current scenario model that simulated an approximate ten year period from 14 February 2007 – 02 October 2016, and to set-up the MIKE SHE future scenario model that simulated from 14 February 2019 – 02 October 2028. This chapter details the analysis methods employed for both MIKE SHE scenarios. Due to the complexity of the MIKE SHE model and the detailed process taken in setting up the models (both current and future), this chapter provides a detailed description of the set-up process. In addition, this chapter details the inputs of the MIKE SHE model, and in some cases these inputs were generated, and thus technically are results. These results were included in the methods chapter for ease of understanding of the process followed, as the MIKE SHE set-up comprises a number of interlinked sequential steps where one step is directly affected by the previous step. As such the methods chapter documents the set-up and some of the input results generated, while the results chapters documents the modelled output results. In addition to the inclusion of input results, model screenshots (termed screen displays) of certain input parameters were included for ease of understanding through visualization. The level of detail included was chosen to exemplify the magnitude of inputs required and to show the researcher's understanding and how she went about addressing all the input needs of the model. This study centres on the set-up of the MIKE SHE model and thus the detail in this chapter is important in illustrating what the set-up entailed and the work effort expended.

4.2 MIKE SHE modelling of the Two Streams sub-catchment

The MIKE SHE model set-up for the Two Streams study site incorporated the results of past research undertaken on-site (Clulow *et al.*, 2011; Kuenene 2013; Everson *et al.*, 2014). To-date, most research conducted on-site has been focused on the larger of the two sub-catchments (Clulow *et al.*, 2011;

Kuenene 2013; Everson *et al*., 2014) and as such, the MIKE SHE modelling study was restricted to the larger sub-catchment (Figure 4.1).

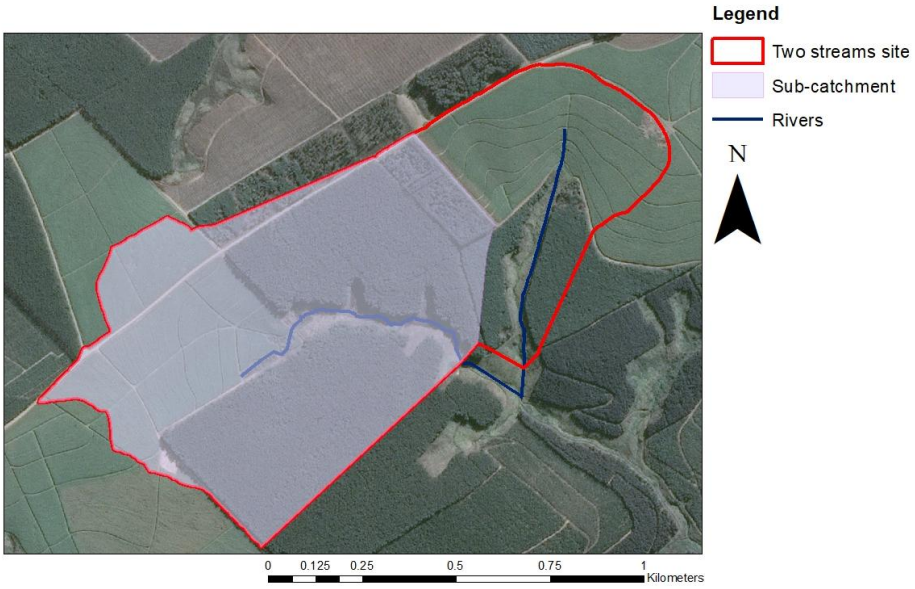

Figure 4.1: The Two Streams sub-catchment.

All data inputs for the MIKE SHE model were set to the same projected coordinate system - WGS 1984 UTM 36S to ensure spatial alignment of the datasets. All time series and spatial data inputs were either generated in, or converted to, MIKE SHE file formats (Table 4.1). Spatial datasets were all inputted in a MIKE SHE grid file format (Table 4.1) as opposed to the more conventional shapefile format and set to the same grid size, ensuring an exact fit of all grid cells. The grid file (raster) format enables easier modelling due to the regular structure of the grid (Hörmann and Floater, 2005). Thus, all shapefile data generated in ArcGIS software were first converted into a MIKE SHE grid series file (.dfs2) prior to being inputted into the MIKE SHE model.

Table 4.1: MIKE SHE files formats.

Data record types	**File format**
Time series files	.dfs0
Profile series files	.dfs1
Grid series files	.dfs2/.dfs3
ET Vegetation Properties file	.etv
UZ Soil Properties file	.uzs

To convert a shapefile into a grid series file (.dfs2) the shapefile was first converted into an .ASCII file format. This conversion was completed in ArcGIS 10.3 using the *Conversion tool – From Raster to ASCII*, and then the grid series file was imported into MIKE SHE and converted into a .dfs2 file. To do so, the *MIKE Zero toolbox* was activated in MIKE SHE and the *Grd2Mike* tool was used. All other inputs that were required in specific file formats (e.g. time series files), were manually inputted directly into the MIKE SHE model (Table 4.2).

Table 4.2: The file formats used for the different data inputs (derived from external sources) as required by the MIKE SHE simulation modules.

Simulated modules	**Data inputs required**	**External sources of data**	**MIKE SHE file format used**
Topography	• DEM	• University of KwaZulu-Natal	• .dfs2
Climate	• Precipitation • ET_{Ref}	• Food and Agriculture Organisation (FAO) AWS • Two Streams mast AWS • South African Weather Services (SAWS) AWS (refer to Table 4.3 for the locations of the AWS's)	• .dfs0
Land use	• Land cover map • Vegetation properties	• University of KwaZulu-Natal • Clulow *et al*. (2011) • Burger (1999) and Dye *et al*. (2008)	• .dfs2 • .etv
OL	• Manning number	• Morgan (2005)	• .dfs2
UZ	• Soil profile definitions • Soil properties	• Kuenene (2013)	• .dfs2 • .uzs
SZ	• Initial potential head	• University of KwaZulu-Natal • Clulow *et al.* (2011)	• .dfs2

The MIKE SHE modelling software has three tabs in which the user works: the set-up tab; the processing tab; and the results tab. The set-up tab was used to input all data to run a MIKE SHE model, the processing tab was used to view all the data processed by MIKE SHE once the set-up was completed, and the results tab housed the results generated by the model that were compared to observed results from the sub-catchment. Data from both the processing tab and the results tab stored information for model validation used once the model set-up and run were completed. Two MIKE

SHE model scenarios were set-up and run. The one scenario described the current scenario of the Two Streams sub-catchment and the second described the future scenario of the sub-catchment (with a change in vegetation from *A. mearnsii* to *E. dunnii*). The MIKE SHE model set-up of both scenarios and model validation methodology are discussed below (Sections 4.3 to 4.5).

4.3 MIKE SHE model set-up – current scenario

The MIKE SHE model set-up was complex, with a number of model modules and processes (Figure 4.2) requiring a multitude of input data (Appendix A).

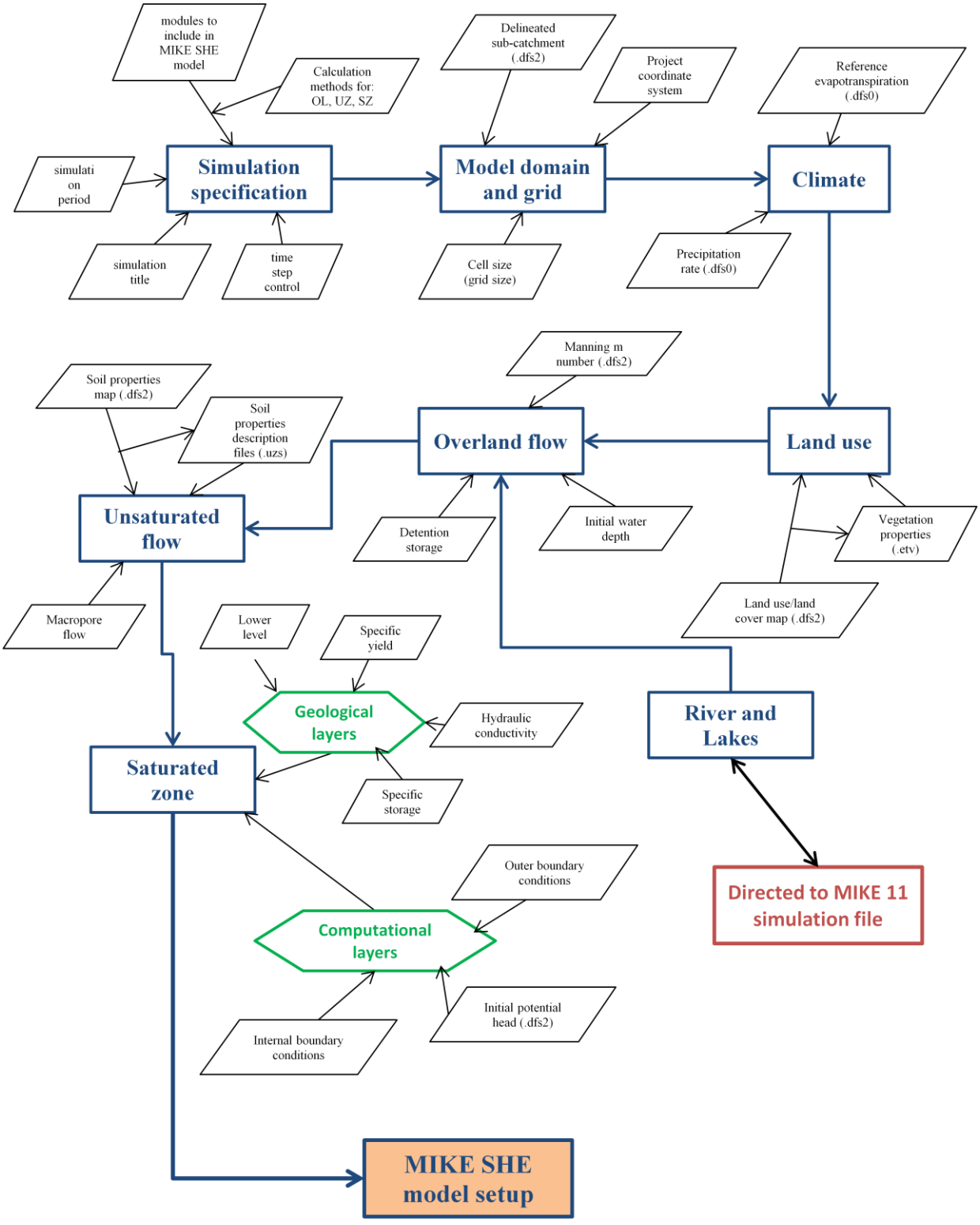

Figure 4.2: Flow chart for the MIKE SHE, current scenario, model set-up.

Given the complexity of the MIKE SHE model setup the processes in operation are multiple, interconnected and feedback into each other making model conceptualisation (Figure 4.3) a difficult

task. The MIKE SHE model set-up was managed using a data tree, which assisted in managing the complexity of the modelling environment by displaying all modules included in the model: *display, simulation specification, model domain and grid, topography, climate, land use, rivers and lakes, overland flow, unsaturated flow, saturated groundwater flow* and *storing of results*. Where necessary, these modules and their inputs have been described in the paragraphs to follow.

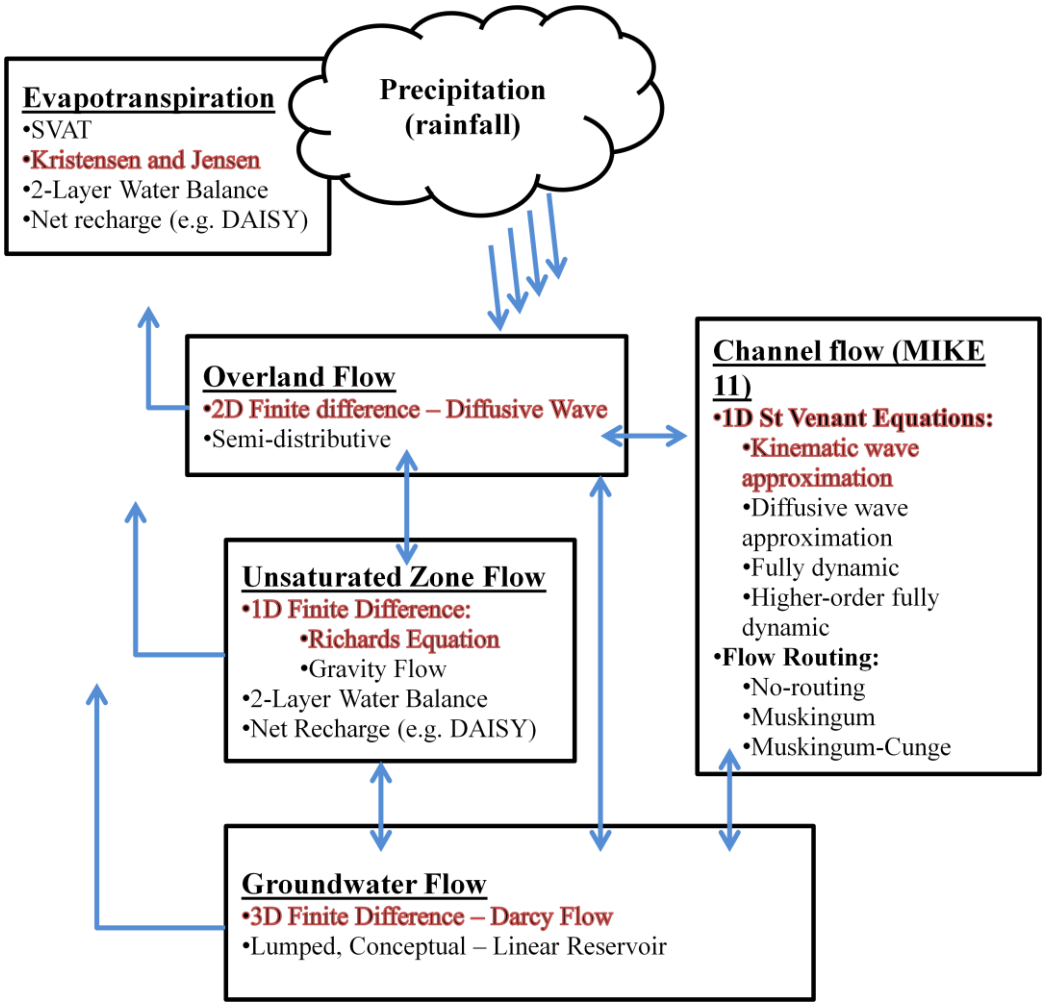

Figure 4.3: Conceptualisation of the MIKE SHE (and related MIKE 11) software. Illustrating the processes that can be modelled (black bulleted points) and the specific processes modelled in this study (red bulleted points). The interconnectedness of the MIKE SHE processes and how water moves through the system is shown by blue directional arrows.

4.3.1 Simulation specification module

The *simulation specification module* (Figure 4.2) specified which components of the hydrological cycle to model and, where applicable, specified the methods used to model certain components (Figure 4.4 and Appendix A). Once the components were selected they were displayed in the set-up MIKE SHE data tree as modules. Under the *simulation specification module* other factors: the *simulation title* and *simulation period*, and the *time step controls*, were defined.

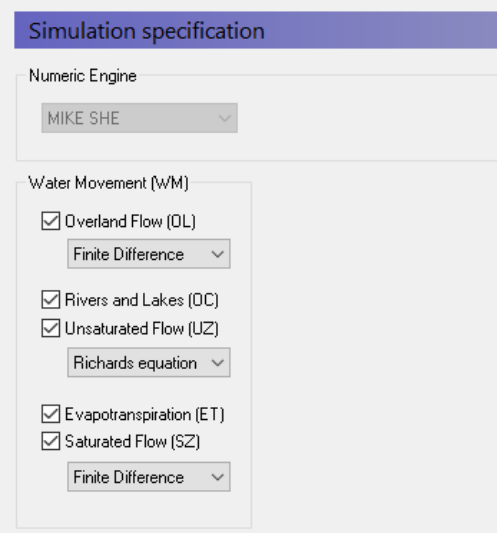

Figure 4.4: Screen display of the hydrological cycle components selected for the MIKE SHE current scenario and the method options chosen for the overland flow, unsaturated flow and saturated flow modules.

The *simulation title* was 'Current Scenario Two Streams 2007 to 2016'. The *simulation period* extended from the 14th of February 2007 – 2nd of October 2016; this period was used as it corresponded to the available length of the rainfall record (described under section 4.3.4). The default settings for the MIKE SHE *time step controls* were used (Figure 4.5 and Appendix A).

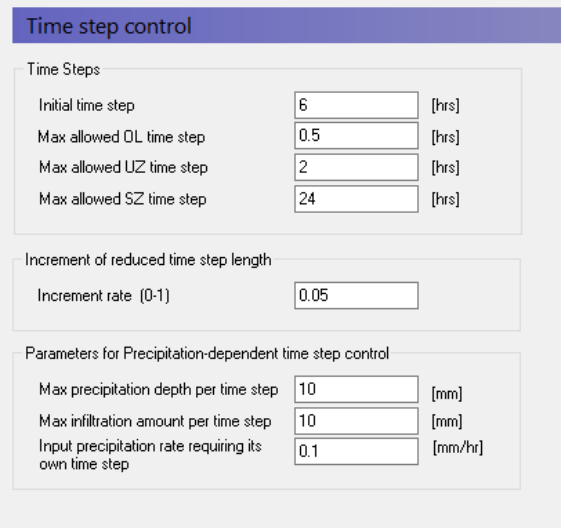

Figure 4.5: Screen display of the default time step control settings used for the MIKE SHE current scenario set-up.

4.3.2 Model domain and grid module

The *model domain and grid module* (Figure 4.2) defined the model area. For this study, the model area was defined by the larger sub-catchment boundary of the site – the boundary used was taken from previous research undertaken at the Two Streams site (Everson *et al.*, 2006, 2014; Clulow *et al.*, 2011). However, on visual inspection of the boundary (Figure 3.2) it appeared to have very straight edges, not typical of a hydrologically defined boundary. Thus, as opposed to using the boundary provided, a new hydrologically defined sub-catchment was delineated using Arc-Hydro in ArcGIS 10.3. Arc-Hydro is used to define drainage patterns for catchments through a set of sequential steps. To delineate catchment or sub-catchment boundaries, the Arc-Hydro software was reliant on the input of a DEM. The DEM input was provided by the Cartographic Unit of the University of KwaZulu-Natal in Pietermaritzburg (described further in section 4.3.3). Once input, the DEM underwent a sequence of processing steps to produce a delineated sub-catchment (Appendix B). Once delineated the sub-catchment boundary (Figure 4.6) was input into MIKE SHE as a .dfs2 file and used to define the model domain and grid size – the file had a cell size of $25m^2$.

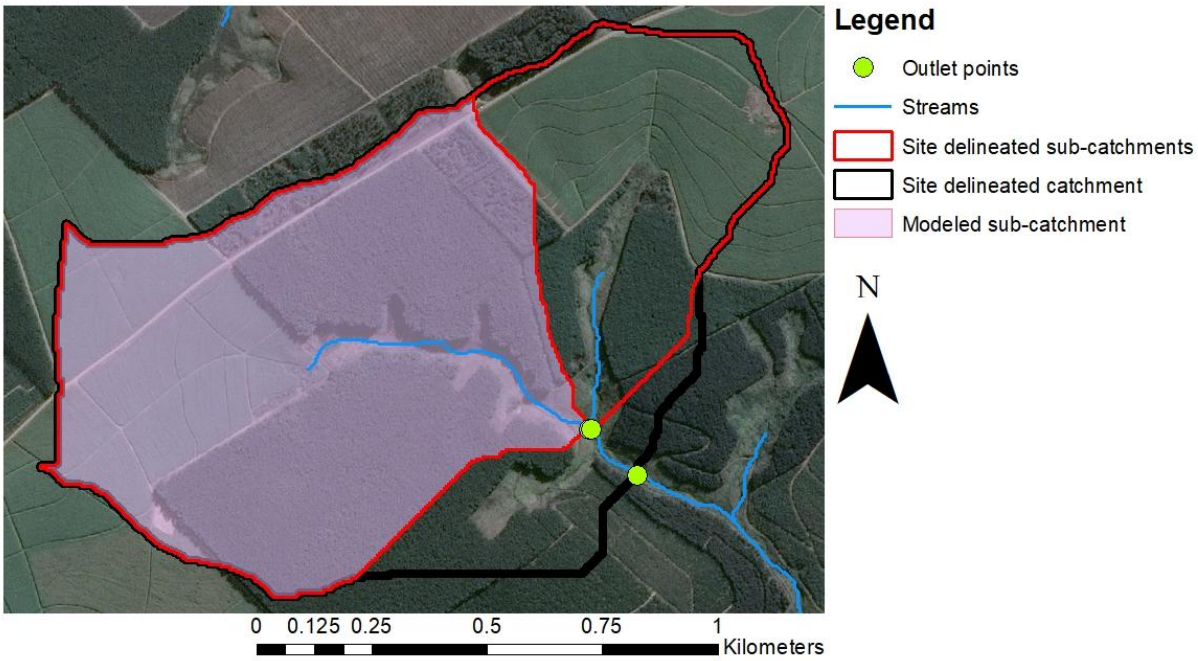

Figure 4.6: The Two Streams catchment boundary and sub-catchment (study site) boundaries delineated through Arc-Hydro tools in ArcGIS 10.3 software.

4.3.3 Topography module

Within MIKE SHE, topography was defined from a DEM. The DEM for the Two Streams site was derived by the Cartographic Unit, Discipline of Geography at the University of KwaZulu-Natal (Pietermaritzburg Campus) from 5 – 10m contours and spot heights (Figure 4.7). The DEM had a resolution of 5m and was input into MIKE SHE as a .dfs2 file.

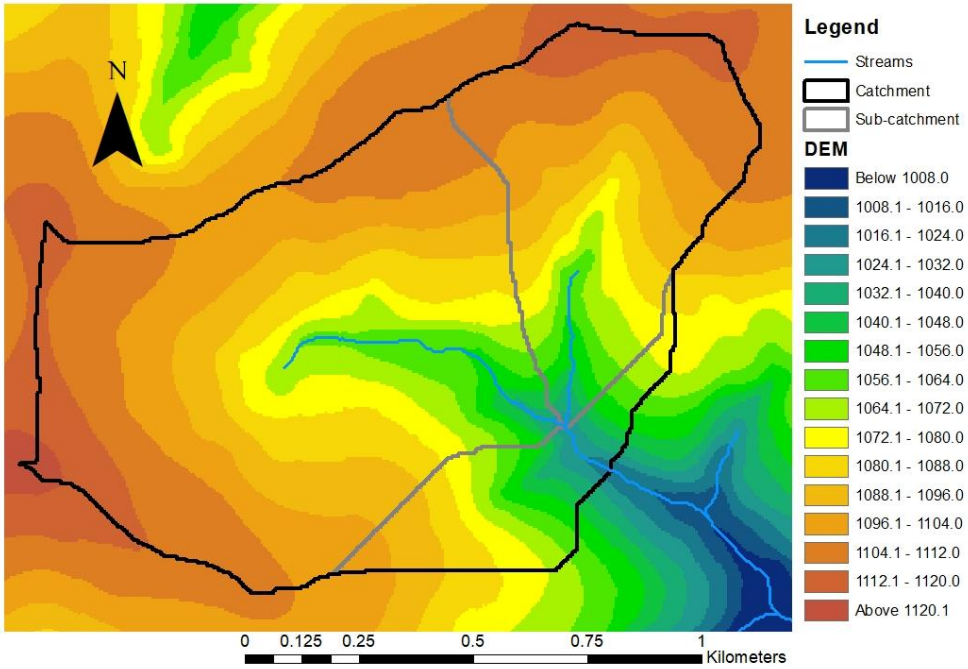

Figure 4.7: 5m Digital Elevation Model (DEM) showing the Two Streams site topography, based on 5m and 10m contours and spot heights.

4.3.4 Climate module

All weather data inputs were input under the *climate module* (Figure 4.2). The *climate module* comprised three sub-modules: *precipitation rate*, *reference evapotranspiration* and *snow melt*. No measure of snow melt had been taken on-site and, due to the infrequency of snowfall in the area, was deemed unnecessary. Thus, the only sub-modules considered for this research were: *precipitation rate* and *reference evapotranspiration*. All climatic data were taken from three AWSs (Table 4.3).

Table 4.3: Coordinates of the locations of the Automatic Weather Station's (AWSs) used in this study.

AWS	Coordinates	Approximate distance from the Two Stream site	Altitude (m)
FAO AWS	29°11'47.9''S; 30°39'58.8''E	1km	2112
Mast AWS	29°12'19.2''S; 30°39'1.3''E	Located on-site	2134
SAWS AWS	29°4'58.8''S; 30°36'10.8''E	15km	2045

Two Campbell Scientific AWSs collect standard atmospheric data at or near to the Two Streams study site. The one station was a FAO registered AWS that had been set-up in a short grassland area,

approximately 1km outside of the Two Streams site (Table 4.3). The FAO AWS (located at an altitude of 2112m) record extended from the 14th of February 2007 – 2nd of October 2016. The second AWS at Two Streams was attached to the top of a 24m lattice mast in the black wattle (*A. mearnsii*) stand (Table 4.3). Originally, the Mast AWS was set-up to provide data for energy balance calculations, to determine ET (Clulow *et al*., 2011; Everson *et al*., 2014). The mast AWS (located at an altitude of 2134m) record extended from 23rd March 2011 – 2nd October 2016. The FAO AWS was considered as the primary AWS record due to the record length and close proximity to the Two Streams site. Gaps in the FAO AWS record were patched using the mast AWS record. Where gaps in the record could not be filled using the mast AWS, the SAWS data for Greytown were used. The SAWS station (located at an altitude of 2045m) was located approximately 15km from the Two Streams site and had a record extending from 14th February 2007 – 2nd October 2016 (Table 4.3).

4.3.4.1 Precipitation rate

In MIKE SHE, precipitation refers to the measured rainfall falling into the defined project domain (DHI software, 2012). In the *precipitation rate* sub-module both the spatial and temporal distribution of rainfall were considered. Daily rainfall data (mm) were input as a time series file (.dfs0) for the period 14 February 2007 – 02 October 2016 (3519 days) and the rainfall was deemed spatially uniform across the sub-catchment (due to the lack of availability of multiple measures of within-catchment rainfall data). Out of the 3519 days modelled, the FAO AWS rainfall record accounted for 2587 days (approximately 73.5%), the mast AWS 812 days (approximately 23.1%), of which 526 days had experienced rainfall and the SAWS record 120 days (approximately 3.4 %), of which 43 days experienced rainfall.

Prior to patching, the AWS records were correlated to determine whether the datasets showed a good linear correlation and thus could be used for patching gaps. The correlation between the FAO AWS record and the mast AWS record were assessed using a scatter plot (Figure 4.8) and a Pearson's correlation coefficient (r) and found to have an extremely significant, very strong, positive, linear correlation, $r = 0.94$ ($P < 1.00 \times 10^{-4}$). This was deemed sufficient to patch the FAO AWS record.

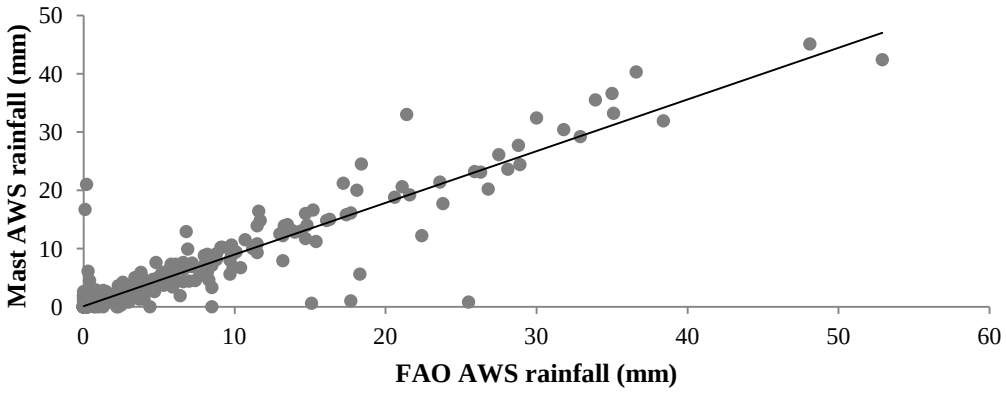

Figure 4.8: Correlation between the FAO Automatic Weather Station (AWS) daily rainfall (mm) record and the mast Automatic Weather Station (AWS) daily rainfall (mm) record.

The SAWS AWS rainfall record was correlated to the combined AWSs record (FAO AWS and mast AWS) and was found to have an extremely significant, positive, linear correlation, r =0.67 ($P < 1.00 \times 10^{-4}$; Figure 4.9). This was deemed sufficient to patch the rainfall record.

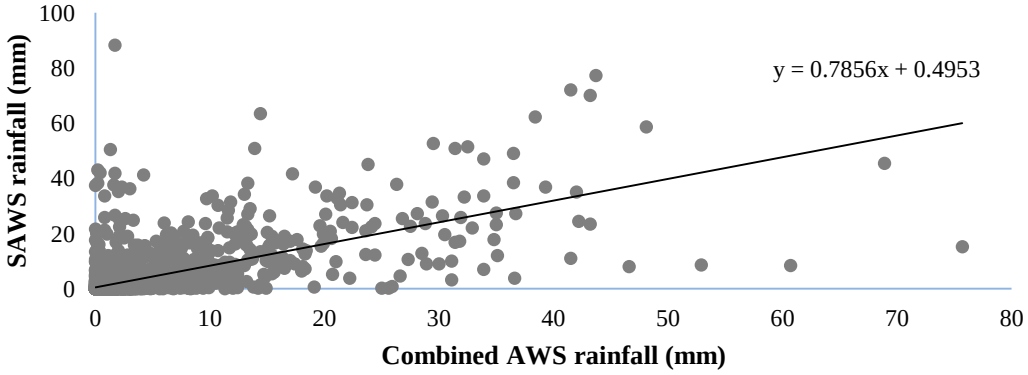

Figure 4.9: Correlation between the combined Automatic Weather Station (AWS) daily rainfall (mm) record for the Two Streams study site and the South African Weather Services' Greytown weather stations daily rainfall (mm) record.

4.3.4.2 Reference evapotranspiration

Reference evapotranspiration (ET_{Ref}), in MIKE SHE, refers to the rate of ET from a reference surface that has an unlimited amount of water (DHI software, 2012). To calculate the ET_{Ref} for the Two Streams sub-catchment the FAO Penman-Monteith method, recommended for use in MIKE SHE (DHI software, 2012), was used (Equation 4.1). It is an internationally recognized method and popular

for many reasons, including the relatively low data requirements (Allen *et al*., 1998). The Penman-Monteith equation for ET_{ref} is reliant on easily acquired weather station data: solar radiation, air temperature, air humidity and wind speed (Zotarelli *et al*., 2015). The calculation of ET_{Ref} using the FAO Penman-Monteith equation, described in Zotarelli *et al*. (2015), was an exhaustive process (Appendix C).

$$ET_{ref} = \frac{0.408\Delta(R_n - G) + \gamma \frac{900}{T + 273} u_2 (e_s - e_a)}{\Delta + \gamma(1 + 0.34u_2)}$$

Equation 4.1: The FAO Penman-Monteith equation for ET_{ref} (Allen *et al*., 1998).

Where: ET_{ref} = the reference evapotranspiration ($mm.day^{-1}$); R_n = the net radiation at the crop surface ($W.m^{-2}$); G = the soil heat flux density (unitless); T = the mean daily air temperature at 2m height (°C); u_2 = the wind speed at 2 m height ($m.sec^{-1}$); e_s = the saturation vapour pressure (kPa); e_a = the actual vapour pressure (kPa); Δ = the slope vapour pressure curve (kPa); and γ = the psychrometric constant (kPa $^oC^{-1}$; Allen *et al*., 1998).

4.3.5 Land use module

The *land use module* (Figure 4.2) was used to define the properties of the land surface and the distribution of vegetation within the Two Streams sub-catchment. The *land use module*, in MIKE SHE, has a *vegetation* sub-module, under which the spatial distribution of vegetation was defined. The land cover map input (as a .dfs2 file) was provided by the Discipline of Geography, University of KwaZulu-Natal (Pietermaritzburg Campus) and was defined using the Ezemvelo KwaZulu-Natal Wildlife (EKZNW) LULC shapefile for the area (Figure 4.10). The LULC map provided had been ground truthed, verified and refined by University staff.

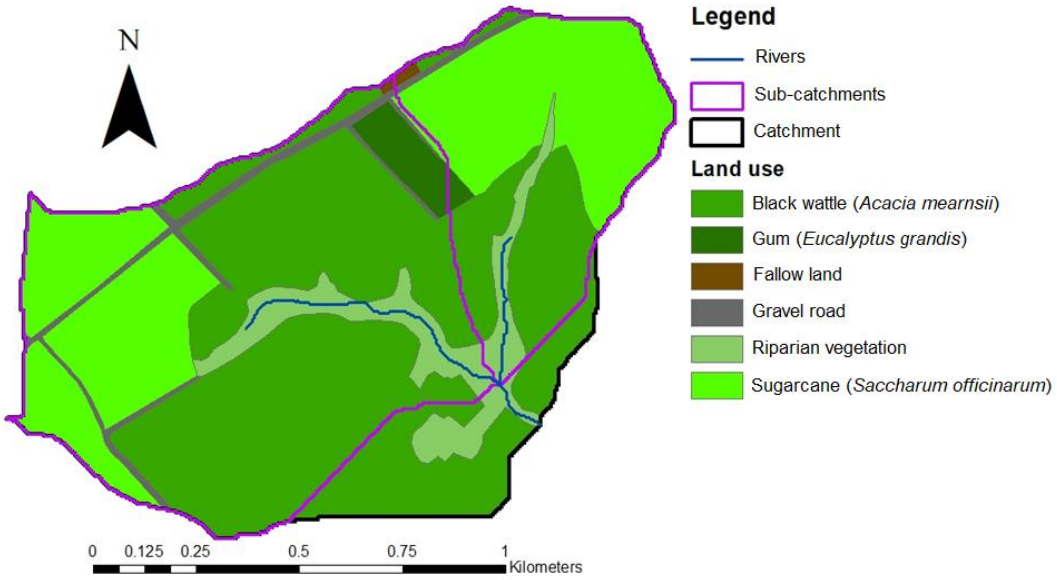

Figure 4.10: Land cover map of the Two Streams catchment, and sub-catchments, as generated using the Ezemvelo KwaZulu-Natal Wildlife (EKZNW) land use and/or land cover shapefile for the area.

Once the vegetation .dfs2 file was input into MIKE SHE, the vegetation properties for each vegetation class were defined. For this study, three vegetation classes were considered: black wattle (*A. mearnsii*), sugarcane (*S. officinarum*) and riparian vegetation. For the black wattle and sugarcane, *vegetation property files* (.etv) were created, as more data were available for these vegetation types than were available on the riparian vegetation. To generate *vegetation property files*, data on LAI, RD and the crop coefficient (K_c) were required (DHI software, 2012).

Leaf area index (LAI) is included in the model as it provides a characteristic value for a specific plant type providing an indication of seasonality and plant stress (DHI software, 2012). Leaf area index (LAI) is defined by Graham and Butts (2005) as being the one-sided area of green leaves per area of ground surface. The LAI of vegetation depends on species composition, development stage and seasonality (Jonckheere *et al*., 2004). In MIKE SHE, the LAI assigned to a vegetation class is based on the average leaf area per grid cell within the model (DHI Software, 2012). Rooting depth (RD) provides an indication of the depth at which water can be extracted from the UZ and, in the case of deep rooting systems, from the SZ (Graham and Butts, 2005; DHI software, 2012). The K_c value is

used in the calculation of the crop reference ET (ET_C) and it is calculated by multiplying K_c by ET_{Ref} (Equation 4.2; DHI software, 2012). To generate the *vegetation property files* for the black wattle and sugarcane, the stages of development of both species were defined and for each stage the LAI, RD and K_c values were specified (Appendix D).

$$ET_C = ET_{Ref} \times K_c$$

Equation 4.2: Calculation of crop reference evapotranspiration (ET_C; DHI software, 2012).

For the black wattle (*A. mearnsii*), LAI values had been measured on-site from August 2006 – October 2013 using a LAI-2000 Plant Canopy Analyzer. The LAI-2000 allows for easy estimation of LAI whereby light readings are taken both below and above the canopy, and transmittances are computed at five angles (LAI-2000 Plant Canopy Analyzer, 1989). Within the LAI-2000, a control unit records the light readings and calculates LAI from the transmittances (LAI-2000 Plant Canopy Analyzer, 1989). The LAI data were input in the *vegetation property file* for the specific days recorded. RD was input as a constant value of 10m throughout the study period. RD had not been determined on-site. However, Everson *et al*. (2014), whilst conducting other studies on soil moisture content, identified *A. mearnsii* tree roots extending to depths deeper than 8m. Thus, a depth of 10m was assumed for the RD. The K_c values for black wattle were taken from the Compoveg database from the ACRU Agrohydrological Modelling System, user manual version 3.00 (Smithers and Schulze, 1995). The black wattle *vegetation property file* comprised 2431 days of varied LAI and K_c value readings and a constant RD (Appendix D).

For the sugarcane (*S. officinarum*), the LAI was determined from Dye *et al*., (2008) in the Seven Oaks region. Based on this study an average LAI value of 3.57 was identified. The *vegetation property file* was used to incorporate harvesting times of the sugarcane crop. According to the farmer who currently owns the sugarcane crop, crops are harvested approximately every 22 months. The last harvest took place at the beginning of October 2017 (Table 4.4). Based on the data provided by the sugarcane farmer, all harvest dates over the study period were calculated. At each harvest time the

LAI was assumed to be 0, sugarcane crops generally take four months to reach maturity (Lin *et al*., 2009). Thus, four months after harvest LAI was recorded as 3.57. This pattern was continued throughout the study period. The RD of the sugarcane was set as 1m based on information from the sugarcane farmer and field observations. The RD was verified in the literature (Dye *et al*., 2008). A constant K_c coefficient value of 0.96 was used for sugarcane, as recommended by Smithers and Schulze (1995).

Table 4.4: Sugarcane harvest periods that fall within the current scenario study period considered.

Harvest month	**Ratoon***
April 2008	5th
February 2010	6th
December 2011	1st
October 2013	2nd
August 2015	3rd
October 2017	4th

*Ratoon refers to a new shoot or sprout growing from the base of a crop plant (i.e. sugarcane), referring to the start of the new growing season. Sugarcane crops are not reseeded after they are cut down; they grow in ratoon cycles, until the crop quality declines at which point they are reseeded. Sugarcane normally grows for six ratoon cycles (Cabral *et al*., 2012).

The riparian vegetation was treated differently from the black wattle and sugarcane, as less information was available on this vegetation class. As opposed to using a *vegetation property file*, constant values for LAI and RD were inputted. The riparian area comprised of a mixture of vegetation types. To determine the LAI of the riparian vegetation, remote sensing was used. Leaf area index (LAI) values were derived from Normalized Difference Vegetation Index (NDVI) calculations undertaken on satellite imagery (discussed below).

The NDVI is a popular vegetation index incorporating the regions of the electromagnetic spectrum showing the highest absorption and highest reflectance of chlorophyll, making it a useful index for vegetation assessment over a wide range of conditions (Bulcock and Jewitt, 2010). The NDVI does not consider topography, making it easier to calculate as no prior knowledge of the ground conditions is required. The NDVI is a ratio of shortwave infrared and red reflectance (Bulcock and Jewitt, 2010; Equation 4.2).

$$\text{NDVI} = \frac{\text{NIR} - \text{red}}{\text{NIR} + \text{red}}$$

Equation 4.3: The Normalized Difference Vegetation Index (NDVI) equation.

Where: Red = the red band (± 600nm to 700nm); and NIR (Near Infrared) = the NIR band (± 750nm to 900nm). The part of the spectrum included in the red and NIR bands will depend on the satellite considered.

For this study, SPOT satellite images were used (Table 4.5). These images were acquired from the South African National Space Agency (SANSA).

Table 4.5: Information on the SPOT satellite imagery acquired from the South African National Space Agency (SANSA).

Date	**Satellite used**	**Band wavelength (nm)**	**Resolution (m)**	**Cloud cover (%)**
01/02/2007	SPOT 5	Red = 610 – 680; NIR = 780 – 890	10	0
17/07/2007	SPOT 5	Red = 610 – 680; NIR = 780 – 890	10	0
19/01/2011	SPOT 4	Red = 610 – 680; NIR = 780 – 890	20	0
31/07/2012	SPOT 5	Red = 610 – 680; NIR = 780 – 890	10	0
04/10/2015	SPOT 5	Red = 610 – 680; NIR = 780 – 890	10	0

Normalized difference vegetation index (NDVI) values were calculated (using 50 random points taken in the riparian zone), for all of the acquired images, and LAI values were derived based on each NDVI value (Appendix D). To calculate the LAI from the NDVI values, an equation to relate LAI and NDVI needed to be used. An equation relating a similar vegetation index, the Soil-adjusted Vegetation Index (SAVI), to LAI was found (Equation 4.3; Bulcock and Jewitt, 2010).

$$\mathrm{LAI} = \frac{-\ln\left(\mathrm{SAVI} + 0.371\right)}{0.48}$$

Equation 4.4: Relationship between Leaf Area Index (LAI) and the Soil-adjusted Vegetation index (SAVI).

The SAVI equation is similar to the NDVI equation (Equation 4.4).

$$\mathrm{SAVI} = \frac{(1 + \mathrm{L})(\mathrm{NIR} - \mathrm{red})}{\mathrm{NIR} + \mathrm{red} + \mathrm{L}}$$

Equation 4.5: The Soil-adjusted Vegetation index (SAVI) equation.

Within the SAVI equation L = 0 in densely vegetated areas; L = 0.5 in sparsely vegetated areas; and L = 1 in areas with no vegetation (Elvidge and Chen, 1995). Based on field observations, the majority of the sub-catchment was densely vegetated, and as such an 'L' value of zero was used. With L = 0 the SAVI equation (Equation 4.4) becomes the NDVI equation (Equation 4.2). Thus, the relationship between LAI and the SAVI (Equation 4.3) was deemed sufficient to derive LAI values for each random point considered (Appendix D). Based on the above process a constant LAI value of 2.01 was calculated (Appendix D). However, there was concern regarding this value due to the resolution of the satellite imagery (Table 4.5), bringing into question the reliability of the LAI data. To determine the validity of the above LAI value obtained, ground measures of LAI were taken.

4.3.5.1 Field validation and ground truthing

Three fieldtrips to the Two Streams site were undertaken. The first fieldtrip took place from the 24th of April 2016 – 30th of April 2016. This fieldtrip was undertaken to gather data on past research undertaken on-site and to become acquainted with the study site. The second fieldtrip was undertaken from the 16th of October 2016 – 21st of October 2016. This fieldtrip involved the gathering of information on past research undertaken on-site and to better understand data previously acquired. The third fieldtrip was undertaken from the 18th of October 2017 – 21st of October 2017. During this fieldtrip, LAI was measured at 20 locations within the riparian vegetation class using a LAI-2200

Plant Canopy Analyzer (Figure 4.11) to determine the average LAI of the riparian vegetation class and to ground truth the average LAI measure derived from satellite imagery.

The LAI-2200 is an upgraded version of the LAI-2000 previously used on-site (making their outputs comparable), to determine LAI of the black wattle stand (Clulow *et al*., 2011). The LAI-2200 calculates LAI and other canopy attributes from light measurements made with a 'fish-eye' optical sensor (148˚ field-of-view; LAI-2200 Plant Canopy Analyser, 2012). Measurements made above and below the canopy are used to calculate canopy light interception at five zenith angles, from which LAI is computed using a model of radiative transfer in vegetative canopies (LAI-2200 Plant Canopy Analyser, 2012). To operate the LAI-2200 a LAI-2250 optical sensor (wand) is connected to a LAI-2270 control unit (console). The LAI-2270 control unit is used to configure the instrument, to store the recorded data and to compute results and the LAI-2250 optical sensor is used to collect the data (LAI-2200 Plant Canopy Analyser, 2012).



Figure 4.11: The LAI-2200 Plant Canopy Analyzer used to measure the average Leaf Area Index (LAI) for the riparian vegetation.

The optical sensor contains high precision optical components, including lenses, optical filters and light sensors and is very sensitive to light (LAI-2200 Plant Canopy Analyser, 2012). The LAI-2250 should ideally be used during times of minimal, uniform light which is not always practically possible, as was the case in the ground truthing fieldtrip visit (LAI-2200 Plant Canopy Analyser,

2012). To account for this limitation, view caps are supplied with the LAI-2250 optical sensor (Figure 4.12) to limit the field of view and block out unwanted light (LAI-2200 Plant Canopy Analyser, 2012). For this study the 90˚ cap was used to limit both the impact of the operator of the instrument and the sun (Figure 4.12).

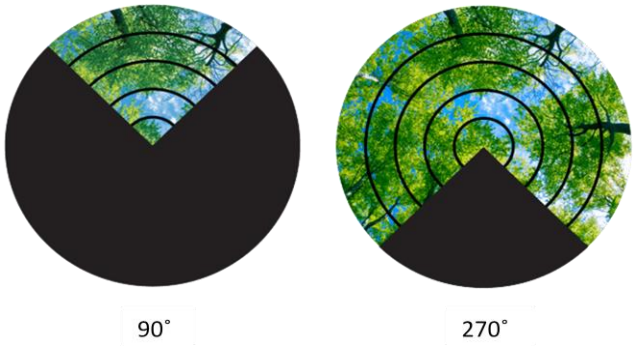

Figure 4.12: Example of view caps used by the LAI-2250 optical sensor (LAI-2200 Plant Canopy Analyser, 2012).

When LAI was measured, using the LAI-2200, the coordinates of the location of the measurement were recorded. Once fieldwork was completed and the average LAI from the 20 samples was obtained it was compared to the LAI measured from the SPOT imagery (Appendix D). Based on the results (section 5.3) a LAI value was obtained and input into MIKE SHE for the riparian vegetation. In addition, a constant RD of 1m was used for the riparian vegetation class.

4.3.6 Overland flow module

In MIKE SHE the *overland flow module* (Figure 4.2) models the interactions between the LULC in the sub-catchment and the properties of the water flowing overland and integrates these OL properties to the *rivers and lakes model* by modelling the interactions between river flow and OL (DHI software, 2012). There are two possible methods for calculating OL in MIKE SHE: the *finite difference method* which uses diffusive wave approximation of the Saint Venant equations, or the *semi-distributed method* which uses a semi-distributed approach based on Manning's equation (DHI software, 2012). The *finite difference method* calculates a more detailed OL and is more suited to small scale study sites, whilst the *semi-distributed method* is of a coarser resolution and more suited to larger regional

scale study sites (DHI software, 2012). The Two Streams study site occupies a small area (79.16ha) and thus the *finite difference method* was used. The *finite difference method* was selected for under the *simulation specification module* (Figure 4.4) and the following items were required for the calculation of OL under the *overland flow module*: Manning number, detention storage and initial water depth.

The Manning number refers to the Manning's m number which is equivalent to the Stickler roughness coefficient and the inverse of the more conventional Manning's n number (Morgan, 2005). Manning's n is the sum of roughness generated by the soil particles, surface micro-topography and vegetation, all acting independently of each other (Morgan, 2005). Manning's n values characteristically range between 0.01 for smooth channels and 0.10 for densely vegetated channels. For Manning's m values this corresponds to values between 100 and 10 respectively. If a Manning's m value of zero (0) is used for a particular cell, then the OL becomes inactive within that cell (DHI software, 2012). For the Two Streams site a different Manning's m value was used for each vegetation class (i.e. black wattle, sugarcane and riparian vegetation). The resistance to OL by the black wattle plantation was determined to be high with a Manning m value of 10, the sugarcane was estimated to have a Manning's m value of 40 based on values recommended in Morgan (2005) for similar crops and the riparian vegetation was provided a Manning's m value of 20 determined by the basal coverage relative to the other land covers considered and based on a recommended value in Morgan (2005) for dense bunch grasses.

The detention storage variable, in MIKE SHE, is used to limit the amount of water that can flow over the ground surface by accounting for ponded water on the surface (DHI software, 2012). The detention storage is a threshold value that must be overcome for OL to take place (DHI software, 2012). The detention storage value used for this study was 2mm uniformly across the study site; this value was a default MIKE SHE setting and considered sufficient given that this has never been investigated on-site. In MIKE SHE, the initial water depth is the depth of water present on the ground surface at the start of the simulation (DHI software, 2012). The initial water depth is usually zero (i.e. no water present on the surface), but can be given a higher value if the area has experienced a

significant amount of rainfall i.e. if there has been a flood or if the site is situated in a wetland or lake area where there is a natural 'film' of water constantly present (DHI software, 2012). For this study, the initial water depth was set at 0mm.

4.3.7 Rivers and lakes module

MIKE SHE software is incapable of modelling the streamflow or water level of terrestrial water bodies and relies on external software extensions to do so (i.e. MIKE 11; Figure 4.13). MIKE SHE links to MIKE 11 software, which is used to model the one-dimensional flow in a river, in this case the river in the Two Streams sub-catchment. However, to generate the input requirements for MIKE 11, MIKE Hydro software (Figure 4.13), which is a graphical user interface framework used for water resources related applications, was used (DHI software, 2012). Thus, MIKE Hydro generated the MIKE 11 files which are linked to the MIKE SHE *rivers and lakes module* (Figure 4.2) to model streamflow (Figure 4.13).

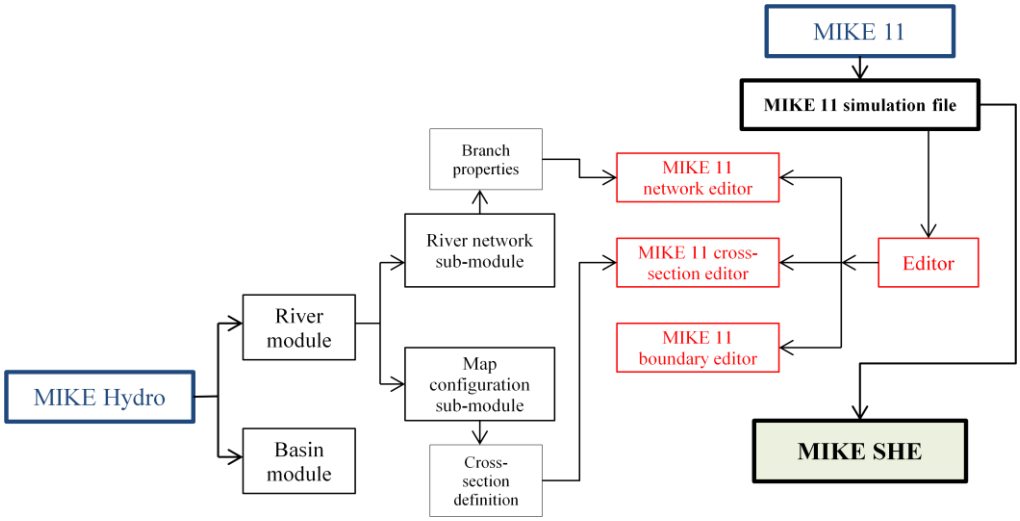

Figure 4.13: Flow chart showing the link between MIKE Hydro, MIKE 11 and MIKE SHE software.

The Two Streams river, located within the sub-catchment of concern, has a weir at which catchment streamflow has been monitored (Everson *et al.*, 2014). The weir is located at approximately 591m along the stream. It is a V-notch weir calibrated by DWAF with a sieve attached to prevent debris

from getting trapped in the V-notch and affecting the water level in the weir (Figure 4.14; Everson *et al*., 2014).



Figure 4.14: The V-notch weir located along the river of the Two Streams larger sub-catchments (Everson *et al*., 2014).

4.3.7.1 Generating MIKE 11 inputs in MIKE Hydro.

The *river module* in MIKE Hydro was used to generate the MIKE 11 inputs required (Figure 4.12). In the *river module*, two sub-modules were considered: *river network* and *map configuration*. The *river network* sub-module is used as the basis for all river applications and was used to input information on river branches. One river (stream) branch was considered for this study and was generated in Arc-Hydro (Appendix B) before being inputted into the *river network* sub-module. Branch properties were defined for the inputted river branch (the branch properties are further explained in Appendix E; Table 4.6).

Table 4.6: Branch properties of the Two Streams stream.

Branch Property	**Model setting used**
Branch name	Two streams stream
Topo ID	Stream 1
Start chainage	0 m
End chainage	748.93 m
Flow direction	Positive
Branch type	Regular

The *map configurations* sub-module was used to define the river cross-sections. Under the *map configurations* sub-module the DEM for the site was input and the option to *use DEM for cross-section digitization* was selected. To generate the cross-sections the *auto generate cross-section* option under the tools tab was selected, the input requirements included the cross-section interval and cross-section width, an interval of 200m and a width of 100m were input and the cross-sections were generated (Figure 4.15).

Following the generation of the river network and river cross-sections all data were exported as MIKE 11 files (Figure 4.13), which all together, made up the *MIKE 11 simulation file*, and were then inputted into the MIKE SHE *rivers and lakes module* (Figure 4.13). The MIKE SHE *rivers and lakes module* is used to direct the MIKE SHE software to the *MIKE 11 simulation file* (for more information on the MIKE 11 and MIKE SHE *rivers and lakes module* set-up, refer to Appendix E).

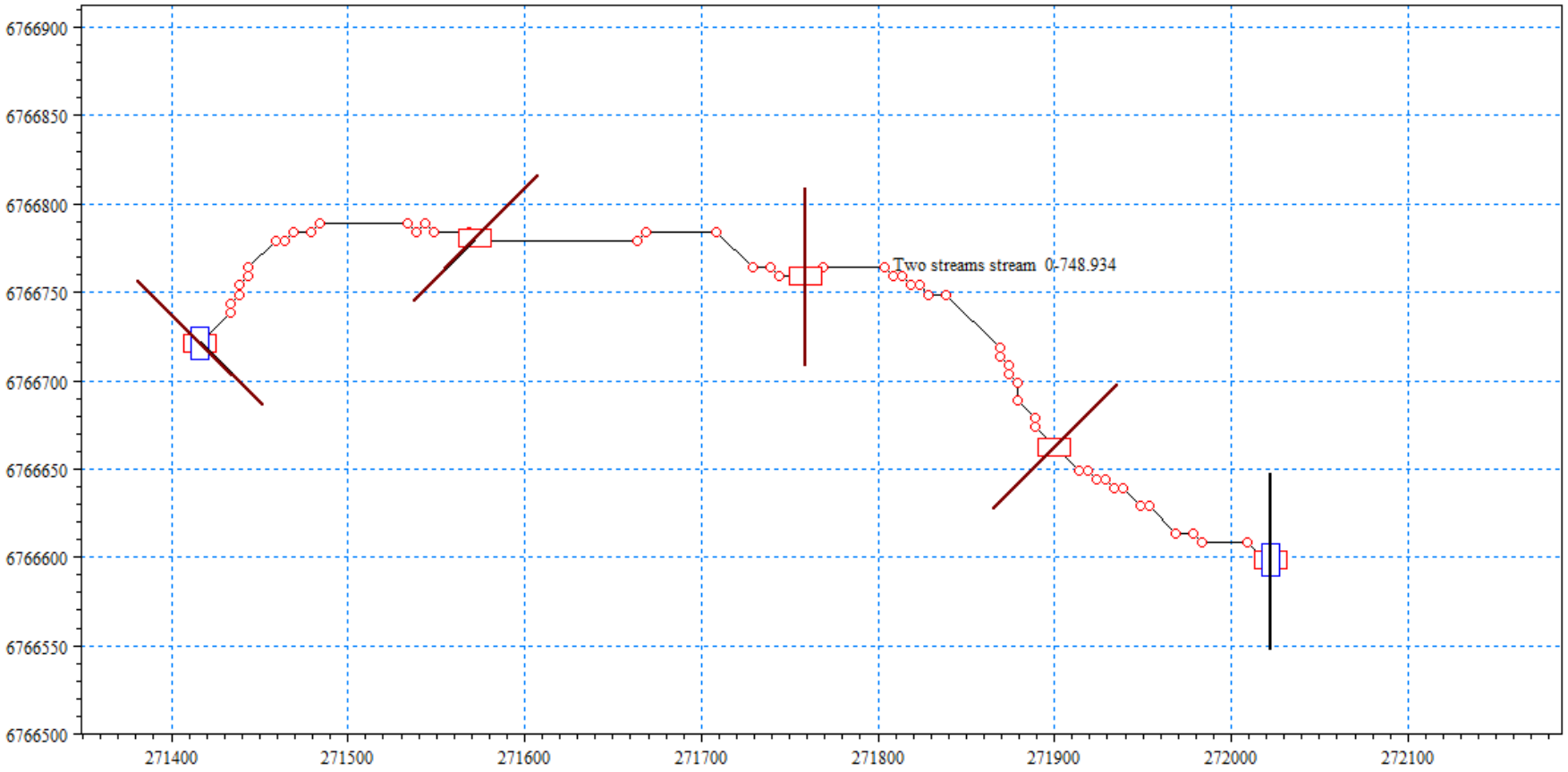

Figure 4.15: Model screen display showing the locations of the cross-sections generated along the length of the Two Streams stream. The stream is mapped on a geo-reference grid (m). The red boxes indicate where cross-sections were generated and the black lines perpendicular to the stream indicate the length and angle the cross-sections were captured at. The blue boxes indicate the start and end chainage points of the river.

4.3.8 Unsaturated flow module

The *unsaturated flow module* (Figure 4.2) in MIKE SHE considers the vertical movement of soil water. The UZ in the hydrological cycle is normally heterogeneous, experiencing dynamic, cyclic changes in soil water when water is added to the system through rainfall, removed through ET, and when water moves through the UZ to the SZ to form GR (DHI software, 2012).

Prior to working in the *unsaturated flow module*, the method used to calculate vertical flow was selected under the simulation specification module (Figure 4.4). There were three options to select from: the full *Richards equation*, a simplified *gravity flow* procedure and a simple *two-layer water balance method*. The full *Richards equation* is the most thorough method when dealing with dynamic unsaturated flow. The simple *two-layer water balance method* is the most simplified method and is more suitable when the water table is shallow and when GR is primarily influenced by ET in the root zone (DHI software, 2012). For this study, the *Richards equation* method was chosen as there was sufficient hydraulic data available. Data used for the *unsaturated flow module* were taken from Kuenene (2013).

Under the *unsaturated flow module* there were certain selections that were made prior to the input of UZ characteristics. The selections included: the *calculation column classification type* (allowing for computational time to be decreased for larger study sites), *macropore flow* (allowing for the inclusion of macropores), and the *initial conditions* (the conditions of soil pressure and water content for the start of the simulation; DHI software, 2012). The study site area is small (79.16ha), therefore the *calculate in all grid points* option was chosen for the *calculation column classification type*. The *none* option was chosen for the *macropore flow* on-site, as the presence of macropores on-site is unknown. The *equilibrium pressure profile* option was chosen for the *initial conditions* as the initial conditions at the start of the simulation were not known and this option overcomes this constraint (Figure 4.16).

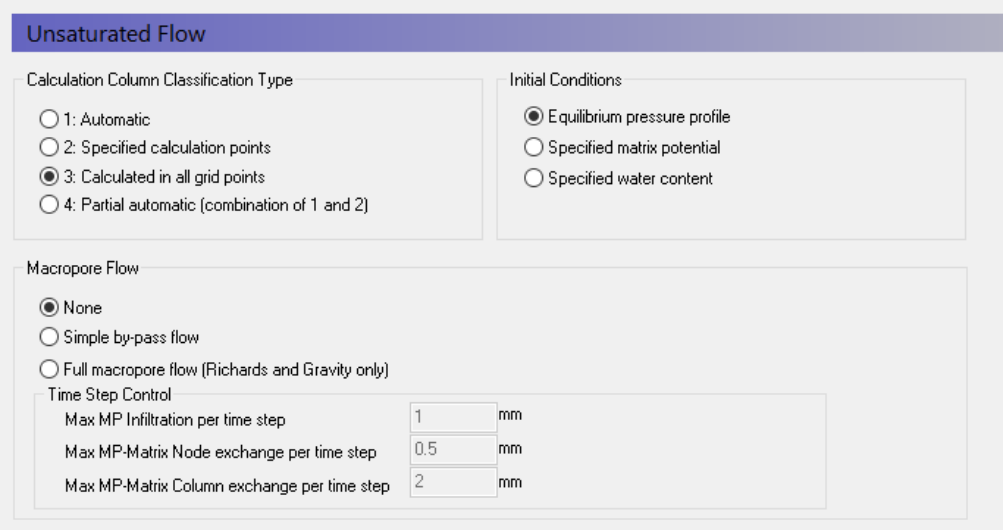

Figure 4.16: Available selection options in the unsaturated zone and the options selected for this study.

4.3.8.1 Soil profile definitions

Kuenene (2013) studied the hydropedological characteristics of the Two Streams sub-catchment and identified seven soil forms, namely: Kranskop (*Kp* 1100), Inanda (*Ia* 1100), Magwa (*Ma* 1200), Katspruit (*Ka* 1000), Oakleaf (*Oa* 1220/1210), Clovelly (*Cv* 2100) and Griffin (*Gf* 1100; Figure 4.17).

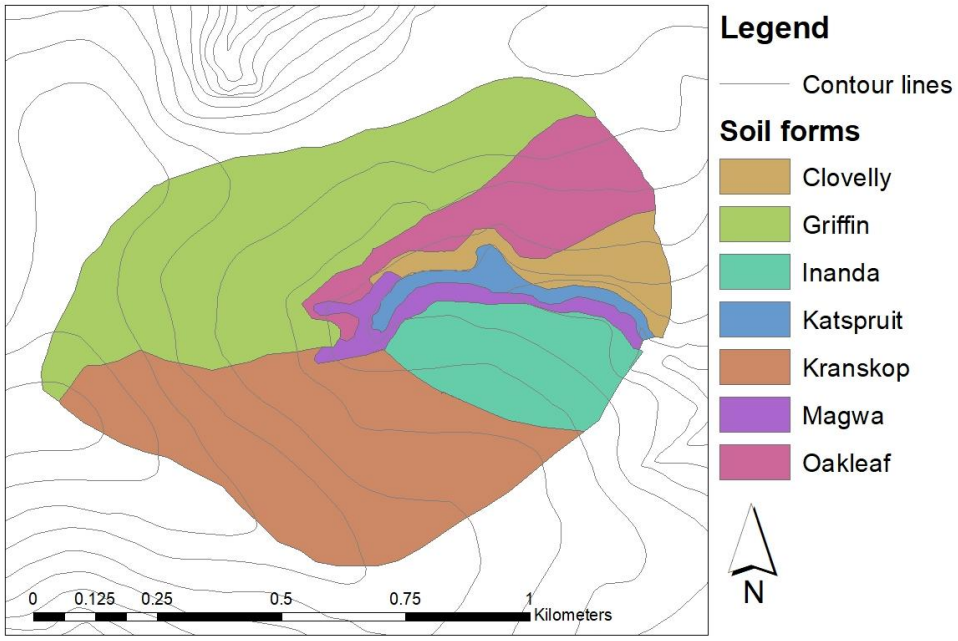

Figure 4.17: Soil map showing the soil forms of the Two Streams sub-catchment (Kuenene, 2013).

The spatially distributed soil data for the Two Streams sub-catchment were input as a .dfs2 file under the soil definitions sub-module of the *unsaturated flow module*. Once input, various hydraulic characteristics were specified for each soil type, including: saturated moisture content (θ_s), residual moisture content (θ_r), and saturated hydraulic conductivity (Ks; Table 4.7; Table 5.3).

Table 4.7: Soil hydraulic characteristics of the soil horizons of the Two Streams sub-catchment (Kuenene, 2013).

Soil form	**Soil horizon**	**Accumulated depth of horizon (mm)**	**Retention curve and Hydraulic conductivity**					**Bulk density ($Mg.m^{-3}$)**
			θ_s ($cm^3.cm^{-3}$)*	**θ_r ($cm^3.cm^{-3}$)***	**α (cm^{-1})***	**n***	**K_s ($m.s^{-1}$)***	
Kranskop *Kp 1100*	ah	400	0.60	0.01	0.02	1.24	1.97×10^{-5}	1.08
	ye	800	0.60	0.08	0.04	1.29	9.53×10^{-5}	1.19
	re	2500	0.54	0.11	0.05	1.34	1.03×10^{-4}	1.24
Inanda *Ia 1100*	ah	400	0.55	0.16	0.04	1.69	1.75×10^{-5}	1.33
	re	2000	0.52	0.21	0.03	1.69	6.39×10^{-5}	1.38
Magwa *Ma 1200*	ah	400	0.54	0.03	0.02	1.21	1.69×10^{-5}	1.06
	ye	1000	0.55	0.21	0.03	1.54	4.94×10^{-5}	1.31
	on	2000	0.54	0.16	0.02	1.45	4.72×10^{-6}	1.34
Katspruit *Ka 1000*	ot	1000	0.62	0.23	0.04	1.83	8.33×10^{-6}	0.95
	G	1200	0.54	0.14	0.05	1.62	1.47×10^{-5}	1.25
Oakleaf *Oa 1220/1210*	ot	400	0.575	0.16	0.025	1.58	5.94×10^{-5}	1.18
	ne	1750	0.535	0.15	0.06	1.63	7.94×10^{-5}	1.33
Clovelly *Cv 2100*	ot	400	0.57	0.15	0.04	1.53	1.83×10^{-5}	1.2
	ye	800	0.53	0.17	0.02	1.76	8.25×10^{-5}	1.25
Griffin *Gf 1100*	ot	400	0.58	0.17	0.04	1.77	2.44×10^{-5}	1.16
	ye	800	0.57	0.11	0.03	1.37	6.25×10^{-5}	1.31
	re	2500	0.54	0.08	0.06	1.26	5.81×10^{-5}	1.33

*θ_s is the saturated moisture content; θ_r is the residual moisture content; α is the inverse of the air entry value; n is the shape parameter; and Ks is the saturated hydraulic conductivity.

Once inputted into the model, MIKE SHE uses the input values to generate soil water retention curves (SWRC; Appendix F) and hydraulic conductivity functions for each soil horizon. Within MIKE SHE

the SWRCs were defined by the van Genuchten model (1980; Equation 4.5). Soil water retention curves (SWRCs) are used to describe the relationship between soil moisture suction (pf) and soil moisture content ($cm^3.cm^{-3}$; DHI software, 2012). The van Genuchten model is one of the most widely used empirical models for describing SWRCs as it is effective for a broad range of soils (Xiang-Wei *et al*., 2010). Within MIKE SHE the hydraulic conductivity function was defined by the Brooks and Corey (1964) model (Equation 4.6), where unsaturated hydraulic conductivity provides a measure of the rate at which water moves through the UZ (DHI software, 2012)

$$\theta(h) = \left[(\theta_s - \theta_r)\left(\frac{1}{1 + (\alpha h)^n}\right)^m\right] + \theta_r$$

Equation 4.6: Van Genuchten soil water retention curve function (DHI software, 2012).

$$K(\theta) = K_{sat}\left(\frac{\theta - \theta_r}{\theta_s - \theta_r}\right)^N$$

Equation 4.7: Brooks and Corey model for soil hydraulic conductivity (DHI software, 2012).

Where: $\theta(h)$ is the water retention curve ($cm^3.cm^{-3}$); h is the suction pressure of the water (cm); θ_s is the saturated water content ($cm^3.cm^{-3}$); θ_r is the residual water content ($cm^3.cm^{-3}$); α is is the inverse of the air entry value (cm^{-1}); and n and m are shape parameters of the van Genuchten relation (unitless); K_{sat} is the saturated hydraulic conductivity ($cm.day^{-1}$); and N is the Brooks and Corey shape parameter (DHI software, 2012).

4.3.9 Saturated groundwater flow module

The *saturated groundwater flow module* (Figure 4.2), in MIKE SHE was used to calculate the saturated subsurface flow and to input geological data. Under the simulation specification module there were two methods to select from for calculating saturated groundwater flow, the *finite difference method* and the *linear reservoir method*. The *finite difference method* allows for the consideration of three-dimensional flow in a heterogeneous aquifer with variations between unconfined and confined

conditions (DHI software, 2012). The *linear reservoir method* provides an alternative to the physically based *finite difference method* and is a compromise between limitations on data availability, the complexity of hydrological response at the catchment scale, and the advantages of model simplicity (DHI software, 2012). For this model, the *finite difference method* was selected as was the case in the *unsaturated flow module* and MIKE SHE requires the continuation of this physics based method (Figure 4.4). However, there were limited data available for the SZ of the Two Streams sub-catchment as research on-site has tended to focus on the surface and UZ (Everson *et al*., 2006, 2014; Clulow *et al*., 2011) and not the SZ.

4.3.9.1 Geological layers sub-module

The underlying geology of the Two Streams sub-catchment was identified as Natal Sandstone by the Council for Geosciences; based on a 1:1000000 geological map. To-date no geological study has been conducted within the Two Streams sub-catchment and thus the hydraulic characteristics of the geology had not been investigated. Various parameters needed to be defined for the geological layer under the *geological layers* sub-module including: *vertical hydraulic conductivity*, *horizontal hydraulic conductivity*, *specific yield* and *specific storage*. None of these parameters had been measured on-site and were all assumed to be uniform across the site (due to data limitations). Values for all of these parameters were taken from recent literature (Demlie and Titus, 2015) or default MIKE SHE values as recommended by the Danish Hydrological Institute (DHI) technical team. The *hydraulic conductivity* is a function of the texture of a material (i.e. soil, rock or vascular plant) and is related to the ease with which water can flow through the material (DHI software, 2012); the *hydraulic conductivity* was assigned a value of $3.20 \times 10^{-5} m.s^{-1}$ (Demlie and Titus, 2015). *Specific yield* is the volume of water released per unit surface area of aquifer per unit decline in head (DHI software, 2012). The specific *yield* was given a value of 1.00×10^{-3}, default value (Appendix A). The *specific storage* (m^{-1}) is the volume of water released per volume of aquifer per unit decline in head (DHI software, 2012); the *specific storage* was given a value of $1.90 \times 10^{-3} m^{-1}$ (Demlie and Titus, 2015).

4.3.9.2 Computational layers sub-module

Under the *computational layers* sub-module the following inputs were required for the Natal Sandstone geological layer: the *initial potential head, outer boundary conditions* and the *internal boundary conditions*. For this study, no *internal boundary conditions* were specified. The *initial potential head* is the starting head for the simulation and the initial 'guess' for steady-state simulations (DHI software, 2012). Data on the *initial potential head* were taken from the water table of the area which was defined using borehole data. There were three boreholes on-site (at the time of the start of the simulation), the data from these boreholes recorded during 2007 – the earliest date recorded to the start of the simulation was 11 October 2007 – were interpolated in ArcGIS 10.3 to produce a water table level for the site. The Inverse Distance Weighting (IDW) interpolation method was used. Once the water table was interpolated it was introduced into MIKE SHE as a .dfs2 file. Thereafter, the water table was subtracted from the topography .dfs2 file to determine elevation above sea level (Figure 4.18).

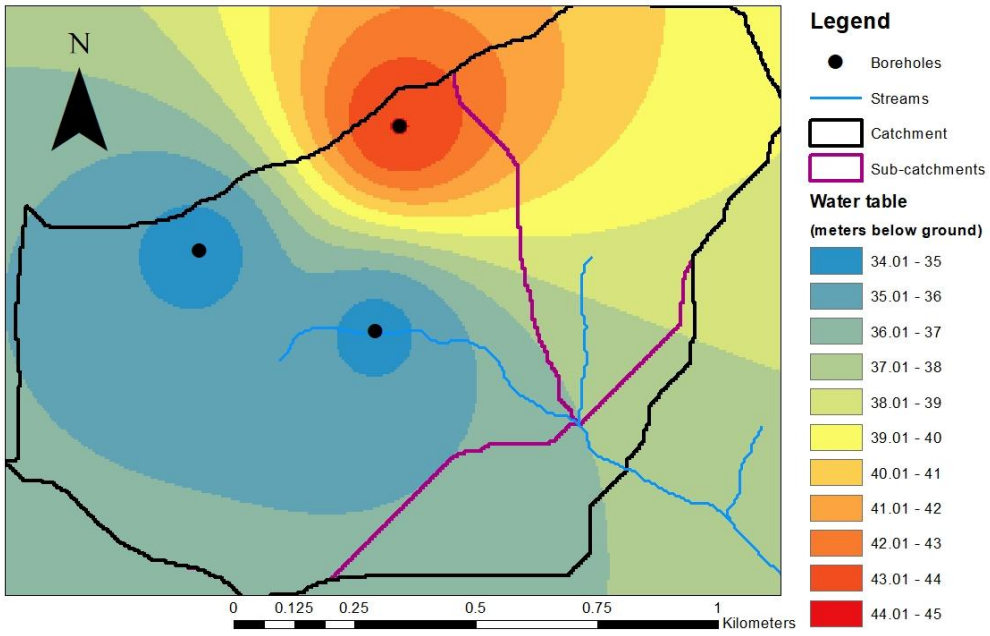

Figure 4.18: Initial water table depth of the Two Streams catchment and sub-catchments for the 11th of October 2007 (the closest date to the start of the simulation – the 14th of February 2007).

The *outer boundary conditions* define the external boundaries of the SZ (DHI software, 2012). There are four possible boundary conditions from which to choose to describe the outer boundary conditions: *fixed head, zero-flux, flux* and *gradient* (DHI software, 2012). *Fixed head* – this option is selected when a head is introduced in the boundary (DHI software, 2012). The *fixed head* can be introduced as a fixed value (m) or as the initial value or it can be linearly interpolated from a time series file (i.e. .dfs0 or .dfs2; DHI software, 2012). *Zero-flux* - this option indicates a no-flow boundary and is the default option in MIKE SHE (DHI software, 2012). *Flux* – this option is used to define constant or time varying flux boundaries where a positive value indicates an inflow into the model (DHI software, 2012). A time varying flux boundary is specified as either a mean step-accumulated streamflow (e.g. $m^3.s^{-1}$) or as a step-accumulated volume (e.g. m^3; DHI software, 2012). *Gradient* – this option is used to describe a gradient (either constant or time varying) that exists between the outer boundary and the internal conditions of the model, where a positive gradient implies a flux into the model. A time varying gradient can either be specified as an instantaneous value or as a percentage (DHI software, 2012). For this study, the outer boundary was specified as having a *zero-flux* boundary. There were limited data available on the SZ of the site, thus no information was available to accurately specify the boundary conditions. However, as the sub-catchment boundary (which defines the extent of the study site) was hydrologically defined for the sub-catchment, a zero flux was assumed throughout.

4.4 Calibration and validation of the MIKE SHE current scenario model

Once the MIKE SHE current scenario model was set-up, the *preprocessed data tool* was run, converting all raw input data into processed data – as the model uses the processed data to run the MIKE SHE model. Following preprocessing, the model was then run against observed findings to determine how well the modelled outputs fit the observed record. Unlike conceptual models, physically-based models do not require extensive hydrological and meteorological data for calibration (Merritt *et al*., 2003; Devi *et al*., 2015); rather physically-based models require a large number of

input parameters to describe the physical characteristics of the sub-catchment (Devi *et al*., 2015; Ma *et al*., 2016). Thus, less emphasis was placed on model calibration than on model set-up.

Calibration and validation of model results is undertaken to build confidence in the model set-up (Singh *et al*., 2017). The observed (measured) datasets used to compare the modelled outputs were streamflow and ET_A. The relationships between the modelled outputs and observed records were analysed through linear correlation and the Pearson's correlation coefficient (r), Root Mean Square Error (RMSE) and tests of statistical significance (discussed further in section 4.6.2). Where the observed and modelled outputs did not relate well or where the relation needed to be improved, calibration was undertaken. Very minimal calibration was undertaken (the process of model calibration and validation is further explained in chapter five).

4.4.1 Storing of results module

To compare the observed data to the MIKE SHE modelled outputs the observed datasets were input into the MIKE SHE set-up under the *storing of results module*. There are three sub-modules under the *storing of results module*: *detailed time series output*, *detailed M11 time series output* and *grid series output*. The *detailed time series output* sub-module allows the user to include specific location time series observed datasets (DHI software, 2012). The observed ET_A record was included under this sub-module. Observed ET_A was measured using a number of different techniques over the years of data collection: large aperture scintillometer, and eddy covariance and surface renewal techniques were employed (Clulow *et al*., 2011; Everson *et al*., 2014). The *detailed M11 time series output* allows the user to add an observed dataset on water level or streamflow (discharge) at a specific chainage point (DHI software, 2012), whereby chainage refers to a measure of distance (DHI software, 2012). The streamflow record was input under this sub-module. The *grid series output* sub-module allows the user to select for the result outputs that will be produced by the model run (DHI software, 2012). Within the *grid series output* sub-module the outputs necessary for water balance calculations were identified and selected for.

4.4.2 MIKE SHE current scenario model run

Once the MIKE SHE current scenario data inputs were processed, the model could be run and the time series data outputs (specified in section 4.4.1) were produced. Once the model run was completed, the modelled *detailed time series output* and the *detailed M11 time series output* could be compared to the observed findings. In addition, water balance calculations for the MIKE SHE current scenario were generated using the *water balance* (.wbl) utility.

Within the MIKE SHE software package, there is a *water balance* utility, which was used to generate water balance data for MIKE SHE simulations. The water balance outputs that can be generated include: water balance diagrams (showing storage depths and storage changes) and model error calculations (Appendix G) – both of which were generated for this study. As part of the model validation process, a water balance summary diagram was generated as it includes a value (mm) for model calculation error. Where an error value greater or smaller than 0mm indicates that the outflows and inflows to the system are not balanced, and thus provides an indication of how accurately the system was modelled.

In addition to providing a value for model calculation error, the water balance summary diagram displays the normalized flows (storage depths), storage changes and model error over a specified time interval (DHI software, 2012). The normalization of values allows for different models or model areas to be compared (DHI software, 2012). The direction of flow is represented by arrows, whilst values with no arrows are indicative of storage. All flows leaving the model and increasing storage are positive. Water balance errors will be positive if the model is generating too much water and the closer the error value is to 0 mm the less calculation difficulty experienced and the better balanced the flow of water in the simulated site (DHI software, 2012). The water balance summary diagram was generated for the total current scenario simulation period, from the 14th of February 2007 – 2nd of

October 2016. Once the model water balance error was determined, the model error was further interpreted to identify where the error occurred within the modelled system.

4.4.3 MIKE SHE current scenario model alterations

As part of the calibration and validation process, the MIKE SHE current scenario model underwent some refinements to provide a better representation of the Two Streams sub-catchment. The model alterations made are described under the MIKE SHE calibration and validation results section (section 5.4).

4.5 MIKE SHE model set-up – future scenario

The future scenario considered the impact a change in forestry plantation, from black wattle (*A. mearnsii*) to *E. dunnii*, would have on the hydrological components of the Two Streams sub-catchment. The future scenario was modelled from the calibrated MIKE SHE current scenario. For the future scenario most of the modules from the current scenario were kept constant, changes were concentrated predominantly in the *land use module*. All changes made to the current scenario are described below.

4.5.1 Simulation specification module

In the *simulation specification module*, the same modules selected for the current scenario were kept constant (Figure 4.4). The only changes to the *simulation specification module* were made to the *simulation title* and the *simulation period*. The *simulation title* was changed to 'Future scenario Two Streams 2019 to 2028' and the *simulation period* was changed to the 14th of February 2019 to the 2nd of October 2028. The simulation dates were chosen to ensure the *simulation period* remained the same as the current scenario *simulation period*, for ease of comparison between the current and future scenario results. The months simulated in the future scenario were kept the same as those in the current scenario simulation to ensure that the climatic data used under the current scenario were relevant for the future scenario.

4.5.2 Modules kept constant for the future scenario

The *model domain and grid module*, for the future scenario, remained the same as for the current scenario, as the study site extent did not change (Figure 4.6). The *topography module* was kept the same as for the current scenario (Figure 4.7). To calculate OL, in the *overland flow module*, information on three categories was required: Manning number, detention storage and initial water depth. Detention storage was maintained at 2mm and initial water depth was maintained at 0mm, as with the current scenario. The Manning numbers stipulated for the riparian and sugarcane (*S. officinarum*) classes were kept the same as for the current scenario. The Manning number used for the black wattle stand was representative of a 'rough' forestry site with a value of 10. For the *E. dunnii* plantation the Manning number was 10 (same as that of the black wattle plantation), as it is a plantation forestry site with a high resistance to flow (Morgan, 2005). Within the *unsaturated flow module*, no changes were made to the soil properties used in the current scenario. Within the *saturated groundwater flow module* no changes were made to the geological layers properties used or to the computational layers properties used for the current scenario.

4.5.3 Climate module

The time series files (.dfs0) created for the MIKE SHE current scenario time period (14 February 2007 – 02 October 2016) were modified to the future scenario time period (14 February 2019 – 02 October 2028). Beside the changes in dates, all climatic data, *precipitation rate* and *reference evapotranspiration*, were kept the same for both the current and future scenarios. A total of 3519 days were modelled in both scenarios.

4.5.4 Land use module

The *land use module*, particularly the black wattle (*A. mearnsii*) vegetation class, was altered for the future scenario to capture the change in vegetation from *A. mearnsii* to *E. dunnii*. There is a paucity of information on *E. dunnii* in the literature, with few to no studies pertaining to LAI or RD. Grant *et al*.

(2012) discuss the distribution of roots of *E. dunnii* under different soil conditions. However roots were only considered to a depth of 1m, thus not providing any information on the depth to which roots extend. To account for the lack of information, data were considered on other *Eucalyptus* species including *E. grandis, E. nitens*, and *E. globulus*. Based on a number of studies (Canadell *et al*., 1996; Battaglia *et al*., 1997; du Toit and Dovey, 2005; Dovey and du Toit, 2006; Dye *et al*., 2008; Le Maire *et al*., 2011) average LAI and RD values were derived, LAI = 3.8 and RD = 8m. The future scenario was modelled over a ten-year period. The first three years of the simulation were modelled with lower LAI and RD values to account for the growth of the newly planted *E. dunnii* plantation, a linear increase in both the LAI and the RD values was assumed for this study (Table 4.8). A linear increase over a short period of time was used as, according to van Dijk and Keenan (2007) in plantation forestry there is a high numbers of stems per hectare planted and thus canopy closure can be achieved rapidly. In addition, *Eucalyptus* plantations have rapid growth rates and are capable of rapid canopy growth if resource availability is conducive (du Toit and Dovey, 2005), as was assumed in this study.

Table 4.8: Leaf Area Index (LAI) and Rooting Depth (RD) values used for *E. dunnii* in the MIKE SHE, future scenario, *land use module*.

Date	**LAI**	**RD (m)**
2/14/2019	0	0
2/14/2020	1.27	4
2/14/2021	2.58	8
2/14/2022 – 10/02/2028	3.8	8

4.5.5 Rivers and lakes module

The river data for the 'Two streams stream' were extended for the future scenario. However, the simulation period was changed to represent that of the future scenario. Other than changes to the simulation period, all data used in the *rivers and lakes module* remained the same.

4.6 Analysis of the MIKE SHE scenario results

To analyze the MIKE SHE results produced from both the current (post validation) and future scenario model simulations, water balance calculations were undertaken and time series data of various water balance components were generated, investigated, compared and statistically analyzed using non-parametric statistical tests. Non-parametric statistical tests were employed over parametric tests as the time series datasets were not found to be normally distributed (Appendix H).

4.6.1 Time series outputs

For the MIKE SHE current scenario, time series outputs were generated for nine water balance components: ET_A, E_t, E_s, evaporation from ponded water (E_p), E_i, canopy interception storage (CIS), depth of OL, I_{UZ}, and GR. These components were assessed for each of the three vegetation classes modelled: sugarcane, riparian and black wattle. For the MIKE SHE future scenario, time series outputs were generated for the *E. dunnii* vegetation class, for the same water balance components as considered for the MIKE SHE current scenario, for ease of comparison with the black wattle outputs.

All time series outputs were made-up of normalized values with units in mm for ease of consistency in comparisons. The time series data were assessed at different temporal scales considering the total, (based on the total simulation period from 14 February 2007 – 02 October 2016), annual, monthly, seasonal and daily data records for each component of each vegetation class. To assess seasonal differences, two seasons were defined dividing the year between the six wettest months (October to March) and the six driest months (April to September), these months formed the summer and winter seasons respectively.

4.6.2 Statistical analysis

The differences in the total and seasonal time series outputs, for the different vegetation classes, were statistically analyzed using 'R' software. Each component considered was tested for normality using the chi-square goodness-of-fit test (Appendix H). The chi-square statistical test provides a measure of

the goodness-of-fit between an observed and an expected dataset (Ghasemi and Zahediasl, 2012). The result of the normality test determined whether parametric or non-parametric tests would be undertaken (Appendix H). For this study non-parametric tests were used (Appendix H): the Kruskal Wallis test by ranks and the two-sample Wilcoxon's signed rank tests. The two-sample Wilcoxon's signed rank test is used to compare the medians of the two populations of concern (Chandler and Scott, 2011). The Kruskal Wallis test by ranks is used for testing whether samples arise from the same distribution. It is used to compare two or more independent samples that are either of equal or different sample size (Chandler and Scott, 2011). Linear regression analysis was carried out to determine the relationship between the different water balance components and the Pearson's correlation coefficient (r) of each linear relationship was determined. RMSE calculations were undertaken to measure the differences between modelled values and the observed values.

4.7 Summary

This chapter detailed the procedure taken in setting up two MIKE SHE model scenarios (current and future) including all input requirements – those which were sourced from past research or literature, those generated or verified through fieldwork and those generated digitally. In addition to the set-up procedures, this chapter detailed the calibration and validation procedure undertaken and the statistical analysis employed in comparing vegetation classes both within and across the two MIKE SHE scenarios (current and future). The model set-up process was written in a sequential approach whereby model inputs are driven by model processes that are used to generate model outputs. Where inputs needed to be generated and are technically results they were included within the methods section for ease of understanding of the sequence followed. Results included in the methods section were: the sub-catchment hydrological boundary, LAI for the riparian vegetation class based on satellite imagery, the river network, river cross-sections, and the interpolated initial water table depth. The methods ultimately detail the procedure taken to address the research aims and objectives of this study.

Chapter Five

MIKE SHE model input characteristics, calibration and validation

5.1 Introduction

This chapter comprises both results and a discussion section and focuses on determining whether the MIKE SHE current scenario model provides a good representation of the Two Streams sub-catchment, by comparing the modelled and observed datasets. The results section describes the biophysical conditions of the sub-catchment, the fieldwork findings and the model calibration and validation process undertaken. The results section distinguishes between ET_{ref} and ET_A records. The discussion section describes the key findings, model uncertainty, the benefits and limitations of the MIKE SHE model and future areas of research.

5.2 Biophysical characteristics of the site

The Two Streams sub-catchment is approximately 79.16ha in size, covering 62.10% of the total catchment area. For the MIKE SHE current scenario, there are three vegetation classes of interest, within the sub-catchment: black wattle (*A. mearnsii*) plantation forestry covering 58.17% of the study site (approximately 46ha), sugarcane (*S. officinarum*), 26.43% (approximately 21ha) and riparian vegetation, 7.36% (approximately 6ha). The average elevation of the sub-catchment is 1092m, ranging from 1028 – 1121m. The black wattle vegetation class has the greatest elevation range and covers the largest area, whilst the sugarcane class has the smallest elevation range (Table 5.1).

Table 5.1: Elevation characteristics of the black wattle, riparian and sugarcane vegetation classes.

Land cover type	Minimum elevation (m)	Maximum elevation (m)	Elevation range (m)	Mean elevation (m)	Standard deviation
Black wattle (*A. mearnsii*)	1043	1111	68	1089	13.81
Riparian	1029	1088	60	1059	11.16
Sugarcane (*S. officinarum*)	1086	1121	35	1106	7.75
Total sub-catchment	**1029**	**1121**	**93**	**1092**	**16.92**

Over the simulation period, rainfall occurs over 1959 days (55.70% of the total days) amounting to 7160.20mm, with annual precipitation ranging from 460 – 960mm, with 2012 experiencing the highest annual rainfall and 2015 the lowest (Figure 5.1). Maximum monthly rainfall is recorded for November 2007 (191.10mm) and minimum for July 2007 (0.30mm). Considering daily rainfall (Figure 5.1), maximum daily rainfall is recorded on the 12th of December 2015 (75.7mm), whilst the lowest rainfall of 0mm is recorded for 1561 days of the simulation.

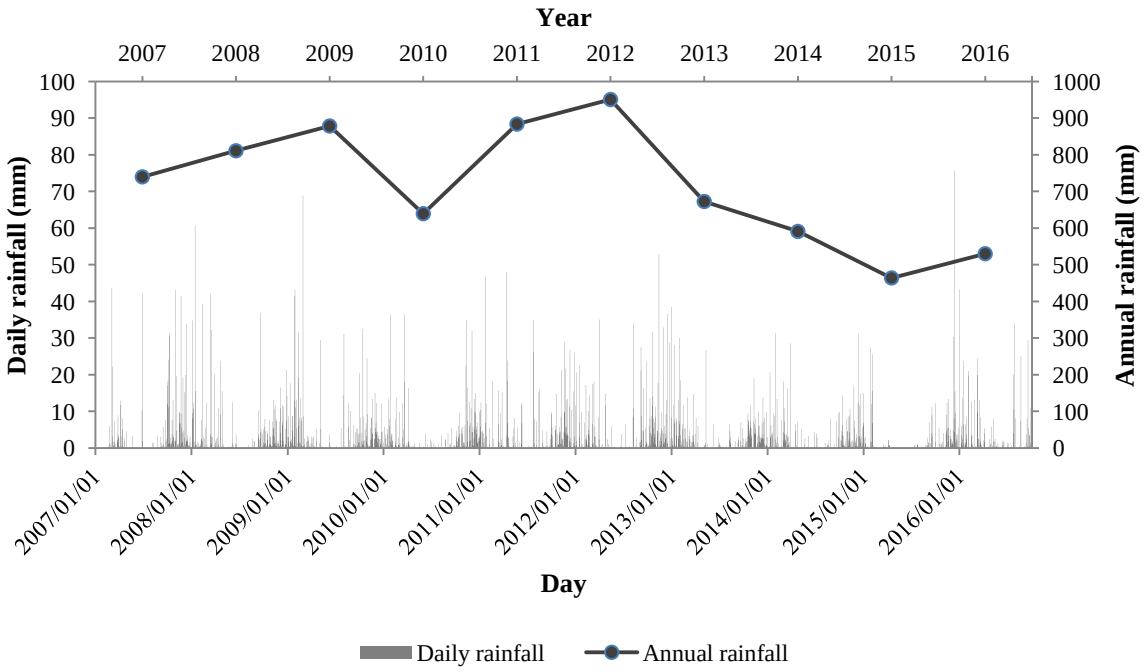

Figure 5.1: Daily and annual rainfall (mm) records that extend from the 14th of February 2007 – 2nd of October 2016, for the Two Streams study site.

The daily ET_{Ref} record (Figure 5.2) was calculated using the FAO Penman-Monteith equation (described under Appendix C) and ranges from 0.01 – 8.08mm, over the simulation period. The cyclic fluctuations in the daily record reflect seasonal changes, with the winter months experiencing lower ET rates than the summer months.

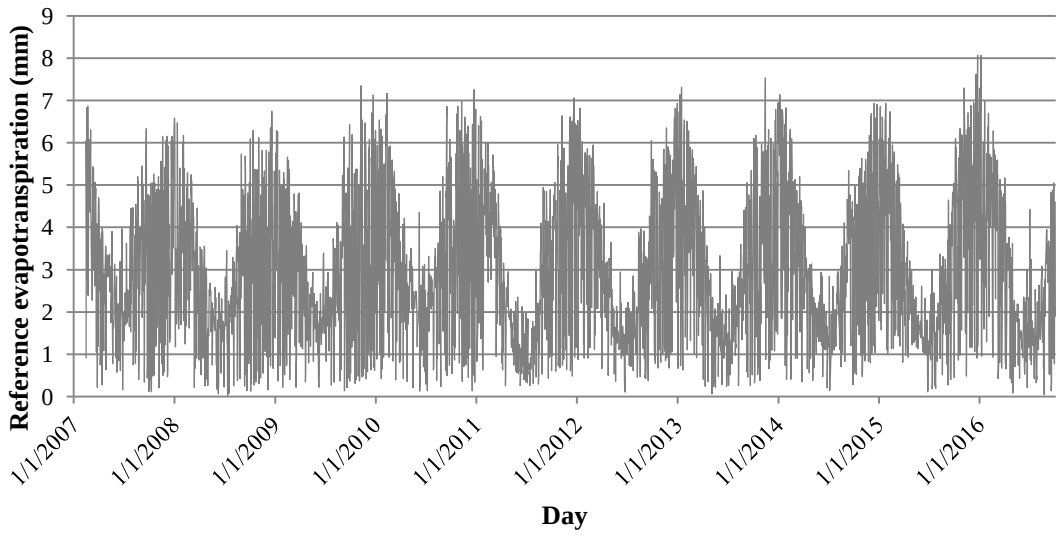

Figure 5.2: Daily reference evapotranspiration (mm) for the Two Streams study site, extending from the 14th of February 2007 – 2nd of October 2016, based on the Penman-Monteith method. Horizontal gridlines included for ease of graph interpretation.

The Two Streams sub-catchment comprises seven soil types (Table 5.2), as classified by Kuenene (2013). The dominant soil types are Kranskop (*Kp* 1100) and Griffin (*Gf* 1100), covering 29 and 35.03% of the sub-catchment respectively. Magwa (*Ma* 1200) and Katspruit (*Ka* 1000) soils cover the smallest portion of the sub-catchment, 3.56 and 2.99% respectively (Table 5.2). Within the three vegetation classes, the sugarcane class comprises predominantly of Griffin (15.21ha), riparian of Magwa (2.24ha) and black wattle of Kranskop (16.38ha; Table 5.2).

Table 5.2: The Soil types of the Two Streams sub-catchment and the soil type coverage extents (ha) in relation to the total area and to the individual vegetation class areas.

Soil type	**Vegetation class**	**Extent of soil coverage of the vegetation class (ha)**	**Total extent of soil coverage (ha)**	**Percentage of total area (%)**
Kranskop (Kp 1100)	Sugarcane	6.43	22.96	29.00
	Riparian	0.15		
	Black wattle	16.38		
Inanda (Ia 1100)	Sugarcane	0	9.15	11.56
	Riparian	0.85		
	Black wattle	8.30		
Magwa (Ma 1200)	Sugarcane	0	2.82	3.56
	Riparian	2.24		
	Black wattle	0.58		
Katspruit (Ka 1000)	Sugarcane	0	2.37	2.99
	Riparian	2.08		
	Black wattle	0.29		
Oakleaf (Oa 1220/1210)	Sugarcane	0.06	8.92	11.27
	Riparian	0.02		
	Black wattle	8.84		
Clovelly (Cv 2100)	Sugarcane	0	5.21	6.58
	Riparian	0.53		
	Black wattle	4.68		
Griffin (Gf 1100)	Sugarcane	15.21	27.73	35.03
	Riparian	3.85×10^{-3}		
	Black wattle	12.52		
Total			79.16	100

Soil texture on-site ranges from fine sandy clay loam to coarse sandy loam (Table 5.3; Kuenene, 2013); with the majority of the soil horizons having a sandy clay loam texture (Table 5.3). The unsaturated soil hydraulic conductivities of the soils range from $4.72 \times 10^{-6} – 1.03 \times 10^{-4}$ $m.s^{-1}$ (Table 5.3). The mean slope on-site ranges from 3.81-11.39˚ for all soils with a maximum slope standard deviation of ±5.51 (Table 5.3). The upland area of the site comprises mostly of Kranskop and Griffin soils, both of which have a relatively low average slope of 4.20˚ (±1.99) and 3.81˚ (±2.18) respectively (Table 5.3). Moving down into the riparian zone the slopes become steeper with the Clovelly and Katspruit soils having the steepest average slopes of 11.39˚ (± 5.51) and 9.06˚ (± 5.28; Table 5.3).

Table 5.3: The soil types of the Two Streams sub-catchment, indicating the horizons, textural classes and slope characteristics of each soil type.

Soil type	Soil horizon	Texture	Hydraulic conductivity ($m.s^{-1}$)	Mean slope (°)	Slope standard deviation
Kranskop	ah	Sand clay loam	1.97×10^{-5}	4.20	1.99
	ye	Sand clay loam	9.53×10^{-5}		
	re	Sand clay loam	1.03×10^{-4}		
Inanda	ah	Sand clay loam	1.75×10^{-5}	8.03	3.82
	re	Clay loam	6.39×10^{-5}		
Magwa	ah	Sand clay loam	1.69×10^{-5}	8.46	4.25
	ye	Clay loam	4.94×10^{-5}		
	on	Clay loam	4.72×10^{-6}		
Katspruit	ot	Clay loam	8.33×10^{-6}	9.06	5.28
	G	Sand clay loam	1.47×10^{-5}		
Oakleaf	ot	Sand clay loam	5.94×10^{-5}	6.41	2.27
	ne	Clay loam	7.94×10^{-5}		
Clovelly	ot	Loam	1.83×10^{-5}	11.39	5.51
	ye	Sand clay loam	8.25×10^{-5}		
Griffin	ot	Sandy loam	2.44×10^{-5}	3.81	2.18
	ye	Sand clay loam	6.25×10^{-5}		
	re	Sand clay loam	5.81×10^{-5}		

5.3 Fieldwork findings

The MIKE SHE model requires an extensive data input (as is evident from chapter four), one such input is LAI. The LAI for the riparian vegetation class was calculated using the LAI-2200 Plant Canopy Analyzer (LAI-2200 Plant Canopy Analyser, 2012), which is the updated version of the apparatus that was previously used to calculate the black wattle LAI of the Two Streams sub-catchment (refer to section 4.3.5; LAI-2000 Plant Canopy Analyzer, 1989). Twenty LAI samples were taken from the riparian vegetation class providing an average LAI of 2.69 and a standard deviation of 1.24 (Table 5.4).

Table 5.4: Leaf Area Index (LAI) measures for the riparian vegetation class, measured using the LAI-2200 Plant Canopy Analyzer. Measures were recorded in October 2017.

Point No.	**LAI**	**Location**	
		Latitude	**Longitude**
1	0.20	29˚12' 23.4" S	30˚39' 02.1" E
2	2.41	29˚12' 24.1" S	30˚39' 01.9" E
3	2.33	29˚12' 24.4" S	30˚39' 01.7" E
4	3.46	29˚12' 24.6" S	30˚39' 01.3" E
5	2.99	29˚12' 24.5" S	30˚39' 00.7" E
6	3.36	29˚12' 24.3" S	30˚39' 00.0" E
7	2.70	29˚12' 24.6" S	30˚38' 57.2" E
8	3.82	29˚12' 24.6" S	30˚38' 56.2" E
9	4.24	29˚12' 24.9" S	30˚38' 55.3" E
10	4.63	29˚12' 25.1" S	30˚38' 55.4" E
11	2.93	29˚12' 25.3" S	30˚38' 55.8" E
12	3.04	29˚12' 25.5" S	30˚38' 55.9" E
13	1.38	29˚12' 25.7" S	30˚38' 56.1" E
14	2.40	29˚12' 25.9" S	30˚38' 56.3" E
15	4.47	29˚12' 25.9" S	30˚38' 56.5" E
16	0.55	29˚12' 26.1" S	30˚38' 56.8" E
17	0.80	29˚12' 25.7" S	30˚38' 56.2" E
18	2.02	29˚12' 25.3" S	30˚38' 55.6" E
19	3.45	29˚12' 24.8" S	30˚38' 55.5" E
20	2.61	29˚12' 24.5" S	30˚38' 56.2" E
Average	**2.69**		
Standard deviation	**1.24**		

The LAI, calculated using the LAI-2200 Plant Canopy Analyzer, was compared to the LAI calculated from SPOT imagery (refer to section 4.3.5 on the calculation process). The SPOT imagery produced an average LAI, for the same 20 point locations of 2.21 and a standard deviation of 0.04 (Table 5.5).

Table 5.5: Leaf Area Index (LAI) calculated for the riparian vegetation class, using ArcGIS 10.3 software and SPOT imagery.

Point No.	**LAI**	**Location**	
		Latitude	**Longitude**
1	2.13	29˚12' 23.4" S	30˚39' 02.1" E
2	2.25	29˚12' 24.1" S	30˚39' 01.9" E
3	2.20	29˚12' 24.4" S	30˚39' 01.7" E
4	2.18	29˚12' 24.6" S	30˚39' 01.3" E
5	2.27	29˚12' 24.5" S	30˚39' 00.7" E
6	2.26	29˚12' 24.3" S	30˚39' 00.0" E
7	2.24	29˚12' 24.6" S	30˚38' 57.2" E
8	2.24	29˚12' 24.6" S	30˚38' 56.2" E
9	2.24	29˚12' 24.9" S	30˚38' 55.3" E
10	2.27	29˚12' 25.1" S	30˚38' 55.4" E
11	2.19	29˚12' 25.3" S	30˚38' 55.8" E
12	2.19	29˚12' 25.5" S	30˚38' 55.9" E
13	2.18	29˚12' 25.7" S	30˚38' 56.1" E
14	2.19	29˚12' 25.9" S	30˚38' 56.3" E
15	2.19	29˚12' 25.9" S	30˚38' 56.5" E
16	2.20	29˚12' 26.1" S	30˚38' 56.8" E
17	2.18	29˚12' 25.7" S	30˚38' 56.2" E
18	2.19	29˚12' 25.3" S	30˚38' 55.6" E
19	2.24	29˚12' 24.8" S	30˚38' 55.5" E
20	2.24	29˚12' 24.5" S	30˚38' 56.2" E
Average	**2.21**		
Standard deviation	**0.04**		

The LAI-2200 LAI and the SPOT LAI had a significant, positive, linear correlation (Figure 5.3), $r = 0.59$ ($P = 5.80 \times 10^{-3}$). There was, however, uncertainty in the SPOT LAI values due to the low imagery resolution (in relation to the size of the study site; discussed further under section 5.6.3). Therefore the LAI-2200 LAI values were deemed to be more representative, and the average LAI of 2.69 (Table 5.4) was used as the riparian LAI input.

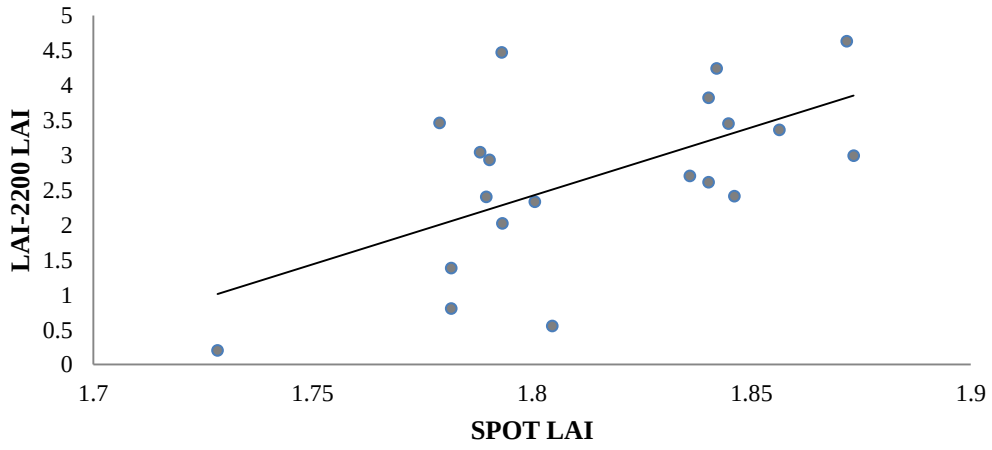

Figure 5.3: Scatter plot of the relationship between the Leaf Area Index (LAI) values calculated from the SPOT imagery and the LAI measures from the LAI-2200 Plant Canopy Analyzer.

5.4 MIKE SHE pre– calibration and validation model outputs

5.4.1 Comparing modelled outputs to observed records.

The observed ET_A record (used to compare to the model ET_A record), is based on data previously recorded from the black wattle class (29°12'19.2''S; 30°39'1.3''E; Clulow *et al*., 2011), over the period 01 October 2011 – 25 October 2013 (Figure 5.4). Over this 756 day period, the total observed ET_A amounted to 2287.70mm. Daily observed ET_A ranged from 0 – 8.10mm, with an average rate of 3.03mm (standard deviation = 1.59). The modelled ET_A record, modelled for the same location over the same time period (Figure 5.4), had a total ET_A rate of 1899.91mm, ranging from 0.05 – 6.24mm, with an average rate of 2.51mm (standard deviation of 1.42).

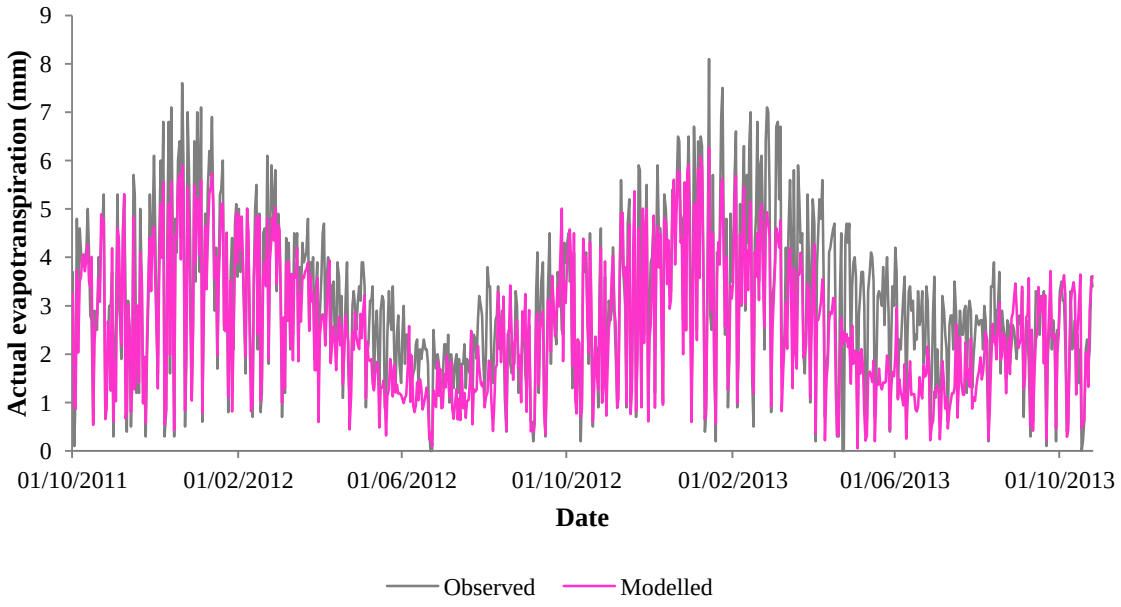

Figure 5.4: The observed and modelled actual evapotranspiration records extending from 01 October 2011 – 25 October 2013, for the Two Streams sub-catchment (29°12'19.2''S; 30°39'1.3''E).

The accumulated observed and modelled ET_A records showed that the model underestimated the ET_A by 10.14% in 2011, 13.30% in 2012 and 23.36% in 2013 and by 16.82% for the total period (01 October 2011 to 25 October 2013; Figure 5.5).

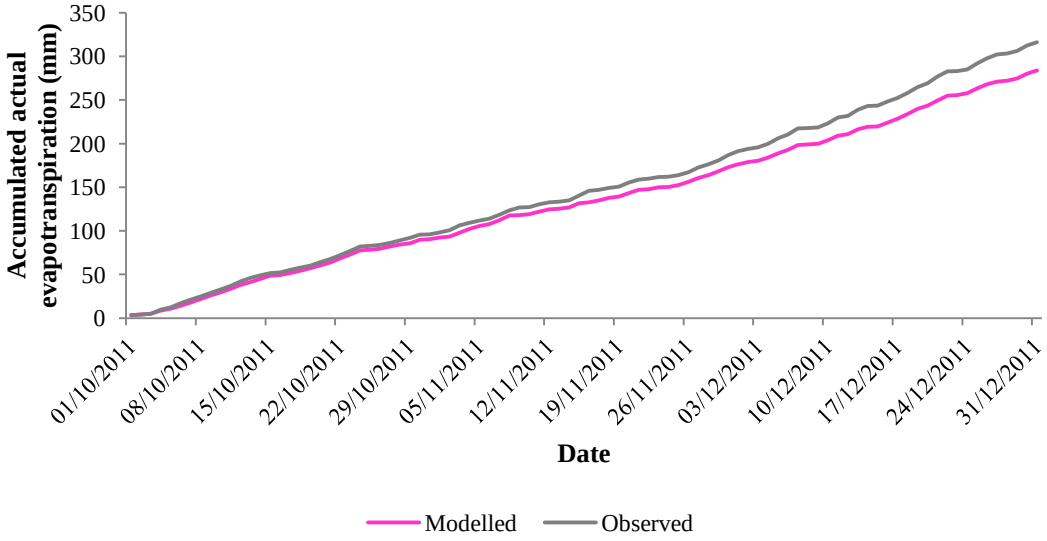

Figure 5.5: Accumulated actual evapotranspiration (mm) records (both observed and modelled) for the period 01 October 2011 – 25 October 2013.

The observed and modelled ET_A records showed a significant, strong positive linear correlation (Figure 5.6), r = 0.86 ($P < 1.00 \times 10^{-4}$) and a RMSE of 0.93, indicating a good fit between the observed and modelled ET_A rates. However, based on the two-sample Wilcoxon signed-ranks test, the two records were significantly different from one another ($P = 4.02 \times 10^{-10}$).

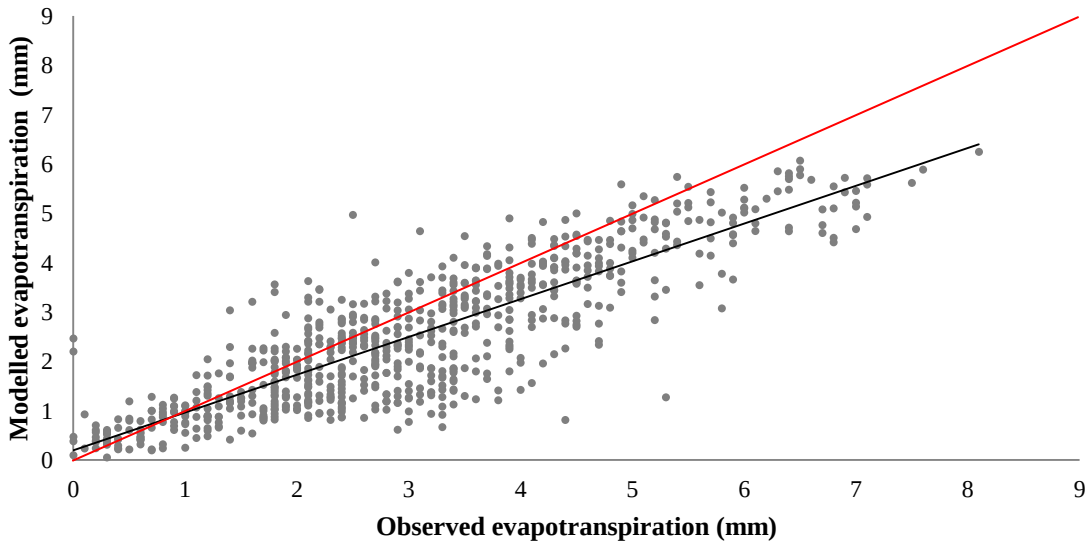

Figure 5.6: Scatter plot comparing the observed and modelled evapotranspiration (mm) rates between 01 October 2011 – 25 October 2013. A 1:1 line is included for comparison (red).

The observed streamflow record for the sub-catchment river extended from 14 February 2007 – 09 December 2013 (Figure 5.7). Over this observed period, low rates of streamflow were recorded, averaging $6.72 \times 10^{-4} m^3.s^{-1}$ and ranging from 1.70×10^{-5} – $5.10 \times 10^{-3} m^3.s^{-1}$. Peak daily streamflow events occurred on the 28th of February 2009 (5.10×10^{-3}) and on the 16th and 26th of October 2013 (4.90×10^{-3} respectively). There was evidence of cyclic fluctuation in the observed streamflow record indicative of seasonality, with the summer months having notably higher streamflow rates than the winter months (Figure 5.7). The modelled streamflow for the sub-catchment amounted to $0 m^3.s^{-1}$ over the study period, indicating that no streamflow was detected by the model (Figure 5.7). As such, no relationship between the observed and modelled streamflow records could be determined. The inability to detect, or lack of streamflow detection, suggests an error in the model set-up, and is discussed further under section 5.4.3.

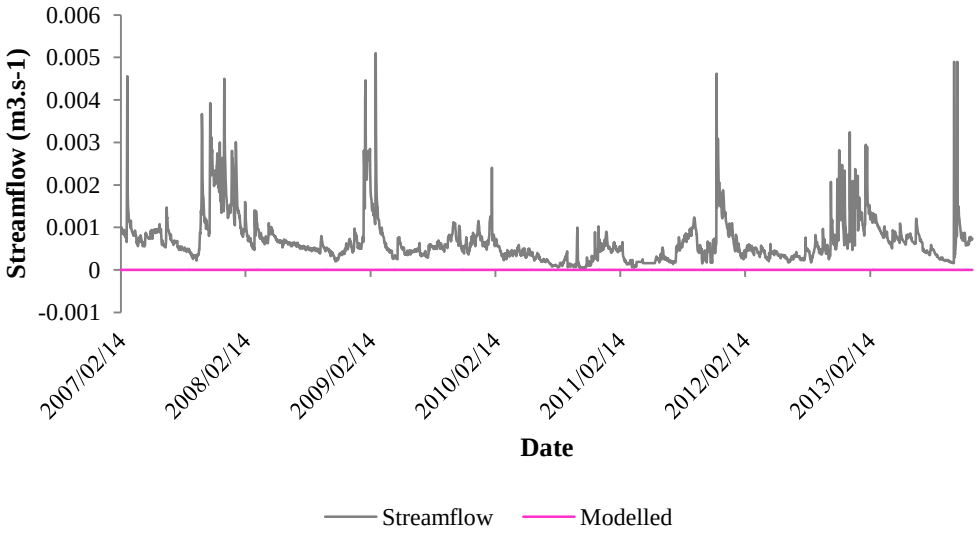

Figure 5.7: Modelled and observed streamflow records for the Two Streams sub-catchment, extending from 14 February 2007 – 09 December 2013.

5.4.2 Initial MIKE SHE water balance summary

A total water balance summary diagram was produced for the modelled area (Figure 5.8) to provide a visual depiction of the flows and storages of water within the modelled area and to identify and quantify model calculation error in the system, calculated through balancing all water inflows and outflows (DHI software, 2012). All values depicted in the water balance diagram have been rounded off to whole numbers and are measured in millimetres (mm). The site water balance diagram had an error of 139mm (Figure 5.8), suggesting that the model generated more water than that available in the modelled system. Findings from the water balance calculation showed: total ET_A to account for 99.06% of the total precipitation, a total loss in sub-surface storage (1454mm) and a movement of 12mm of water from the SZ to OL section (infilt. incl. Evap; Figure 5.8). Furthermore, there was no change in OL storage or in canopy storage and a movement of 150mm of water out of the modelled area from the OL component (Figure 5.8). The water balance diagram provided no indication of any interaction between the modelled stream and the adjacent or connected hydrological components of OL, and subsurface water zones (Figure 5.8).

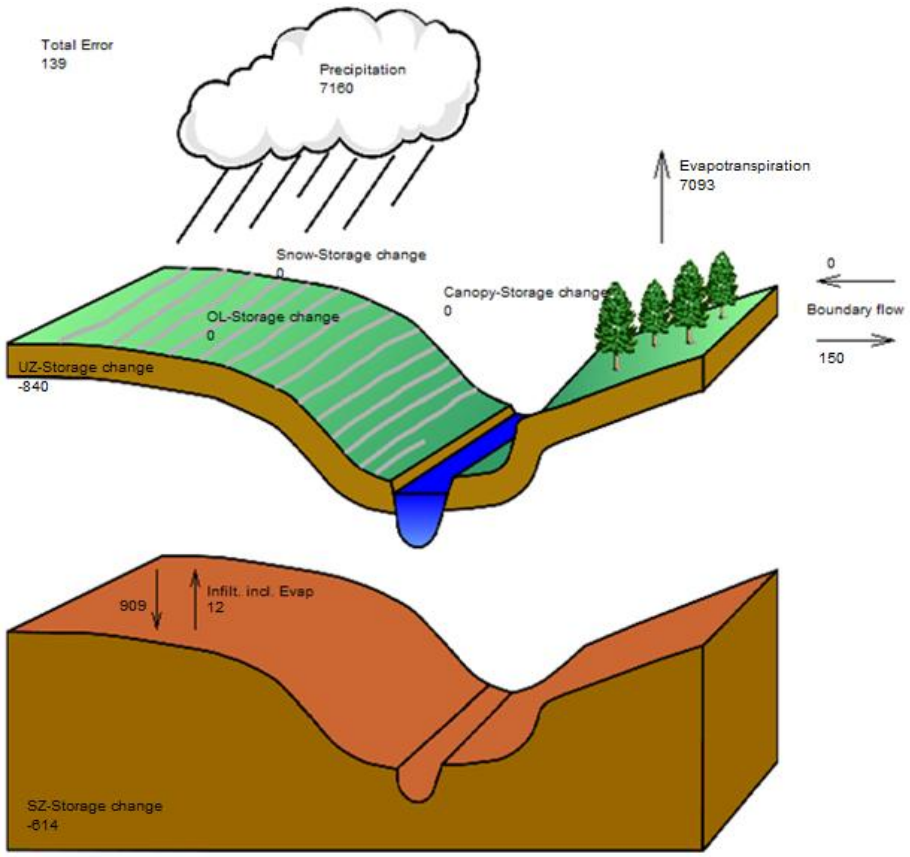

Figure 5.8: MIKE SHE accumulated water balance diagram showing the normalized flows (mm) within the modelled area over the simulated period (14 February 2007 – 02 October 2016) for the MIKE SHE current scenario (pre-validation) run.

To investigate the cause of the model error (139mm) from the water balance diagram (Figure 5.8), the four MIKE SHE water balance sections (CI, OL, UZ and SZ) were considered separately and individual section errors were determined (Table 5.6). On inspection of the individual section errors, majority of the error was concentrated in the OL section, 99.83% (Table 5.6). This error can predominantly be attributed to water moving out of the model area as OL boundary outflow (150mm) and to the water moving from the SZ to the OL section (12mm; Figure 5.8). From the diagram and streamflow results it is clear no water is being held by the river (discussed further below).

Table 5.6: Water balance errors of the MIKE SHE current scenario model.

Water balance components	**CI**	**OL**	**UZ**	**SZ**	**Total**
Accumulated error (mm)	0.22	138.94	0.02	-0.01	**139.17**

5.4.3 Correcting the MIKE SHE river component

Based on the pre-validation model run, it appears the MIKE 11 river component was incorrectly modelled. To determine why this occurred and to correct for it, input data and processed data (inputs processed by the model prior to model run) were reassessed. Within the *river and lakes* processed data module there is a *bank minus ground* section which indicates how the river layer overlays the topography within each grid cell of the model, i.e. topography minus river cross-sectional height (DHI software, 2012). The output of this section showed the river to be located between approximately 4 – 26m above the ground surface (Figure 5.9), essentially floating above the land, explaining why no streamflow was being generated by the model. This error arose predominately from user error and calculation difficulty within the MIKE Hydro software where initially the river was incorrectly geo-referenced and thus did not align with the topography layer. Furthermore, the cross-sections were spaced too far apart (five cross-section profiles were generated over the 750m river) to accurately capture the stream shape.

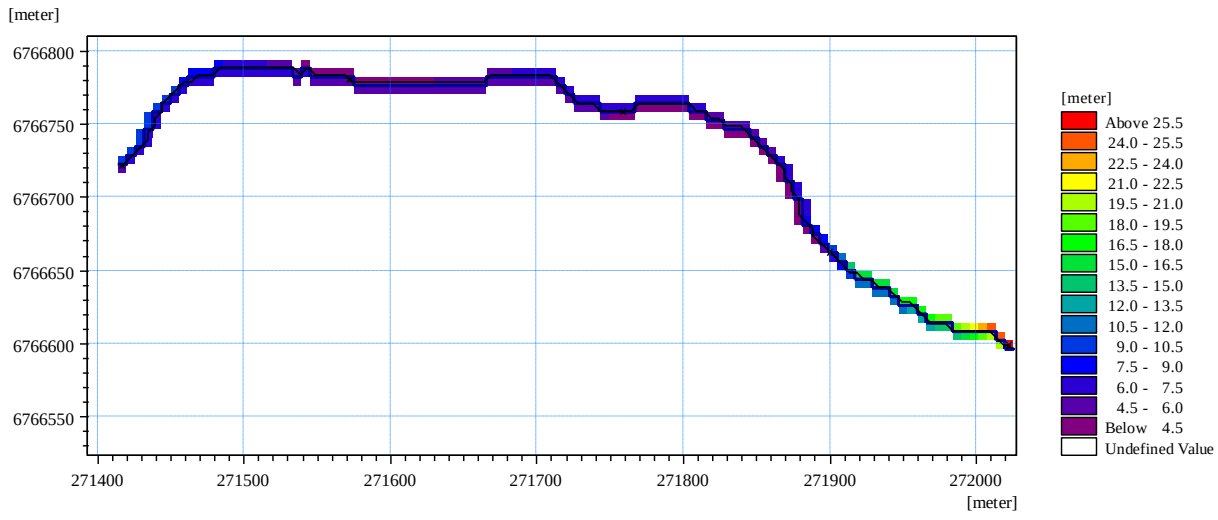

Figure 5.9: Model screen display of the river bank level minus ground level map produced in the processed data section of the MIKE SHE simulation.

To correct for this error, the river was correctly geo-referenced to WGS 1984 UTM 36S projected coordinate system and reintroduced into MIKE Hydro and an additional four cross-sections were added (amounting to nine cross-sections along the course of the river), to provide greater detail on the

river (Figure 5.10). Calibration was needed to further refine the cross-sections by smoothing their edges, as the cross-sections were computer generated and had terraced sides not representative of natural stream banks. In addition, where it was found to be necessary, through the calibration process the stream bank vertical heights were adjusted to even out where uneven stream banks led to elevation discrepancies between the topography and river layers.

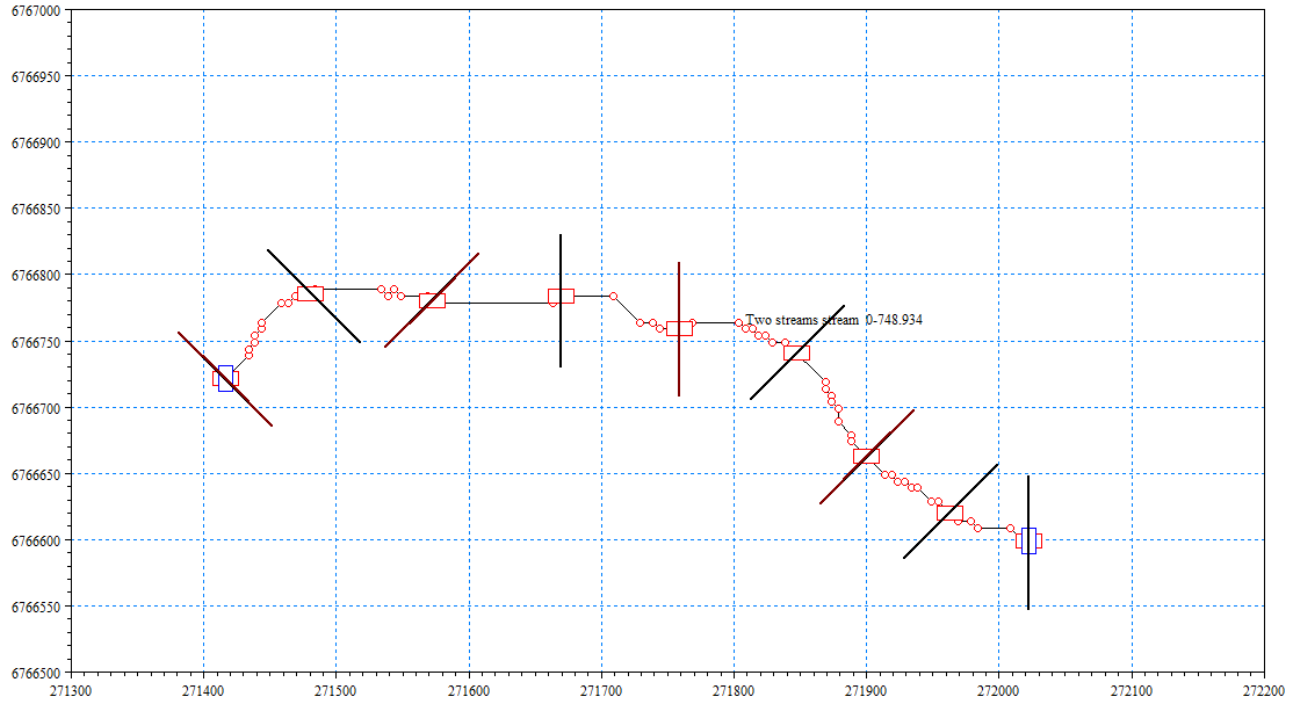

Figure 5.10: Model screen display showing the locations of the new cross-sections generated along the length of the Two Streams stream. The x- and y-axis represent the MIKE SHE geographically positioned grid (m). The red boxes indicate where cross-sections were generated and the black lines perpendicular to the stream indicate the length and angle the cross-sections were captured at. The blue boxes indicate the start and end chainage points of the river.

Once the new cross-sections were finalised, the pre-processing of data in MIKE SHE was run. The new *bank minus ground* section was greatly improved (Figure 5.11) with the river being located between 1.2m above the ground and 4.4m below the ground. This was sufficient for this study as the topography layer has a grid size of 5m x 5m, and thus the discrepancy between topography and streamflow would fall within one grid size, which is the highest accuracy at which the modelled data

can be considered. Furthermore, the river appears to fall predominantly between -1.2m – 0m below ground, with only small portions falling outside of this range (Figure 5.11).

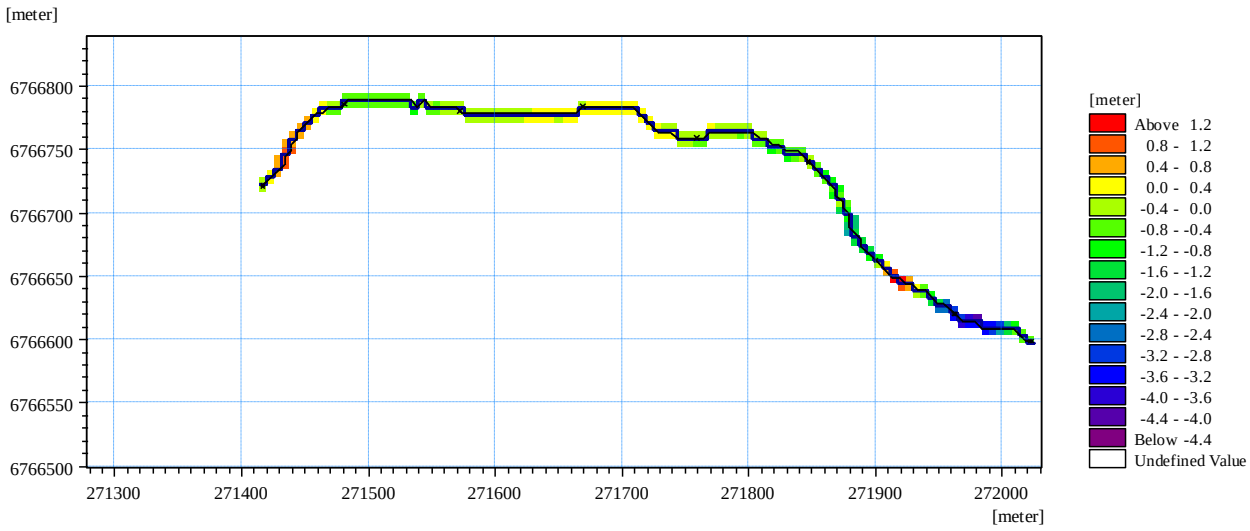

Figure 5.11: Model screen display of the river bank level minus ground level map produced in the processed data section of the MIKE SHE simulation once the cross-sections were altered.

5.4.4 Alterations to the model simulation run time

In addition to the river changes, the model time step control properties were also refined, to decrease model run time, as the model was taking in excess of three days to run, making output generation a lengthy process and not practical due to the requirements of the set-up, calibration and validation processes to run numerous iterations. Originally the run time settings were left to their default values (Figure 4.4; Appendix A). These default values were altered to decrease the model run time, particularly decreasing the maximum OL and UZ time steps, reducing overall runtime to approximately a day (Appendix A).

5.5 MIKE SHE current scenario model refinement results

Once the above alterations were made, the refined MIKE SHE current scenario model was run. From the refined model outputs, the modelled ET_A record did not change significantly from the initial run, with only a minor increase in total modelled ET_A from 1899.91 – 1907.78mm. No further attempts

were made to refine the modelled ET_A as attempts to improve model fit would require a trial and error approach, which would not provide a true representation of the response of the model to the input data.

The calibrated, modelled streamflow record (Figure 5.12), showed a marked improvement from the initial MIKE SHE model run and produced an average streamflow of 3.68 x $10^{-4}m^3.s^{-1}$ (standard deviation of 1.14 x 10^{-3}) for the total simulated period, with the streamflow ranging from 0 – 1.20 x $10^{-2}m^3.s^{-1}$. There was a total of 2995 days out of a total 3519 days (approximately 85% of the total days) where no streamflow was modelled.

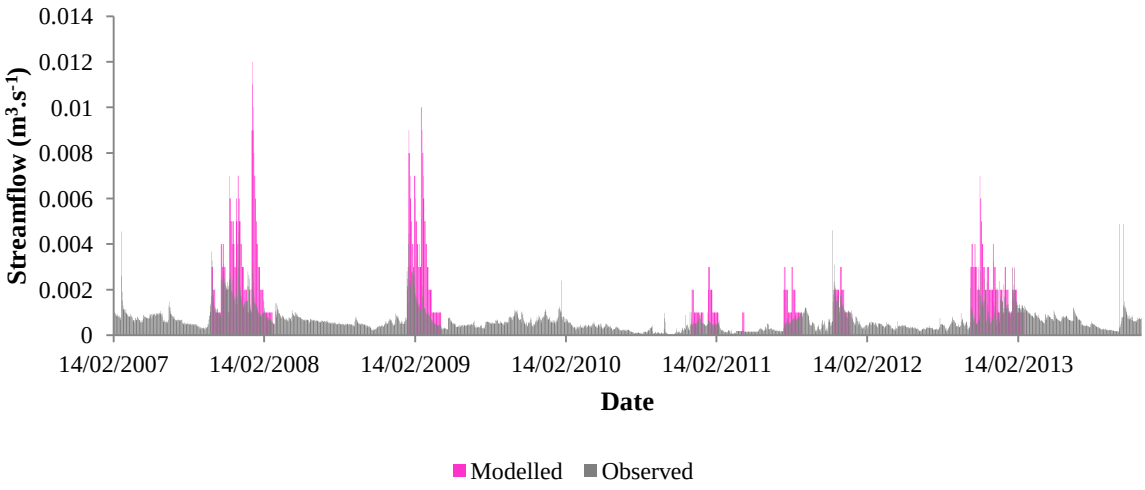

Figure 5.12: Modelled and observed streamflow records, following model validation, for the period 14 February 2007 – 09 December 2013.

Comparing the observed and calibrated modelled streamflow records, the total observed streamflow amounted to 1.67$m^3.s^{-1}$, which is equivalent to 182.30mm, whilst the total modelled streamflow amounted to 1.28$m^3.s^{-1}$ (139.97mm), over the observed streamflow record time period from 14 February 2007 – 09 December 2013. This is a 0.39$m^3.s^{-1}$ (42.33mm) under-prediction in streamflow and, even though it is an insignificant quantity, it does constitute a 23.22% under-prediction.

Considering only the days over the observed streamflow period (14 February 2007 – 09 December 2013) when the model detected streamflow (510 days), the modelled streamflow exceeded the observed streamflow by 0.63mm (49.22% of modelled streamflow). Thus, for the 510 days the model detected streamflow, the modelled streamflow exceeded the observed streamflow, more so than when considering the total observed streamflow record time period (Figure 5.12). The accumulated daily streamflow records (modelled and observed) displayed different patterns over the simulation period (Figure 5.13), with the modelled output having a more stepped response than that of the observed record. The stepped response in the modelled accumulated streamflow (Figure 5.13) shows how streamflow was only experienced over some periods, with extended periods of no streamflow, with the days experiencing streamflow creating a vertical rise in the accumulation record whilst the days that do not experience streamflow result in a no change in the accumulated record (Figure 5.13).

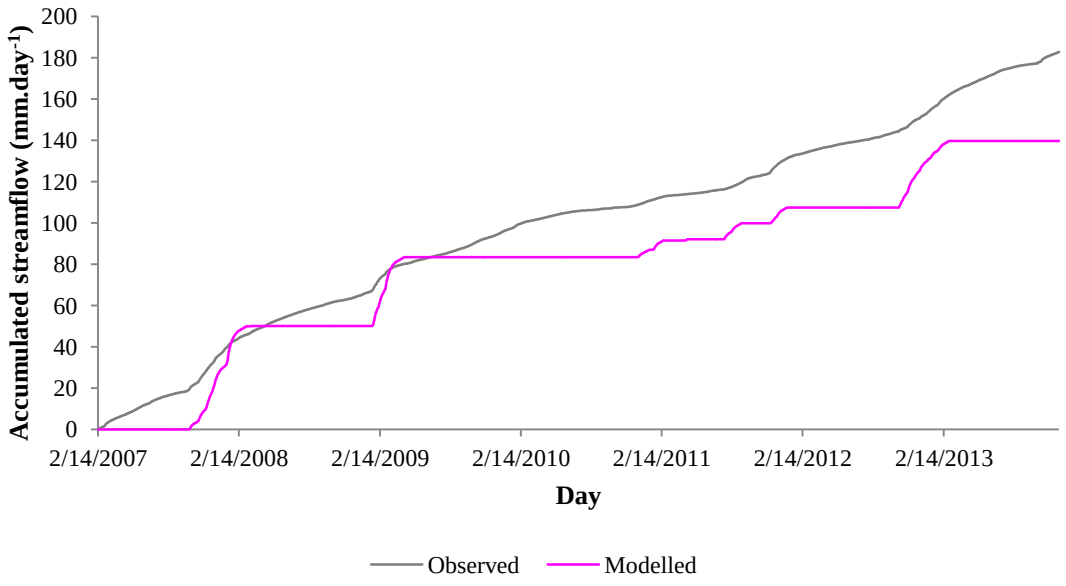

Figure 5.13: Accumulated streamflow records (mm), both observed and modelled, for the period 14 February 2007 – 09 December 2013.

Correlating the calibrated, modelled streamflow record to the observed streamflow record over the observed period, from 14 February 2007 – 09 December 2013, the two records show a significant, positive linear correlation (Figure 5.14), $r = 0.67$ ($P < 1.00 \times 10^{-4}$). However, based on the two-sample

Wilcoxon signed-ranks test, the observed and modelled streamflow records were significantly different from one another ($P < 1.00 \times 10^{-4}$). Correlating the streamflow records (both observed and modelled) to the rainfall record both streamflow records did not correlate well to the rainfall record, but were significant, $r = 0.31$ ($P < 1.00 \times 10^{-4}$) and $r = 0.21$ ($P < 1.00 \times 10^{-4}$) for the observed and modelled streamflow records respectively.

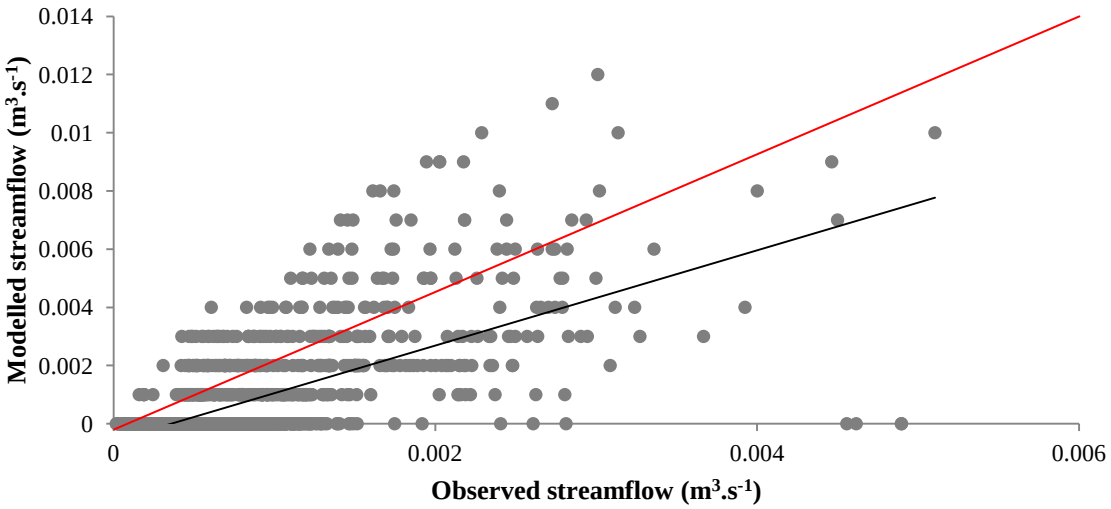

Figure 5.14: Scatter plot of the relationship between the observed and modelled streamflow records ($m^3.s^{-1}$) for the Two Streams sub-catchment, over the period 14 February 2007 – 09 December 2013. 1:1 line included as well for comparison (red).

Comparing the observed and modelled streamflow records, the eight months with the least difference between modelled and observed streamflow produce differences ranging from 3.21×10^{-4} – $8.88 \times 10^{-3} m^3.s^{-1}$ (Table 5.7). The month with the smallest difference between observed and modelled streamflow was April 2011, with an average RMSE of 3.66×10^{-4} (Table 5.7).

Table 5.7: Monthly streamflow records showing the greatest similarity between the observed and modelled records – over days when rainfall was detected by the model.

Month	**Observed streamflow ($m^3.s^{-1}$)**	**Modelled streamflow ($m^3.s^{-1}$)**	**Differences (Observed – modelled)**	**Difference between observed and modelled (%)**	**Monthly average RMSE**
October 2007	$4.01 \times 10^{--2}$	3.60×10^{-2}	4.15×10^{-3}	10.22	6.98×10^{-4}
January 2009	3.71×10^{-2}	4.00×10^{-2}	-2.95×10^{-3}	7.25*	1.91×10^{-3}
April 2009	1.16×10^{-2}	1.70×10^{-2}	-5.45×10^{-3}	31.76*	4.54×10^{-4}
December 2010	1.59×10^{-2}	2.20×10^{-2}	-6.06×10^{-3}	27.73*	7.53×10^{-4}
February 2011	1.21×10^{-2}	2.10×10^{-2}	-8.88×10^{-3}	42.38*	6.60×10^{-4}
April 2011	5.32×10^{-3}	5.00×10^{-3}	3.21×10^{-4}	6.02	3.66×10^{-4}
July 2011	7.68×10^{-3}	1.50×10^{-2}	-7.32×10^{-3}	48.80*	9.38×10^{-4}
February 2013	4.01×10^{-2}	3.90×10^{-2}	1.11×10^{-3}	2.74	3.19×10^{-4}

*Differences where the modelled streamflow exceeded the observed streamflow.

The streamflow records of the eight months with the greatest differences between observed and modelled streamflow had differences ranging from $2.72 \times 10^{-2} – 8.85 \times 10^{-2} m^3.s^{-1}$ (Table 5.8). The greatest monthly difference is observed for January 2008, with an average RMSE of 4.29×10^{-3} (Table 5.8).

Table 5.8: Monthly streamflow records showing the greatest difference between the observed and modelled records over days when rainfall was detected by the model.

Month	**Observed streamflow ($m^3.s^{-1}$)**	**Modelled streamflow ($m^3.s^{-1}$)**	**Differences (Observed – modelled)**	**Difference between observed and modelled (%)**	**Monthly average RMSE**
November 2007	7.21×10^{-2}	0.11	-3.49×10^{-2}	34.45*	1.92×10^{-3}
December 2007	5.81×10^{-2}	0.13	-6.79×10^{-2}	55.31*	2.41×10^{-3}
January 2008	5.25×10^{-2}	0.14	-8.85×10^{-2}	62.50*	4.29×10^{-3}
February 2009	5.70×10^{-2}	0.13	-7.60×10^{-2}	56.15*	3.03×10^{-3}
March 2009	3.27×10^{-2}	0.12	-8.23×10^{-2}	72.75*	3.36×10^{-3}
August 2011	2.08×10^{-2}	4.80×10^{-2}	-2.72×10^{-2}	56.67*	1.09×10^{-3}
November 2012	3.62×10^{-2}	9.70×10^{-2}	-6.08×10^{-2}	62.68*	2.33×10^{-3}
December 2012	3.16×10^{-2}	7.00×10^{-2}	-3.84×10^{-2}	54.86*	1.46×10^{-3}

*Differences where the modelled streamflow exceeded the observed streamflow.

Considering the 50 days experiencing the largest amount of rainfall, nine of these days show a good response in streamflow (i.e. an increase in rainfall was reflected by an increase in streamflow) , whilst 27 days do not show a good response in streamflow (Table 5.9). Thus, individual peaks in rainfall are not well reflected in streamflow. Particularly noticeable is that no streamflow was modelled on the 12th of December 2015, which experiences the highest daily rainfall rate of 75.7mm (Table 5.9).

Table 5.9: How well or poorly represented the largest rainfall events were in the modelled streamflow record.

Representation	**Date (dd/mm/yy)**	**Rainfall event (mm)**	**Modelled streamflow ($m^3.s^{-1}$)**
Well represented	01/11/07	43.2	0.004
	21/11/07	41.5	0.006
	12/12/07	33.9	0.007
	14/01/08	60.7	0.009
	28/01/09	43.2	0.008
	11/02/09	31.8	0.007
	28/02/09	68.9	0.01
	13/11/12	52.9	0.007
	15/12/12	36.6	0.004
Poorly represented	04/03/07	43.7	0
	27/06/07	42.2	0
	08/10/07	31.4	0
	11/03/08	42	0
	15/03/08	32.2	0
	20/09/08	36.7	0
	04/05/09	29.5	0
	02/08/09	31.1	0
	12/10/09	32.5	0
	26/01/10	36.5	0
	20/03/10	36.5	0
	10/11/10	35	0
	03/12/10	31.9	0
	13/04/11	48.1	0
	21/11/11	28.9	0
	31/03/12	35.1	0
	08/08/12	33.9	0
	06/09/12	27.5	0
	30/01/14	31.4	0
	27/03/14	28.5	0
	12/12/14	31.1	0
	28/01/15	27.3	0

	08/12/15	30.3	0
	12/12/15	75.7	0
	01/01/16	43.2	0
	26/07/16	33.9	0
	17/09/16	29.4	0

5.5.1 Calibrated model water balance summary

A water balance summary diagram was generated for the calibrated and validated MIKE SHE current scenario (Figure 5.15) and compared to the MIKE SHE current scenario water balance generated prior to validation (Figure 5.8). The calibrated water balance has an improved error value of 0mm (Figure 5.15), in relation to the pre-calibrated error value of 139mm (Figure 5.8). There is now an upward exchange between the river and the SZ, of 15mm (Figure 5.15), where previously there was no water movement specified to or from the river (Figure 5.8). The total ET_A for the simulation period was 7105.54mm, similar to the pre-calibrated scenario, and accounted for 99.24% of the total precipitation falling on the site (Figure 5.15). The recharge to the SZ decreased from the pre-calibrated run (Figure 5.8) by 31.73mm to 877.44mm (Figure 5.15). The accuracy of the changes in the total water balance, from pre- to post-calibration and validation cannot be verified due to a lack of calibration datasets for the study site. However based on the alterations and refinements made on the ET_A and streamflow records, the other water balance values are believed to be improvements on the pre-calibrated model water balance as the hydrological cycle is an interconnected process where improvements in one component should assist in the better reflection of the process response in subsequent components (Hendriks, 2010).

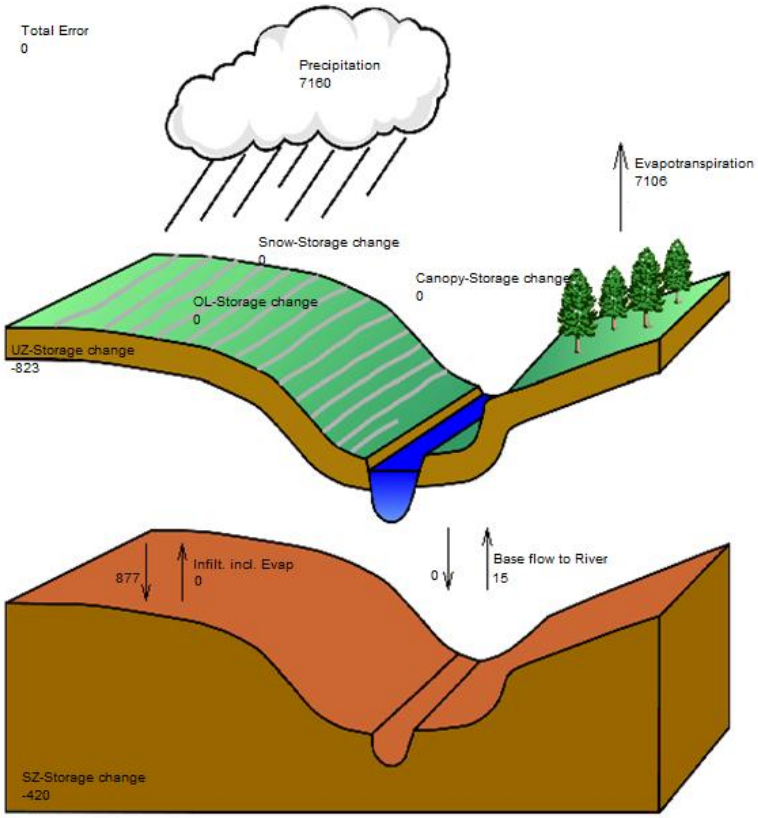

Figure 5.15: MIKE SHE validated total water balance diagram showing the normalized flows (mm) within the modelled area over the entire simulated period (14 February 2007 – 02 October 2016).

On closer examination of the error in the calibrated and validated MIKE SHE current scenario model (Table 5.10), the error in the OL component has been reduced from 138.94 – 0.04mm giving the modelled area an overall water balance error of -0.27mm (Table 5.10).

Table 5.10: The water balance errors of the calibrated MIKE SHE current scenario model.

Water balance components	**CI**	**OL**	**UZ**	**SZ**	**Total**
Accumulated error (mm)	-0.04	0.04	-0.12	-0.15	**-0.27**

5.6 Discussion

Based on the results described above this discussion considers the key findings and decisions made in the model set-up, calibration and validation processes.

5.6.1 Soil characteristics of the Two Streams sub-catchment

The soil types and soil physical properties data considered for this study were taken from a hydropedology study of the Two Streams sub-catchment (Kuenene, 2013). Based on the soil study findings (Kuenene, 2013), the soil texture of the seven Two Streams sub-catchment soils fall within four textural classes, as defined by the United States Department of Agriculture (USDA; Soil Survey Division Staff, 1993; Figure 5.16) based on the percentage of sand, silt and clay, these classes are: loam, sandy loam, sandy clay loam and clay loam (Table 5.3). The sandy loam and sandy clay loam soils both have a relatively high percentage of sand ranging between 50 – 80% (Figure 5.16). The loam and clay loam soils both have a proportionate composition of sand and silt ranging between 30 – 50% for loam and between 20 – 50% for clay loam (Figure 5.16). The clay loam and sandy clay loam soils have the highest percentage of clay (compared to the sandy loam and loam soils) ranging between 20 – 30% (Figure 5.16).

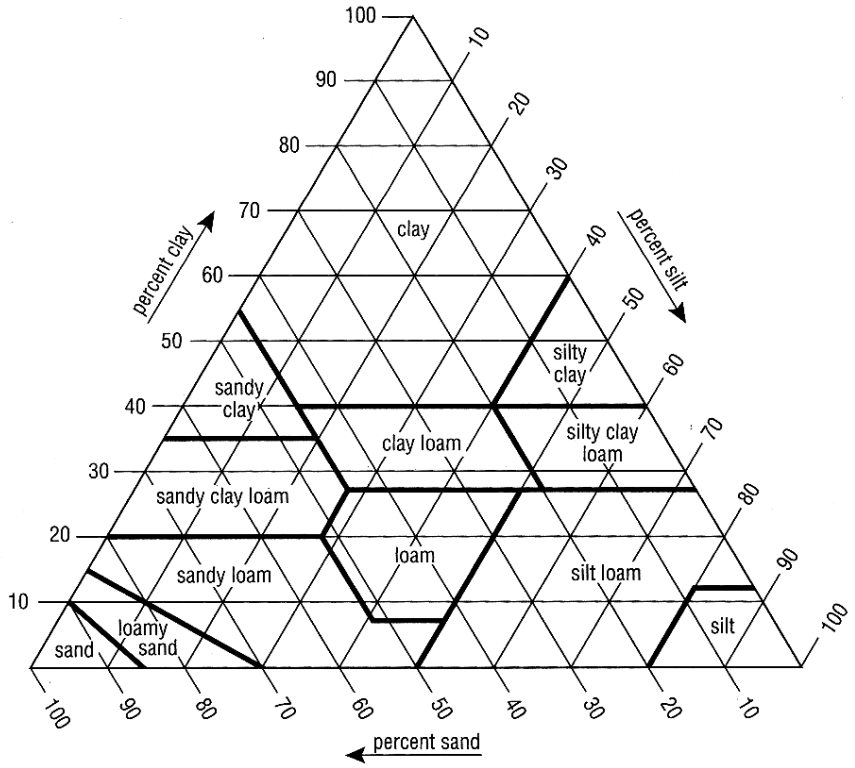

Figure 5.16: Soil textural class pyramid, developed by the United States Department of Agriculture (USDA), to define soil textural classes based on percentage sand, silt and clay (Soil Survey Division Staff, 1993).

Sandy soils have larger pores than clay soils and are more permeable, with sand particles varying in size from very fine (0.05mm) to very coarse (2.00mm) in average diameter, while clay has finer soil particles finer than 2.00 x 10^{-3}mm in average diameter. Silt particles are in between sand and clay particles ranging in size from 2.00 x 10^{-3} – 0.05mm (Daniels and Haering, 2006). In general water infiltrates more quickly and moves more freely in coarse-textured or sandy soils and sandy soils retain less water than fine-textured, clayey soils (Daniels and Haering, 2006; Hillel, 2008).

Unsaturated soil hydraulic conductivity determines the rate at which water moves through the UZ ($m.s^{-1}$), with a higher rate of hydraulic conductivity indicative of faster water movement (Hillel, 2008; Şen, 2015). According to Hillel (2008) soil hydraulic conductivities for sandy textured soils generally range between 10^{-5} – $10^{-4}m.s^{-1}$, and between 10^{-9} – $10^{-6}m.s^{-1}$ for clayey soils. For this study soil hydraulic conductivities fall within the 10^{-5} – $10^{-4}m.s^{-1}$ range and thus are more sandy than clayey for all soil texture types indicative of fast rates of water movement. Furthermore, when comparing the soil hydraulic conductivities for the different textural classes to those in the unsaturated soils hydraulic database (UNSODA; Leij *et al*., 1996), the Kuenene (2013) hydraulic conductivities were generally higher (Table 5.11), further exemplifying the high rates of conductivities in this study which lead to greater rates of I_{UZ} and lower rates of streamflow or OL (Miao and Ni, 2009). I_{UZ} and OL are considered in chapter six.

Table 5.11: Comparing the unsaturated hydraulic conductivities of the Kuenene (2013), to those of the UNSODA database (Leij *et al*., 1994).

Soil type	**Soil horizon**	**Soil textural class**	**Unsaturated hydraulic conductivity ($m.s^{-1}$)**	
			Kuenene (2013) soils	**UNSODA soils (Leij *et al*., 1994)**
Clovelly	ot	loam	1.83×10^{-5}	3.00×10^{-6}
	ye	Sandy clay loam	8.25×10^{-5}	3.77×10^{-6}
Griffin	ot	Sandy loam	2.44×10^{-5}	1.27×10^{-5}
	ye	Sandy clay loam	6.25×10^{-5}	3.77×10^{-6}
	re	Sandy clay loam	5.81×10^{-5}	3.77×10^{-6}
Inanda	ah	Sandy clay loam	1.75×10^{-5}	3.77×10^{-6}
	re	Clay loam	6.39×10^{-5}	7.49×10^{-7}
Kranskop	ah	Sandy clay loam	1.97×10^{-5}	3.77×10^{-6}
	ye	Sandy clay loam	9.53×10^{-5}	3.77×10^{-6}
	re	Sandy clay loam	1.03×10^{-4}	3.77×10^{-6}
Magwa	ah	Sandy clay loam	1.69×10^{-5}	3.77×10^{-6}
	ye	Clay loam	4.94×10^{-5}	7.49×10^{-7}
	on	Clay loam	4.72×10^{-6}	7.49×10^{-7}
Oakleaf	ot	Sandy clay loam	5.94×10^{-5}	3.77×10^{-6}
	ne	Clay loam	7.94×10^{-5}	7.49×10^{-7}
Katspruit	ot	Clay loam	8.33×10^{-6}	7.49×10^{-7}
	G	Sandy clay loam	1.47×10^{-5}	3.77×10^{-6}

*Coloured blocks indicate the higher hydraulic conductivity rates when comparing those attained from Kuenene (2013) to those from Leij *et al*. (1994)

5.6.2 Model uncertainty

Inherently the processes of model set-up, calibration and validation are subject to model uncertainty, as no hydrological model is able to truly replicate reality and rather hydrological models serve as imperfect abstractions, simplifications and interpretations of reality (Loucks *et al*., 2005; Ma *et al*., 2016). According to Renard *et al*. (2010), hydrological model uncertainty can arise from one or a multiple of four possible sources: 1) Input uncertainty, including errors in sampling techniques or measurement errors of the spatial and temporal input data employed; 2) Output uncertainty, including errors in the modelled spatial and temporal outputs; 3) Structural uncertainty, results from the simplification of hydrological processes within the model that creates a degree of uncertainty in the model itself; and 4) Parametric uncertainty, resulting from uncertainties and limitations that arise due to the calibration process.

The description of inherent model uncertainty is not to create a pessimistic perception of the Two Streams model set-up but rather to be used to make readers aware that no model is without fault. In addition, as model uncertainty can arise from a number of sources, the description illustrates that in cases such as this study, knowing all sources of uncertainty or error is difficult for such a complicated model. However where error was suspected in the model, efforts were taken to reduce model error. These errors are discussed below.

5.6.3 Leaf Area Index (LAI)

One data input that required much effort was LAI, in particular the determination of the riparian vegetation class LAI. The riparian zone of the Two Streams sub-catchment comprises a diverse range of species. For example, *Setaria megaphylla*, *Aristida junciformis*, *Urtica urens*, *Solanum mauritianum*, *Lantana camara*, are a few of the species that have been observed within the Two Streams sub-catchment riparian zone. The presence of a diverse range of species is common for riparian zones (Zaimes *et al*., 2011) which, through past forestry clearing practices and lack of proper management, had invaded and/or colonized the area (Figure 5.17). The high species number made it difficult to consult relevant literature in determining an average LAI, as was possible for the more homogeneous sugarcane vegetation class. Instead, in an attempt to simplify the LAI determination process, LAI was calculated from remotely sensed satellite imagery.



Figure 5.17: Photographs taken during fieldtrips showing the heterogeneity of the species composition of the Two Streams sub-catchment riparian zone.

Remote sensing (RS) is advantageous in the provision of rapid, widespread coverage of spatially distributed data, which helps in minimizing the need for field data collection (Khalil, 2017). The limitation with using the remotely sensed SPOT imagery was that the resolution of the data ranged between 10 – 20m. Due to the small study site size (79.16ha) a resolution higher than 10m would be required to distinguish between the different vegetation classes, in particular the heterogeneous riparian vegetation class which is a narrow strip of land covering 5.83ha. The low resolution of the imagery brings the precision of the NDVIs generated (that were used to calculate LAI) into question (Figure 5.17), as much of the detail in the SPOT imagery and resulting NDVIs is lost due to the low resolution (Figure 5.17). Data of a higher resolution is preferable for use in areas with small features

or where there are fine-scale variations in LULC (Fisher *et al*., 2018). The lower the resolution the less likely small scale changes are detectable, as the change is smaller than the data pixel size, and imagery detail can only be detected to pixel size (Fisher *et al*., 2018).

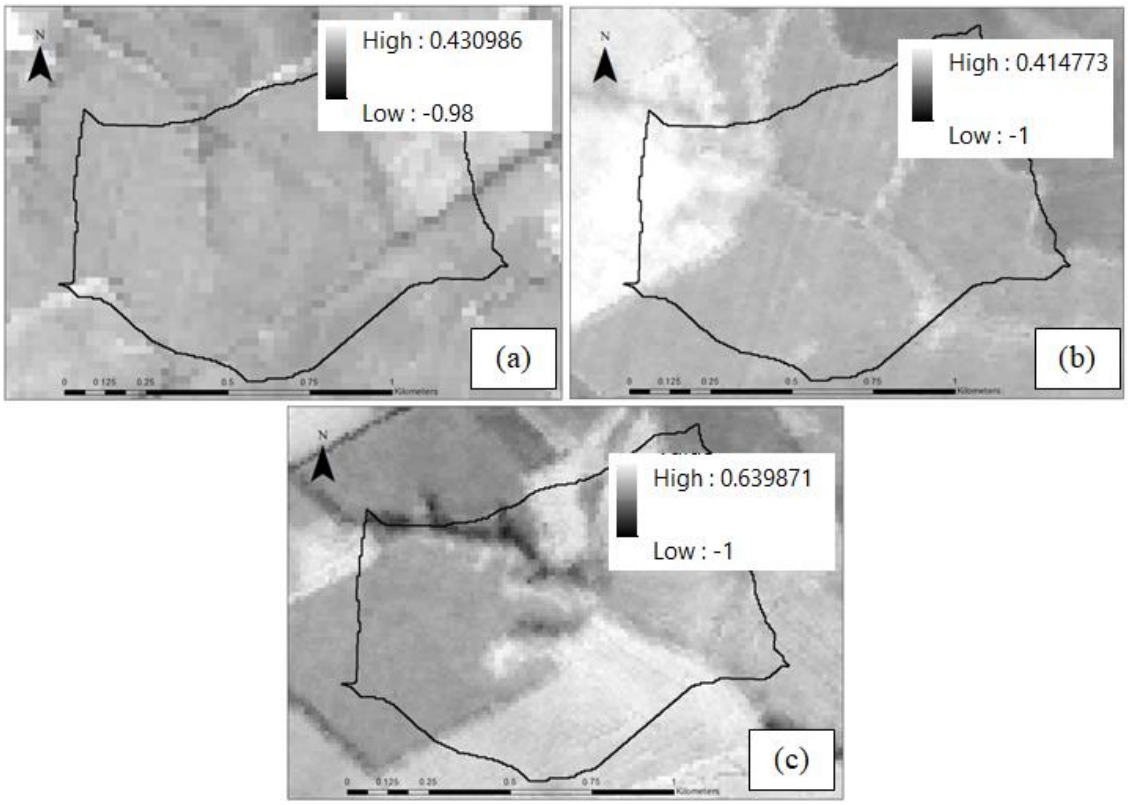

Figure 5.18: The normalized difference vegetation indices (NDVIs) generated from the SPOT satellite imagery attained for the Two Streams site showing the effect of low resolution on the data. (a) 20m resolution – image taken on 19 January 2011; (b) 10m resolution – image taken on 01 February 2007; (c) 10m resolution – image taken on 31 July 2012.

To verify and enable the capturing of the spatial heterogeneity of the riparian vegetation class, ground-based LAI measures were taken using a LAI-2200 Plant Canopy Analyser (described previously under section 4.3.5.1). The LAI-2200 LAI measures showed great variation (mean LAI = 2.69 and standard deviation = 1.24) suggesting a range of coverage in the area, illustrating the spatial heterogeneity of the riparian zone. This was found to be an improved detection than that achieved through remotely sensed calculations which showed very similar LAI measures and illustrated less variation in the measures with a mean LAI = 2.21 and standard deviation = 0.04. Thus, given a lack of

confidence in the remotely sensed LAI average measure, the LAI-2200 LAI measure was taken, instead, as the average LAI measure for the riparian vegetation class. The only uncertainty in using the LAI-2200 average measure is that it was not taken over the simulation period (October 2017).

5.6.4 Model calibration and validation

Model calibration and validation were carried out to evaluate model performance and to improve the realism of the modelled results (Singh *et al*., 2017). Ideally calibration and validation should be undertaken using different datasets to limit the chance of model parameter uncertainty (Legessea *et al*., 2003; Renard *et al*., 2010). However, in the case of this study, calibration and validation were undertaken using the same datasets, because of limited observed data records. The minimal calibration, necessary to improve model cross-sections bank heights and shape, was based on a trial and error approach. However this was kept to a minimum to limit the chance of curve fitting or equifinality that would lead to model parameter uncertainty (Loucks *et al*., 2005; Ma *et al*., 2016). Equifinality arises when more than one modelled parameter set is able to achieve a good fit with the observed data, resulting in more than one viable modelled response, and therefore determining the true or most realistic representation of the parameter cannot be achieved (Ma *et al*., 2016).

5.6.4.1 Water balance calculations

The water balance calculation in MIKE SHE is a useful tool to summarise accumulated flow and storage processes that occur within the different model components and provides a detailed assessment of where model errors are concentrated (Appendix G; DHI software, 2012). In comparison to the simplified water balance calculation procedures proposed by Thornthwaite and Mather (1957; Equation 2.1), the MIKE SHE water balance calculation provides a higher level of detail enabling the easier specification and quantification of hydrological outputs and calculation error in the system. Model calibration can be a lengthy process, particularly for a complex physically-based model such as MIKE SHE, because of the numerous input requirements and model processes run and the integration of the surface and subsurface processes that make room for high uncertainty. The detailed water

balance calculation assists in compartmentalising the multitude of processes and viewing the data in a more simplified manner (DHI software, 2012). Although specific error is not identified within the calculation it is separated into different model components, identifying the general part of the system the error will be located (Table 5.6 and 5.10).

5.6.4.2 Evapotranspiration

Comparing the observed and modelled ET_A records, they showed a significant, strong, positive linear correlation, $r = 0.86$ ($P < 1.00 \times 10^{-4}$), indicating them to be well correlated. However, despite this close correlation the two records were significantly different based on the Wilcoxon's signed-ranks test (described under section 5.4.1). This resulted as the modelled ET_A under predicted the observed record by approximately 16.82%. This is a concern given that ET forms the largest component of the water balance calculation and is necessary to determine the total sub-catchment water use (Zhang *et al*., 2001). The accurate estimation of ET is essential for an accurate water balance calculation and any inaccuracies will have negative knock-on effects on all the other water balance components. For example, Westerhoff (2015) described how if the ET_A record is overestimated by 10% there is an under-estimation of annual GR of 5%. This too could have a significant impact on the under/over estimation of streamflow (Zhao *et al*., 2013). However, the discrepancy may not result in such a level of impact as described in Stockle *et al*. (1991) who suggested that there is a reasonable margin of tolerance to ET under-prediction which is likely linked to the water holding capacity of the soil, reporting that an 11 – 16% under-prediction in ET did not impact on the overall corn yield of the area, when comparing the observed and actual yields.

Within MIKE SHE, ET_A is derived from empirically derived equations that follow the work of Kristensen and Jensen (1975). These equations require inputs of: LAI, RD, ET_{Ref} and K_c (DHI software, 2012). Thus, the under-estimation of ET_A could be as a result of the under-prediction of any one or multiple of these factors. The ET_{Ref} rate was calculated using the Penman-Monteith equation, following the steps outlined by Zotarelli *et al*. (2015) and was reliant on the climatic datasets from the

three AWSs (described in section 4.3.4). Given the multitude of datasets used, correlated and patched (Appendix C) and the multitude of calculations undertaken to determine ET_{Ref} (Zotarelli *et al*., 2015), there is a degree of uncertainty in the calculation of ET_{Ref}, pertaining particularly to the climatic input datasets used. Studies have found error pertaining to ET calculations to be related to climatic data (Gong *et al*., 2006). Thus, more regulated collection of climatic data is required on-site to minimise the need for patching of records.

5.6.4.3 Streamflow

Comparing the observed and modelled streamflow records (post validation) they were found to have a significant, positive linear correlation, $r = 0.67$ ($P < 1.00 \times 10^{-4}$). The modelled streamflow under-predicted the observed streamflow by $0.39 m^3.s^{-1}$ (an approximate 23.35% under-prediction) and the two datasets were found to be significantly different from each other based on the Wilcoxon signed-ranks test. Overall, both the accumulated observed and modelled streamflow records were both minimal over the simulation period (or observation period); if converted into mm the accumulated observed and modelled streamflow amounted to only 182.73mm and 139.71mm respectively over the observation period. The under-prediction in the modelled streamflow could be as a result of model structural uncertainty, input uncertainty (in the observed streamflow record) or output uncertainty (the under-prediction in ET; Loucks *et al*., 2005; Renard *et al*., 2010).

Model structural uncertainty describes the errors in the model structure compared to the real world system such as the approximations made by the numerical methods employed in the model. No matter how good hydrological parameter values are, there will always be residual model error (Loucks *et al*., 2005). Model structural uncertainty or weakness in the model may be more evident in outputs of smaller measures (Loucks *et al*., 2005). Error in the observed streamflow record is expected to exist given that, over the years of research, streamflow has been worked on and captured by a range of different people and at times there have been weir failures in the sub-catchment that have been attempted to be corrected for within the data record (Clulow *et al*., 2011), suggesting a level of uncertainty in the data.

Comparing the modelled streamflow record (mm) to the daily rainfall record (mm), they had a significant, weak positive linear correlation, $r = 0.21$ ($P < 1.00 \times 10^{-4}$), showing a poor relationship between rainfall and streamflow. Of the higher daily rainfall records not all were reflected in the streamflow record, specifically the 12th of December 2015, when the observed daily rainfall was 75.7mm and the daily modelled streamflow was 0mm. The lack of correlation between the rainfall and streamflow records is believed to be as a result of model output uncertainty (Renard *et al*., 2010) in the observed streamflow record (discussed in the previous paragraph). In addition, the lack of correlation could be attributed to other hydrological processes at work in the sub-catchment as the relationship between streamflow and rainfall is not necessarily linear (Gordon *et al*., 2004). Streamflow is not only influenced by, or just a reflection of, the rainfall falling within the sub-catchment, other influencing factors include: I_{UZ}, ET and human influence, which can lead to hydrological anomalies observed in the streamflow record (Miao and Ni, 2009). Streamflow will show strong correlation to rainfall as long as rainfall intensity is higher than I_{UZ} or land storage capacity and as long as there is minimal water E_t from deep soil water reserves (Miao and Ni, 2009).

A study by Scott and Lesch (1997) also found a weak correlation between streamflow and rainfall and indicated a delayed return of streamflow following plantation clearing. A possible reason for the delayed return of streamflow was attributed to the desiccation of deep, soil-water reserves to a wetness level below that needed to generate streamflow. Before streamflow could occur these reserves would need to be replenished, thus leading to an irregular response in streamflow (Scott and Lesch, 1997). Given that this model only ran for 10 years a longer period would be needed to truly determine if there is a lagged response in streamflow. Scott *et al*. (2000) also found that the effects of afforestation on streamflow may become lagged if the reservoir becomes depleted, and that storage of water in the catchment can vary from year to year leading to irregular streamflow responses. This notion would also aid in explaining the stepped response observed in the accumulated modelled streamflow showing periods where continuous rainfall is received over an extended period to then produce streamflow whilst for the remainder of the simulated days no rainfall was received. The

stepped nature is indicated of sequential periods of peaked streamflow followed by no streamflow. This irregular pattern in streamflow that only sees a response in streamflow with prolonged periods of rainfall may be attributed to the dynamics of deeper soil water reserves. Given the lack of data on deeper soils and geology this is a key limitation in understanding the soil water dynamics of the catchment and explaining the response in streamflow observed. The irregular stepped response in streamflow could also be as a result of antecedent moisture conditions which change continuously in a catchment and can have a significant accumulative effect on streamflow (De Michele and Salvadori, 2002). Antecedent moisture conditions are explained and discussed further under section 6.9.3 Runoff and infiltration.

5.6.5 The benefits and limitations of the MIKE SHE model for the Two Streams study site.

Based on the model set-up, input requirements, model run and calibration and validation processes, the benefits and limitations of the MIKE SHE software for the Two Streams sub-catchment have been identified. MIKE SHE is capable of expressing the spatial heterogeneity of the natural system through its spatial mapping abilities and small grid (cell) size calculation unit. This study employed a small grid size of $25m^2$ and, where practicable most inputs were spatially mapped including LULC, soil and initial potential head. The small cell size allowed for detailed model outputs, which resulted in slow processing times, so much so that the model run time setting had to be altered. Initially the model run time exceeded three days, which was not practical considering the need to iteratively run the model multiple times to explore the effects of varying parameter values. Shorter run times were achieved by altering the run time default settings. In the future when computer capabilities permit, the run times can be decreased to attain a smaller time step and thus more temporal detail.

The MIKE SHE model is a complex modelling software requiring multidisciplinary inputs in fields inclusive of hydrogeology, soil science, agronomy and computational hydraulics, for which one person would not be completely qualified and ideally an experienced modelling team would be most suitable (Ma *et al*., 2016). Without the presence of a modelling team, the process becomes time

consuming to understand all of the different disciplinary input requirements and modelling processes. In addition to the need for a multidisciplinary approach, the large data requirements in the numerous model parameters, coupled with the complex modelling structure, can lead to the over-parameterization of the model (Graham and Butts, 2005). For this study, the OL and UZ parameters could be modelled using complex physically-based methods due to the availability of data (Figure 4.3), whilst the limited data available for the SZ would have best been modelled using more conceptual means requiring less data inputs. However, once the option to select for the more complicated UZ method is used, this is carried through to the SZ requiring a more detailed description of SZ properties than was available. This resulted in the input of model default values and, where available, data from relevant literature. This inevitably will cause a degree of uncertainty in the model outputs.

One of the greatest benefits of using a physically-based model such as MIKE SHE is that it is capable of exploring the mechanisms of hydrological processes in response to the environment and environmental change, rather than simply pursuing an improved fit between the modelled and observed outputs (Ma *et al*., 2016). As such, it is capable of providing a more realistic interpretation of reality in comparison to more conceptual modelling approaches. Due to the nature of physically-based models, they require more parameter inputs than more conceptual approaches; however they also require less calibration (Abbott *et al*., 1986; Merritt *et al*., 2003; Devi *et al*., 2015). The physics basis of these models and detailed parameter inputs and data outputs all coupled with the spatial and temporal heterogeneity capabilities of MIKE SHE, make hydrological forecasting more realistic than more conceptual approaches (Devi *et al*., 2015; Ma *et al*., 2016). A further benefit of using MIKE SHE is the water balance calculation utility and graphical user interface, allowing for ease of visual interpretation of large quantities of input and output datasets and easy exchange of data between external software and programmes, including Microsoft Excel and ArcGIS (Graham and Butts, 2005; DHI software, 2012).

5.6.6 Future areas of research

Based on the results presented, and the experience gained, in this chapter, key areas for future research have been identified: research on model sensitivity of the MIKE SHE model for use in the Two Streams sub-catchment, improved streamflow data recording, improved parameter estimation, improved streamflow generation processes, groundwater monitoring and continued hydrological data collection. From the above discussion it is clear that there is a degree of uncertainty in the modelling of the Two Streams sub-catchment. This uncertainty is difficult to address as sources are not easily identifiable and can be as a result of an accumulation of error. To determine where focus should be placed in improving the modelling capabilities of MIKE SHE, for the Two Streams sub-catchment, a sensitivity analysis should be undertaken. Different parameters impact the modelling outputs differently and having a better understanding of which parameters have greater effect on model output can be useful in identifying where future hydrological research should be focussed. This will help reduce the number of parameters that have little impact on overall outputs and improve the efficiency of carrying out a simulation, thereby reducing the disturbance of insensitive parameters (Ma *et al*., 2016).

Improving the streamflow data recording and collection procedure will improve the reliability of the current observed streamflow record and will assist in future hydrological modelling studies. By ensuring consistency in the methodological approach employed for data collection and recording, as well as, improving the frequency and consistency in the frequency of data collection will improve the streamflow data recording process. Extending hydrological research on-site will add to the hydrological database and provide improved model inputs or calibration datasets. For the MIKE SHE model improved research into hydro-geological properties of the Two Streams sub-catchment would be beneficial and allow for the more accurate coupling of surface-subsurface hydrological processes allowing for the development of a more comprehensive hydrological model to better understand the hydrological cycling and better address issues of water resource management on-site.

5.7 Conclusion

The MIKE SHE model set-up required much data, as where possible, physical data intensive processes were selected for. The input data used were either from past studies, relevant primary and secondary literature sources, generated or collected. Of the input data taken from past studies, large amounts required adaptation to fit into the model environment, as data had to be patched, cleaned and converted to appropriate units. Once all data were input the model was run and model outputs generated. On consideration of these outputs, the reliability and accuracy was determined through a combined calibration and validation process following which a finalized hydrological set-up was arrived at to describe the Two Streams sub-catchment current scenario.

This MIKE SHE model study is, to-date, the most exhaustive hydrological modelling approach taken for the Two Streams sub-catchment, and has been useful in providing an initial baseline onto which further research can be built, and in highlighting some of the hydrological research limitations and uncertainties on-site. Although the modelled data outputs used in the validation process were not significantly similar to their observed counterparts, they were well correlated with low RMSE. Based on the strong linear correlation, low RMSE and minimized water balance error, the calibrated model was deemed to be able to produce usable outputs in understanding the hydrological characteristics of the Two Streams sub-catchment and deemed sufficient for use in assessing the comparisons in the land cover hydrological outputs of the current scenario (chapter six). Furthermore, the calibrated and validated model set-up was deemed sufficient for use as the basis for the simulation of the MIKE SHE predicted future scenario (set-up process described under section 4.5 and results and discussion presented in chapter seven).

Chapter Six

Comparing the MIKE SHE current scenario vegetation class model outputs

6.1 Introduction

This chapter compares the MIKE SHE current scenario (post-validation) model outputs of the sugarcane, riparian and black wattle vegetation classes and comprises of both a results and a discussion section. The results section compares the hydrological outputs generated from the calibrated and validated MIKE SHE current scenario model. All of the outputs have normalized values (to the size of the vegetation class) for ease of comparison. Comparisons are made at varying temporal scales considering the total, annual, monthly, seasonal and daily outputs. To assess seasonal differences, two seasons were defined, dividing the year between the six wettest months (October to March) and the six driest months (April to September), forming the summer and winter seasons respectively. The significance of the differences in the total and seasonal outputs were determined using the Kruskal Wallis test by ranks and the two-sampled Wilcoxon's signed ranks test, both tests are non-parametric. Non-parametric tests were employed over parametric tests as initially chi-squared goodness of fit tests were conducted on all model outputs to determine whether the outputs were parametric or not, and all were found to be non-parametric (Appendix H). The discussion section focuses on key findings and critically evaluates the sub-catchment spatial heterogeneity and vegetation management aspects of the holistic hydrological system.

6.2 Evapotranspiration

The total accumulated ET_A (refer to as ET from here) rates for all three vegetation classes are high, with all accounting for more than 95% of the total rainfall record (Table 6.1). The black wattle class has the highest total ET (7206.93mm), exceeding total rainfall by 0.66%, and sugarcane the lowest (6892.84mm), accounting for 96.28% of the total rainfall (Table 6.1). All three ET outputs are

significantly different ($P = 6.28 \times 10^{-8}$), based on the Kruskal Wallis test by ranks (Table 6.2). However, comparing the classes two at a time, using the two-sample Wilcoxon's signed ranks test, the sugarcane and riparian ET outputs are not significantly different (P = 0.76; Table 6.2).

Table 6.1: The accumulated total, summer and winter evapotranspiration rates for the sugarcane, riparian and black wattle vegetation classes.

Accumulated rates	**Sugarcane**	**Riparian**	**Black wattle**
Total ET (mm)	6892.84	6995.59	7206.93
Total summer ET (mm)	4514.22	4926.57	4557.64
Total summer ET as % of total ET	65.49	70342	63.24
Total winter ET (mm)	2378.62	2069.02	2649.29
Total winter ET as % of total ET	34.51	29.58	36.76
Total ET as % of total rainfall	96.28	97.71	100.66

The ET rates for only the summer months, of all three vegetation classes, are significantly higher than those of the winter months ($P < 2.20 \times 10^{-16}$; Table 6.2), and account for more than 60% of the total ET outputs (Table 6.1). The riparian class has the highest total summer ET rate (4926.57mm), while sugarcane has the lowest (4514.22mm; Table 6.1). Over the winter months, the black wattle has the highest total ET (2649.29mm) and the riparian the lowest (2069.02mm; Table 6.1). The ET rate of the black wattle class was high, with ET predominantly occurring over the summer months. However in comparison to the other two vegetation classes, the winter ET contributed more to the total black wattle total ET (Table 6.1).

Table 6.2: Statistical significance of the evapotranspiration outputs of the sugarcane, riparian and black wattle vegetation classes, compared using the Kruskal Wallis test by ranks and the two-sample Wilcoxon's signed rank non-parametric tests.

	Statistical test employed	**Outputs compared**	**P-value**	**Are the outputs significantly different?****
Total ET	Kruskal Wallis test by ranks	All three	$P = 6.28 \times 10^{-8}$	Yes
	Two-sampled Wilcoxon's signed ranks test	Sugarcane and riparian	$P = 0.76$	No
		Sugarcane and black wattle	$P = 5.56 \times 10^{-7}$	Yes
		Riparian and black wattle	$P = 6.93 \times 10^{-7}$	Yes
Comparing summer and winter ET	Two-sampled Wilcoxon's signed ranks test	Sugarcane	$P < 2.20 \times 10^{-16}$	Yes
		Riparian	$P < 2.20 \times 10^{-16}$	Yes
		Black wattle	$P < 2.20 \times 10^{-16}$	Yes

*Coloured blocks indicate relationships of insignificant difference.
**Where vegetation classes are significantly different (yes) – $P < 0.05$, and where vegetation classes are not significantly different (no) – $P > 0.05$.

The daily ET outputs for all three vegetation classes show cyclic fluctuations, which correspond to seasonal variation, with the summer days experiencing higher rates than the winter days (Figure 6.1). For the sugarcane daily output, where the ET rates drop to 0mm the sugarcane is harvested. This occurs five times over the simulation period (Table 4.4; Figure 6.1). The annual ET rates for all three classes are low in 2007 and 2016 (Figure 6.1) as both the start (2007) and final (2016) simulated years are not complete years. All three classes have low ET in 2015 and high in 2012 (Figure 6.1), which correspond to the lowest and highest annual rainfall rates respectively (Figure 5.1). The sugarcane and riparian classes both show lower ET rates in 2010. This decline does not occur in the black wattle output (Figure 6.1). The black wattle class has the largest annual range (598.09mm) and the sugarcane the smallest (400.33mm).

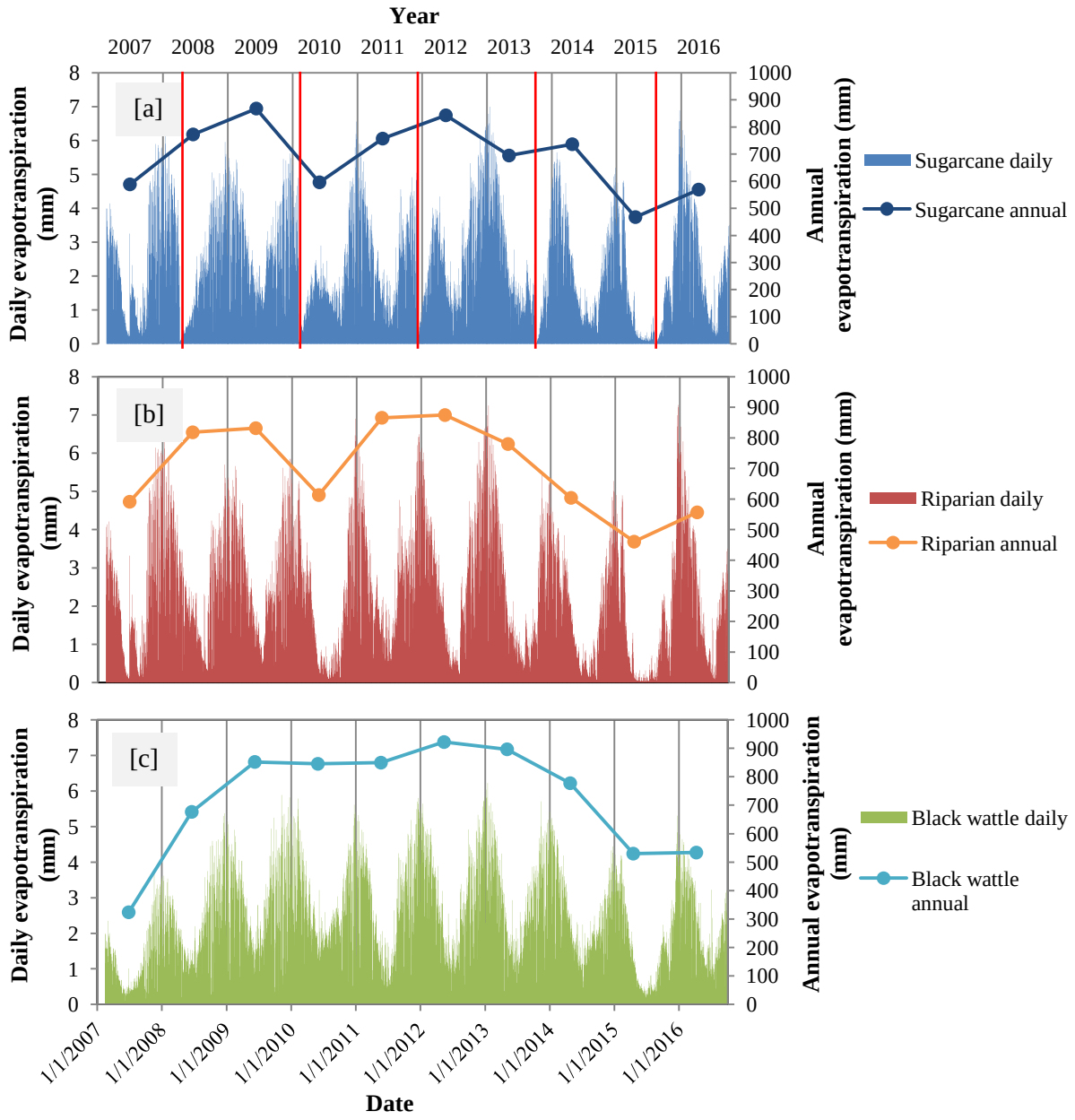

Figure 6.1: Daily and annual evapotranspiration outputs for the [a] sugarcane, [b] riparian and [c] black wattle vegetation classes, modelled over the total simulation period (14 February 2007 – 02 October 2016). In addition, the sugarcane harvest dates are indicated in [a] with red lines.

The averaged monthly ET totals are higher for the riparian class over the summer months and generally lower over the winter months, while the black wattle has higher rates over the winter months (Figure 6.2). The riparian class has the largest monthly range (89.79mm) and black wattle the smallest (65.13mm).

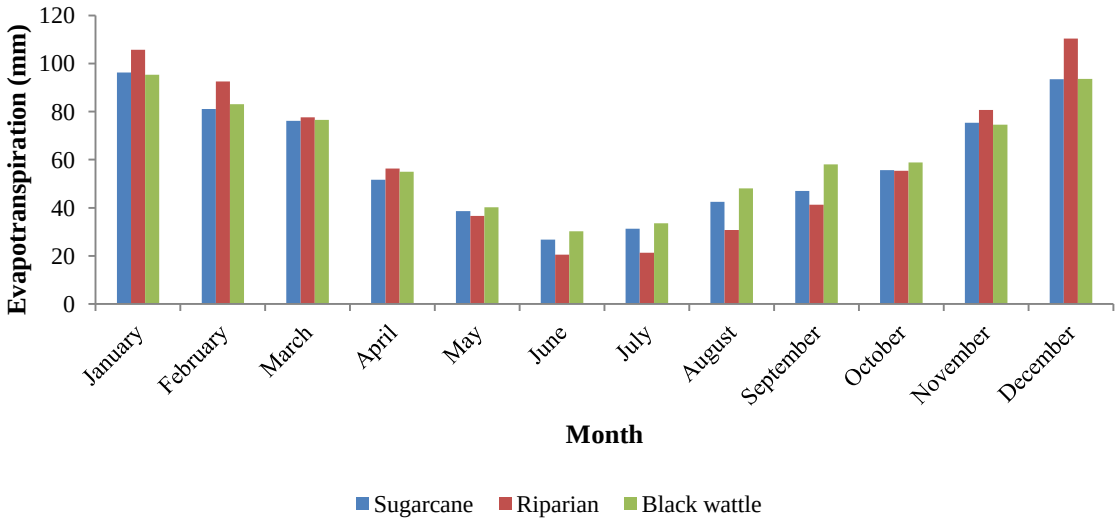

Figure 6.2: Averaged monthly evapotranspiration for the sugarcane, riparian and black wattle vegetation classes for the total simulated period (14 February 2007 – 02 October 2016). The averages exclude the incomplete months of February 2007 and October 2016.

6.3 Evapotranspiration components

Within MIKE SHE the total ET rate comprises of: E_t, E_s, E_i, E_p and evaporation from the SZ (DHI software, 2012). All of these components are investigated below except for evaporation from the SZ as, based on the modelled outputs, no evaporation occurred directly from the SZ.

For each vegetation class, ET comprised predominantly of E_t, accounting for more than 60% of total ET for all three vegetation classes (Table 6.3). Total E_t is highest for the black wattle class (4604.01mm) and lowest for the riparian (4231.35mm) and all E_t rates are significantly different ($P = 1.67 \times 10^{-11}$), when compared together (Table 6.4). However, comparing the outputs two at a time, the sugarcane and riparian rates are not significantly different ($P = 0.11$; Table 6.4). The E_t total outputs show strong seasonal differences, with the summer months accounting for more than 60% of the total output, for each vegetation class. This is verified through the two-sample Wilcoxon's signed ranks test which found the seasonal differences to be statistically significant ($P < 2.20 \times 10^{-16}$; Table 6.4).

Table 6.3: Totals of each evaporation component including overall simulated total and seasonal totals for the summer and winter season.

ET component	Vegetation class	Total (mm)	Total as % of total ET	Summer (mm)	Summer (% of total)	Winter (mm)	Winter (% of total)
E_t	Sugarcane	4330.44	62.83	2783.26	63.23	1592.18	36.77
	Riparian	4231.35	60.49	2987.75	70.61	1243.6	29.39
	Black wattle	4604.01	63.88	2782.82	60.44	1821.19	39.56
E_s	Sugarcane	1377.69	19.99	879.11	63.81	498.58	36.19
	Riparian	1622.59	23.19	1082.36	66.71	540.23	33.29
	Black wattle	1523.18	21.13	962.03	63.16	561.15	36.84
E_i	Sugarcane	1168.33	16.95	881.8	75.48	286.53	24.52
	Riparian	1124.34	16.07	840.61	74.76	283.73	25.24
	Black wattle	1066.92	14.80	801.08	75.08	265.84	24.92
E_p	Sugarcane	16.38	0.24	15.05	91.88	1.33	8.12
	Riparian	17.31	0.25	15.85	91.57	1.46	8.43
	Black wattle	12.83	0.18	11.73	91.43	1.10	8.57

Soil evaporation (E_s) rates contribute between 19.99 – 21.13% of total ET for the three vegetation classes and are highest for the riparian class (1622.59mm) and lowest for sugarcane (1377.69mm; Table 6.3). All E_s outputs are significantly different ($P = 6.37 \times 10^{-12}$), when compared together and when compared two at a time. The riparian and black wattle class outputs are not significantly different ($P = 0.16$; Table 6.4). Similarly to E_t, and all of the other ET component outputs, E_s shows strong, significant ($P < 2.20 \times 10^{-16}$) seasonal differences (Table 6.4), with the summer months accounting for more than 60% of the total E_s rates for all three vegetation classes (Table 6.3).

Evaporation from interception (E_i) rates account for approximately 15% of total ET for all of the vegetation classes (Table 6.3) and are highest for the sugarcane class (1168.33mm) and lowest for the black wattle class (1066.92mm). However these rates are not significantly different for any of the vegetation classes ($P = 0.75$; Table 6.4). The summer months account for more than 70% of the total E_i output (Table 6.3), and the summer and winter E_i rates are significantly different for all three vegetation classes ($P = < 2.20 \times 10^{-16}$; Table 6.4).

The E_p rates are very low for all three vegetation classes, contributing little to total ET rates (< 0.30%; Table 6.3). They are highest for the riparian class (17.31mm) and lowest for black wattle (12.83mm). However the riparian and black wattle class outputs are not significantly different (P = 0.40; Table 6.4). More than 90% of the total E_p outputs occur over the summer months, for all three vegetation classes, with less than 1.50mm occurring over the winter months (Table 6.3). The strong seasonal distinction is verified through the lack of significance between the seasons of each vegetation class ($P < 2.20 \times 10^{-16}$; Table 6.4).

Table 6.4: Statistical significance of the total and seasonal transpiration, soil evaporation, evaporation from interception and evaporation from ponded water outputs of the sugarcane, riparian and black wattle vegetation classes, compared using the Kruskal Wallis test by ranks and the two-sample Wilcoxon's signed ranks non-parametric tests.

ET components		**Statistical test employed**	**Outputs compared**	**P-value**	**Are the outputs significantly different?****
E_t	**Comparing total**	Kruskal Wallis test by ranks	All three	$P = 1.67 \times 10^{-11}$	Yes
		Two-sampled Wilcoxon's signed ranks test	Sugarcane and riparian	P = 0.11	No
			Sugarcane and black wattle	$P < 2.20 \times 10^{-16}$	Yes
			Riparian and black wattle	$P = 1.20 \times 10^{-11}$	Yes
	Comparing summer and winter	Two-sampled Wilcoxon's signed ranks test	Sugarcane	$P < 2.20 \times 10^{-16}$	Yes
			Riparian	$P < 2.20 \times 10^{-16}$	Yes
			Black wattle	$P < 2.20 \times 10^{-16}$	Yes
E_s	**Comparing total**	Kruskal Wallis test by ranks	All three	$P = 6.37 \times 10^{-12}$	Yes
		Two-sampled Wilcoxon's signed ranks test	Sugarcane and riparian	$P = 3.77 \times 10^{-11}$	Yes
			Sugarcane and black wattle	$P = 1.85 \times 10^{-8}$	Yes
			Riparian and black wattle	P = 0.16	No
	Comparing summer and winter	Two-sampled Wilcoxon's signed ranks test	Sugarcane	$P < 2.20 \times 10^{-16}$	Yes
			Riparian	$P < 2.20 \times 10^{-16}$	Yes
			Black wattle	$P < 2.20 \times 10^{-16}$	Yes
E_i	**Comparing total**	Kruskal Wallis test by ranks	All three	P = 0.75	No
		Two-sampled	Sugarcane and riparian	P = 0.62	No
			Sugarcane and black wattle	P = 0.42	No

		Wilcoxon's signed ranks test	Riparian and black wattle	P = 0.95	No
	Comparing summer and winter	Two-sampled Wilcoxon's signed ranks test	Sugarcane	$P < 2.20 \times 10^{-16}$	Yes
			Riparian	$P < 2.20 \times 10^{-16}$	Yes
			Black wattle	$P < 2.20 \times 10^{-16}$	Yes
E_p	**Comparing total**	Kruskal Wallis test by ranks	All three	P = 0.01	Yes
		Two-sampled Wilcoxon's signed ranks test	Sugarcane and riparian	P = 0.04	Yes
			Sugarcane and black wattle	$P = 3.86 \times 10^{-3}$	Yes
			Riparian and black wattle	P = 0.40	No
	Comparing summer and winter	Two-sampled Wilcoxon's signed ranks test	Sugarcane	$P < 2.20 \times 10^{-16}$	Yes
			Riparian	$P < 2.20 \times 10^{-16}$	Yes
			Black wattle	$P < 2.20 \times 10^{-16}$	Yes

*Coloured blocks indicate relationships of insignificant difference.
**Where vegetation classes are significantly different (yes) – $P < 0.05$ and where vegetation classes are not significantly different (no) – $P > 0.05$.

The daily outputs support the previous findings of seasonality with the E_t and E_s outputs, for all vegetation classes, showing cyclical fluctuations that display seasonal differences, where the winter months experience lower rates than the summer months (Figure 6.3). The E_p outputs show seasonal differences in daily data. However, over the winter seasons little to no E_p occurs for any of the vegetation classes (Figure 6.3). For all three vegetation classes, the majority of the simulated days do not experience E_p (Figure 6.3). For the sugarcane output, 82.92% of the simulated days (2918 days) record no E_p; for the riparian 79.54% (2799 days); and for the black wattle, 82.24% (2894 days). The daily E_i outputs show seasonal differences. These are more evident during the times when the rates are more erratic, between 2007 – 2009, between 2011 – 2012 and periods in 2013 and 2016 (Figure 6.3).

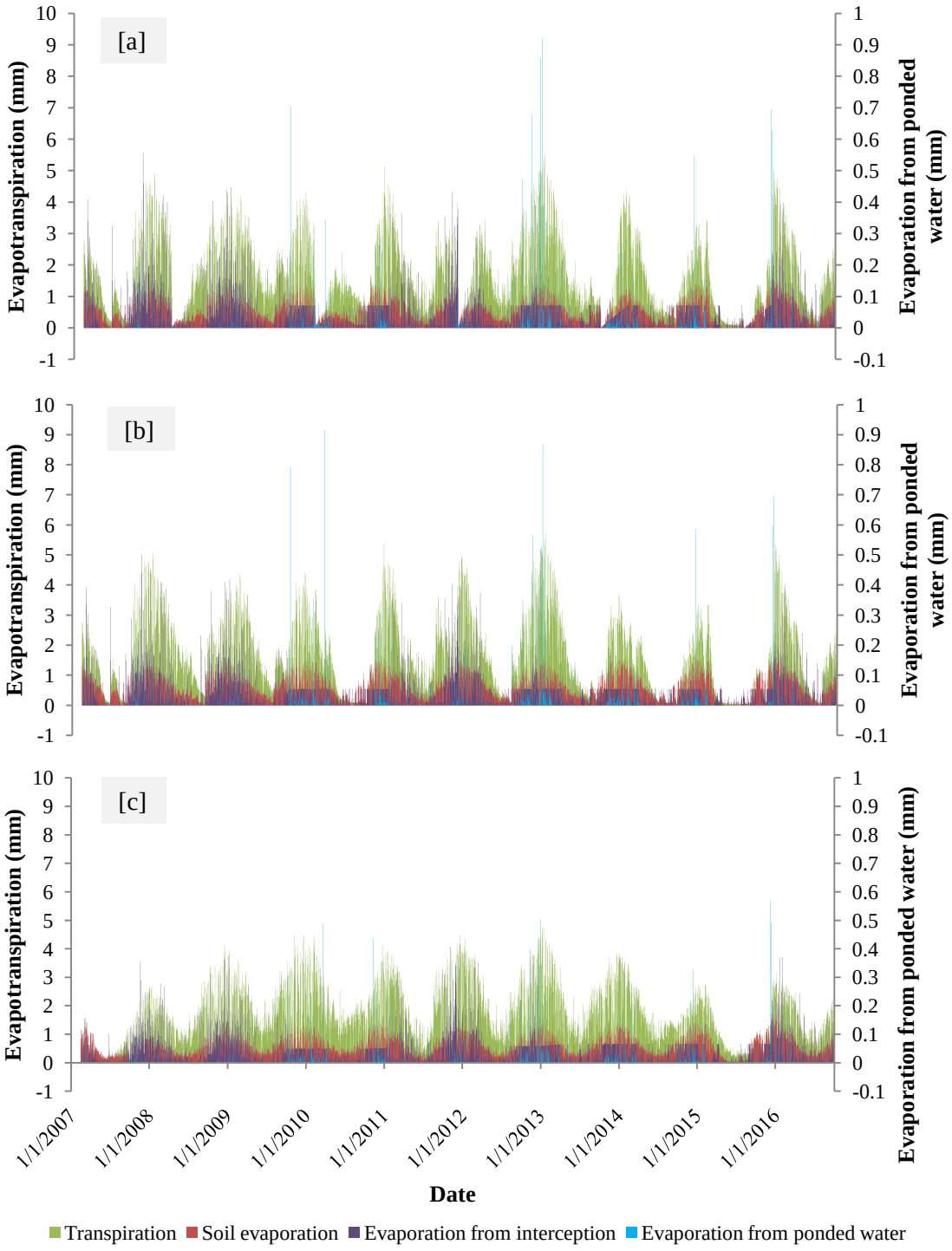

Figure 6.3: Daily transpiration, soil evaporation, evaporation from interception and evaporation from ponded water (separate vertical axis) outputs, for the [a] sugarcane, [b] riparian, and [c] black wattle vegetation classes.

The annual E_t rates for the sugarcane and riparian classes are similar, whilst the black wattle rates differ, most noticeably in 2010 where annual E_t increases from the previous year, whilst for the other class a decrease in E_t is experienced (Figure 6.4). The black wattle output has a noticeably higher

annual E_t in 2013, in comparison to the annual records of the other classes, and a noticeably lower rate in 2007 (Figure 6.4). The annual black wattle E_t range is the largest (493.72mm) and sugarcane the smallest (275.82mm). The annual E_s outputs of all three vegetation classes follow similar trends with 2007 and 2016 experiencing lower rates that the remainder of the simulated years (Figure 6.4). Overall the sugarcane E_s rates are noticeably lower than those of the other classes (Figure 6.4). The riparian class had the largest annual E_s range (63.67mm) and sugarcane the smallest (45.06mm). The annual E_i rates of all three vegetation classes showed similar trends, with the largest difference observed between 2007 – 2008 and the smallest between 2010 – 2012 (Figure 6.4). The sugarcane class has the largest range in annual E_i (97.77mm) and black wattle the smallest (79.65mm). The annual E_p outputs all show a similar trend (Figure 6.4), with the highest annual range seen in sugarcane (4.43mm) and lowest in black wattle (2.67mm).

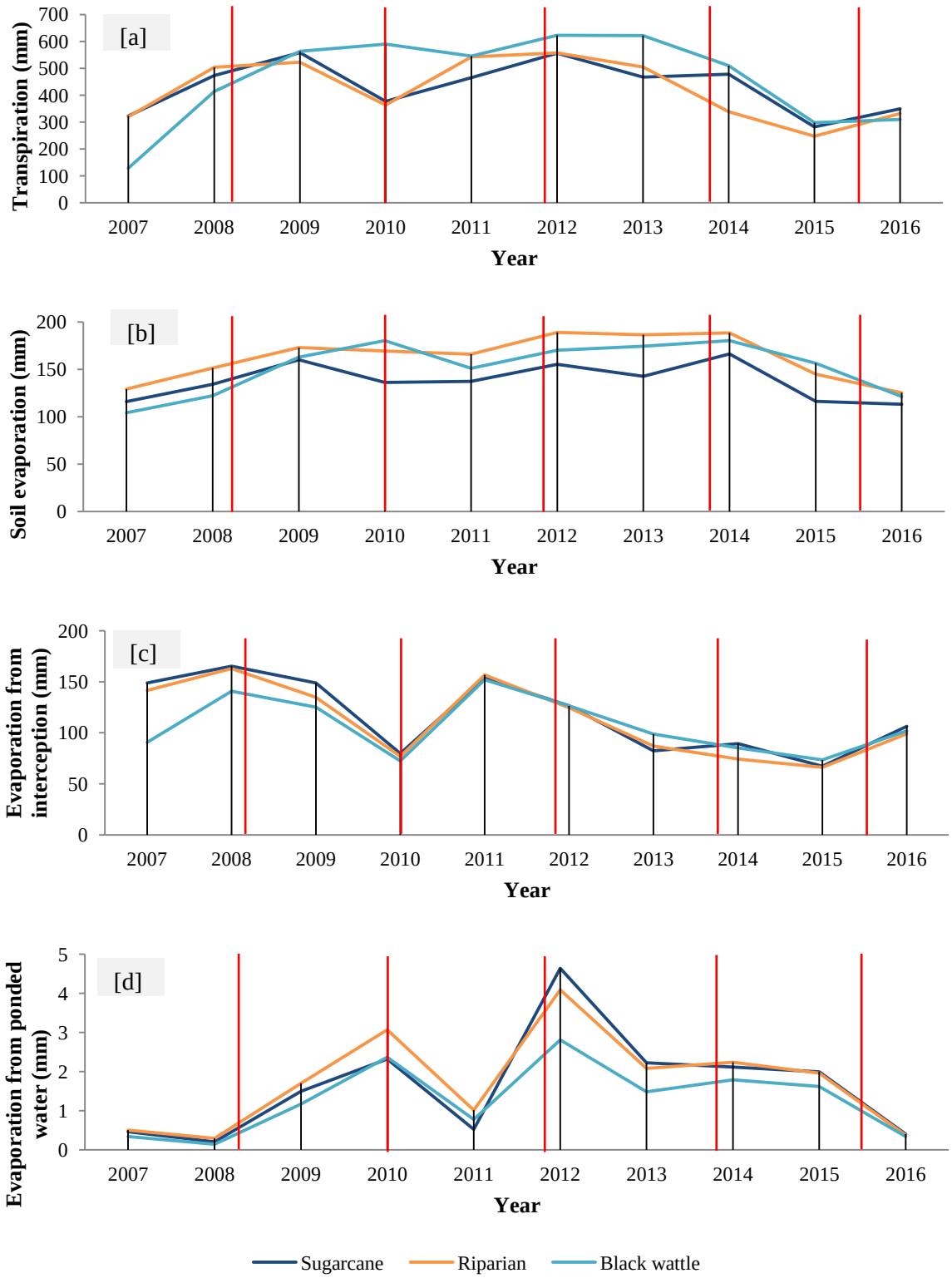

Figure 6.4: Annual rates of [a] transpiration, [b] soil evaporation, [c] evaporation from interception and [d] evaporation from ponded water for the sugarcane, riparian and black wattle vegetation classes over the total simulated period (14 February 2007 – 02 October 2016). In addition, the sugarcane harvest dates are indicated in each graph with red lines.

6.4 Canopy interception storage (CIS)

The total accumulated CIS rates are low for all three vegetation classes, accounting for < 1% of the total rainfall (Table 6.5). The total summer CIS outputs, for all classes, account for approximately 54% of their respective totals (Table 6.5). Thus, the winter and summer seasons do not display as noticeable differences in CI as is evident from the ET outputs. However, the seasonal differences are significantly different from one another for each vegetation class ($P < 0.05$; Table 6.6).

Table 6.5: Accumulated total, summer and winter canopy interception storage rates for the sugarcane, riparian and black wattle vegetation classes, captured over the simulation period (14 February 2007 – 02 October 2016).

Accumulated rates	**Sugarcane**	**Riparian**	**Black wattle**
Total CIS (mm)	44.64	29.89	34.14
Total CIS as % of total rainfall	0.62	0.42	0.48
Total summer CIS (mm)	24.44	16.05	18.57
Total summer CIS as % of total CIS	54.75	53.70	54.39
Total winter CIS (mm)	20.20	13.84	15.57
Total winter CIS as % of total CIS	45.25	46.30	45.61

Sugarcane has the largest total, summer and winter CIS rates (44.64mm, 24.44mm and 20.20mm respectively), whilst the riparian class has the lowest (29.89mm, 16.05mm and 13.84mm, respectively; Table 6.5). The sugarcane and riparian CIS records are significantly different from one another ($P = 8.40 \times 10^{-4}$; Table 6.6).

Table 6.6: Statistical significance of the total and seasonal canopy interception storage outputs of the sugarcane, riparian and black wattle vegetation classes, compared using the Kruskal Wallis test by ranks and the two-sample Wilcoxon's signed ranks non-parametric tests.

	Statistical test employed	**Outputs compared**	**P-value**	**Are the outputs significantly different?****
Total CIS	Kruskal Wallis test by ranks	All three	$P = 3.83 \times 10^{-3}$	Yes
	Two-sampled Wilcoxon's signed ranks test	Sugarcane and riparian	$P = 8.40 \times 10^{-4}$	Yes
		Sugarcane and black wattle	P = 0.12	No
		Riparian and black wattle	P = 0.07	No
Comparing summer and winter CIS	Two-sampled Wilcoxon's signed ranks test	Sugarcane	$P = 1.59 \times 10^{-5}$	Yes
		Riparian	$P = 4.59 \times 10^{-3}$	Yes
		Black wattle	$P = 1.06 \times 10^{-3}$	Yes

*Coloured blocks indicate relationships of insignificant difference.
**Where vegetation classes are significantly different (yes) – $P < 0.05$ and where vegetation classes are not significantly different (no) – $P > 0.05$.

The daily CIS outputs (Figure 6.5) demonstrate no seasonal fluctuations (Figure 6.1), supporting the above findings showing little seasonal difference in CIS. The majority of the simulation period experiences no CIS, for all three vegetation classes (Figure 6.5). The sugarcane daily CIS ranges from 0 – 0.18mm, with 87.33% of the total simulated days experiencing no CIS (3074 days), the riparian ranges from 0 – 0.13mm, with 89.57% of the total days experiencing no interception storage (3153 days), and the black wattle rates range between 0 – 0.17mm, with 88.21% of days experiencing no CIS (3105 days).

The annual sugarcane CIS rates exceed those of the other classes until 2013 during which time the riparian and black wattle annual rates are similar (Figure 6.5). After 2013, the sugarcane and black wattle classes have similar annual rates for the remainder of the simulation, whilst the riparian annual rates are lower (Figure 6.5). The sugarcane CIS output show the largest annual range (7.12mm), whilst the riparian (5.81mm) and black wattle (5.88mm) outputs have similar annual ranges.

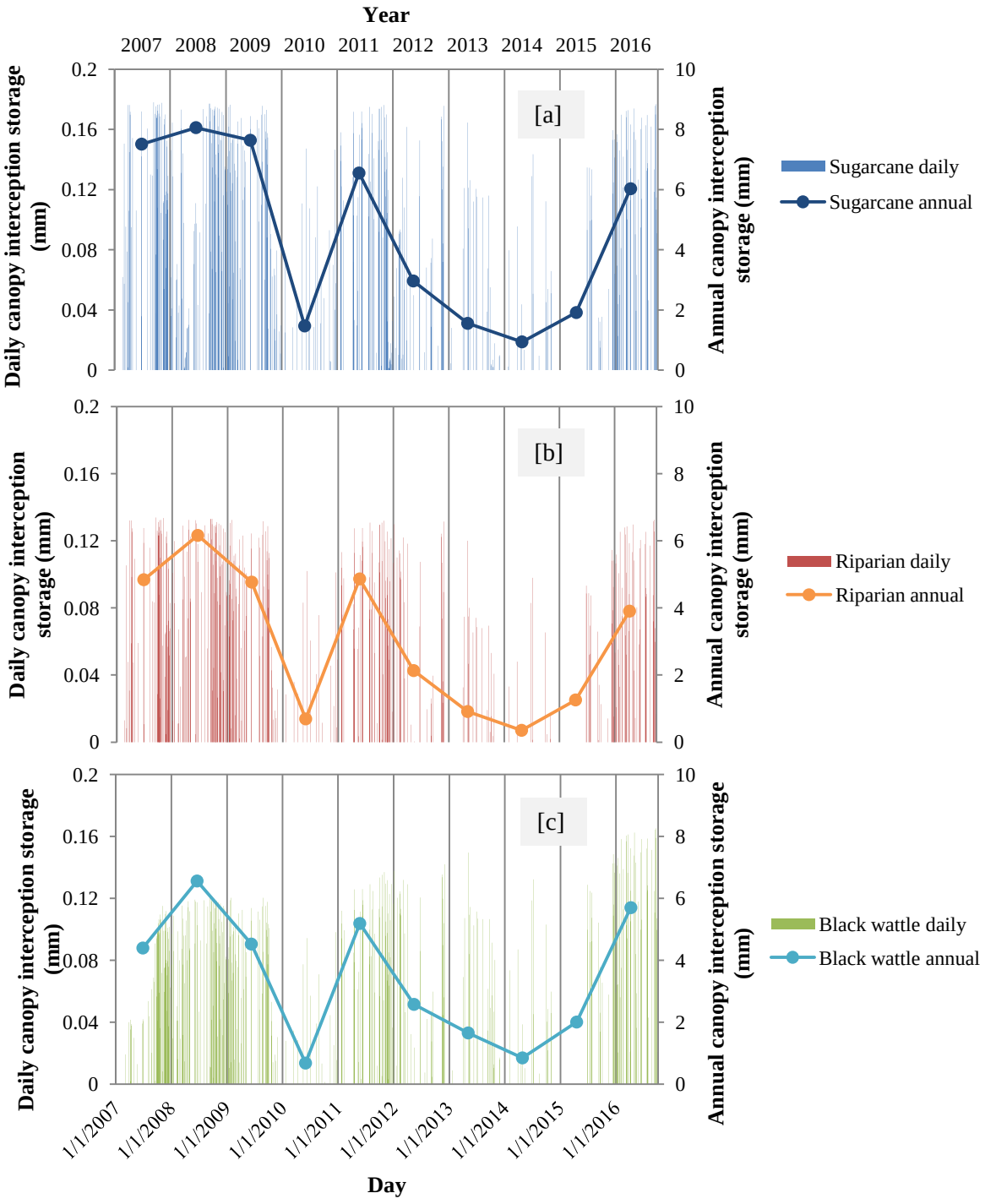

Figure 6.5: Daily and annual canopy interception storage outputs for the [a] sugarcane, [b] riparian and [c] black wattle vegetation classes, modelled over the total simulation period (14 February 2007 – 02 October 2016).

Together CIS and E_i make-up the total amount of water intercepted by the canopy (DHI software, 2012). Correlating the annual CIS and E_i outputs, all comparisons produce strong positive, significant,

linear correlations, r = 0.89 (P = 5.00 x 10^{-4}), 0.91 (P = 3.00 x 10^{-4}) and 0.70 (P = 0.02) for the sugarcane, riparian and black wattle classes respectively.

The monthly sugarcane rates are higher than those of the other vegetation classes for each month, whilst the riparian rates are lowest for the majority of months (Figure 6.6). The months of September, October and November had the highest rates of CIS for all three vegetation classes, while May had the lowest monthly rates (Figure 6.6). Thus, a seasonal pattern was less evident in the monthly CIS rates than was evident in the ET outputs.

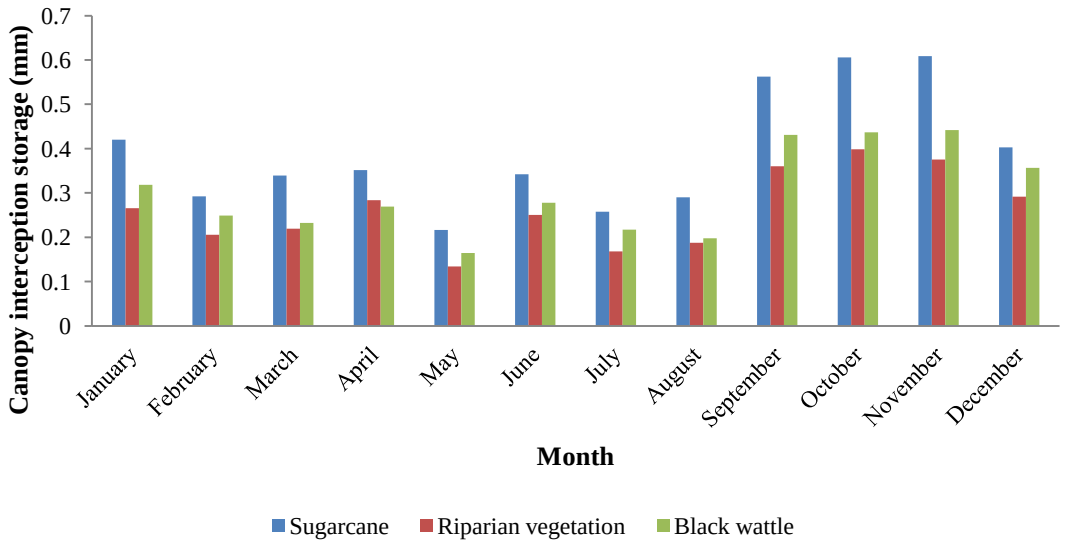

Figure 6.6: Averaged monthly canopy interception storage for the sugarcane, riparian and black wattle vegetation classes for the total simulated period (14 February 2007 – 02 October 2016). The averages exclude February 2007 and October 2016.

In MIKE SHE LAI defines the plant canopy characteristics (DHI software, 2012) and as such can have an influencing factor on the rates of E_t (and subsequently total ET) and CI (including both evaporation and storage) as both of these factors have a direct interaction with vegetation (Hendriks, 2010). Correlating the monthly black wattle ET and LAI rates (Figure 6.7), they have a significant, strong, positive linear correlation, r = 0.74 (P < 1.00 x 10^{-4}). Similarly, the monthly E_t and LAI rates have a significant, strong, positive linear correlation (Figure 6.7), r = 0.79 (P < 1.00 x 10^{-4}).

Correlating the monthly black wattle CI (CIS and E_i) and black wattle LAI, they have a significant, positive linear correlation (Figure 6.7), r = 0.46 (P = 0.03). The LAI of the other vegetation classes are not correlated to their respective ET, E_t and CI rates as these LAI rates are averaged over the simulation period showing limited variation in relation to a real world situation (section 4.3.5).

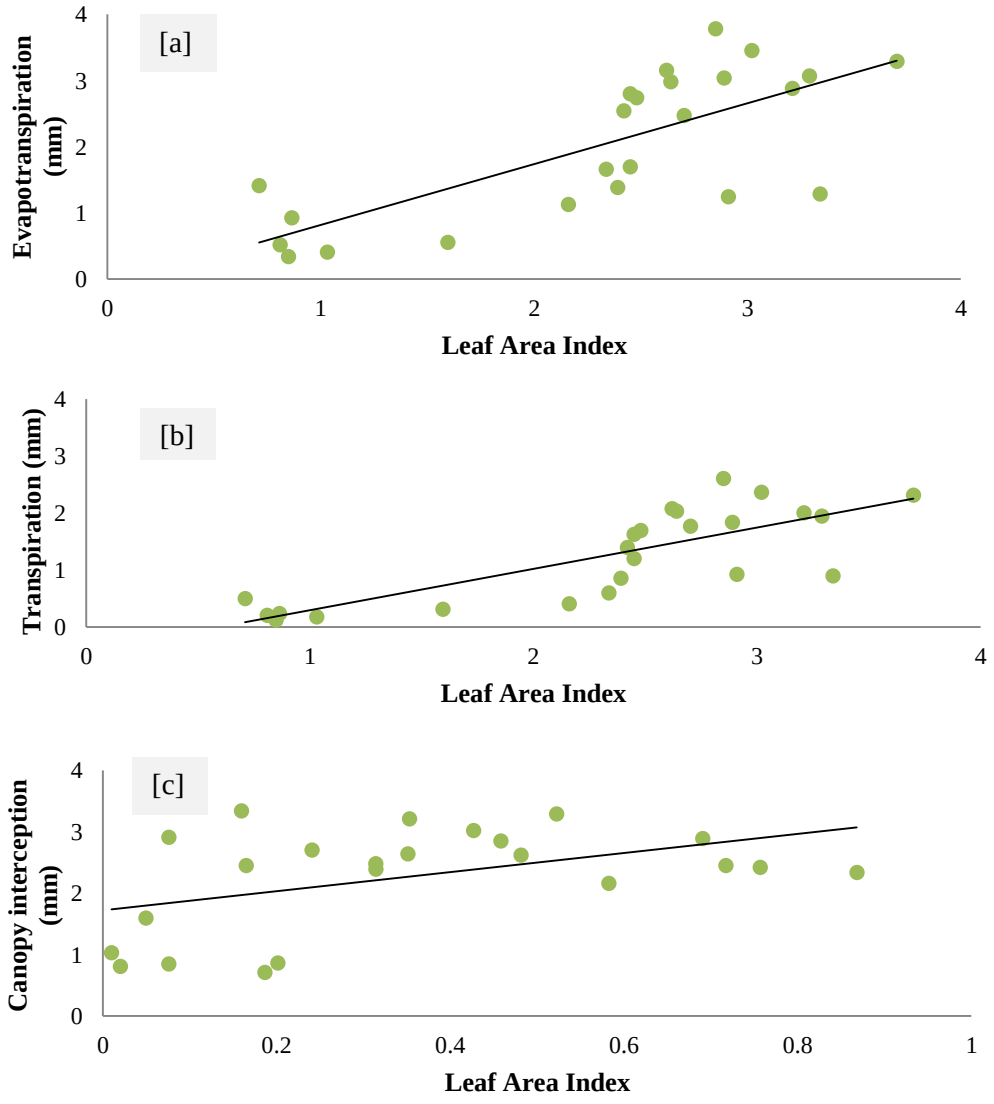

Figure 6.7: Scatter plots showing the relationship between monthly [a] evapotranspiration, [b] transpiration, and [c] canopy interception, and monthly Leaf Area Index (LAI), for the black wattle vegetation class over the period February 2007 – October 2013.

6.5 Depth of overland flow

The depth of OL outputs are low for all three vegetation classes, accounting for approximately 3.00 x 10^{-5}% of the total precipitation (Table 6.7). The riparian class has the highest total depth of OL (2.55 x 10^{-3}mm) and black wattle the lowest (1.95 x 10^{-3}mm; Table 6.7). All depth of OL outputs are significantly different from one another, based on the Kruskal Wallis test by ranks ($P < 2.20 \times 10^{-16}$; Table 6.8). However when comparing the vegetation class outputs using the two-sample Wilcoxon's signed ranks test the sugarcane and riparian outputs are not significantly different (P = 0.07; Table 6.8).

Table 6.7: Accumulated total, summer and winter depth of overland flow values for the sugarcane, riparian and black wattle vegetation classes, captured over the simulation period (14 February 2007 – 02 October 2016).

Accumulated rates	**Sugarcane**	**Riparian**	**Black wattle**
Total depth of OL (mm)	2.26 x 10^{-3}	2.55 x 10^{-3}	1.95 x 10^{-3}
Total depth of OL as % of total rainfall	3.16 x 10^{-5}	3.56 x 10^{-5}	2.72 x 10^{-5}
Summer depth of OL (mm)	1.68 x 10^{-3}	1.90 x 10^{-3}	1.36 x 10^{-3}
Summer depth of OL as % of total depth of OL	74.35	74.57	69.83
Winter depth of OL (mm)	5.80 x 10^{-4}	6.45 x 10^{-4}	5.83 x 10^{-4}
Winter depth of OL as % of total depth of OL	25.65	25.43	30.17

The total depth of OL values are higher for the summer months (than the winter months) accounting for between 70 – 75% of the total outputs for all three vegetation classes (Table 6.7). However, despite the differences in total seasonal depth of OL, the black wattle output shows no significant difference between seasons (P = 0.82; Table 6.8).

Table 6.8: Statistical significance of the total and seasonal depth of overland flow outputs of the sugarcane, riparian and black wattle vegetation classes, compared using the Kruskal Wallis test by ranks and the two-sample Wilcoxon's signed ranks non-parametric tests.

	Statistical test employed	**Outputs compared**	**P-value**	**Are the outputs significantly different?****
Total depth of OL	Kruskal Wallis test by ranks	All three	$P < 2.20 \times 10^{-16}$	Yes
	Two-sampled Wilcoxon's signed ranks test	Sugarcane and riparian	$P = 0.07$	No
		Sugarcane and black wattle	$P < 2.20 \times 10^{-16}$	Yes
		Riparian and black wattle	$P < 2.20 \times 10^{-16}$	Yes
Comparing summer and winter depth of OL	Two-sampled Wilcoxon's signed ranks test	Sugarcane	$P = 2.92 \times 10^{-14}$	Yes
		Riparian	$P = 2.67 \times 10^{-11}$	Yes
		Black wattle	$P = 0.82$	No

*Coloured blocks indicate relationships of insignificant difference.
**Where vegetation classes are significantly different (yes) – $P < 0.05$ and where vegetation classes are not significantly different (no) – $P > 0.05$.

The annual depths of OL values are highest in 2014 for the sugarcane and riparian vegetation classes and highest in 2013 for the black wattle class, and lowest in 2016 for all three vegetation classes (Figure 6.8). There is a peak in the annual depth of OL outputs for all three vegetation classes in 2010, followed by a steep decline in annual values in 2011 (Figure 6.8). The daily depth of OL outputs show a peak rate significantly greater than all other simulated days on the 28th of January 2015 (Figure 6.8), with this single day accounting for 6.72% (sugarcane), 8.95% (riparian) and 5.40% (black wattle) of the total respective OL values (Table 6.9).

Table 6.9: Daily depth of overland flow values for the 28th of January 2015 for the sugarcane, riparian and black wattle vegetation classes.

Vegetation class	**Date of highest simulated daily depth of** OL	**Depth of** OL **(mm)**	**Total simulated daily depth of** OL **(mm)**	**Highest simulated as % of total**
Sugarcane	28 January 2015	1.52×10^{-4}	2.26×10^{-3}	6.72
Riparian	28 January 2015	2.28×10^{-4}	2.55×10^{-3}	8.95
Black wattle	28 January 2015	1.05×10^{-4}	1.95×10^{-3}	5.40

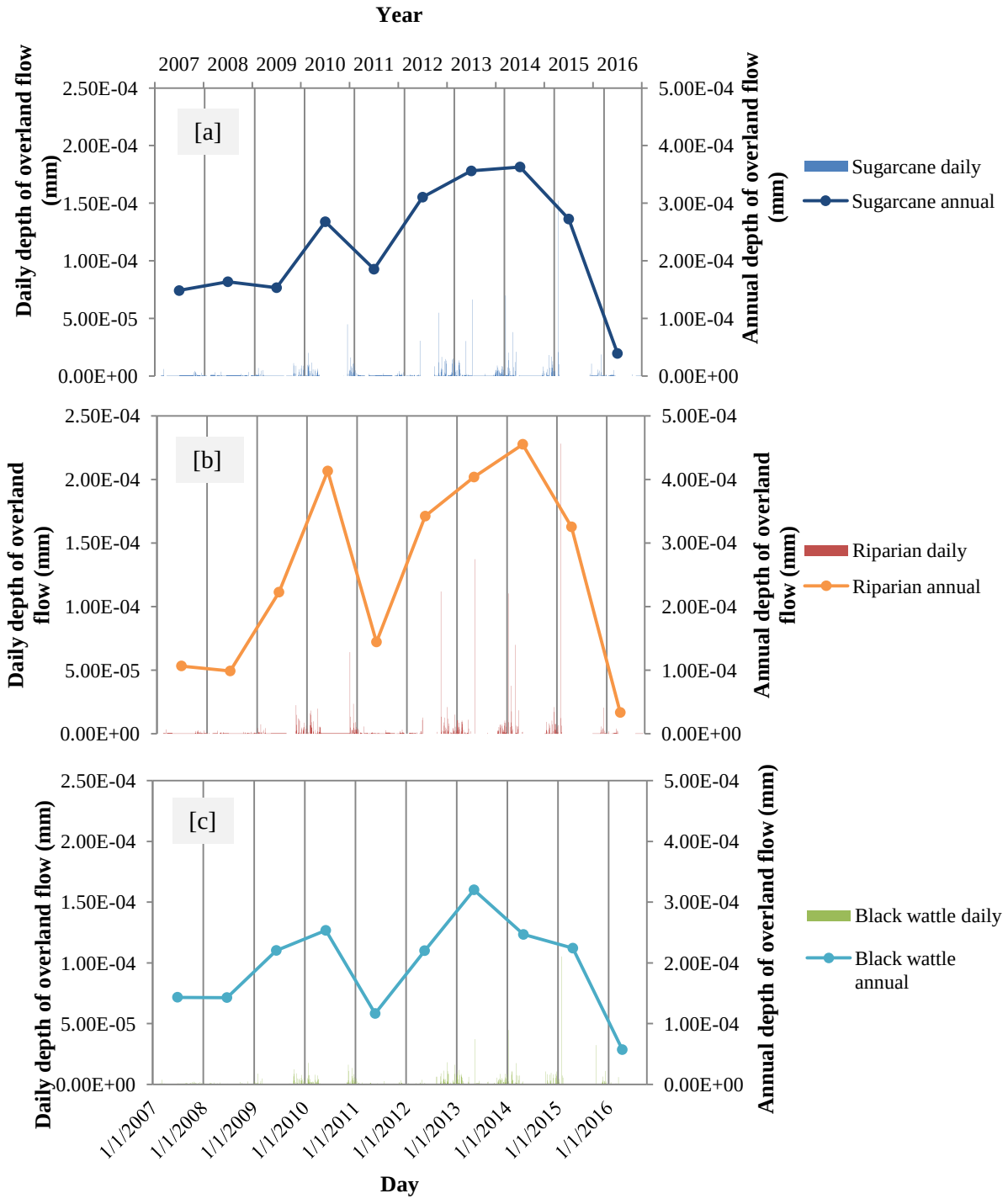

Figure 6.8: Daily and annual depth of overland flow outputs for the [a] sugarcane, [b] riparian and [c] black wattle vegetation classes, modelled over the total simulation period (14 February 2007 – 02 October 2016).

To identify the cause of this peak in depth of OL, climatic conditions are considered. On the 28th of January 2015 daily rainfall was 27.3mm, this was the highest rainfall experienced in January 2015

which had an average rainfall of 2.17mm and a total rainfall of 67.4mm (Figure 6.9). However, this was lower that the highest daily rainfall experienced over the simulation of 75.7mm (12 December 2015; Figure 5.1). The daily average temperature was approximately 16˚C which was lower than the monthly average of 20˚C (Figure 6.9). Thus, for January 2015, the 28th experienced the highest rainfall and relatively low temperatures.

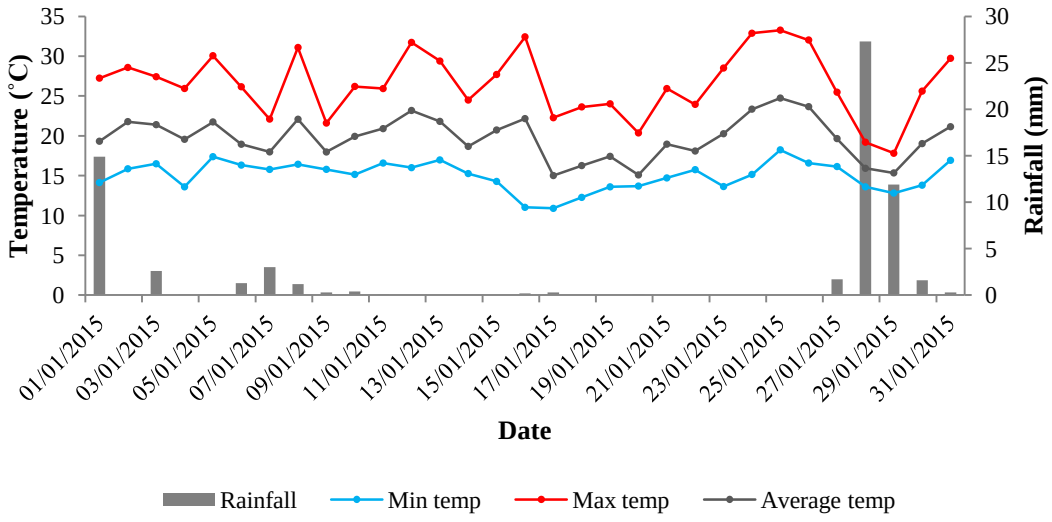

Figure 6.9: Daily rainfall (mm) and temperature (˚C) measures for January 2015, for the Two Streams study site.

This could suggest that more water was available for OL as less water was evaporated due to the lack of radiant energy. The average ET was lowest for the 28th of January 2015 in comparison to the rest of the month, amounting to 0.95mm (Figure 6.10). This is much lower than the averaged ET for January 2015 (2.86mm). The I_{UZ} rate was greatest for the 28th of January 2015, in comparison to the rest of the month (Figure 6.10), justifying why, despite being the largest rate of depth of OL, over the simulation period, the rate was still low (Table 6.9).

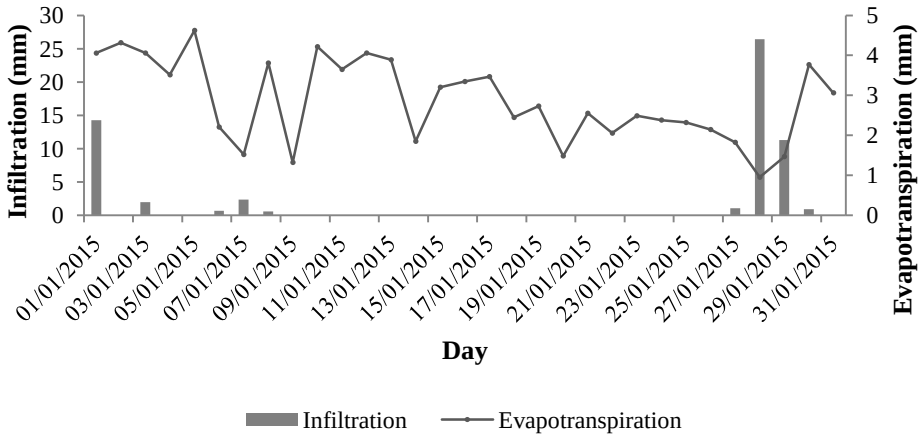

Figure 6.10: Daily average infiltration (mm) and average evapotranspiration (mm) measures for January 2015, for the Two Streams study site.

The spatial variation in the depth of OL for the 28th of January 2015 (Figure 6.11) shows discrete homogeneous patches of depth of OL. Each patch corresponds to the different soil types of the sub-catchment (Figure 4.15), with the Magwa and Clovelly soils having higher rates of depth of OL (> 2.60 x 10^{-4}) and the Oakleaf soil having lower rates of depth of OL (< 2.00 x 10^{-5}; Figure 6.11).

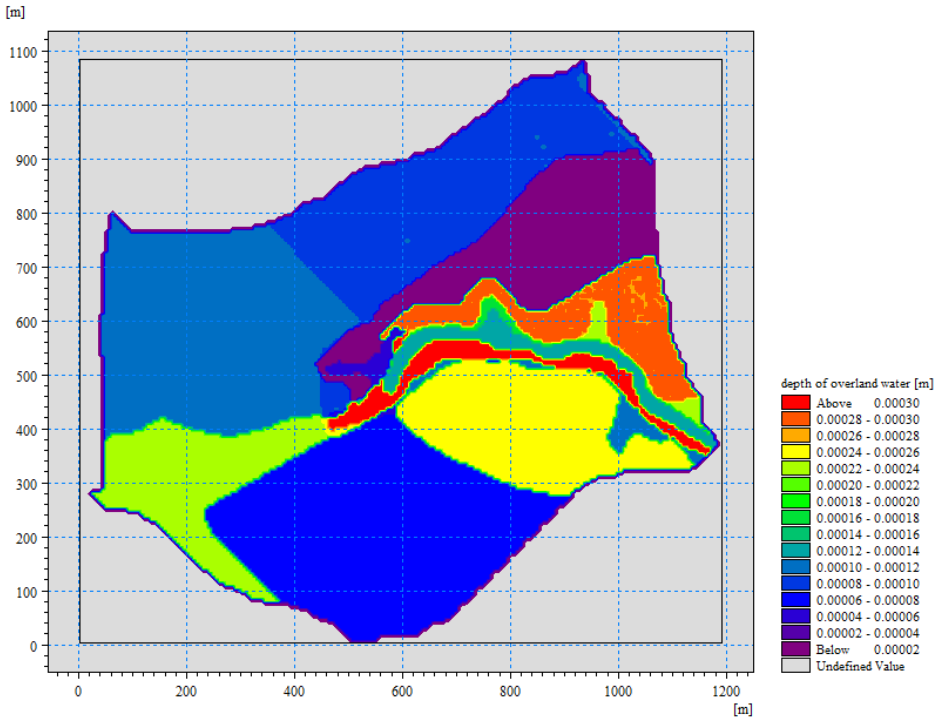

Figure 6.11: Model screen display of the spatially explicit depth of overland flow values for the 28th of January 2015, for the Two Streams study site.

Depth of overland flow (OL) and I_{UZ} (results presented in section 6.6) are expected to be interlinked processes having a resultant impact on each other, as if more I_{UZ} occurs there should be less water available as OL. Correlating the annual depth of OL rates to those of I_{UZ}, all vegetation classes show insignificant, weak linear correlations, r = 0.06 (sugarcane), 0.05 (riparian) and 8.37 x 10^{-4} (black wattle; Table 6.10). The amount of OL (i.e. water present on the ground surface) will impact the amount of evaporation taking place, where the more water present on the surface is expected to allow for greater rates of evaporation. Correlating the annual depth of OL rates and the E_p rates, for all three vegetation class, they have significant, strong positive linear correlations, r = 0.71 (sugarcane), 0.81 (riparian) and 0.70 (black wattle; Table 6.10).

Table 6.10: Pearson's correlation coefficients based on the linear correlations between the annual depth of overland flow and infiltration rates, and annual depth of overland flow and evaporation from ponded water rates for the three vegetation classes: sugarcane, riparian and black wattle.

Correlation	**Vegetation class**	**Relationship**	**Pearson's correlation coefficient (r)**	**Significance of the Pearson's correlation***
Depth of OL and I_{UZ}	Sugarcane	Positive	0.06	P = 0.86
	Riparian	Negative	0.05	P = 0.89
	Black wattle	Positive	8.37 x 10^{-4}	P = 0.99
Depth of OL and E_p	Sugarcane	Positive	0.71	P = 0.02
	Riparian	Positive	0.81	P = 0.01
	Black wattle	Positive	0.70	P = 0.03

* Pearson's correlation coefficients are significant when P < 0.05 and not significant when P > 0.05.
** Coloured blocks indicate Pearson's correlation coefficients that are not significant (P > 0.05).

6.6 Infiltration to the unsaturated zone (I_{UZ})

Outside of total ET, I_{UZ} accounts for the largest proportion of total rainfall (> 80%) for each vegetation class (Table 6.11). The I_{UZ} rates of the three vegetation classes are similar (Table 6.11), and showed no significant differences (P = 0.78; Table 6.12).

Table 6.11: Accumulated total, summer and winter infiltration (mm) rates for the sugarcane, riparian and black wattle vegetation classes, captured over the simulation period (14 February 2007 – 02 October 2016).

Accumulated rates	**Sugarcane**	**Riparian**	**Black wattle**
Total I_{UZ} (mm)	5974.79	6017.85	6079.76
Total I_{UZ} as % of total rainfall	83.45	84.05	84.92
Summer I_{UZ} (mm)	4628.69	4669.00	4712.66
Summer I_{UZ} as % of total I_{UZ}	77.47	77.59	77.51
Winter I_{UZ} (mm)	1346.10	1348.85	1367.10
Winter I_{UZ} as % of total I_{UZ}	22.53	22.41	22.49

Black wattle has the highest total, summer and winter I_{UZ} rates (6079.76mm, 4712.66mm and 1367.10mm respectively), whilst sugarcane the lowest (5974.79mm, 4628.69mm, 1346.10mm; Table 6.11). The total summer I_{UZ} rates exceed those of, and are significantly different ($P < 2.2 \times 10^{-16}$; Table 6.12) to, the winter rates, for each vegetation class, accounting for approximately 78% of the total I_{UZ} outputs for all three classes (Table 6.11). For all three vegetation classes, water use (ET) exceeded I_{UZ} every year, with the total differences of 918.05mm (sugarcane), 977.74mm (riparian) and 1127.17mm (black wattle).

Table 6.12: Statistical significance of the total and seasonal infiltration outputs of the sugarcane, riparian and black wattle vegetation classes, compared using the Kruskal Wallis test by ranks and the two-sample Wilcoxon's signed ranks non-parametric tests.

	Statistical test employed	**Outputs compared**	**P-value**	**Are the outputs significantly different?****
Total I_{UZ}	Kruskal Wallis test by ranks	All three	P = 0.78	No
	Two-sampled Wilcoxon's signed ranks test	Sugarcane and riparian	P = 0.82	No
		Sugarcane and black wattle	P = 0.48	No
		Riparian and black wattle	P = 0.64	No
Comparing summer and winter I_{UZ}	Two-sampled Wilcoxon's signed ranks test	Sugarcane	$P < 2.2 \times 10^{-16}$	Yes
		Riparian	$P < 2.2 \times 10^{-16}$	Yes
		Black wattle	$P < 2.2 \times 10^{-16}$	Yes

*Coloured blocks indicate relationships of insignificant difference.
**Where vegetation classes are significantly different (yes) – $P < 0.05$ and where vegetation classes are not significantly different (no) – $P > 0.05$.

The daily I_{UZ} outputs all display cyclic fluctuations, demonstrating what appear to be seasonal variations, with the summer months experiencing higher rates than the winter months (Figure 6.12). Peak daily rates of I_{UZ} are experienced on the 12th of December 2015, 28th of February 2009 and 14th of January 2008 for all three vegetation classes (Figure 6.12). These dates correspond with the peak daily rainfall rates, with highest amount of rainfall (75.7mm) experienced on the 12th of December 2015 and 68.9mm and 60.7mm of rainfall experienced on the 28th of February 2009 and 14th of January 2008 respectively (Figure 5.1). The annual I_{UZ} rates of the three vegetation classes are similar (Figure 6.12), with the greatest difference occurring in 2007, where the black wattle rate exceeds that of the other vegetation classes (Figure 6.12). Comparing the annual ranges of I_{UZ}, the black wattle and sugarcane ranges were similar, 432.48mm and 425.03mm respectively.

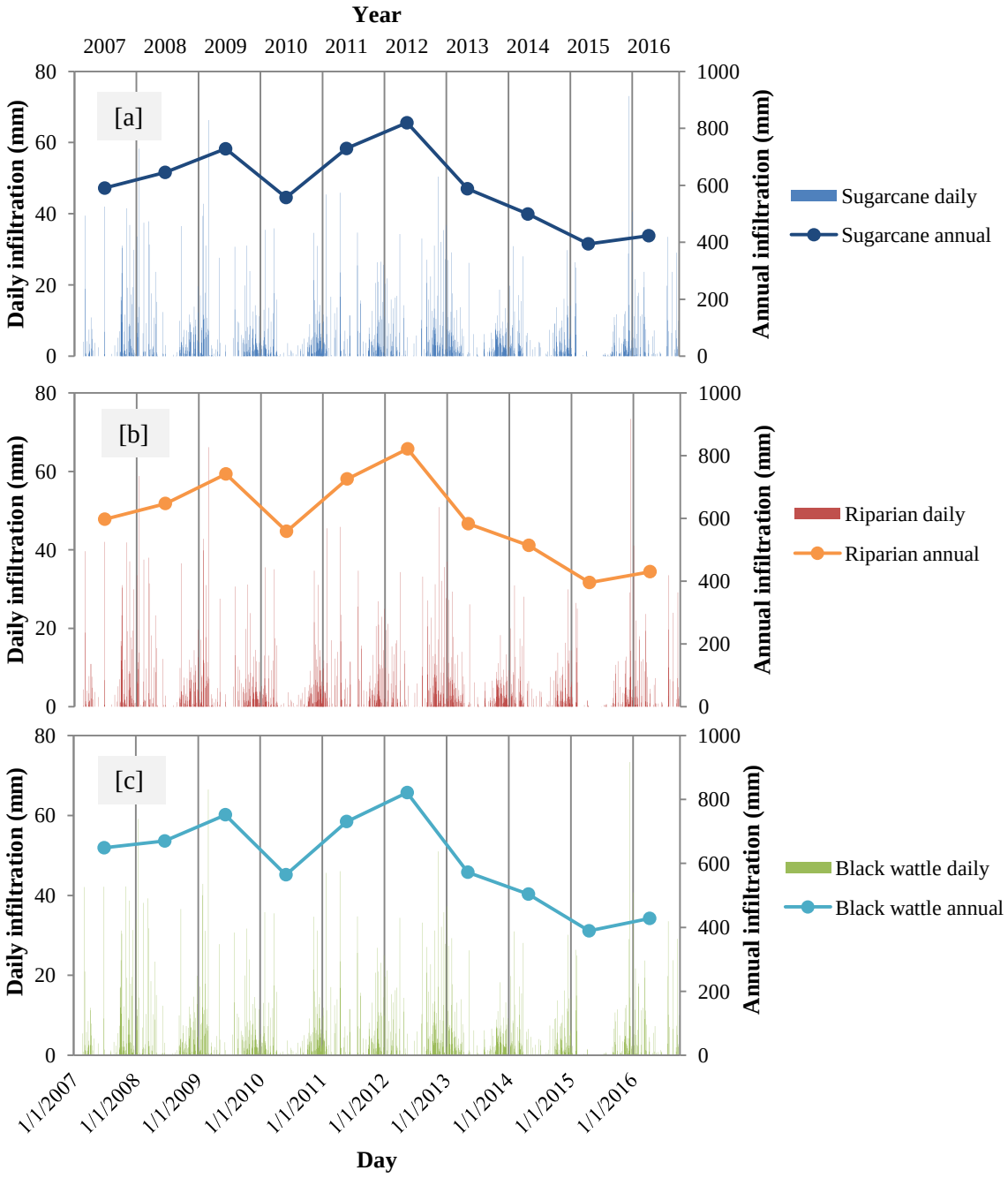

Figure 6.12: Daily and annual infiltration outputs for the [a] sugarcane, [b] riparian and [c] black wattle vegetation classes, modelled over the total simulation period (14 February 2007 – 02 October 2016).

The averaged monthly I_{UZ} totals are similar for all three vegetation classes (Figure 6.13), with the black wattle monthly rates being slightly higher. There is a clear seasonal distinction with the summer months having higher rates than the winter months (Figure 6.13). All three vegetation

classes have similar ranges in monthly I_{UZ} rates of 94.99mm (sugarcane), 94.95mm (riparian) and 95.48mm (black wattle).

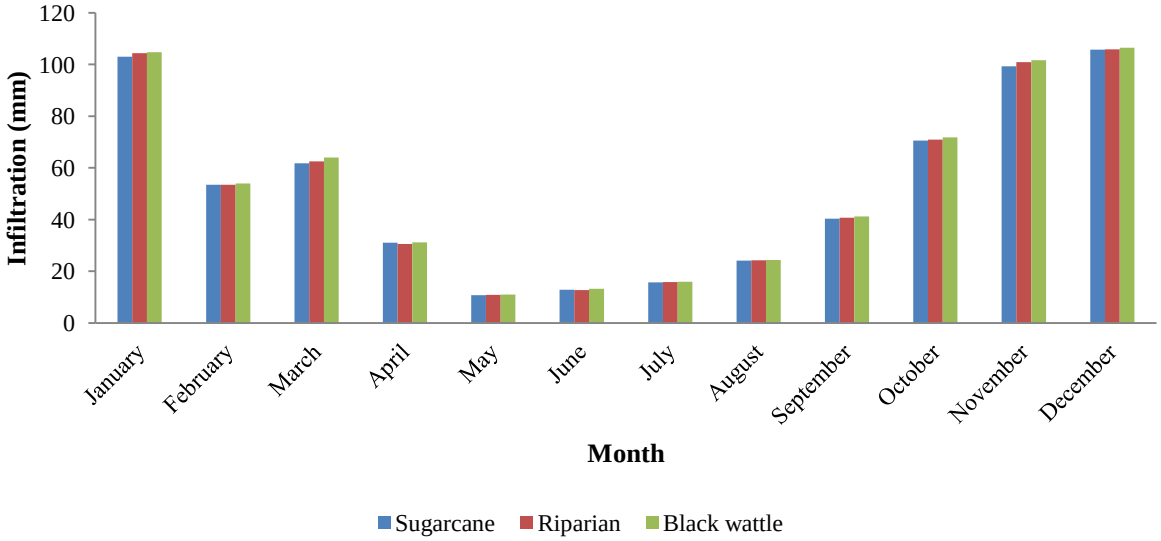

Figure 6.13: Monthly infiltration rates of the sugarcane, riparian and black wattle vegetation classes for the total simulated period (14 February 2007 – 02 October 2016). The averages exclude February 2007 and October 2016.

Comparing the total I_{UZ} rates modelled for each soil types in the Two Streams sub-catchment (Table 6.13), the Griffin soil has the lowest total I_{UZ} rate of 6018.27mm and Oakleaf the highest (6084.00mm; Table 6.13).

Table 6.13: Total infiltration rates of the different soil types of the Two Streams sub-catchment.

Soil type	**Total I_{UZ} (mm)**
Kranskop	6053.79
Inanda	6068.78
Magwa	6032.19
Clovelly	6069.28
Oakleaf	6084.00
Katspruit	6024.79
Griffin	6018.27

The soil I_{UZ} rates are similar for the different soil types with no two soil I_{UZ} records differing significantly ($P > 0.05$) based on the Wilcoxon's signed ranks test (Table 6.14).

Table 6.14: Statistical significance of the daily infiltration rates of the different soil types that fall within the Two Streams sub-catchment, compared using two-sample Wilcoxon's signed ranks non-parametric tests.

Soils compared	**P-value**	**Are the outputs significantly different?***
Kranskop and Inanda	0.48	No
Kranskop and Magwa	0.52	No
Kranskop and Clovelly	0.47	No
Kranskop and Oakleaf	0.91	No
Kranskop and Katspruit	0.43	No
Kranskop and Griffin	0.79	No
Inanda and Magwa	0.95	No
Inanda and Clovelly	0.99	No
Inanda and Oakleaf	0.55	No
Inanda and Katspruit	0.93	No
Inanda and Griffin	0.66	No
Magwa and Clovelly	0.94	No
Magwa and Oakleaf	0.59	No
Magwa and Katspruit	0.88	No
Magwa and Griffin	0.70	No
Clovelly and Oakleaf	0.54	No
Clovelly and Katspruit	0.95	No
Clovelly and Griffin	0.65	No
Oakleaf and Katspruit	0.50	No
Oakleaf and Griffin	0.88	No
Katspruit and Griffin	0.60	No

*Where vegetation classes are significantly different (yes) – $P < 0.05$ and where vegetation classes are not significantly different (no) – $P > 0.05$.

6.7 Recharge to the saturated zone

Groundwater recharge (GR) accounts for more than 10% of the total rainfall for all three vegetation classes (Table 6.15). The riparian class has the highest total recharge (1006.95mm), while sugarcane the lowest (781.82mm; Table 6.15). However, the riparian and black wattle recharge records are not significantly different from one another ($P = 0.38$; Table 6.16).

Table 6.15: : Accumulated total, summer and winter groundwater recharge (mm) rates for the sugarcane, riparian and black wattle vegetation classes, captured over the simulation period (14 February 2007 – 02 October 2016).

Accumulated rates	**Sugarcane**	**Riparian**	**Black wattle**
Total GR (mm)	781.82	1006.95	903.06
Total GR as % of total rainfall	10.67	14.06	12.32
Summer GR (mm)	399.51	523.47	461.42
Summer GR as % of total GR	52.32	51.93	52.31
Winter GR (mm)	364.09	483.48	420.63
Winter GR as % of total GR	47.68	48.07	47.69

The winter GR rates account for approximately 48% of the total recharge for all vegetation classes, indicating little seasonal variation. This is supported by the Wilcoxon's signed ranks test findings that show no significant differences between the seasonal records of the three vegetation classes ($P > 0.05$; Table 6.16).

Table 6.16: Statistical significance of the total and seasonal groundwater recharge outputs of the sugarcane, riparian and black wattle vegetation classes, compared using the Kruskal Wallis test by ranks and the two-sample Wilcoxon's signed ranks non-parametric tests.

	Statistical test employed	**Outputs compared**	**P-value**	**Are the outputs significantly different?****
Total GR	Kruskal Wallis test by ranks	All three	$P < 2.20 \times 10^{-16}$	Yes
	Two-sampled Wilcoxon's signed ranks test	Sugarcane and riparian	$P = 3.17 \times 10^{-7}$	Yes
		Sugarcane and black wattle	$P < 2.20 \times 10^{-16}$	Yes
		Riparian and black wattle	$P = 0.38$	No
Comparing summer and winter GR	Two-sampled Wilcoxon's signed ranks test	Sugarcane	$P = 0.68$	No
		Riparian	$P = 0.37$	No
		Black wattle	$P = 0.72$	No

*Coloured blocks indicate relationships of insignificant difference.
**Where vegetation classes are significantly different (yes) – $P < 0.05$ and where vegetation classes are not significantly different (no) – $P > 0.05$.

The daily GR outputs show periods of more variable recharge between 2007 – 2009, in 2011 and in 2016 (Figure 6.14). Seasonal changes are not evident in the daily outputs, supporting the above findings that show there to be little variability between the summer and winter rates. The annual

recharge rates show a declining trend over the simulation period (Figure 6.14), with 2008 experiencing the highest annual rates and 2016 the lowest, for all vegetation classes (Figure 6.14). The black wattle class has the largest annual range (83.24mm) and sugarcane the smallest (62.98mm).

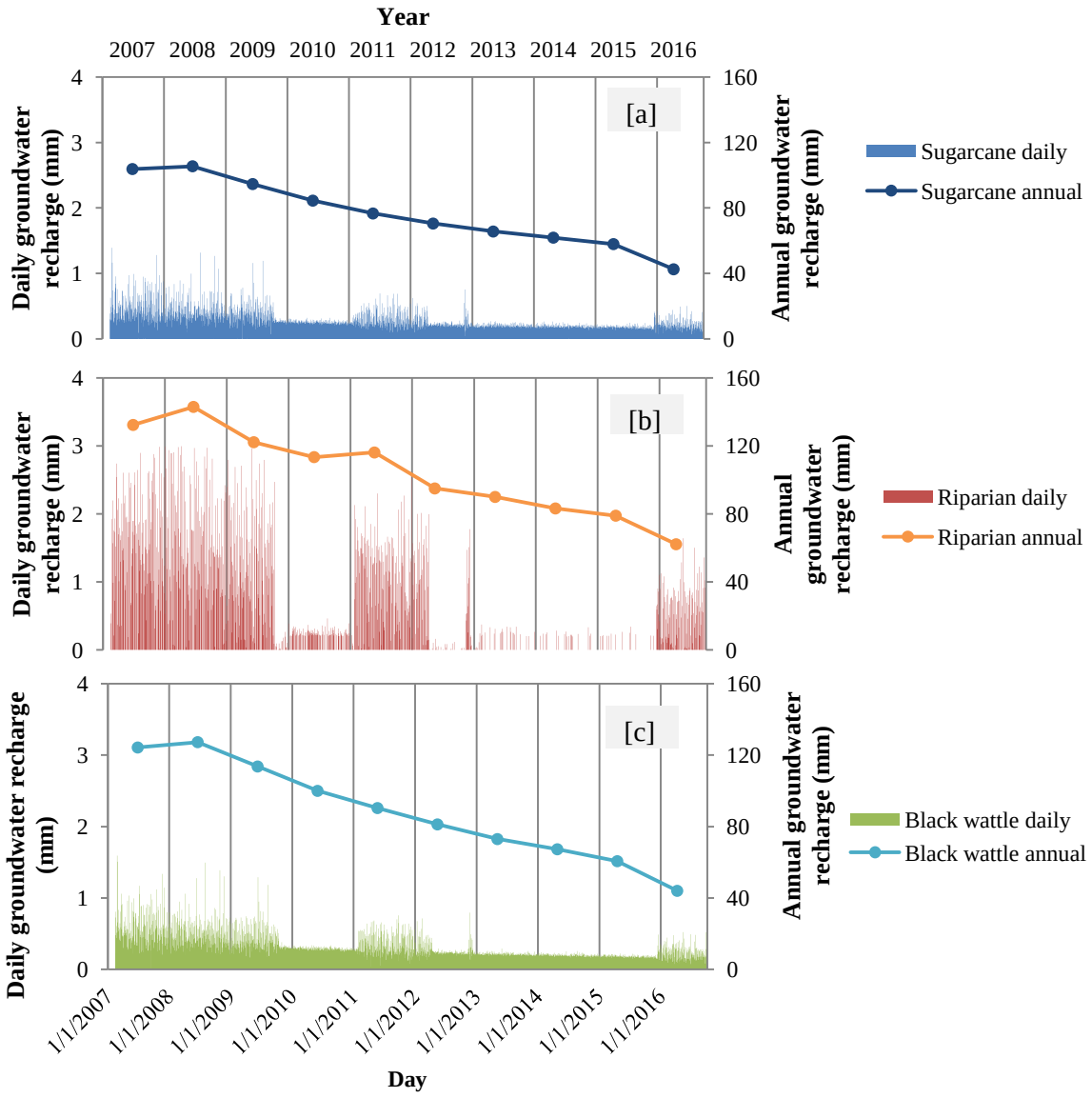

Figure 6.14: Daily and annual groundwater recharge outputs for the [a] sugarcane, [b] riparian and [c] black wattle vegetation classes, modelled over the total simulation period (14 February 2007 – 02 October 2016).

There is no indication of seasonal differences in the monthly GR for all three vegetation classes (Figure 6.15). For every month, the riparian class has the highest monthly recharge rates and sugarcane the lowest (Figure 6.15). All three vegetation class recharge outputs show little difference

in their respective averaged monthly rates with standard deviations of 0.26 (sugarcane), 0.22 (riparian) and 0.32 (black wattle). Similarly, the ranges in monthly recharge are low for all three vegetation classes, 0.86mm (sugarcane), 0.63mm (riparian) and 1.07mm (black wattle).

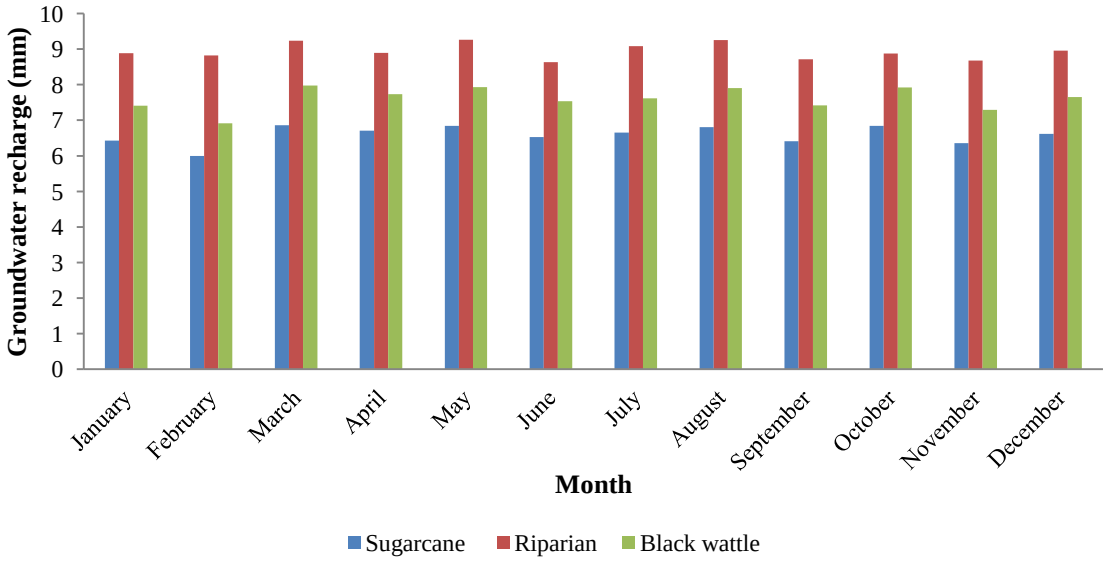

Figure 6.15: Mean monthly groundwater recharge rates of the sugarcane, riparian and black wattle vegetation classes for the total simulated period (14 February 2007 – 02 October 2016). The averages exclude February 2007 and October 2016.

6.8 Correlation and comparison of the vegetation class hydrological outputs

Correlating the hydrological outputs of the different vegetation class, all showed significant ($P < 0.05$), strong linear correlations ($r > 0.63$), except for the GR outputs, where $r = 0.37$ (riparian and black wattle; Table 6.17). This suggests that the riparian GR output differs most between vegetation classes. The I_{UZ} outputs show the strongest correlations, $P = 0.99$, suggesting the greatest similarity between the different vegetation class outputs (Table 6.17). Overall, the average r for all comparisons was 0.86 suggesting that the different vegetation classes have similar hydrological responses (Table 6.17).

Table 6.17: Pearson's correlation coefficients based on linear correlation between the vegetation class outputs of the different hydrological components, considered for this study.

Hydrological component	Vegetation classes compared	Pearson's correlation coefficient (r)	Significance of Pearson's correlation*
ET	Sugarcane and riparian	0.74	$P = 5.00 \times 10^{-4}$
	Sugarcane and black wattle	0.63	P = 0.04
	Riparian and black wattle	0.74	P = 0.03
E_t	Sugarcane and riparian	0.84	$P = 1.30 \times 10^{-3}$
	Sugarcane and black wattle	0.78	P = 0.01
	Riparian and black wattle	0.82	P = 0.03
E_s	Sugarcane and riparian	0.92	$P = 4.00 \times 10^{-4}$
	Sugarcane and black wattle	0.89	P = 0.02
	Riparian and black wattle	0.94	$P = 1.10 \times 10^{-3}$
E_i	Sugarcane and riparian	0.96	$P < 1.00 \times 10^{-4}$
	Sugarcane and black wattle	0.94	$P = 3.90 \times 10^{-3}$
	Riparian and black wattle	0.97	$P = 1.60 \times 10^{-3}$
E_p	Sugarcane and riparian	0.93	$P < 1.00 \times 10^{-4}$
	Sugarcane and black wattle	0.91	$P < 1.00 \times 10^{-4}$
	Riparian and black wattle	0.94	$P < 1.00 \times 10^{-4}$
CIS	Sugarcane and riparian	0.95	$P = 1.00 \times 10^{-4}$
	Sugarcane and black wattle	0.93	$P = 1.60 \times 10^{-3}$
	Riparian and black wattle	0.94	$P = 8.00 \times 10^{-4}$
Depth of OL	Sugarcane and riparian	0.94	$P = 2.20 \times 10^{-3}$
	Sugarcane and black wattle	0.89	P = 0.02
	Riparian and black wattle	0.86	$P = 1.60 \times 10^{-3}$
I_{UZ}	Sugarcane and riparian	0.99	$P < 1.00 \times 10^{-4}$
	Sugarcane and black wattle	0.99	$P < 1.00 \times 10^{-4}$
	Riparian and black wattle	0.99	$P < 1.00 \times 10^{-4}$
GR	Sugarcane and riparian	0.64	$P < 1.00 \times 10^{-4}$
	Sugarcane and black wattle	0.84	$P < 1.00 \times 10^{-4}$
	Riparian and black wattle	0.37	$P < 1.00 \times 10^{-4}$

* Pearson's correlation coefficients are significant when $P < 0.05$ and not significant when $P > 0.05$.

Correlating the hydrological components of the three vegetation classes to the rainfall record for the study site, the I_{UZ} rates show very strong, significant, linear correlations to rainfall, $r = 0.99$ ($P < 1.00 \times 10^{-4}$), for all three vegetation classes (Table 6.18). The E_s, E_p and depth of OL outputs all show weak linear correlations to rainfall (Table 6.18). Overall, black wattle outputs show weaker linear correlations to rainfall than the other two vegetation classes. Particularly noticeable is the ET, E_t and E_s correlations (Table 6.18).

Table 6.18: Pearson's correlation coefficients based on linear correlation between the hydrological components of the sugarcane, riparian and black wattle vegetation classes and the rainfall record of the Two Streams sub-catchment.

Linear comparison	**Pearson's correlation coefficient***		
	Sugarcane	**Riparian**	**Black wattle**
ET and rainfall	0.84	0.91	0.46
E_t and rainfall	0.76	0.87	0.42
E_s and rainfall	0.47	0.38	5.48×10^{-3}
E_i and rainfall	0.78	0.80	0.80
E_p and rainfall	0.17	0.15	0.05
CIS and rainfall	0.48	0.51	0.37
Depth of OL and rainfall	0.06	0.19	0.06
I_{UZ} and rainfall	0.99	0.99	0.99
GR and rainfall	0.58	0.63	0.61

* Pearson's correlation coefficients are significant when $P < 0.05$ and not significant when $P > 0.05$.
** Coloured blocks indicate Pearson's correlations are not significant ($P > 0.05$).

6.9 Discussion

This discussion elaborates on the key findings made in the comparison of the sugarcane, riparian and black wattle hydrological components, as generated by the calibrated MIKE SHE current scenario model.

6.9.1 Evapotranspiration

Evapotranspiration (ET) is an important component of the water balance calculation, accounting for the largest proportion of precipitation (Zhang *et al*., 1999), and is an important component in land hydrological processes for determining the exchange of moisture and energy between and within the soil, vegetation and atmosphere of a system (Bian *et al*., 2018). The total ET outputs for this study comprised of: E_t, E_s, E_i and E_p. Each of these components was individually investigated and combined as total ET. The ability of MIKE SHE software to separate the ET rate into its constituent components allows for a more accurate prediction of total ET, which not all hydrological modelling software programmes are capable of doing. Savenije (2004) highlights that many hydrological models

disregard or underestimate E_i. This is a concern as E_i is one of the most important processes in hydrological modelling, especially for tall vegetation like forests. The ability of models to distinguish between the different ET components is necessary for understanding ecosystem processes such as plant-water availability, water-use efficiency and vegetation patterns (Raz-Yaseef *et al*., 2010). Moreover, E_i is one of the first processes to take place in the chain of interlinked hydrological modelling processes (DHI software, 2012). Thus, the underestimation or exclusion of this variable will introduce model error into the system at the onset of the modelling process (Savenije, 2004).

Total ET provides an indication of how much water is used by the sub-catchment and is predominantly controlled by the amount of available water, energy and vegetation characteristics (Bian *et al*., 2018). This explains why the summer months, which receive more radiant energy and precipitation, have greater ET rates than the winter months (Table 6.1; van Dijk and Keenan, 2008; Hasenmueller and Criss, 2013). Considering the influence of vegetation characteristics, black wattle is an exotic forest plantation, comprising fast growing trees, with deep rooting systems that have a high water uptake (Versfeld *et al*., 1998; Dye *et al*., 2001; van Wilgen *et al*., 2001; Le Maitre *et al*., 2002; Clulow *et al*., 2011; Chamier *et al*., 2012; Everson *et al*., 2014). Plantation forests typically have higher rates of ET than other vegetation types (Calder *et al*., 1997; Vertessy, 2001; Dye and Jarmain, 2004; Liu *et al*., 2016) as was found in this study (Table 6.1).

6.9.2 Limitations in the model inputs governing evapotranspiration components and canopy interception

The vegetation characteristics modelled have a large impact on the modelled outputs generated (Bian *et al*., 2018), particularly LAI and RD (DHI software, 2012). For this study it was found that LAI influences E_t rates and subsequent ET rates (Figure 6.7). These findings are reaffirmed by the findings of Bian *et al*. (2018) and Liu *et al*. (2016). Bian *et al*. (2018) found ET and LAI to have a high correlation at both the catchment and sub-catchment scale and similarly, Liu *et al*. (2016) found that increasing trends in LAI generally increased annual ET. In addition, LAI defines the canopy structure impacting on CI processes of CIS and E_i (Figure 6.7), by defining the density of the canopy

(Jonckheere *et al*., 2004). Subsequently, LAI influences evaporation from the ground surface and the soil as the greater the canopy coverage, the more shading of the ground surface reduces rates of evaporation. For evaporation to occur, water needs to be exposed to the conducive climatic conditions of radiant energy and wind (Hendriks, 2010; Bulcock and Jewitt, 2012), which are limited under dense canopy coverage.

In MIKE SHE, the dependence on LAI exclusively to define vegetation canopy characteristics is a limitation in the modelling software as different vegetation species may have the same LAI. However, they have different canopy storage capacities depending on their leaf and canopy characteristics (Bulcock and Jewitt, 2012; Klamerus-Iwan, 2014). Canopy interception (CI) and ET rates will differ with leaf structures and angles, plant surface states, tree spacing and management practices (Bulcock and Jewitt, 2012; Klamerus-Iwan, 2014). The leaf structure of the vegetation classes on-site differs. Black wattle have compound leaves with small densely packed leaflets covered in fine hairs (Glen and van Wyk, 2016). The density of the leaves and the resistance to flow caused by the rough hairy surface allows for rainfall to be held by the vegetation. Sugarcane leaves have a larger surface area, are less densely packed and are smoother, allowing water to move off the leaves at a faster rate, and allowing for more water to be held on a single leaf at a given time (Cuadra *et al*., 2012). These factors are not considered in MIKE SHE but can impact on rates of ET and CI (Bulcock and Jewitt, 2012).

The sensitivity of the MIKE SHE outputs to LAI (as identified by the strong influence LAI has on the hydrological outputs), stresses the importance of accuracy in modelling this input. This is a limitation of this study. Leaf area index (LAI) is site specific as different areas experience different growing conditions, impacting on LAI (Dye *et al*., 2004). Thus employing LAI estimates from other studies for the sugarcane class is a limitation in this study. The riparian classes LAI inputs were based on averaged fieldwork findings, which is again a limitation, as, in reality, LAI should not be averaged but rather fluctuate with changes in vegetation phenology and season (Jonckheere *et al*., 2004). Indigenous vegetation leaf area will increase rapidly following germination and once vegetation reaches maturity green leaf area will be at a maximum, following which vegetation senescence will

decrease leaf area (Calder and Dye, 2001). The fact that fluctuations in riparian LAI were not captured could lead to a possible over-prediction in riparian hydrological outputs as periods of senescence would lower vegetation coverage decreasing CI and ET rates (Calder and Dye, 2001). If hydrological research continues on-site it would be beneficial to develop a database of LAI for future hydrological modelling.

Vegetation RD is another important model input indicating the extent of the active rooting zone, which is the area from where ET can take place, and thus, the greater the RD extent the greater the access to soil water reserves (Schulze *et al*., 1996; Zhu *et al*., 2018). This is particularly important for deep rooted vegetation in the dry winter seasons allowing vegetation to escape drought stress and continue growing during the dry season by keeping stomata open allowing for continued E_t (Bruijnzeel, 2004; Cai *et al*., 2018). This was observed in this study where ET rates exceed rainfall over the winter months for black wattle.

Hydrological models often only measure roots down to a 200mm depth, disregarding the possible importance of root access to deeper soil layers (Lu *et al*., 2011). In the case of MIKE SHE, input data on plant RDs are flexible to user data availability (DHI software, 2012). However, a limitation in MIKE SHE software capabilities it that it assumes an exponential decline in root mass with soil depth implying that most water abstraction occurs in the shallow soil layers, and thus could under-estimate deep soil water abstraction. This rooting behaviour is typical of many vegetation types, as found by Canadell *et al.* (1996), who stipulated that a majority of roots occur above 1m into the soil, after which root biomass decreases. However, this under-emphasises the importance of deep roots in the water cycle which is a concern as in more arid environments trees have adapted to depend more heavily on reliable deeper stored water (Dye *et al*., 2004; Cai *et al*., 2018), leading to the proliferation of roots where water is present. An example of this was shown by Kimber (1974) for *Eucalyptus marginata* in Western Australia (Figure 6.16). The design of MIKE SHE therefore severely limits water uptake in deep soils/subsoils, and this needs to be addressed in order to simulate tree water use under these conditions.

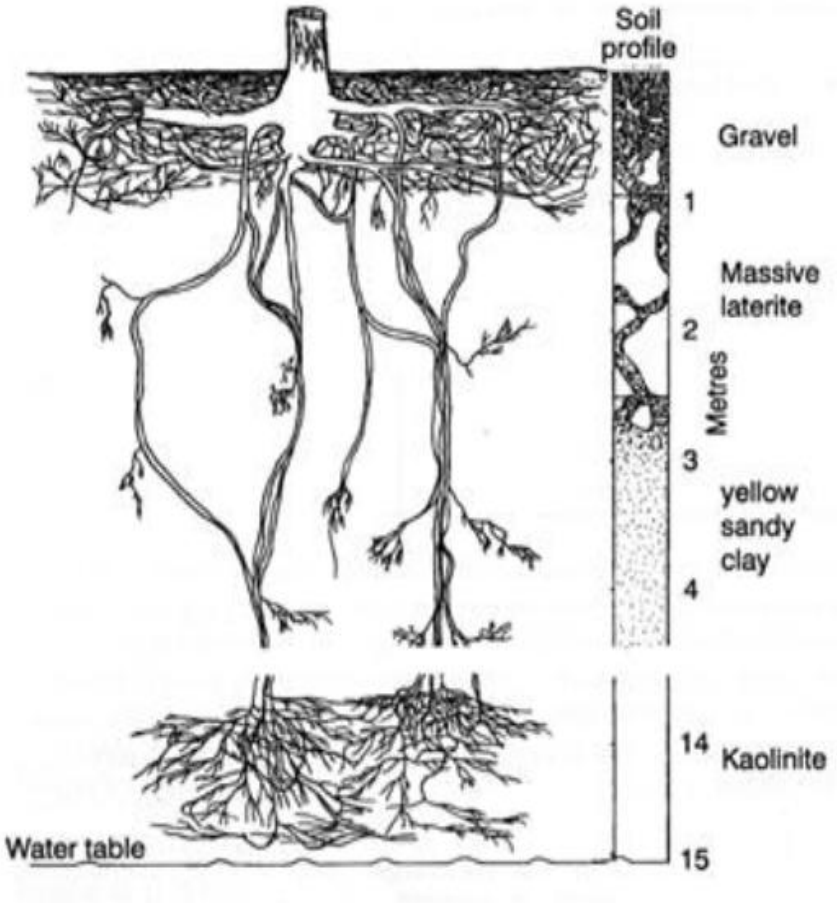

Figure 6.16: Diagram showing the nature of a deep, *E. marginata*, rooting system (Kimber, 1974).

A further important input governing ET and CI is rainfall. The intensity, duration and raindrop size all impact on hydrological processes such as vegetative rainfall adhesion (Kozak *et al*., 2007; Bulcock and Jewitt, 2012; Raz-Yaseef *et al*., 2012; Morbidelli *et al*., 2018). This study employed a daily rainfall record (Figure 5.1) as opposed to a smaller temporal period of hours or even minutes. A smaller temporal scale would allow for improved precision in rainfall intensity. Based on a study by Smithen and Schulze (1982) conducted in South Africa, rainfall intensity cannot adequately be determined based on daily rainfall records, requiring shorter intervals in defining storm intensity. This is a limitation in this dataset as hydrological components such as CI (Kozak *et al*., 2007), I_{UZ} (Daniels and Haering, 2006; Bothma *et al*., 2012; Morbidelli *et al*., 2018) and E_t (Raz-Yaseef *et al*., 2012) are influenced predominantly not by rainfall itself but more by storm intensity and duration.

According to Raz-Yaseef *et al*. (2012), E_t, or more precisely the ratio of E_t to ET, is more influenced by large storm events of greater than 30mm than by precipitation itself. Greater precision in rainfall intensity and storm duration would better determine hydrological capacity thresholds, for example the time-lag between the start of rainfall and the start of runoff (Johnston *et al*., 1980) and between the start of rainfall and GR (van Wyk *et al*., 2012). The reason rainfall was not considered at a smaller temporal scale was due to the patching requirements and the insufficient data that would have led to great uncertainty (Renard *et al*., 2010). The completeness of rainfall records of different temporal scales needs to be improved upon in future research at the Two Streams study site.

6.9.3 Runoff and infiltration

Daily depth of OL was highest on the 28th of January 2015 for all three vegetation classes (Table 6.9). The 28th of January 2015 experienced the highest daily rainfall, lower temperatures and lowest ET in relation to the rest of the month (January 2015; Figure 6.9 and 6.10). Infiltration (I_{UZ}) rates were highest for the 28th of January 2015, in relation to the rest of the month (Figure 6.10), but coupled with the low rates of ET and high rainfall lead to greater depth of OL. However, OL rates were minimal for all three vegetation classes and this event does not constitute a significant impact on overall site hydrology. This event could also be attributed to antecedent moisture conditions which change continuously in a catchment and can have a significant effect on the runoff or flood response of a catchment (De Michele and Salvadori, 2002). Antecedent moisture conditions give an indication of the state of wetness of the catchment (James and Roulet, 2009) and if the catchment is in a wet state, possibly achieved through prolonged wetting of the catchment, then additional rainfall will lead to a larger response in runoff than if the catchment was in a dry state (James and Roulet, 2009). Such antecedent moisture conditions coupled with considerations on storm characteristics can lead to very different responses in runoff or streamflow from rainfall event to rainfall event (Biron *et al*., 1999). Studies have documented sharp increases in water levels (Biron *et al*., 1999), dramatic increases in runoff ratios (James and Roulet, 2009) and non-linear responses in streamflow to rainfall or storm events (James and Roulet, 2009)

To better investigate the event, higher temporal precision on the climatic data would be required to determine rainfall intensity and duration, and to identify storm events. A high intensity, high volume, short time period rainfall event may produce greater OL than a lower intensity prolonged rainfall event, as water has less time to evaporate or infiltrate (Mu *et al*., 2015). In addition further investigation into antecendent moisture conditions of the catchment should also be investigated further. This is out of the scope of the project given the limitations on rainfall data and as the depth of OL values were so minimal and inconsequential to the site water balance.

All three vegetation classes experienced very low depth of OL values (Table 6.7) and E_p rates (Table 6.3). This is predominantly attributed to the high I_{UZ} in the sub-catchment (Table 6.11), as when water reaches the ground surface it will infiltrate. Once the I_{UZ} threshold is reached water will then flow as OL (DHI software, 2012). Infiltration (I_{UZ}) is influenced by a number of factors such as soil, climate and topography. Soil factors include: the influence of vegetation, macropores, and soil moisture content (Cerdá, 1997), soil profile characteristics of soil depth, soil hydraulic properties, soil texture, soil structure, soil horizons and underlying parent geology (Bothma *et al*., 2012; Morbidelli *et al*., 2018). Climatic factors include: the amount, duration and intensity of rainfall events (Daniels and Haering, 2006; Bothma *et al*., 2012; Morbidelli *et al*., 2018), and topographical factors such as slope (Daniels and Haering, 2006) are important.

The limitations in this study that have an impact on the rate of I_{UZ} were the lack of spatial variability in the climatic and geological data inputs and the lack of knowledge on macropore flow. Further investigation into the geological properties of the site is required as the data used to model geology were taken from relevant regional literature and was not site-specific (Demlie and Titus, 2015). Further geological investigation should involve spatially mapping the underlying geology, determination of spatially explicit saturated hydraulic conductivity and determination of subsurface macropore presence or identification of preferential flow pathways.

Considering the soil water retention capabilities of the soil (Appendix F), the soils had relatively high rates of water retention, in comparison to the calculated UNSODA soil water retention capabilities (Appendix F). This, coupled with the findings described previously (section 5.6.1) on soil hydraulic conductivity, which showed the soils modelled for this study to have high rates of hydraulic conductivity and thus, fast rates of water movement through the soil (Hillel, 2008), have led to the high I_{UZ} observed.

Research conducted by Cook (2012) suggests that MIKE SHE is sensitive to hydraulic conductivity, stressing the importance of this input parameter. The hydraulic conductivity input is important within MIKE SHE as it determines the amount of water that infiltrates versus the amount that will form surface runoff. The high hydraulic conductivities lead to higher rates of I_{UZ} and limited OL (Şen, 2015). Depth of OL and the rate of I_{UZ} are interrelated processes, whereby depth of OL and the initial soil moisture distribution near the soil surface control the rate of I_{UZ}, which itself influences the depth of OL (Wallach *et al*., 1997). The depth of OL and I_{UZ} rates were found to have insignificant weak linear correlation (Table 6.10). The fast rates of water movement through the soil resulted in the I_{UZ} rates and rainfall rates demonstrating strong linear correlations for all vegetation classes. In addition, the effects of seasonality are generally found to be greater for well-drained soil (typically sandy soils), where an increased subsurface runoff and drainage are experienced (Yokoo *et al*., 2008), as is the case in this study, where soils had a high sand content and high hydraulic conductivities (refer to section 5.6.1).

6.9.4 Groundwater recharge

The amount of water that recharges the SZ is dependent on the amount of infiltrated water that leaves the bottom of the soil zone to become part of the groundwater zone (Zhang *et al*., 1999; Harlow, 2018). Thus it is the downward exchange from the unsaturated to the SZ (DHI software, 2012). Determining GR requires modelling of the interactions between the hydrological processes including: I_{UZ}, surface runoff, ET and variations in groundwater levels (Jyrkama and Sykes, 2007). As recharge

is one of the last processes to take place in the chain of events within a hydrological model, the calculation of recharge is complex and there is much uncertainty in the prediction thereof (Jyrkama and Sykes, 2007). This uncertainty is further increased by the limitations in the SZ data. For improved recharge estimates, more detailed investigation and more accurate spatial consideration of the SZ needs to be undertaken.

An advantage of MIKE SHE software, over other hydrological modelling software, is its ability to couple the surface and subsurface hydrological interactions (DHI software, 2012), allowing for a more accurate determination of GR by encompassing a more inclusive physical consideration of determinant factors (Graham and Butts, 2005; DHI software, 2012). Thus, as no other fully integrated models have been employed for use on the study site (Everson *et al*., 2006, 2014; Clulow *et al*., 2011); this MIKE SHE model provides the best depiction, so far, of the hydrology and specifically GR on-site.

The total GR was highest for the riparian class, and lowest for sugarcane (Table 6.15). The riparian vegetation class is believed to have higher rates of recharge as these zones generally support larger quantities of water than the surrounding upland areas (Zaimes *et al*., 2011). Riparian zones generally have different sources of water from that of upland areas, where precipitation is the primary source (Zaimes *et al*., 2011). In riparian zones water is received through precipitation, OL, subsurface flow and GR (Zaimes *et al*., 2011) resulting in riparian zones having great moisture availability. This justification supports the high rates of evaporation found within the riparian zone (Table 6.1), as driven by greater water availability.

The annual GR showed a clear declining trend over the simulated years, with each subsequent year, from 2008, having lower rates of recharge than the previous (Figure 6.14). This could be as a result of the accumulated interactions between ET and I_{UZ}, as GR will increase if increased I_{UZ} outweighs increased water use (van Dijk and Keenan, 2007). However, research has found there to be a lagged

response in hydrological changes, whereby the effects of plantation establishment on GR may only be clearly evident after several decades (Vertessy, 2001).

Given the dynamic plantation history of the Two Stream study site, longer-term hydrological investigation is required for GR to be accurately depicted and understood. Similarly so for the GR seasonality, where seasonally GR rates were not significantly different from one another (Table 6.16), with the summer rates being slightly higher than the winter rates (Table 6.15). The recharge outputs demonstrated weaker correlation to the rainfall record than both the ET and I_{UZ} outputs (Table 6.18), suggesting that other factors interact to derive GR, such as the lateral exchange of water between the different vegetation classes or soil types, lateral exchange across the hydrologically defined boundary of the study site, upward movement of water from the saturated to the UZ and exchange between the river and the SZ (DHI software, 2012). These factors, coupled with a potential time-lag or delayed response in recharge, all contribute to the inter-annual variations observed in the recharge rates.

6.9.5 The riparian zone

Comparing the three vegetation classes, the riparian zone did not show markedly different responses in comparison to the plantation classes. Both sugarcane and black wattle have been recognised in the literature for their high water use in South Africa (Dye and Versfeld, 2007). Plantation forestry (inclusive of black wattles) in South Africa is listed as a 'Stream Flow Reduction Activity' in the National Water Act (NWA, Act 36 of 1998). To-date, plantation forestry is the only activity to be listed under this category. According to Dye and Versfeld (2007), the only other activity that could be listed as a 'Stream Flow Reduction Activity' is sugarcane, which is believed to use approximately half as much water as plantation forestry. Given the high water usage of these plantations, it is surprising that the riparian zone, which has previously been cleared of forestry (Clulow *et al*., 2011), would produce hydrological outputs comparable to these water intensive vegetation types. This indicates a potential weakness or uncertainty, either in the model itself or in the input data used. Within the Two Streams study site, research studies on hydrology have been undertaken for decades with the focus

primarily on the black wattle stand while less focus has been placed on the sugarcane and riparian zones (Everson *et al.*, 2006, 2014; Clulow *et al.*, 2011). Thus the lack of data on the riparian vegetation meant little observed historical data was available for input into the model and data employed was based on current day findings over shorter time periods. In recent years, research has started to extend into the sugarcane. However, for a fruitful and representative understanding of the hydrological conditions and behaviour of the modelled system, a more holistic approach to research needs to be undertaken. The holistic view needs to take the entire Two Streams hydrological system into consideration. Riparian zones are important transitional zones linking the terrestrial and aquatic environments. Although streamflow in this sub-catchment is severely limited, the correct management of riparian zones should bring about an increase in streamflow.

In South Africa, studies have found streamflow to increase by up to 44% per 10% of the catchment cleared within the first year of clearing of forestry plantations (Scott, 1999). A study by Prinsloo and Scott (1999) considered the changes in streamflow following the clearing of invasive wattle *(Acacia mearnsii* and *A. longifolia)* from riparian zones in three small catchments in the Western Cape Province, South Africa. The study found there to be a marked increase in streamflow in all three catchments following clearing. The streamflow increases in the three catchments were 8.8, 10.4 and 12 $m^3.day^{-1}$ per ha cleared (Prinsloo and Scott, 1999).

6.9.6 Sub-catchment heterogeneity

The study site was small (79.16ha) for a modelling based study (Graham and Butts, 2005) and so for accurate depiction of spatial heterogeneity a small grid size of $25m^2$ was used to achieve the smallest scale possible (restricted by spatial resolution of input datasets) at which model processes could be investigated. The input datasets were predominantly dependent on past research mostly undertaken on-site, however where data were scarce, inputs were based on literature with sources from other regional sites. Considering spatial heterogeneity, not all inputs captured spatial heterogeneity, with the rainfall record and the geology being spatially uniform. In addition, no significant differences were

observed in the I_{UZ} rates across the site (Table 6.12), suggesting spatial homogeneity. The lack of heterogeneity in these key input datasets resulted in variable patterns of statistical significance in the component results produced, with no two vegetation classes showing clear significant differences in all inputs.

The homogeneity of the inputs, as they are currently and as they have been used for this study, brings into question the need for the use of such a physically-based exhaustive model. More simplified, lumped conceptual modelling approaches simplify site heterogeneity by dividing the area into HRUs of homogenous factors, thereby simplifying site complexity and allowing for a faster model run time (Devi *et al*., 2015). Conceptual models are less data intensive and, based on current homogeneity, may produce results equivalent to the MIKE SHE output. However, further research into the subsurface characteristics and dynamics of the riparian zone will allow for improved understanding of the heterogeneity in the hydrological system and will then allow for the more effective re-evaluation of the benefits in relation to the work effort expended in setting up, running and calibrating a MIKE SHE model.

6.10 Conclusion

This chapter investigates the differences between the hydrological responses of the three main vegetation classes of the Two Streams sub-catchment, namely: black wattle forestry plantation (*A. mearnsii*), sugarcane plantation (*S. officinarum*) and the riparian zone. The hydrological components, for each of the vegetation classes, were investigated both within each vegetation class and between the different vegetation classes. The study results show black wattle to have higher rates of ET and the riparian vegetation to have higher rates of I_{UZ} and GR. The MIKE SHE current scenario model set-up has, to-date, provided a thorough consideration of the holistic hydrological cycle of the Two Streams sub-catchment, supplying insight into the dominant hydrological processes. The study comprehends the effect plantation forestry has on the sub-catchment, showing water use to be higher than for the sugarcane and riparian vegetation classes, over the winter months. However, this did not occur during

the summer months. This study highlights how the deep rooting system of the black wattle plantation allows for increased E_t during the winter months. There were however data limitations. The input requirements of the MIKE SHE model are detailed and further hydrological research should focus on improving research into the subsurface conditions of the Two Streams sub-catchment, increasing spatial heterogeneity in hydrological data outputs and on improving water use efficiency through the implementation of a more holistic research approach and improved management of the riparian zone.

Chapter Seven

Impact of a change in plantation forestry on hydrological characteristics of the Two Streams sub-catchment

7.1 Introduction

This chapter comprises of results and a discussion section focusing on comparing the hydrological outputs that result from a change in land cover from black wattle (*A. mearnsii*) to *E. dunnii* plantation forestry in the Two Streams sub-catchment. This was achieved by comparing the outputs of the two scenarios, *A. mearnsii* from the MIKE SHE modelled current scenario and *E. dunnii* from the MIKE SHE predicted future scenario. Both the current and future scenarios ran for the same length (3519 days), approximately ten years, as determined by the climatic data input record length (refer to section 4.3.4). The current scenario ran from 14 February 2007 – 02 October 2016 and the future scenario from 14 February 2019 – 02 October 2028.

For ease of comparison, and because the future scenario is a hypothetical case, actual years are not referred to in this chapter and rather referred to between year one and ten, i.e. 2007 and 2019 are referred to as year one and 2016 and 2028 as year ten. The differences between the MIKE SHE current and future scenarios have been elaborated on in section 4.5, where it stipulates that changes between the two scenarios were enacted mostly in the *land use module*, with most of the other modules kept constant (Appendix A). To assess the seasonal differences, two seasons are defined dividing the year between the six wettest months (October to March) and the six driest months (April to September), forming the summer and winter seasons respectively. The differences in the daily outputs, of the different plantation species, are statistically analyzed using non-parametric tests (Appendix H) and linear correlation and Pearson's correlation coefficients (r) are calculated to compare the hydrological outputs of the two plantation types. The discussion focuses on key findings, limitations and uncertainty, and where *A. mearnsii* findings have been elaborated on in chapter six, less emphasis is placed on these findings in this chapter, to avoid repetition.

7.2 Comparison and correlation of totaled model outputs

Total accumulated ET is highest for *E. dunnii* (7274.21mm), as is the total summer ET (4638.35mm), whilst *A. mearnsii* has the highest winter ET (2635.86mm; Table 7.1). The accumulated total ET rates of *A. mearnsii* and *E. dunnii* exceed total rainfall by 0.66 and 1.60% respectively (Table 7.1). Evapotranspiration (ET) comprises E_t, E_s, E_i and E_p. As part of ET, E_t accounts for 63.88 and 57.30% of the *A. mearnsii* and *E. dunnii* plantation types respectively, and total accumulated E_t is highest for *A. mearnsii* (4604.01mm; Table 7.1). Total E_s accounts for between 21.13 – 26.45% of total evapotranspration for *A. mearnsii* and *E. dunnii* respectively, whilst E_i accounts for between 14.80 – 16.06% respectively (Table 7.1). *E. dunnii* has higher rates of E_s, E_i and E_p in comparison to *A. mearnsii* (Table 7.1). Each ET component demonstrates strong seasonal differences between the total summer and total winter rates (Table 7.1), with the summer rates accounting for more than 60% of the totals for all ET components, for both plantation types (Table 7.1).

Table 7.1: The accumulated totals (overall simulated total and seasonal totals) for evapotranspiration and the evapotranspiration components: transpiration, soil evaporation, evaporation from interception and evaporation from ponded water, for the *A. mearnsii* and *E. dunnii* plantation species.

ET component	**Species**	**Total (mm)**	**Total as % total rainfall**	**Total as % of total ET**	**Summer (mm)**	**Summer (% of total)**	**Winter (mm)**	**Winter (% of total)**
E_t	*A. mearnsii*	4604.01	64.31	63.88	2782.82	60.44	1821.19	39.56
	E. dunnii	4168.06	58.22	57.30	2508.93	60.19	1659.13	39.81
E_s	*A. mearnsii*	1523.18	21.27	21.13	962.03	63.16	561.15	36.84
	E. dunnii	1924.06	26.87	26.45	1240.77	64.49	683.29	35.51
E_i	*A. mearnsii*	1066.92	14.90	14.80	801.08	75.08	265.84	24.92
	E. dunnii	1167.88	16.31	16.06	875.55	74.97	292.33	25.03
E_p	*A. mearnsii*	12.83	0.18	0.18	11.73	91.43	1.10	8.57
	E. dunnii	14.22	0.20	0.20	13.11	92.19	1.11	7.81
Total ET	***A. mearnsii***	**7206.93**	**100.66**	**100.00**	**4557.64**	**63.24**	**2649.29**	**36.76**
	E. dunnii	**7274.21**	**101.60**	**100.00**	**4638.35**	**63.76**	**2635.86**	**36.24**

The accumulated total CIS rates for both species are relatively low, in relation to the totals of the outputs considered, amounting to less than 0.5% of the total rainfall (Table 7.2). Unlike total ET, CIS rates do not show strong seasonal differences, with the accumulated summer rates accounting for 54.39 and 50.01% of the accumulated total CIS rates of *A. mearnsii* and *E. dunnii*, respectively (Table 7.2).

The accumulated total depth of OL values are low for both species, in relation to the other outputs considered, reflecting an insignificant portion of accumulated rainfall (approximately 2.70×10^{-5}% for both species; Table 7.2), and are similar for both *A. mearnsii* and *E. dunnii*, amounting to 1.95×10^{-3}mm and 1.94×10^{-3}mm respectively (Table 7.2). The accumulated total summer depth of OL values exceed those of the winter values accounting for approximately 70% for both plantations (Table 7.2).

The accumulated total I_{UZ} rates are high for both species, with total rates reflecting more than 80% of the accumulated rainfall (Table 7.2). In relation to the other hydrological components considered, only the ET totals exceed those of the I_{UZ} (Table 7.2). *A. mearnsii* has the highest total I_{UZ} (6079.76mm) and the highest summer (4712.66mm) and winter rates (1367.10mm; Table 7.2). The I_{UZ} rates demonstrate strong seasonal differences, with the summer months accounting for approximately 77.50% of the total I_{UZ} rates of both species (Table 7.2).

The accumulated total GR rate for *A. mearnsii* (903.06mm) exceeds that of *E. dunnii* (862.23mm) and both totals account for approximately 12% of the total rainfall record (Table 7.2). The total summer and winter GR rates of *A. mearnsii* (471.13mm and 431.93mm, respectively) exceed those of *E. dunnii* (452.67mm and 409.56mm, respectively; Table 7.2). The GR rates do not display strong seasonal differences between the total summer and winter seasons, with the summer totals accounting for just over half, 52.17% and 52.50%, of the total GR of *A. mearnsii* and *E. dunnii* respectively (Table 7.2).

Table 7.2: The accumulated 10-year totals (overall simulated total and seasonal totals) for the canopy interception storage, depth of overland flow, infiltration and groundwater recharge outputs, for the *A. mearnsii* and *E. dunnii* plantation types.

Hydrological component	**Species**	**Total (mm)**	**Total as % of total rainfall**	**Summer (mm)**	**Summer (% of total)**	**Winter (mm)**	**Winter (% of total)**
CIS	*A. mearnsii*	34.14	0.48	18.57	54.39	15.57	45.61
	E. dunnii	34.81	0.49	17.41	50.01	17.40	49.99
Depth of OL	*A. mearnsii*	1.95×10^{-3}	2.72×10^{-5}	1.36×10^{-3}	69.99	5.83×10^{-4}	30.01
	E. dunnii	1.94×10^{-3}	2.71×10^{-5}	1.39×10^{-3}	71.75	5.48×10^{-4}	28.25
I_{UZ}	*A. mearnsii*	6079.76	84.92	4712.66	77.51	1367.10	22.49
	E. dunnii	5977.41	83.49	4636.74	77.57	1340.67	22.43
GR	*A. mearnsii*	903.06	12.61	471.13	52.17	431.93	47.83
	E. dunnii	862.23	12.04	452.67	52.50	409.56	47.50

7.3 Annual differences in hydrological outputs

Based on the annual differences in ET (*E. dunnii* minus *A. mearnsii*), *E. dunnii* has higher annual rates over the first three years, exceeding those of *A. mearnsii* by 18.30%, thereafter *A. mearnsii* has higher annual rates, exceeding those of *E. dunnii* by 6.06% (Figure 7.1a). The annual differences in E_t demonstrate that *E. dunnii* rates only exceed those of *A. mearnsii* in the third simulated year (by 9.43%; Figure 7.1b). The annual *E. dunnii* E_s rates exceed the *A. mearnsii* rates for every simulated year (Figure 7.1c), particularly for the first two years where *A. mearnsii* rates are less than half of *E. dunnii* rates. The differences in annual E_p rates are minimal for all simulated years (Figure 7.1d). However, the largest differences are observed in the first two simulated years, where the *E. dunnii* rates exceed *A. mearnsii* rates by 76.35%. The annual E_i rates are higher for *A. mearnsii* for the first simulated year (24.14% higher), and thereafter are higher for *E. dunnii* (Figure 7.1e).

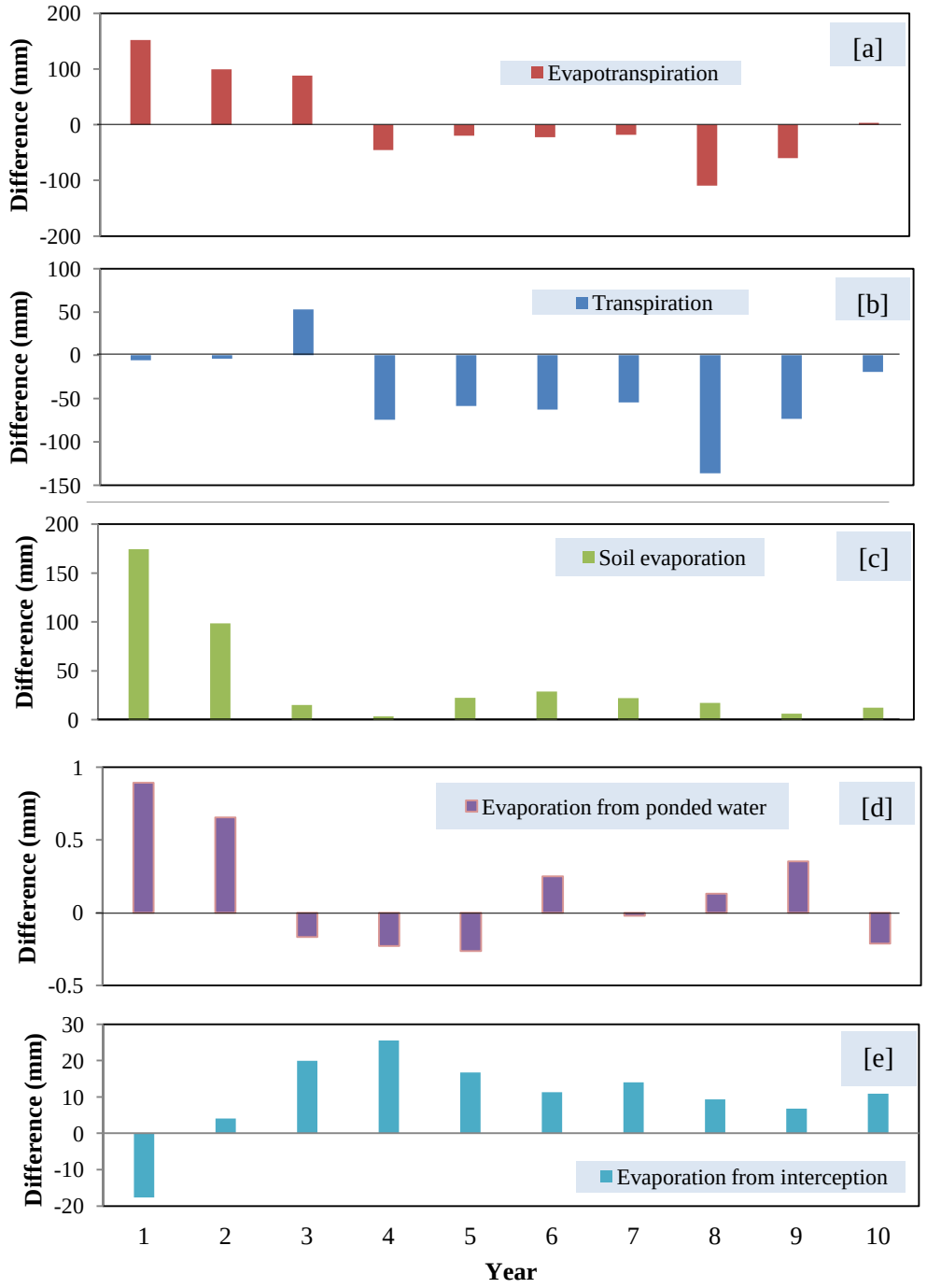

Figure 7.1: Differences between the [a] evapotranspiration, [b] transpiration, [c] soil evaporation, [d] evaporation from ponded water, [e] and evaporation from interception rates for the *E. dunnii* and *A. mearnsii* plantation species (*E. dunnii* minus *A. mearnsii*). For rates > 0 *E. dunnii* rates exceed *A. mearnsii* rates, while rates < 0 *A. mearnsii* exceeded *E. dunnii.*

From the annual differences in ET and the ET components, noticeable differences are observed for the first year or two years of the simulations, which relate to the changes in LAI modelled (Figure 7.2).

Over the first two simulated years vegetation establishment was low for both species. From the third simulated year *E. dunnii* LAI increased above that of *A. mearnsii*, this continued up until the seventh year when *A. mearnsii* LAI exceeded that of *E. dunnii* (Figure 7.2). As the *E. dunnii* LAI exceeded that of *A. mearnsii* so there was less difference in E_s and E_p (Figure 7.1). The E_t rates were greater for *E. dunnii* in the third simulated year that related to the peak RD of *E. dunnii* (Figure 7.2), thereafter *A. mearnsii* E_t rates were greater (Figure 7.1b).

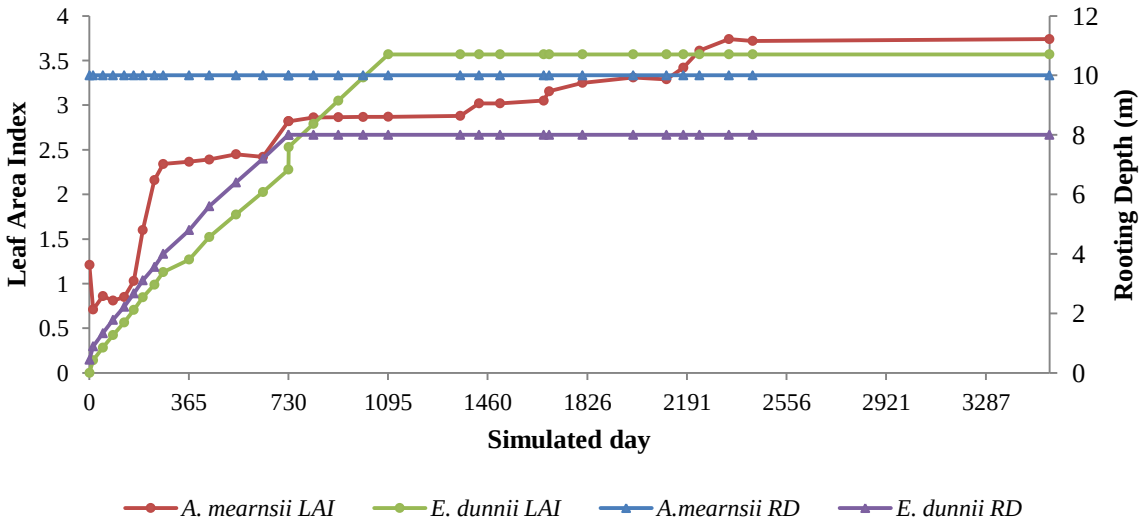

Figure 7.2: Modelled Leaf Area Index (LAI) and Rooting Depth (RD) of *A. mearnsii* and *E. dunnii*.

A. mearnsii has higher annual rates of CIS for the first two years of the simulations (by more >50%); thereafter *E. dunnii* annual CIS was higher (Figure 7.3a). Similarly, after two years the LAI of *E. dunnii* started to exceed that of *A. mearnsii* (Figure 7.2) indicating that *E. dunnii* then had greater canopy coverage and more chance of CI. Similar results were found for the difference between the annual E_i rates of the two species (Figure 7.1e), where E_i was higher for *A. mearnsii* for the first simulated year, but as LAI started to increase for *E. dunnii* (Figure 7.2), so *E. dunnii* had higher rates of E_i with the denser canopy capable of intercepting and making more water available for E_i.

The differences between the annual depth of OL values (*E. dunnii* minus *A. mearnsii*) demonstrate greater variation (Figure 7.3b) than is observed between the annual differences of the other

hydrological components (Figure 7.1 and 7.3); however the values are minimal with little impact to the overall water balance of the site (Table 7.9). *E. dunnii* has a higher annual I_{UZ} rate only for the first simulated year, exceeding that of *A. mearnsii* by 2.58% (Figure 7.3c), whilst annual GR rates are higher for *A. mearnsii* for every simulated year (Figure 7.3d), demonstrating a decreasing trend with the annual differences becoming smaller from the first to the tenth simulated year (Figure 7.3d).

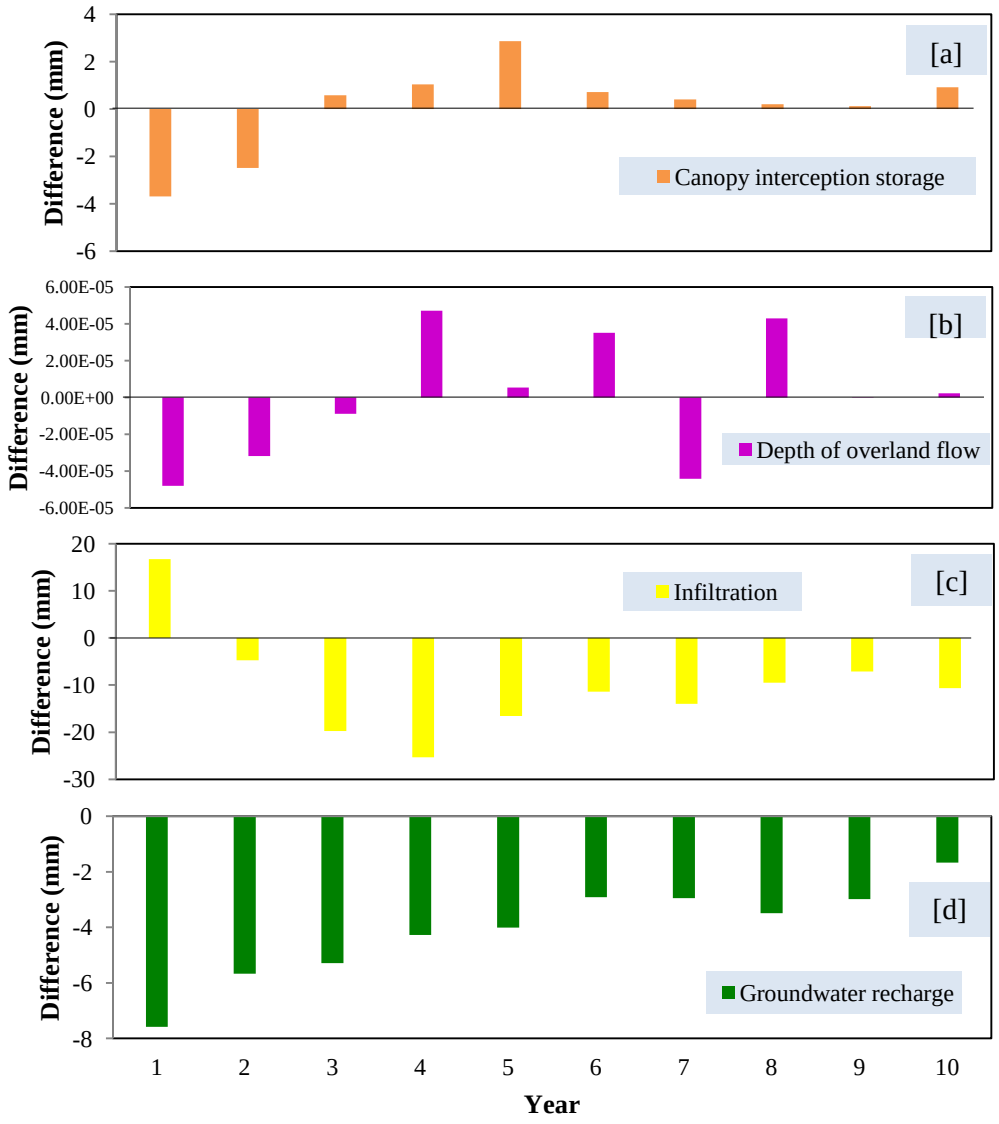

Figure 7.3: Differences between the [a] canopy interception storage, [b] depth of overland flow, [c] infiltration, and [d] groundwater recharge rates of the *E. dunnii* and *A. mearnsii* plantation species (*E. dunnii* minus *A. mearnsii*). For rates > 0 *E. dunnii* rates exceed *A. mearnsii* rates, while rates < 0 *A. mearnsii* exceeded *E. dunnii*.

E. dunnii ET, depth of OL and GR outputs all display stronger linear correlation to rainfall than those *A. mearnsii* outputs, while *A. mearnsii* display stronger linear correlation for the CIS component (Table 7.3). The annual I_{UZ} and rainfall rates demonstrate the strongest linear correlations for both species, r = 0.99 ($P < 1.00 \times 10^{-4}$; Table 7.3).

Table 7.3: Correlation results (Pearson's correlation coefficients) of the daily hydrological components of the *A mearnsii* and *E. dunnii* vegetation classes.

Hydrological component	**Pearson's correlation coefficient (r) of linear regression***	
	Comparing annual *A mearnsii* component to rainfall	**Comparing annual *E. dunnii* component to rainfall**
ET	0.46	0.71
CIS	0.37	0.34
Depth of OL	0.06	0.09
I_{UZ}	0.99	0.99
GR	0.60	0.61

* Pearson's correlation coefficients are significant when $P < 0.05$ and not significant when $P > 0.05$.
**Coloured blocks are not significant ($P > 0.05$).

7.4 Comparison of daily modelled outputs

The accumulated daily ET rates of both species are similar, being higher for *E. dunnii* for the first simulated years and higher for *A. mearnsii* for the latter simulated years (Figure 7.4a). The similarities visible in the daily ET outputs is reaffirmed by the Wilcoxon's signed ranks test that indicate no significant difference between the two outputs ($P = 0.47$; Table 7.4).

Table 7.4: Statistical significance of the daily hydrological component outputs of the *A. mearnsii* and *E. dunnii* plantation types compared using the two-sample Wilcoxon's signed rank non-parametric test.

Hydrological component compared	**P-Value**	**Were the plantation types significantly different?**
ET	0.47	No (P > 0.05)
E_t	5.69×10^{-6}	Yes (P < 0.05)
E_s	$< 2.20 \times 10^{-16}$	Yes (P < 0.05)
E_i	0.08	No (P > 0.05)
E_p	0.93	No (P > 0.05)
CIS	0.35	No (P > 0.05)
Depth of OL	3.17×10^{-5}	Yes (P < 0.05)
I_{UZ}	0.55	No (P > 0.05)
GR	1.58×10^{-5}	Yes (P < 0.05)

*Coloured blocks indicate relationships of insignificant difference.
**Where plantation types are significantly different (yes) – P < 0.05, and where plantation types are not significantly different (no) – P > 0.05.

The accumulated daily E_t rates are similar for both species up until the sixth simulated year after which *A. mearnsii* accumulated E_t rates start to exceed those of *E. dunnii*, continuing on an increasing trajectory until the end of the simulation periods (Figure 7.4b). The daily E_t outputs of the two species are significantly different from one another ($P = 5.69 \times 10^{-6}$; Table 7.4). The accumulated daily E_s rates (Figure 7.4c) differ significantly ($P < 2.20 \times 10^{-16}$; Table 7.4) for the two species, with *E. dunnii* having higher rates throughout the simulations (Figure 7.4c). The accumulated daily E_p rates are low for both species, but are larger for *E. dunnii* throughout the simulations (Figure 7.4d). Despite the distinct similarities in daily accumulated rates, the E_p outputs are not significantly different (P = 0.93; Table 7.4). The daily accumulated E_i outputs are similar for the first four years; thereafter the accumulated *E. dunnii* rates exceed those of *A. mearnsii*, continuing on the increasing trajectory until the end of the simulation periods (Figure 7.4e). There is however, no significant difference between the two E_i outputs (P = 0.08; Table 7.4).

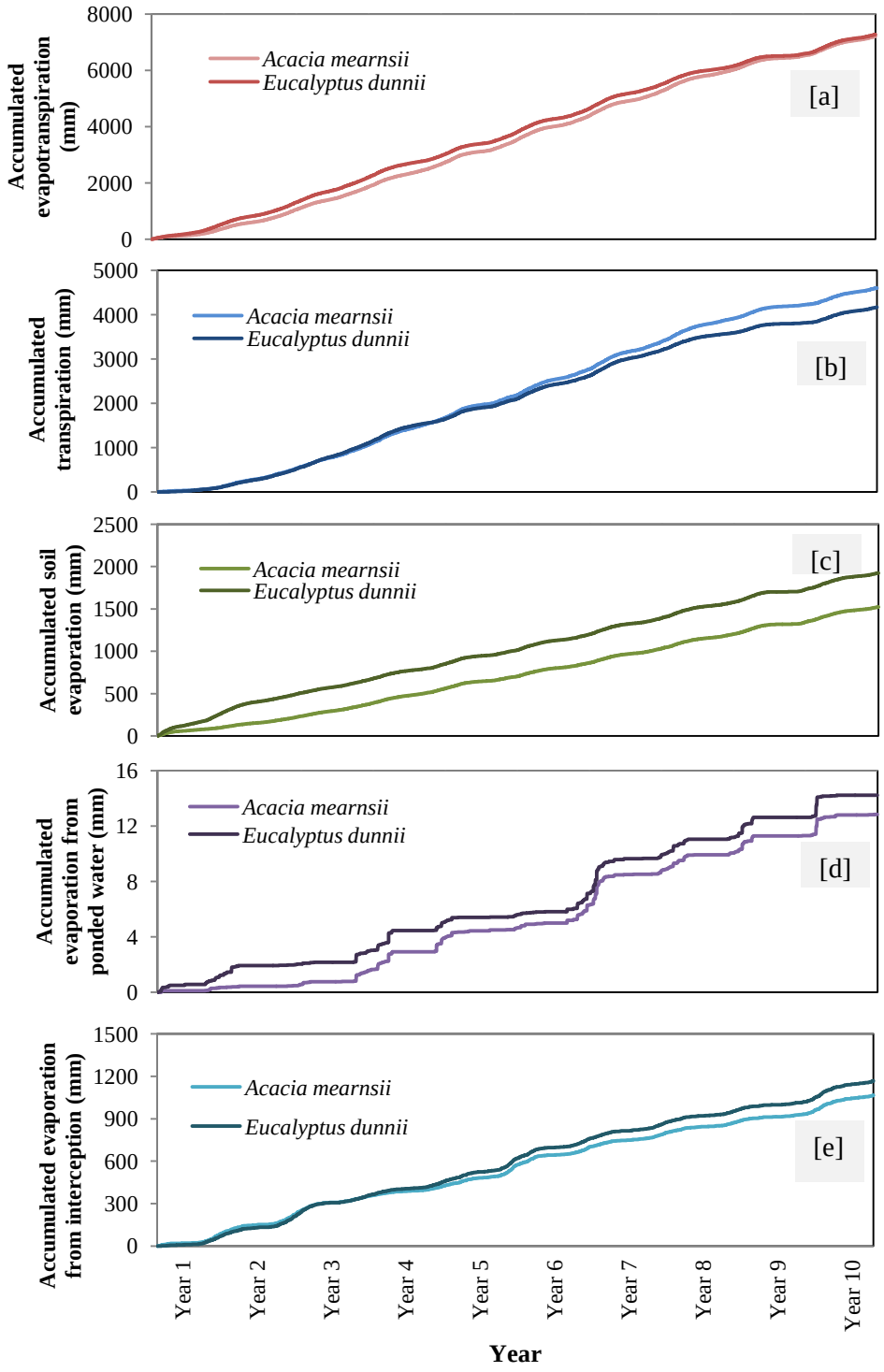

Figure 7.4: Accumulated daily [a] evapotranspiration, [b] transpiration, [c] soil evaporation, [d] evaporation from ponded water, [e] evaporation from interception rates of the *A. mearnsii* and *E. dunnii* plantation species.

The accumulated daily CIS rates are higher for *A. mearnsii* for the first six simulated years. Thereafter, the *E. dunnii* rates increase and the accumulated daily records remain similar until the end of the simulations (Figure 7.5a). There is no significant difference between the two CIS outputs (P = 0.35;

Table 7.4). Both plantation types have low daily values of depth of OL (Figure 7.5b) with accumulated quantities by the end of each simulation amounting to less than 2.10×10^{-3}mm. Despite the similarity in the accumulated daily values, there is a significant difference between the depth of OL outputs ($P = 3.17 \times 10^{-5}$; Table 7.4).

The accumulated daily I_{UZ} rates display the greatest similarity in accumulated daily rates (Figure 7.5c), in comparison to all other accumulated daily outputs considered (Figure 7.4 and 7.5) and the daily I_{UZ} outputs are not significantly different from one another ($P = 0.55$; Table 7.4). Comparing the accumulated daily GR rates, *A. mearnsii* has higher accumulated daily rates than *E. dunnii*, with the accumulated daily difference increasing over the simulation periods (Figure 7.5d). The GR daily outputs are significantly different from one another ($P = 1.58 \times 10^{-5}$; Table 7.4). In comparison with the daily accumulated records of the other hydrological components, there is little inter-annual variation for both plantation types.

Overall, the accumulated daily rates demonstrate similar pattern responses for both species modelled, for all of the outputs considered (Figure 7.4 and 7.5). The inter-annual variability observed in the accumulated daily rates display a stepped response, indicative of seasonal differences, with the summer months having higher rates than the winter months. The terraced pattern is noticeable in the ET, E_t, E_s, E_p, E_i, depth of OL and I_{UZ} outputs (Figure 7.4 and 7.5), particularly so in the E_p records (Figure 7.4d), where *A. mearnsii* daily record experienced no OL for 79.54% of the total simulation (2799 days) and *E. dunnii* experienced no OL for 79.97% of the total simulation (2814 days), with no OL occurring predominantly over the winter months, thus creating a more stepped response between the summer and winter seasons (Figure 7.5b).

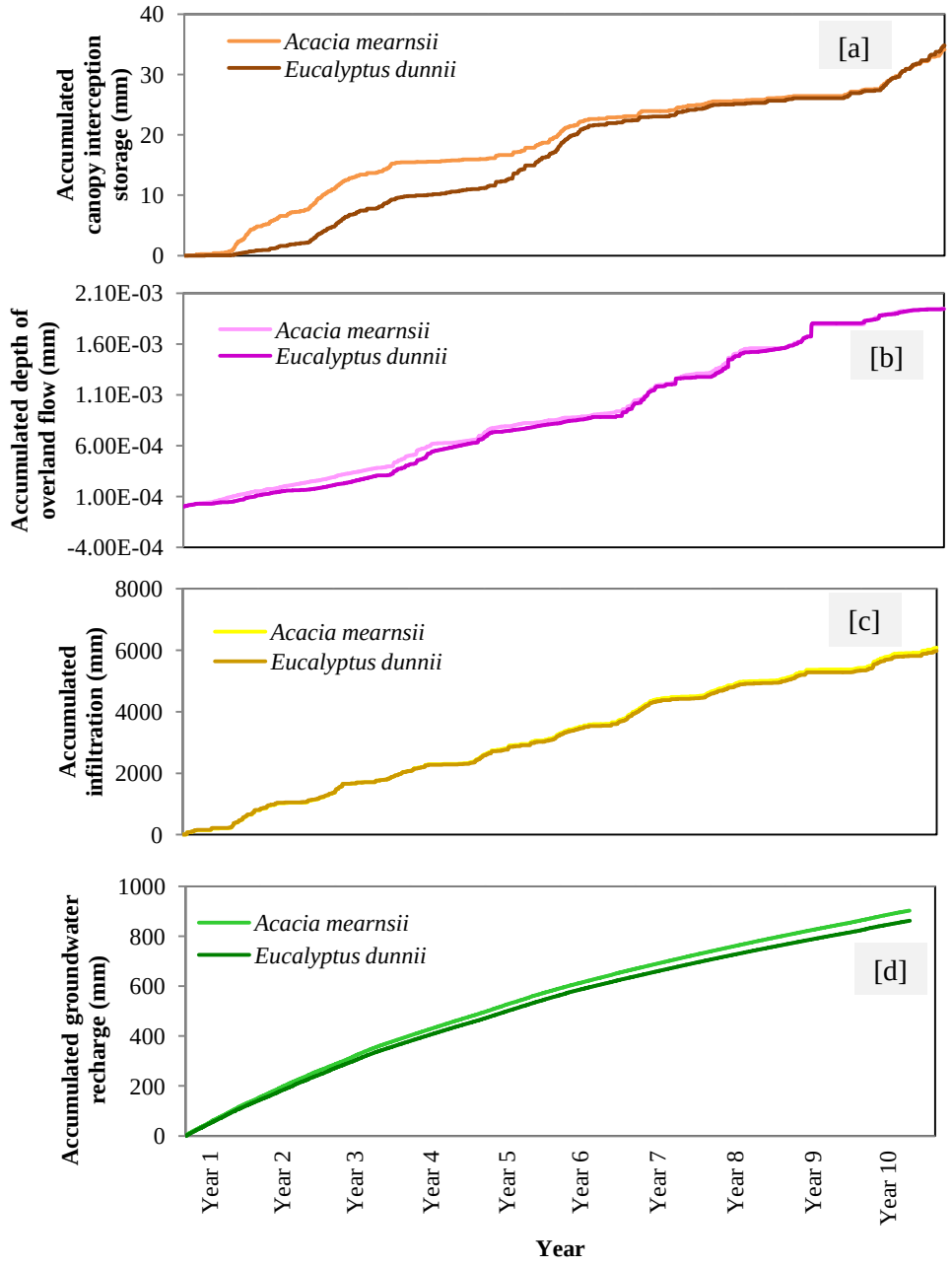

Figure 7.5: Accumulated daily [a] canopy interception storage, [b] depth of overland flow, [c] infiltration, and [d] groundwater recharge rates of the *A. mearnsii* and *E. dunnii* plantation species.

Linear correlations were undertaken and Pearson's correlation coefficients were calculated to compare the hydrological component outputs of the two species (Table 7.5). All of the hydrological component outputs, except for the GR, demonstrate strong linear correlations; r ranges between 0.79 – 0.99 (Table 7.5). The daily I_{UZ} rates have the strongest linear correlations, r = 0.99 ($P < 1.00 \times 10^{-4}$) while the GR daily rates have the weakest linear correlation, r = 0.24 ($P < 1.00 \times 10^{-4}$; Table 7.5).

Table 7.5: Pearson's correlation coefficients based on linear correlation between each annual hydrological output and annual rainfall.

Hydrological component	**Pearson's correlation coefficient (r)**	**Significance of Pearson's correlation coefficient***
	Comparing daily *A mearnsii* and *E. dunnii* component	
ET	0.97	$P = 2.00 \times 10^{-4}$
CIS	0.79	P = 0.02
Depth of OL	0.92	$P = 1.60 \times 10^{-3}$
I_{UZ}	0.99	$P < 1.00 \times 10^{-4}$
GR	0.24	$P < 1.00 \times 10^{-4}$

* Pearson's correlation coefficients are significant when P < 0.05 and not significant when P > 0.05.

It is expected that the more water available on the surface, the greater the chance of evaporation. Thus correlating the annual E_p rates and depth of OL values a strong, significant, linear correlation is expected, and was found to be true for both plantation types, r = 0.70 (P = 0.04) and 0.78 (P = 0.01) for *A. mearnsii* and *E. dunnii* respectively (Table 7.6). Correlating the variables that make-up CI (i.e. E_i and CIS), they demonstrated a significant, strong, linear correlation of r = 0.70 (P = 0.01) and r = 0.79 (P = 0.01) respectively. Correlating the *A. mearnsii* annual rates of E_S and I_{UZ}, as it is expected that the more water infiltrating the soil the more water is available for E_S, they demonstrated no linear correlation, r = 0.03 (P = 0.89; Table 7.6). Similarly, the annual rates of *E. dunnii* demonstrated a significant, weak, linear correlation, r = 0.44 (P = 0.20; Table 7.6).

Table 7.6: Pearson's correlation coefficients based on linear correlation across the outputs of: evaporation from ponded water and depth of overland flow, evaporation from interception and canopy interception storage, and soil evaporation and infiltration for the *A. mearnsii* and *E. dunnii* plantation types.

Outputs compared	**Pearson's correlation coefficient (r) of *A. mearnsii* outputs***	**Pearson's correlation coefficient (r) of *E. dunnii* outputs***
E_p and depth of OL	0.70	0.78
E_i and CIS	0.70	0.79
E_s and I_{UZ}	0.03	0.44

* Pearson's correlation coefficients are significant when P < 0.05 and not significant when P > 0.05.
**Coloured blocks indicate Pearson's correlation is not significant (P > 0.05).

7.5 Monthly and seasonal comparisons of the hydrological outputs

The monthly ET rates display similar patterned responses with the wet summer months having higher rates than the dry winter months for both species (Figure 7.6).

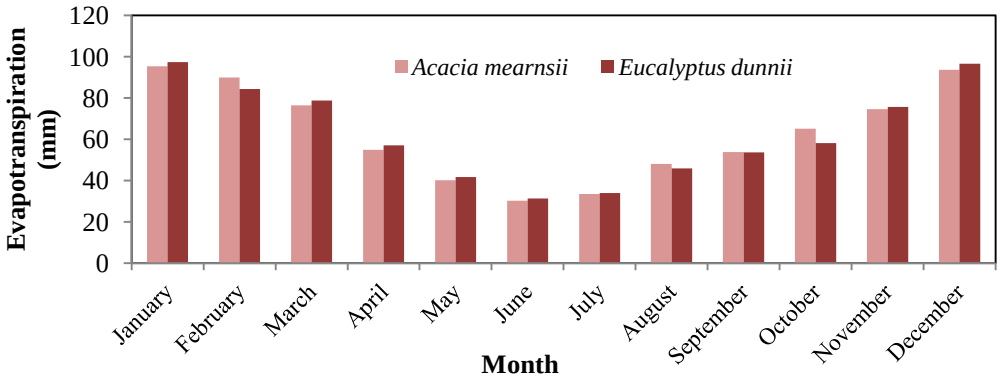

Figure 7.6: Averaged monthly evapotranspiration totals for the *A. mearnsii* and *E. dunnii* plantation types for the total simulated periods.

The *A. mearnsii* monthly ET rates are separated into their ET components (E_t, E_s, E_p and E_i) to determine the percentage each component contributes to total monthly ET (Table 7.7). Transpiration (E_t) accounts for between 55.65 – 71.54% of the monthly totals, with the winter month ET experiencing a greater percentage contribution of E_t than the summer months (Table 7.7). June and July have the highest percentage contribution of E_t while October and November have the lowest (Table 7.7). Soil evaporation (E_S) accounts for between 20.36 – 24.25% of the monthly ET rates of *A. mearnsii* with September having the highest monthly contribution and June the lowest (Table 7.7). The *A. mearnsii* monthly E_i accounts for between 8.10 – 23.57% of the monthly ET rates (Table 7.7). The E_i rates contribute the least to overall monthly ET during the winter months (June and August) and highest during the summer months (October and November; Table 7.7). Overall, the E_p rates contribute negligibly to monthly ET rates, with percentage contribution ranging from 0 – 0.49% (Table 7.7). The E_p contributes most over the summer months and least over the winter months (Table 7.7).

Table 7.7: Percentage composition (transpiration, soil evaporation, evaporation from interception and evaporation from ponded water) of the monthly *A. mearnsii* evapotranspiration rates.

Month	E_t **as % of monthly ET**	E_s **as % of monthly ET**	E_i **as % of monthly ET**	E_p **as % of monthly ET**
January	63.22	20.59	15.91	0.28
February	65.80	20.61	13.52	0.08
March	63.15	21.47	15.19	0.19
April	66.95	21.44	11.56	0.05
May	69.79	20.53	9.67	0.01
June	71.54	20.36	8.10	0
July	70.69	20.99	8.30	0.02
August	70.88	20.49	8.57	0.05
September	62.66	24.25	13.01	0.08
October	57.50	22.12	20.18	0.19
November	55.65	20.48	23.57	0.30
December	60.06	20.74	18.71	0.49

The monthly *E. dunnii* E_t rates account for the largest percentage (ranging from 47.83 – 66.57%) of the monthly *E. dunnii* ET rates (Table 7.8). Transpiration (E_t) contributed most to the total month ET over the winter months (Table 7.8). The *E. dunnii* E_t rates have a smaller percentage contribution to total ET than is seen for *A. mearnsii* (Table 7.7), contributing between 55.65 – 71.54% of the monthly ET rates (Table 7.8). The *E. dunnii* E_s rates contribute most to monthly ET over October and November and least over May and June (Table 7.8). The *E. dunnii* monthly E_i rates account for between 8.78 – 24.20% of the monthly ET rates (Table 7.8); this is higher than the percentage contribution observed for *A. mearnsii* (Table 7.7). The E_i rates have the lowest percentage contribution during the winter months (June to August) and highest during the summer months (October and November; Table 7.8), similar to observations made for *A. mearnsii* (Table 7.7). The *E. dunnii* E_p contribute very little to monthly ET, with percentage contribution ranging from 0 – 0.54% (Table 7.8), similar to the percentages observed for *A. mearnsii* (Table 7.7). The *E. dunnii* E_p contribution to total monthly ET is highest over the summer months and lowest over the winter months (Table 7.8), yet negligible to total ET.

Table 7.8: Percentage composition (transpiration, soil evaporation, evaporation from interception and evaporation from ponded water) of the monthly *E. dunnii* evapotranspiration rates.

Month	**E_t as % of monthly ET**	**E_s as % of monthly ET**	**E_i as % of monthly ET**	**E_p as % of monthly ET**
January	56.22	25.15	18.37	0.26
February	59.17	26.31	14.41	0.11
March	56.67	27.84	15.25	0.23
April	61.39	27.03	11.52	0.06
May	65.22	24.56	10.20	0.01
June	66.57	24.63	8.78	0.02
July	65.79	25.39	8.82	0
August	64.74	25.22	10.00	0.05
September	57.36	27.51	15.05	0.08
October	47.83	28.79	23.15	0.24
November	48.31	27.21	24.20	0.28
December	53.40	26.08	19.97	0.54

The monthly CIS rates of both species demonstrate little monthly seasonal variation between the wet summer months and dry winter months (Figure 7.7a). For *A. mearnsii*, monthly CIS is lowest between February – August and highest between September – January (Figure 7.7a). *E. dunnii* has less evidence of monthly variations in CIS. September has the highest rates, whilst February and May the lowest (Figure 7.7a). Over June, the CIS rates are most similar for the two species, whilst for October they have the biggest difference in rates (Figure 7.7a). The monthly depth of OL values for the two species display strong seasonal variations between the wet summer months and the dry winter months (Figure 7.7b). Noticeably the months of June, July and August have much lower values than all other months, whilst the months of January and December have much higher values (Figure 7.7b).

The monthly I_{UZ} rates are similar for both species, for all months of the year. However, for every month *A. mearnsii* I_{UZ} rates slightly exceed those of *E. dunnii* (Figure 7.7c). For both species, the monthly I_{UZ} rates demonstrate clear seasonal distinctions with the wet summer months having noticeably higher I_{UZ} rates than the dry winter months (Figure 7.7c). December experiences the highest rates of I_{UZ}, while May the lowest (Figure 7.7c). The monthly GR rates are highest every

month for *A. mearnsii* (Figure 7.7d). For both plantation species, there is little monthly distinction in GR, with the largest differences observed over October and December. June has the lowest GR rates for both species (Figure 7.7d).

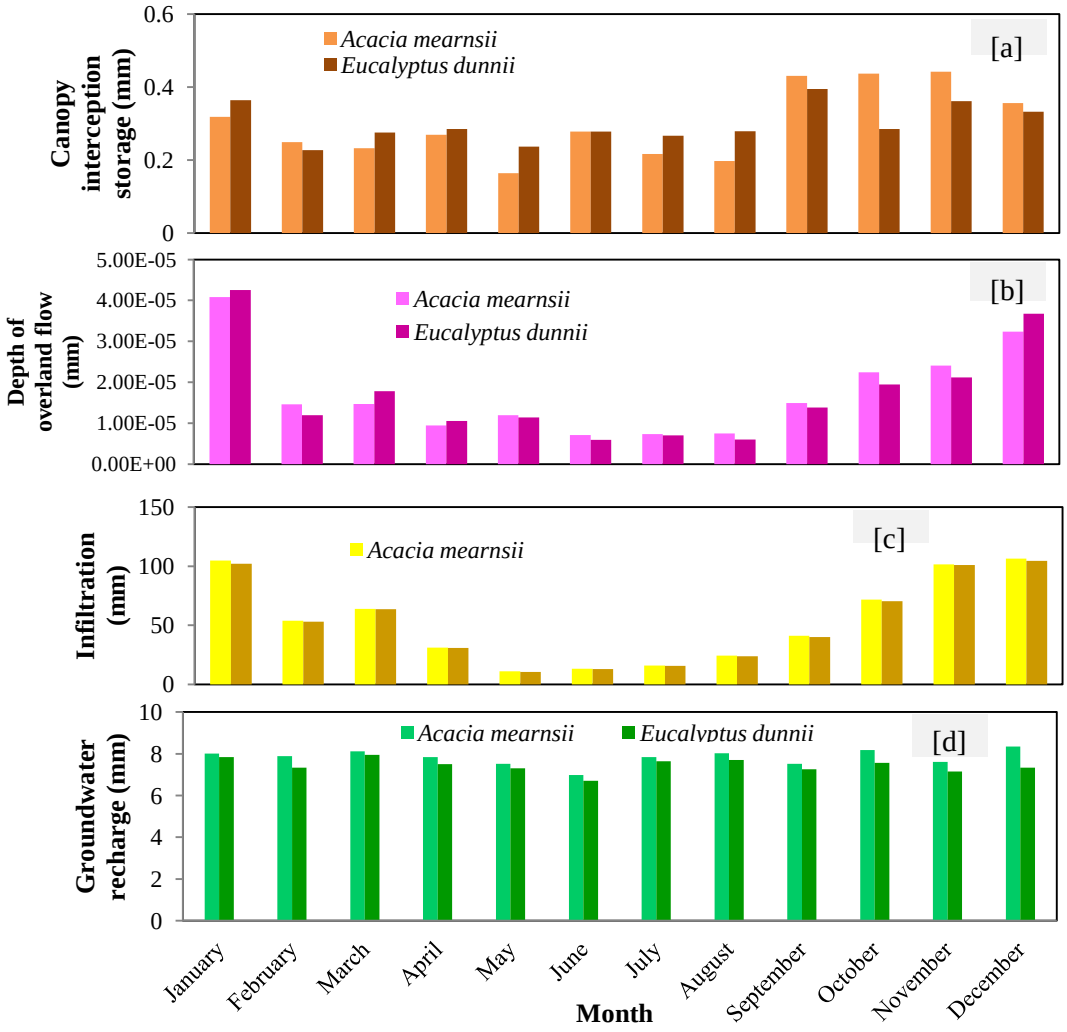

Figure 7.7: Averaged monthly [a] canopy interception storage, [b] depth of overland flow, [c] infiltration, and [d] groundwater recharge rates for the *A. mearnsii* and *E. dunnii* plantation types for the total simulated period.

7.6 Comparing the water balances of the two plantation types

Comparing the water balance, water storages and water balance error of both plantation species, there is a negligible loss in *A. mearnsii* CIS (1.12×10^{-6}mm) and a negligible gain in *E. dunnii* CIS (4.67×10^{-5} mm; Table 7.9). Both *A. mearnsii* and *E. dunnii* experience a similar, yet negligible, gain in overland storage (1.95×10^{-3} and 1.94×10^{-3}mm, respectively; Table 7.9). The larger and more

significant storage changes for both species are in the unsaturated and SZ storage, where both *A. mearnsii* and *E. dunnii* experience a loss in sub-surface storage equivalent to 1484.06 and 1492.83mm, respectively (Table 7.9). Overall, both species display a similar hydrological response, with the greatest differences observed between E_t and E_s rates (Table 7.9). Comparing the SZ inflow and outflow of water, both species experience a net outflow, greater for *A. mearnsii* (1436.33mm) than for *E. dunnii* (1377.97mm; Table 7.9).

Table 7.9: Summary of the water balance component rates and errors for the *A. mearnsii* and *E. dunnii* plantation types (mm), from the start to the end of 10 year modelled period.

Water balance components for error calculation		***A. mearnsii***	***E. dunnii***
CI	Total precipitation reaching the canopy	-7159.50	-7159.50
	Canopy throughfall to ponded water	6092.63	5991.65
	Evaporation from intercepted storage	1066.92	1167.88
	Change in interception storage	-1.12×10^{-6}	4.67×10^{-5}
	Error in CI	**0.05**	**0.03**
OL	Canopy throughfall to ponded water	-6092.63	-5991.65
	E_p	12.83	14.22
	I_{UZ} from ponded water	6079.76	5977.41
	Change in overland storage	1.95×10^{-3}	1.94×10^{-3}
	Error in OL	**-0.04**	**-0.02**
UZ	I_{UZ} from ponded water	-6079.76	-5977.41
	Evaporation from the UZ	1523.18	1924.06
	E_t from the root zone	4604.01	4168.06
	Recharge to the SZ	903.06	862.23
	UZ storage	-950.80	-977.08
	Error in UZ	**-0.31**	**-0.14**
SZ	Recharge to the SZ	-903.06	-862.23
	SZ boundary inflow	-935.48	-844.50
	SZ boundary outflow	2371.81	2222.47
	Change in SZ storage	-533.26	-515.75
	SZ to river exchange	0.00	0.00
	Error in SZ	**0.01**	**-0.01**
Total error		**-0.29**	**-0.14**

7.7 Discussion

This discussion elaborates on the key findings and where findings have been elaborated on in chapter six, less emphasis is placed on those findings in this chapter to avoid repetition. Of particular interest was to compare water use of the two plantation species. Furthermore the discussion addresses the limitations encountered in the study including the uncertainty in the MIKE SHE future scenario (*E. dunnii*) predictions.

7.7.1 Comparing the water use and invasive nature of *A. mearnsii* and *E. dunnii*.

In South Africa, *A. mearnsii* and *E. dunnii* plantations are categorized as exotic species, indigenous to Australia and acknowledged for their fast growth rates and high demand on water resources (Le Maitre *et al*., 2016). The fast growth rates give these and other exotic forestry species a competitive advantage over indigenous forestry and motivate for their use as plantation species (Albaugh *et al*., 2013). However, a major limitation for use of exotics in plantation forestry is their excessive water use in relation to indigenous vegetation, which arises due to their deep rooting systems, evergreen nature and high ET rates demands (Dye and Jarmain, 2004; Albaugh *et al*., 2013; Le Maitre *et al*., 2016). This is a concern given the water scarcity experienced in South Africa (Claassen, 2010).

A. mearnsii has been identified as the most pervasive and widespread tree invader in South Africa (Versfeld *et al*., 1998), based on coverage extent and water use (Le Maitre *et al*., 2000). In terms of total invaded area, *A. mearnsii* is the third highest ranked species, whilst *Eucalyptus* spp. are not within the top ten (Le Maitre *et al*., 2000). In terms of water use, *A. mearnsii* has been identified as the greatest water user in comparison to other tree invaders in South Africa, whilst *Eucalyptus* spp. have been listed as number six of the 25 invasive plants with the greatest water use (Le Maitre *et al*., 2000). The high water use restricts catchment or sub-catchment streamflow and depletes deep soil water reserves (Dye *et al*., 2001).

The excessive water use of *A. mearnsii* is exacerbated by the tendency of this species to spread rapidly from planting sites, particularly into riparian zones, forming dense thickets of high LAI and density (Dye *et al*., 2001; Albaugh *et al*., 2013). The spread into riparian zones and the subsequent spread downstream through rivers or streams are of concern in the management of *A. mearnsii* (Dye and Jarmain, 2004). Within riparian zones, *A. mearnsii* tends to use more water than when located in the upper reaches of a catchment or sub-catchment, as more water is available and ET (particularly E_t) is less restricted in dry winter seasons allowing for continued growth over the winter months (Le Maitre *et al*., 2000). Thus, invasive trees in riparian zones have a greater impact on water resources than they would in the upper reaches of a catchment or sub-catchment, where water availability is more of a restriction to growth and ET (Dye and Jarmain, 2004).

There is a paucity of research on *E. dunnii*, and this study found no research conducted on the invasive nature of *E. dunnii*. Instead the focus was placed on the evidence for the invasive nature of other *Eucalyptus* spp. (Le Maitre *et al*., 2000; Forsyth *et al*., 2004; Rejmánek and Richardson, 2011; Albaugh *et al*., 2013; Le Maitre *et al*., 2016). Eucalypts have the greatest cultivation extent in South Africa, but have been shown to be markedly less invasive than many other invasive species, including *A. mearnsii* (Rejmánek and Richardson, 2011; Albaugh *et al*., 2013). Where eucalypts have invaded they rarely spread large distances from planting sites and their regeneration is sporadic (Forsyth *et al*., 2004; Albaugh *et al*., 2013). According to Rejmánek and Richardson (2011), the reason for the limited invasions of eucalypts is due to limited seed dispersal, high seedling mortality, or lack of compatible ectomycorrhizal fungi. The invasive nature of *Eucalyptus* spp. was investigated by Forsyth *et al*. (2004), who found most eucalypts to be non-invasive, with only three species showing invasive tendencies: red river gum (*Eucalyptus camaldulensis*), flooded gum (*Eucalyptus grandis*) and spider gum (*Eucalyptus conferruminata*).

In general, it appears that exotic *Eucalyptus* spp. are less invasive in terms of their propensity to spread from their place of establishment and use less water than exotic *Acacia* spp. (Le Maitre *et al*., 2000). Thus, based on the literature considered above, *E. dunnii* as a *Eucalyptus* species, appears to be

a preferential plantation species, requiring less management intervention to reduce spread into the riparian zones or into downstream catchments and having a lower impact on water quantity than *A. mearnsii* (Le Maitre *et al*., 2000; Rejmánek and Richardson, 2011; Albaugh *et al*., 2013; Le Maitre *et al*., 2016). In addition, it is acknowledged that there are differences between plantation species and invasive species. Even if the plantation and invasive species is the same species they behave differently under different circumstances, with invasive species occurring in greater densities and being largely prevalent in riparian zones (Dye *et al*., 2001; Albaugh *et al*., 2013).

Comparing the findings from the literature to those made in this study, they are in contradiction. For this study, a change in plantation from *A. mearnsii* to *E. dunnii*, led to a greater loss in ET and total sub-surface storage, suggesting that *E. dunnii* is the greater water user. This does not relate well to the above findings that suggest *A. mearnsii* to be the greater water user. Reasons for the discrepancy in the findings could possibly be that the above literature were concerned with invasive species in total and not just plantations (Le Maitre *et al*., 2000). Within South Africa, exotic plantations consume approximately 93mm.yr^{-1} of rainfall, while invaded areas use about 190mm.yr^{-1} (Le Maitre *et al*., 2000). The difference in these rates is believed to be as a result of the concentration of invasive species in riparian zones (Le Maitre *et al*., 2000), and as *A. mearnsii* has a greater tendency for invasion into riparian zones, this species is likely to have a greater water use (Dye and Jarmain, 2004).

However, in terms of water use there are concerns for both *A. mearnsii* and *E. dunnii*, with ET rates for both species exceeding the rates of rainfall over the simulation periods (Table 7.1) and with both species resulting in a significant loss in unsaturated and SZ storage (Table 7.9). Given the paucity of hydrological data and research on *E. dunnii*, this investigation provides a preliminary assessment and future research should focus on improving the *E. dunnii* hydrological dataset and specifically the MIKE SHE model parameters.

7.7.2 Contributing to the understanding of genus exchange

Genus exchange concerns the impacts of plantation species exchanges (Scott and Gush, 2017) and is quite a contentious issue in South Africa given the stringent legal restrictions imposed on forestry by the National Water Act (NWA, Act 36 of 1998). From previous discussion it is clear that different plantation species use water differently (Chapter 7 results) and thus two species will have different impacts on water resources. The Department of Water and Sanitation (DWS) published Government Gazette no. 39324 (2015) stipulating the regulations on afforestation genus exchanges in terms of the NWA. Under this notice any existing afforestation water user who is planning to exchange the genus of their plantation needs to apply for the proposed exchange. As such each exchange is heavily regulated and requires knowledge of the water use properties of the plantation of concern. If the planned exchange will result in greater water use, the area proposed for plantation may have to be reduced to counteract the negative impacts on the hydrological cycle. Based on this studies results, *E. dunni* is shown to be a greater water user than *A. mearnsii*. This genus exchange would thus result in greater water use and legally this may be an issue when applying for the appropriate licensing. However, given the paucity of research on *E. dunnii* further research is required to more accurately quantify the species water use within the Two Streams sub-catchment.

Biologically the exchange of one species for another can have a number of impacts. This is particularly noticeable if there is an exchange from an invasive to a non-invasive or native plantation or visa versa (Strauss, 2001). With an exchange from an invasive to a native plantation forest there is greater exchange of biota between the plantation and surrounding ecosystem with the native plantation providing resources and corridors for native biota (Strauss, 2001). Given the lack of data on the invasive nature of *E. dunnii* it is unclear how the plantation ecosystem and surrounds will respond to such a genus exchange and as such further research into *E. dunnii* is required to investigate this exchange. The beneficial aspect of this genus exchange is that the baseline conditions of the study site are fairly well known given the extensive research that has taken place within the Two Streams sub-catchment (Everson *et al.*, 2006, 2014; Clulow *et al.*, 2011). As such, changes in hydrological processes will be more noticeable for example changes in streamflow or evapotranspiration.

Baselining in plantation forestry studies is an issue especially in terms of legal classifications of SFRAs (Gush *et al*., 2002; Jewitt *et al*., 2009).

7.7.3 Transpiration and soil evaporation

As discussed above, the ET rates of both species were high (Table 7.1). ET rates for both *A. mearnsii* and *E. dunnii* exceeded rainfall rates, which could suggest inaccuracies in modeling and also brings into question the ability for MIKE SHE to adequately simulate periods of water deficit. The precipitation modelled was only in the form of rainfall, however this region is known to experience extensive mist and fog (Mucina and Rutherford, 2006; Clulow *et al*., 2011; Everson *et al*., 2014) which could significantly contribute to total precipitation, and thus rates of ET would not appear as excessive.

The high ET rate is predominantly as a result of E_t which accounts for the largest portion of ET for both vegetation classes, followed by E_s (Table 7.1). Together they account for >80% of total ET for both *A. mearnsii* and *E. dunnii* (Table 7.1), and are the greatest evapotranspirative drivers of water loss. The greatest differences observed between the two classes were seen in E_t and E_s rates (Table 7.9), where *A. mearnsii* experienced longer more sustained access to groundwater reserves from the start of the simulation, whilst *E. dunnii* experienced slower root and canopy establishment at the start of the simulation leading to greater exposure of the ground surface. Greater exposure of the ground to atmospheric conditions of increased radiant energy, increased soil temperature and wind all drive evaporation (van Dijk and Keenan, 2008; Hasenmueller and Criss, 2013), whilst access to deep soil water reserves allows for continued growth during the dry season and for vegetation stomata to remain open, increasing E_t (Dye and Jarmain, 2004; Cai *et al*., 2018). The soil physical characteristics, including hydraulic conductivity, determine the quantity of water accumulating in the topsoil and in the root zone. Water that accumulates in the topsoil controls E_s whilst water accumulating in the root zone controls E_t (Raz-Yaseef *et al*., 2012). These differences in E_s and E_t were driven predominantly by the vegetation and soil characteristics of the site (sections 6.9.2, 6.9.3 and Appendix F).

The partitioning of ET into the dominant constituent components of E_t, E_s and E_i is necessary in understanding not just the hydrological cycle but also other connected system responses such as fluxes in latent heat (energy cycling) and carbon cycling (Lawrence *et al*., 2005). The partitioning of ET into the constituent components conforms to the study findings that E_t is the dominant component of ET (Williams *et al*., 2004; Lawrence *et al*., 2005). However, when the canopy is sparse, the partitioning of evapotranpiration becomes more complicated and E_s can, at times, dominate (Raz-Yaseef *et al*., 2012). This inversely proportional relationship between E_s and E_t was found true for this study, where at the start of the simulations E_t was low and E_s was high due to limited vegetation coverage – particularly noticeable for *E. dunnii*. Thereafter the *E. dunnii* canopy coverage became denser and E_t rates exceeded E_s.

7.7.4 Hydrological processes and capacity thresholds

Within the MIKE SHE model, at the onset of rainfall, the capacity of the canopy to intercept water is the initial process to occur (DHI software, 2012). Canopy interception (CI) refers both to the water evaporated from CI and the water stored in the canopy (Hendriks, 2010). Canopy interception storage (CIS) depends strongly on rainfall characteristics, and vegetation characteristics: vegetation type and stage of vegetation development (Kozak *et al*., 2007).

Considering the constituent parts of CI (E_i and CIS), CIS (Table 7.2) contributes less to total CI than does E_i (Table 7.1) for both plantation types, highlighting the high evaporative potential of both species canopies, due to the direct exposure to solar radiation and wind (Bulcock and Jewitt, 2012). Furthermore, the E_i rates display strong seasonal differences as a result of the direct exposure to climatic elements, whilst CIS did not display clear seasonal distinction between the wet summer and dry winter months. This is believed to be as a consequence of the evergreen nature of both canopies and fast growth rates that allow for sustained dense canopy coverage (van Wilgen *et al*., 2001;

Chamier *et al.*, 2012; Albaugh *et al*., 2013; Le Maitre *et al*., 2016). Thus, the canopies physiological capacity to store water is not governed by seasonality.

Canopy interception (CI) is an important factor in the forest water balance accounting for a significant portion of precipitation (Dye and Versfeld, 1992, Savenije, 2004; Everson *et al*., 2006). The most comparable CI findings to this study were found by Bulcock and Jewitt (2012), who studied CI at the Two Streams catchment between April 2008 – March 2011. They found the CI by *A. mearnsii* to account for 27.7% of precipitation. Considering the results obtained by Bulcock and Jewitt (2012), over the same period of time for this study, CI for *A. mearnsii* amounted to 15.44%. In comparison to the findings of the Bulcock and Jewitt (2012) study, this study had an under-prediction of interception of more than 10% of precipitation. This highlights a potential weakness in the model or input data employed possibly requiring the refinement in the way MIKE SHE conceptualises and parameterises interception. This shortfall would need to be verified through further studies, as an under-prediction in CI will affect the total water balance of the system. Outside of the possibility of weakness in the study, possible reasons for the discrepancies are that Bulcock and Jewitt (2012) considered the entire catchment, whilst this study focussed only on the research intensive sub-catchment, and due to different temporal consideration in precipitation (discussed previously under section 6.9.2).

The precipitation, not intercepted by the vegetation canopy, will move as throughfall to the ground surface, at which stage it will either infiltrate into the soil surface or flow overland as runoff (Hendriks, 2010; DHI software, 2012). Given the high hydraulic conductivity and high soil water retention capability of the soils of the Two Streams sub-catchment (described in section 5.6.1 and Appendix F), water easily infiltrates through the soil and less water is available for OL or runoff. This study found daily I_{UZ} to be strongly correlated to daily rainfall, and to account for over 80% of total rainfall for both plantation species. The I_{UZ} rates were not significantly different between the two species; however *A. mearnsii* rates are higher. Overall, *E. dunnii* has denser coverage and higher ET rates than that of *A. mearnsii*, resulting in less water available to infiltrate in comparison to *A. mearnsii*.

OL rates and the E_p rates were minute for both species as they are proportional to the rate of I_{UZ} (discussed previously section 6.9.3). For OL to occur, the threshold of water ponding on the ground surface must first be overcome (DHI software, 2012) – refer to section 4.3.6. A hydrological process not included in the MIKE SHE model, and that has a significant impact on the amount of water ponding on the surface, is that of litter interception. Litter interception is an important component in forestry ecosystems where tree litter accumulates on the forest floor acting as a barrier to I_{UZ} and can lead to surface runoff, once the litter interception threshold is reached (Bulcock and Jewitt, 2012). Litterfall within forestry plantations can contribute to a significant portion of total biomass. For example, du Toit, (2008) found annual, foliar, litterfall to range from 4.79 – 5.92Mg.ha^{-1} in a young *Eucalyptus grandis* stand in South Africa.

The amount of litter intercepting precipitation is an important concept in the Two Streams study site given the high rates of I_{UZ} that occur, as this would reduce the rates of I_{UZ} and increase surface runoff and E_p. Litter interception was not included in this study, but for the same study site, Bulcock and Jewitt (2012) found litter interception to account for 6.60% of precipitation for the *A. mearnsii* plantation. This accounts for a significant portion of rainfall that would then not be infiltrating the soil. Thus, by including litter interception into the study the rates of I_{UZ} might be reduced and OL and the evaporation thereof may increase, resulting in improved streamflow. This is a limitation in MIKE SHE modelling capabilities, and future hydrological modelling studies should work to include litter interception, in particular in plantation forests where this is clearly a significant water storage process.

Each of the hydrological processes described above causes a delay in the subsequent processes in the hydrological cycle, as each process is dependent on the previous, and each hydrological component has threshold capacities to overcome prior to the occurrence of the subsequent process (DHI software, 2012). As a result, by the time water starts to move through the deeper soil layers into the SZ, there is a significant time-lag (Vertessy, 2001). It has been found that the effects of plantation establishment on GR may only truly be evident after several decades due to the lagged response in hydrological

changes (Vertessy, 2001). This explains why GR showed a weak correlation to rainfall. In addition, this can explain the steady daily accumulation in GR, as small fluctuations in hydrological events are less reflected, thus there is a lack of quick responses in GR and a rather more stable addition over time (van Wyk *et al*., 2012).

In this study, GR accounts for 12.61 and 12.04% of total rainfall for *A. mearnsii* and *E. dunnii* respectively (Table 7.2). In accordance with the findings of Silveira *et al*. (2016), the *E. dunnii* recharge falls within the range presented in the literature of 4 to 39% of rainfall for areas dominated with *Eucalyptus* spp. forestry. However, it is difficult to compare and generalize GR rates across studies at different locations (Silveira *et al*., 2016). Variables such as rainfall, soil types, geological conditions, water table depths and land uses all have an effect on groundwater (Jyrkama and Sykes, 2007) making the rate of GR location or study specific. Results of GR in relation to plantation forestry establishment or afforestation have demonstrated contradicting results. Fan *et al*. (2014) reported a reduction in GR, while Krishnaswamy *et al*. (2013) reported an increase, and Wyatt *et al.* (2015) demonstrated a mixed response that varies in time.

7.7.5 Limitations in research

A significant limitation to this study is the generalized use of hydrological data of other *Eucalyptus* spp. to define *E. dunnii* (refer to section 4.5.4). This is a concern over the generic consideration of the species but also because research has found that differences in water use by exotic plantations are greater between genera than within genera (Görgens and van Wilgen, 2004). This brings into question the accuracy of using generalized data from a number of different *Eucalyptus* species. This is not an easily addressed limitation given the paucity of data available on the species and given the detailed and temporally lengthy data inputs required by MIKE SHE. However, given that the Two Streams sub-catchment is a research site, it provides an excellent opportunity and working environment to extend research given the long-term establishment of infrastructure in place and the good working

relationship established with Mondi that allows for continuation of research and the involvement of researchers in decision making processes, such as harvest times.

In addition there is concern over the uncertainties that emerge from using historical data to quantify future hydrological processes. This concern arises as the accuracy of the model outputs can never be determined through comparison with observed data and calibration procedures (Ma *et al*., 2016). As Lane and Richards (2001) argue, successful model prediction achieved through calibration and validation procedures is restricted both in time and space. Thus, modelled outputs cannot be truly universally validated, as they are restricted by data availability (Ma *et al*., 2016). In addition du Toit *et al*., (2010) describe how multiple rotations of forestry plantations could lead to declines in soil physical properties. Such effects would not accurately be accurately projected in modelling of future scenarios based on historical data.

The final limitation is that both scenarios (current and future) were run as separate processes and not a continuation as would be the reality of the situation, and so there may be 'legacy effects' missed in the simulation such as soil moisture carryover, or soil moisture depletion (Raz-Yaseef *et al*., 2012). Such legacy effects would not have been able to be captured for either the current or future scenarios, this is a concern given the long history of plantation forestry on-site and the potential legacy effects in operation. In addition the separation in the two scenarios did not allow for the examination of the clear felling period and the potential impact of harvesting on the hydrological characteristics of the site. This was out of the scope of this project, but would be useful to investigate in the future. Harvesting can alter site characteristics and influence long-term site productivity (du Toit *et al*., 2010), that would not be accurately captured in predictive modelling scenarios were legacy effects or residual effects or not accurately captured. In addition, future research should also focus on improving monitoring of soil water, soil water balance, penetration into the UZ and water movement to the SZ, all of which would greatly improve MIKE SHE modelling capabilities.

7.8 Conclusion

To compare the different forestry plantations of the MIKE SHE modelled current scenario (*A. mearnsii*) and the MIKE SHE predicted future scenario (*E. dunnii*), certain hydrological components of the water balance diagrams were investigated at different temporal periods from total, annual, seasonal, monthly and daily. The results found both plantation types to be high water users, with the ET rates for both classes exceeding rainfall. Overall, *E. dunnii* used more water through ET and UZ storage, whilst *A. mearnsii* used more deep soil water through E_t, particularly over winter. This chapter highlights the limitations of this study and where future research should be focussed. The limitations included the lack of data on *E. dunnii*, the lack of inclusion of litter interception within MIKE SHE and the inherent uncertainty of basing future model predictions on historic data. Future research should focus on improving hydrological knowledge on *E. dunnii*, and extending the hydrological focus to deeper groundwater investigations and canopy litter interception, all of which will improve hydrological modelling capabilities. This chapter provides a preliminary assessment of the potential impact of changing forestry plantation from *A. mearnsii* to *E. dunnii*.

Chapter Eight

Conclusion

8.1 Summary of study findings

This dissertation determines the effectiveness of using MIKE SHE hydrological modelling software to simulate the hydrological characteristics of the Two Streams sub-catchment, following which the hydrological outputs of the resulting MIKE SHE model are then used to deduce differences in hydrology with differences in land cover and a change in land cover. This dissertation effectively demonstrates the capabilities of the MIKE SHE model for use in the Two Streams sub-catchment and highlights the key advantages and limitations of using the MIKE SHE model.

The MIKE SHE set-up for the study site is to-date the most exhaustive and holistic hydrological modelling approach taken for the Two Streams sub-catchment, supplying insight into the dominant hydrological processes in operation and the overall water use of the hydrological system. The capabilities of the MIKE SHE software, to incorporate detailed spatial and temporal datasets, is a beneficial attribute in small study sites, such as the Two Streams sub-catchment, allowing for greater precision and heterogeneous expression of hydrological variables.

A key finding in the study was that the vegetation classes considered did not display as big a difference in their water balance outputs as observed in literature (Calder, 1997; Vertessy, 2001; Raz-Yaseef *et al*., 2012; Warburton *et al*., 2012). This is believed to be due to the limited spatially explicit data inputs, specifically rainfall and geology. This brings into question the need to use such a physically-based, data intensive model. Where, instead, a more simplified, lumped conceptual model may be able to perform the same function (Merritt *et al.*, 2003; Devi *et al*., 2015). The study site is, however, recognised for the extensive hydrological research conducted on-site and provides a great opportunity for future hydrological research, and thus using a more simplified model may be less time consuming and yield similar results. However, addressing some of the key hydrological data

limitations that would increase spatial heterogeneity would allow for a more accurate depiction of the Two Streams study site and be more beneficial in understanding site hydrological physical processes.

In addition, one of the greatest benefits of using a physically-based model, such as MIKE SHE, is that it is capable of exploring the mechanisms of hydrological processes in response to the environment and environmental change, rather than simply pursuing an improved fit between the modelled and observed outputs (Ma *et al*., 2016). As such, the MIKE SHE model provides a more realistic interpretation of reality in comparison to more conceptual modelling approaches. Furthermore, the physics basis of the modelling software and small scale modelling allows for more realistic hydrological forecasting than more conceptual approaches (Devi *et al*., 2015; Ma *et al*., 2016).

A major challenge faced was acquiring data from past research studies of the site. The Two Streams site has for many decades been run as a hydrological research catchment and should thus have a plethora of data available for hydrological modelling. However, access limitations to these data meant that the model could only be run for a ten-year period and calibration and validation were restricted to single datasets. In addition, data limitations for the period modelled for this study included: smaller temporal intervals of rainfall, the need for verification and greater consistency in capturing of the streamflow record, LAI and RD of the riparian and sugarcane vegetation classes, spatial mapping of geological layers, hydraulic conductivity of geological layers, specific yield and specific storage of geological layers, borehole data for water table mapping and identification of macropore flow or preferential flow paths. Addressing these data limitations will improve spatial heterogeneity of the modelled system, improve model accuracy and allow for the effective re-evaluation of the benefits in relation to the work effort expended in setting up, running and calibrating the MIKE SHE model for the Two Streams sub-catchment.

Limitations with using MIKE SHE were that canopy litter interception was not captured by the model despite being a significant process in forestry ecosystems, where plant litter on the canopy floor can intercept as much as 6.6% in *A. mearnsii* plantations (Bulcock and Jewitt, 2012). Another limitation is

that LAI is the only vegetation index used to define vegetation canopy characteristics, as different tree species may have the same LAI but have very different canopy storage capacities depending on their specific leaf and canopy characteristics (Bulcock and Jewitt, 2012; Klamerus-Iwan, 2014). Other limitations included model uncertainty, long model run time and in-depth data requirements.

The advantages of using the MIKE SHE model include the flexible nature of the software that allow user preferences to determine the underlying equations that govern hydrological processes as dependent on data availability and time constraints of the study site, as a result the MIKE SHE model can be as complicated or simplified as needed (DHI software, 2012). This flexibility allows for the capturing of spatial and temporal heterogeneity in MIKE SHE, that allow for greater precision in modelling. Another advantage is the more complicated water balance calculation, that improves on the basic water balance calculation derived by Thornthwaite and Mather (1957) and the graphical user interface that allows for easy visual interpretation and manipulation of large quantities of input and output datasets (DHI software, 2012). The ability for MIKE SHE software programmes to separate the ET rate into its constituent components of E_t, E_s, E_i and E_p is another advantage of the modelling software, allowing for more accurate predictions of total ET and more accurate understanding of ecosystem processes like plant water availability, water-use efficiency and vegetation patterns (Raz-Yaseef *et al*., 2010). Not all hydrological modelling software programmes model the separate ET constituents (Savenije, 2004; Everson *et al*., 2014), making MIKE SHE a better model choice.

Key findings from the study included that the validation processes undertaken resulted in both the streamflow and ET records (observed and modelled) having good linear correlation. Both plantation forests (*A. mearnsii* and *E. dunnii*) had total ET rates that exceeded total rainfall and this was only the case during the winter months when deeper roots allowed for greater access to deeper soil water reserves and were not only dependent on rainfall for water input. The black wattle class was a greater water user in comparison to the sugarcane and riparian vegetation classes (based on ET rates and subsurface storage losses), whilst *E. dunnii* was a greater water user in relation to black wattle in terms of ET and subsurface storage losses. The ET rates between the vegetation classes of the current

scenario were statistically different whilst those of the future scenario were not. Infiltration (I_{UZ}) rates were high for all vegetation classes and showed no statistical differences between vegetation classes or between soil types. All annual I_{UZ} records showed strong linear correlations to rainfall. The soil types for the site have high soil water retentions and high hydraulic conductivities allowing for fast water movement through the soil increasing the rates of I_{UZ}. Groundwater recharge (GR) rates did not show distinct monthly or seasonal differences with no statistical differences between the winter and summer seasons for all vegetation classes. Groundwater recharge (GR) rates did not correlate well to rainfall. The total rates of CIS, depth of OL and streamflow were all very low for every vegetation class considered.

8.2 Future research

Research going forward should concentrate on addressing the data limitations discussed above, as this would improve the hydrological modelling of the Two Streams sub-catchment. Preventing degradation of water resources and reducing water use is important in South Africa, given that it is a water scarce country (Claassen, 2010). As such, research should focus on improving water use efficiency of the Two Streams study site. Efficiency can be improved through the implementation of a more holistic consideration of site hydrology and through focus on improving management strategies, specifically within the riparian zone (i.e. vegetation clearance and monitoring).

As part of achieving a more holistic model for the site, studies should incorporate soil erosion, given that research on Two Streams is now starting to consider soil erosion through sediment plot studies. Soil erosion is influenced predominantly by, and dependent on, hydrological processes (Le Roux, 2012) and thus having a well developed physically based knowledge of hydrology on-site can greatly aid in understanding soil erosion processes. Previous studies on MIKE SHE have shown the capabilities of linking MIKE SHE to external sediment erosion software to model sediment erosion (Wicks and Bathurst, 1996; DHI, Unknown). Wicks and Bathurst (1996) employed SHESED, which is a physically based, spatially distributed erosion and sediment yield component of MIKE SHE,

whilst DHI (Unknown) documents the incorporation of RUSLE software into MIKE SHE software for modelling soil erosion. The incorporation of a soil erosion extension within the MIKE SHE model was out of the scope of this dissertation as it would require significant programming knowledge to incorporate this extension. This is not a readily available software package from DHI. However, a soil erosion extension would be a good focus for future research on the Two Streams catchment and a valuable addition to the larger WRC project – WRC project No K5/2402: "Assessing the impact of erosion and sediment yield from different land uses in farming and forestry systems and their effect on water resources in selected catchments of South Africa."

8.3 Conclusion

Within South Africa, water is a limiting factor to growth and development and so understanding hydrological processes and quantifying both natural and anthropogenic impacts on water availability is crucial in water resource management (Forrester *et al*., 2011; Ma *et al*., 2016; Toohey *et al*., 2018). Understanding these processes and quantifying these impacts is difficult due to the complexity of the hydrological system and requires a holistic consideration of the dynamic hydrological cycle (Hendriks, 2010; Mimikou *et al*., 2016). The complexity, dynamic character and need for holistic consideration have brought about the need for, and development of, deterministic physically-based hydrological models, such as MIKE SHE (Devi *et al*., 2015). The physical consideration and multitude of input parameters from various disciplines required by deterministic physically-based models aims to reduce the bias between the model system and reality (Castagné, 2007), and although may never truly represent reality, they can provide a good approximation (Ma *et al*., 2016). MIKE SHE allows for spatial and temporal consideration of processes through the incorporation of time series flexibility and spatial mapping through GIS (DHI software, 2012). The flexibility in data inputs both in time and space allows for greater precision in modelling changes (Graham and Butts, 2005), both natural and anthropogenic, such as land cover change (Vogel *et al*., 2015).

The interdisciplinary approach taken in MIKE SHE allows for the development of an in-depth understanding of the dynamics of the connectedness between human and natural systems and thus can be used to determine more holistic and effective solutions to resolve the complex water problems that the world faces today (Vogel *et al*., 2015). This study provides a holistic quantification of the hydrological cycle of the Two Streams sub-catchment and quantifies the hydrological impact of land cover and the change thereof on hydrological processes and water availability. This study provides a platform of consolidated hydrological data onto which research can build to better understand the effects of land cover on hydrology. This study is important given the water scarce nature of the country and the negative impacts of plantation forestry on water resources. The improved understanding of the hydrological system of the Two Streams sub-catchment can be used to inform plantation establishment into the future.

In addition limitations in modelling capabilities are improving, and will continue to improve, over time and thus will become less of a concern in modelling based studies (Devi *et al*., 2015). Hydrological models are constantly and rapidly being improved and advancing in complexity, capabilities, data requirements, user flexibility, ease of operation and processing time and thus over time the spatial and temporal constraints in hydrological modelling will improve enabling further insight into hydrological processes (Rangecroft *et al*., 2018).

References

Abbott, M.B., Bathurst, J.C., Cunge, J.A., O'Connell, P.E. and Rasmussen, J., 1986: An introduction to the European Hydrological System – Systeme Hydrologique Europeen, "SHE", 2: structure of a physically-based, distributed modeling system, *Journal of Hydrology*, 61, 61-77.

Aduah, M.S., Jewitt, G.P.W., Warburton, M.L., 2017: Assessing suitability of the ACRU hydrological model in a rainforest catchment in Ghana, West Africa, *Water Science*, 31(2), 198-214.

Aksoy, H. and Kavass, L., 2005: A review of hillslope and watershed scale erosion and sediment transport models, *Catena*, 64, 247-271.

Albaugh, J.M., Dye, P.J. and King, J.S., 2013: *Eucalyptus* and water use in South Africa, *International Journal of Forestry Research*, 2013, Article ID 852540.

Albhaisi, M., Brendonck, L. and Batelaan, O., 2013: Predicted impacts of land use change on groundwater recharge of the upper Berg catchment, South Africa, *Water SA*, 39(2), 211-220.

Allen, R.G., Pereira, L.S., Raes, D. and Smith, M., 1998: Crop evapotranspiration: guidelines for computing crop water requirements, Irrigation and Drainage Paper No. 56, Food and Agriculture Organization of the United Nations, Italy.

Arheimer, B. and Olsson, J., 2003: Integration and coupling of hydrological models with water quality models: Applications in Europe, Report of the Swedish Meteorological and Hydrological Institute, Norrkoping Sweden.

Arnold, J.G., Moriasi, D.N., Gassman, P.W., Abbaspour, K.C., White, M.J., Srinivasan, R., Santhi, C., Harmel, R.D., van Griensven, A., Van Liew, M.W., Kannan, N. and Jha, M.K., 2012: SWAT:

Model use, calibration, and validation, *American Society of Agricultural and Biological Engineers*, 55(4), 1491-1508.

Ashton, P.J., Harwick, D. and Breen, C., 2008: Changes in water availability and demand within South Africa's shared river basins as determinants of regional social and ecological resilience, in M. Burns and A.v.B. Weaver (eds.), *Advancing sustainability science in South Africa*, Stellenbosch University Press, Stellenbosch, 279-310.

Bathurst, J.C., 1986: Physically-based distributed modeling of an upland catchment using the Systeme Hydrologique Europeen, *Journal of Hydrology*, 79, 79-102.

Battaglia, M. and Sands, P., 1997: Modelling site productivity of *Eucalyptus globulus* in response to climatic and site factors, *Australian Journal of Plant Physiology*, 24(6), 831-850.

Bauhus, J., Khanna, P.K. and Menden, N., 2000: Aboveground and belowground interactions in mixed plantations of *Eucalyptus globulus* and *Acacia mearnsii*, *Canadian Journal of Forest Research*, 30, 1886-1894.

Bauhus, J., van Winden, A.P. and Nicotra, A.B., 2004: Aboveground interactions and productivity in mixed-species plantations of *Acacia mearnsii* and *Eucalyptus globulus*, C*anadian Journal of Forest Research*, 34, 686-694.

Bergström, S., 1992: *THE HBV model- its structure and applications*, SMHI Reports Hydrology No. 4, ISSN 0283-1104.

Bergström, S. and Graham, P.L., 1998: On the scale problem in hydrological modelling, *Journal of Hydrology*, 211, 253-265.

Beven, K., 1997: TOPMODEL: a critique, *Hydrological Processes*, 11, 1069-1085.

Beven, K.J., Lamb, R., Quinn, P., Ronanwvie, R. and Freer, J., 1995: TOPMODEL, in V.P. Singh (ed.), *Computer models of watershed hydrology*, Water Resources Publications, Colorado, 627-668.

Bian, Z., Gu, Y., Zhao, J., Pan, Y., Li, Y., Zeng, C. and Wang, L., 2018: Simulation of evapotranspiration based on leaf area index, precipitation and pan evaporation: A case study of Poyang Lake watershed, China, *Ecohydrology and Hydrobiology*, (in press).

Birkel, C., Soulsby, C. and Tetzlaff, D., 2012: Modelling the impacts of land-cover change on streamflow dynamics of a tropical rainforest headwater catchment, *Hydrological Sciences Journal*, 57(8), 1543-1561.

Biron, P.M., Roy, A.G., Courschesne, F., Hendershot, W.H., Côte, B. and Fyles, J., 1999: The effects of antecedent moisture conditions on the relationship of hydrology to hydrochemistry in a small forested watershed, *Hydrological Processes*, 13, 1541-1555.

Blöschl, G., Ardoin-Bardin, S., Bonell, M., Dorninger, M., Goodrich, D., Gutknecht, D., Matamoros, D., Merz, B., Shand, P. and Szolgay, J., 2007: At what scales do climate variability and land cover change impact on flooding and low flows?, *Hydrological Processes*, 21(9), 1241-1247.

Blöschl, G. and Sivapalan, M., 1995: Scale issues in hydrological modeling: A review, *Hydrological Processes*, 9, 251-290.

Bosch, J.M., 1979: Treatment effects on annual and dry period streamflow at Cathedral Peak, *South African Forestry Journal*, 108(1), 29-38.

Bothma, C.B., van Rensburg, L.D. and Le Roux, P.A.L., 2012: Rainfall intensity and soil physical properties influence on infiltration and runoff under in-field rainwater harvesting conditions, *Irrigation and Drainage*, 61, 41-49.

Brooks, R.H. and Corey, A.T., 1964: *Hydraulic properties of porous media*, Hydrology Paper no. 3, Civil Engineering Department, Colorado State University, Colorado.

Bruijnzeel, L.A., 2004: Hydrological functions of tropical forests: not seeing the soil for the trees? *Agriculture, Ecosystems and Environment*, 104, 185-228.

Bulcock, H.H. and Jewitt, G.P.W., 2010: Spatial mapping of leaf area index using hyperspectral remote sensing for hydrological applications with a particular focus on interception, *Hydrology and Earth System Sciences*, 14, 383-392.

Bulcock, H.H. and Jewitt, G.P.W., 2012: Field data collection and analysis of canopy and litter interception in commercial forest plantations in the KwaZulu-Natal Midlands, South Africa, *Hydrology and Earth Systems Sciences*, 16, 3717-3728.

Burger, C., 1999: *Comparative evaporation measurements above commercial forestry and sugarcane canopies in the KwaZulu-Natal Midlands*, Masters in Science (MSc) dissertation, University of KwaZulu-Natal, Pietermaritzburg.

Burt, T., Pinay, G., Matheson, F., Haycock, N., Butturini, A., Clement, J., Danielescu, S., Dowrick, D., Hefting, M., Hillbricht-Ilkowska, A. and Maitre, V., 2002: Water table fluctuations in the riparian zone: comparative results from a pan-European experiment, *Journal of Hydrology*, 265, 129-148.

Butts, M.B., Overgaard, J., Viaene, P., Dubicki, A., Strońska, K., Szalinska, W., Lewandowski, A., Olszewski, T. and Kolerski, T., 2005: Flexible process-based hydrological modelling framework for flood forecasting - MIKE SHE, Proceedings of the International Conference, *Innovation, advances and implementation of flood forecasting technology*, Tromso, Norway, 17-19.

Buytaert, W., Iñiguez, V. and De Bièvre, B., 2007: The effects of afforestation and cultivation on water yield in the Andean Pa´ramo, *Forest Ecology and Management*, 251, 22-30.

Cabral, O.M.R., Rocha, H.R., Gash, J.H., Ligo, M.A.V., Tatsch, J.D., Freitas, H.C. and Brasilio, E., 2012: Water use in a sugarcane plantation, *Global Change Biology Bioenergy*, 4, 555-565.

Cai, G., Vanderborght, J., Langensiepen, M., Schnepf, A., Hűging, H. and Vereecken, H., 2017: Root growth, water uptake, and sap flow of winter wheat in response to different soil water conditions, *Hydrology and Earth Systems Sciences*, 22, 2449-2470.

Calder, I.R., 1990: *Evaporation in the uplands*, John Wiley and Sons Ltd., Chichester, UK, 40-75.

Calder, I. and Dye, P., 2001: Hydrological impacts of invasive alien plants, L*and Use and Water Resources Research*, 1, 1-12.

Calder, I.R., Rosier, P.T.W., Prasanna, K.T. and Parameswarappa, S., 1997: Eucalyptus water use greater than rainfall input – a possible explanation from southern India, *Hydrology and Earth System Sciences*, 1(2), 249-256.

Canadell, J., Jackson, R.B., Ehleringer, J.R., Mooney, H.A., Sala, O.E. and Schulze, E.D., 1996: Maximum rooting depth of vegetation types at the global scale, *Oecologia*, 108, 583-595.

Castagné, N., 2007: Physically-based modelling, in A. Luciani and C. Cadoz (eds.), *Enaction and enactive interfaces: A handbook of terms,* Enactive Systems Books, 237-238.

Cerdá, A., 1997: Seasonal changes of the infiltration rates in a Mediterranean scrubland on limestone, *Journal of Hydrology*, 198, 209-225.

Chamier, J., Schachtschneider, K., Le Maitre, D.C., Ashton, P.J. and van Wilgen, B.W., 2012: Impacts of invasive alien plants on water quality, with particular emphasis on South Africa, *Water SA*, 38(2), 345-356.

Chandler, R.E. and Scott, M., 2011: *Statistical methods for trend detection and analysis in the environmental sciences*, Wiley, Chichester, West Sussex, UK, 3-167.

Clark, D.J., Hughes, D.A., Smithers, J.C., Thornton-Dibb, S.L.C., Lutchminarain, A. and Forsyth, D.A., 2012: Deployment, maintenance, and further development of SPATSIM-HDSF: Volume 1, WRC Report no. 1870/1/12, Pretoria, South Africa.

Clinton, B.D., 2011: Stream water responses to timber harvest: Riparian buffer width effectiveness, *Forest Ecology and Management*, 261, 979-988.

Clulow, A.D., Everson, C.S. and Gish, M.B., 2011: The long-term impact of *Acacia mearnsii* trees on evaporation, streamflow and groundwater resources, WRC Report No. TT 505/11, Pretoria, South Africa.

Claassen, M., 2010: How much water do we have? in CSIR (ed.), *A CSIR perspective on water in South Africa*, CSIR Report No. CSIR/NRE/PW/IR/2011/0012/A, South Africa, 4-7.

Christiaens, K. and Feyen, J., 2001: Analysis of uncertainties associated with different methods to determine soil hydraulic properties and their propagation in the distributed hydrological MIKE SHE model, *Journal of Hydrology*, 246, 63-81.

Cook, A., 2012: Development of an integrated surface and subsurface model of the Everglades National Park, Florida International University, Paper 634.

Cuadra, S.V., Costa, M.H., Kucharik, C.J., de Rocha, H.R., Tatsch, J.D., Inman-Bamber, G., da Rocha, R.P., Leite, C.C. and Cabral, O.M.R., 2012: A biophysical model of sugarcane growth, *Global Change Biology Bioenergy*, 4, 36-48.

DAFF, 2012a: *State of the forests report: 2010-2012*, Report by the Department of Agriculture, Forestry and Fisheries, South Africa.

DAFF, 2012b: *Strategic plan for the Department of Agriculture, Forestry and Fisheries: 2012/13-2016/17*, Report by the Department of Agriculture, Forestry and Fisheries, South Africa.

Daniels, W.L. and Haering, K.C., 2006: Concepts of Basic Soil Science, in K.C. Haering and G.K. Evanylo (eds.), *The Mid-Atlantic Nutrient Management Handbook*, Mid-Atlantic Regional Water Program, Virginia Tech., 33-52.

da Silva, V.P.R., da Silva, B.B., Albuquerque, W.G., Borges, C.J.R., de Sousa, I.F. and Neto, J.D., 2013: Crop coefficient, water requirements, yield and water use efficiency of sugarcane growth in Brazil, *Agricultural Water Management*, 128, 102-109.

da Silva, V.P.R., Silva, M.T., Singh, V.P., de Souza, E.P., Braga, C.C., de Holanda, R.M., Almeida, R.S.R., de Sousa, F.A.S. and Braga, A.C.R., 2018: Simulation of stream flow and hydrological response to land-cover changes in a tropical river basin, *Catena*, 162, 166-176.

De Michele, C. and Salvadori, G., 2002: On the derived flood frequency distribution: Analytical formulation and the influence of antecedent soil moisture condition, *Journal of Hydrology*, 262, 245-258.

DeFries, R. and Eshleman, K.N., 2004: Land-use change and hydrologic processes: a major focus for the future, *Hydrological Processes*, 18, 2183-2186.

Demaria, E.M., Nijssen, B. and Wagner, T., 2007: Monte Carlo sensitivity analysis of land surface parameters using the Variable Infiltration Capacity model, *Journal of Geophysical Research*, 112, D11113, doi:10.1029/2006JD007534.

Demlie, M. and Titus, R., 2015: Hydrogeological and hydrogeochemical characteristics of the Natal Group Sandstone, South Africa, *South African Journal of Geology*, 118 (1), 33-44.

De Roo, A.P.J., 1996: Soil erosion in assessment using GIS, *Geographical Information Systems in Hydrology*, 26, 339-356.

Devi, G.K., Ganasri, B.P. and Dwarakish, G.S., 2015: A review on hydrological models, *Aquatic Procedia*, 4, 1001-1007.

DHI software, 2012: *MIKE SHE user manual: Volume 1: User guide*, MIKE by DHI Edition 2012.

DHI, Unknown: Assessing soil erosion: Modelling catchment soil losses due to climate change, land use management and erosion control development, DHI solutions, https://www.dhigroup.com/-/media/shared%20content/dhi/flyers%20and%20pdf/solution%20flyers/assessing-soil-erosion-dhi-solution-flyer.pdf

Dovey, S.B. and du Toit, B., 2006: Calibration of LAI-2000 canopy analyser with leaf area index in a young eucalypt stand, *Trees*, 20(3), 273-277.

du Toit, B., 2008: Effects of site management on growth, biomass partitioning and light use efficiency in a young stand of Eucalyptus grandis in South Africa, *Forest Ecology and Management*, 255, 2324-2336.

du Toit, B. and Dovey, S.B., 2005: Effect of site management on leaf area, early biomass development, and stand growth efficiency of a *Eucalyptus grandis* plantation in South Africa, *Canadian Journal of Forest Research*, 35, 891-900.

du Toit, B., Smith, C.W., Little, K.M., Boreham, G. and Pallett, R.N., 2010: Intensive, site specific silviculture: Manipulating resource availability at establishment for improved stand productivity. A review of South African research, *Forest Ecology and Management*, 259, 1836-1845.

Dye, P., Moses, G., Vilakazi, P., Ndlela, R. and Royappen, M., 2001: Comparative water use of wattle thickets and indigenous plant communities at riparian sites in the Western Cape and KwaZulu-Natal, *Water SA*, 27(4), 529-538.

Dye, P.J. and Croke, B.F.W., 2003: Evaluation of streamflow predictions by the IHACRES rainfall-runoff model in two South African catchments, *Environmental Modelling and Software*, 18(8-9), 705-712.

Dye, P.J., Jacobs, S. and Drew, D., 2004: Verification of 3-PG growth and water-use predictions in twelve *Eucalyptus* plantation stands in Zululand, South Africa, *Forest Ecology and Management*, 193, 197-218.

Dye, P. and Jarmain, C., 2004: Water use by black wattle (*Acacia mearnsii*): implications for the link between removal of invading trees and catchment streamflow response, S*outh African Journal of Science*, 100, 40-44.

Dye, P. and Versfeld, D., 2007: Managing the hydrological impacts of South African plantation forests: an overview, *Forest Ecology and Management*, 251, 121-128.

Dye, P.J., Jarmain, C., le Maitre, D., Everson, C.S., Gush, M. and Clulow, A., 2008: Modeling vegetation water use for general application in different categories of vegetation, WRC Report No. 1319/1/08, Pretoria, South Africa.

Dye, P.J. and Weiersbye, I.M., 2010: *The Mine Woodlands Project in the Witwatersrand Basin gold fields of South Africa: Strategy and progres*s, Mine Water and Innovative Thinking, Sydney, Nova Scotia.

Dzikiti, S., Schachtschneider, K., Naiken, V., Gush, M.B. and Le Maitre, D.C., 2013: Comparison of water-use by alien invasive pine trees growing in riparian and non-riparian zones in the Western Cape Province, South Africa, *Forest Ecology and Management*, 293, 92-102.

Easton, Z.M., Fuka, D.R., White, E.D., Collick, A.S., Biruk Ashagre, B., McCartney, M., Awulachew, S.B., Ahmed, A.A. and Steenhuis, T.S., 2010: A multi basin SWAT model analysis of runoff and sedimentation in the Blue Nile, Ethiopia, *Hydrology and Earth System Sciences*, 14, 1827-1841.

Eggert, B., Berg, P., Haerter, J.O., Jacob, D. and Moseley, C., 2015: Temporal and spatial scaling impacts on extreme precipitation, *Atmospheric, Chemistry and Physics*, 15, 5957-5971.

El-Nasr, A.A., Arnold, J.G., Feyen, J. and Berlamont, J., 2005: Modelling the hydrology of a catchment using a distributed and a semi-distributed model, *Hydrological Processes*, 19(3), 573-587.

Elvidge, C, D. and Chen, Z., 1995: Comparison of broad-band and narrow-band red and near-infrared vegetation indices, *Remote Sensing of Environment*, 54(1), 38-48.

Everson, C.S., Gush, M., Moodley, M., Jarmain, C., Govender, M. and Dye, P., 2006: Can effective management of the riparian zone vegetation significantly reduce the cost of catchment management and enable greater productivity of land resources, WRC Report No. K5/1284, CSIR, Pretoria, South Africa.

Everson, C.S., Dye, P.J., Gush, M.B. and Everson, T.M., 2011: Water use of grasslands, agroforestry systems and indigenous forests, *Water SA*, 37(5), 781-788.

Everson, C.S., Clulow, A.D., Becker, M., Watson, A., Ngubo, C., Bulcock, H., Mengistu, M., Lorentz, S. and Demlie, M., 2014: The long term impact of *Acacia mearnsii* trees on evaporation, streamflow, low flows and ground water resources. Phase II: Understanding the controlling environmental variables and soil water processes over a full crop rotation, WRC Report No. 2022/1/13, Pretoria, South Africa.

Fan, J., Oestergaard, K.T., Guyot, A. and Lockington, D., 2014: Estimating groundwater recharge and evapotranspiration from water table fluctuations under three vegetation covers in a coastal sandy aquifer of subtropical Australia, *Journal of Hydrology*, 519, 1120-1129.

Farley, K.A., Jobbágy, E.G. and Jackson, R.B., 2005: Effects of afforestation on water yield: a global synthesis with implications for policy, *Global Change Biology*, 11, 1565-1576.

Feddes, R.A., Hoff, H., Bruen, M., Dawson, T., de Rosnay, R., Dirmeyer, P., Jackson, R.B., Kabat, P., Kleidon, A., Lilly, A. and Pitman, A.J., 2001: Modeling root water uptake in hydrological and climate models, *Bulletin of the American Meteorological Society*, 82(12), 2797-2810.

Fisher, J.R.B., Acosta, E.A., Dennedy-Frank, P.J., Kroeger, T. and Boucher, T.M., 2018: Impact of satellite imagery spatial resolution on land use classification accuracy and modeled water quality, *Remote Sensing in Ecology and Conservation*, 4(2), 137-149.

Fohrer, N., Haverkamp, S., Eckhardt, K. and Frede, H.G., 2001: Hydrologic response to land use changes on the catchment scale, *Physics and Chemistry of the Earth*, 26 (7-8), 577-582.

Forrester, D.I., Theiveyanathan, S., Collopy, J.J. and Marcar, N.E., 2011: Enhanced water use efficiency in a mixed *Eucalyptus globulus* and *Acacia mearnsii* plantation, *Forest Ecology and Management*, 259, 1761-1770.

Forsyth, G.G., Richardson, D.M., Brown, P.J. and van Wilgen, B.W., 2004: A rapid assessment of the invasive status of *Eucalyptus* species in two South African provinces, *South African Journal of Science*, 100, 75-77.

Gangodagamage, C., 2001: Hydrological modeling using remote sensing and GIS, *22nd Asian Conference on Remote Sensing*, 5-9 November 2001, Singapore.

Gassman, P. W., J. R. Williams, X. Wang, A. Saleh, E. Osei, L. M. Hauck, R. C. Izaurralde, and J. D. Flowers, 2010. The Agricultural Policy/Environmental eXtender (APEX) model: An emerging tool for landscape and watershed environmental analyses, *Transactions of the ASABE*, 53(3), 711-740.

Ghanbarian-Alavijeh, B., Liaghat, A., Guan-Hua, H. and van Genuchten, M.T.H., 2010: Estimation of the van Genuchten soil water retention properties from soil textural data, *Pedosphere*, 20(4), 456-465.

Ghasemi, A. and Zahediasl, S., 2012: Normality tests for statistical analysis: A guide for non-statisticians, *International Journal of Endocrinology and Metabolism*, 10(2), 486-489.

Glen, H. And van Wyk, B., 2016: *Guide to trees introduced into Southern Africa*, Struik Nature, Cape Town, South Africa, 210-426.

Golmohammadi, G., Prasher, S., Madani, A. and Rudra, R., 2014: Evaluating three hydrological distributed watershed models: MIKE-SHE, APEX, SWAT, *Hydrology*, 1(1), 20-39, doi:10.3390/hydrology1010020.

Gong, L., Xu, C., Chen, D., Halldin, S. and Chen, Y.D., 2006: Sensitivity of the Penman–Monteith reference evapotranspiration to key climatic variables in the Changjiang (Yangtze River) basin, *Journal of Hydrology*, 329, 620-629.

Gordon, N.D., McMahon, T.A., Finlayson, B.L., Gippel, C.J. and Nathan, R.J., 2004: *Stream Hydrology: An Introduction for ecologists*, John Wiley and Sons Ltd, Chichester, UK, 49-74.

Görgens, A.H.M. and van Wilgen, B.W., 2004: Invasive alien plants and water resources in South Africa: current understanding, predictive ability and research challenges, *South African Journal of Science*, 100, 27-33.

Govender, M. and Everson, C.S., 2005: Modelling streamflow from two small South African experimental catchments using the SWAT model, *Hydrological Processes*, 19, 683-692.

Graham, D.N. and Butts, M.B., 2005: Flexible, integrated watershed modelling with MIKE SHE, in V.P. Singh and D.K. Frevert (eds.), *Watershed Models*, CRC Press, Florida, USA, 245-272.

Grant, J.C., Nichols, J.D., Yao, R.L., Smith, R.G., Brennan, P.D. and Vanclay, J.K., 2012: Depth distribution of roots of *E. dunnii* and *Corymbia citriodora* subsp. *variegata* in different soil conditions, *Forest Ecology and Management*, 269, 249-258.

Gush, M.B., Scott, D.F., Jewitt, G.P.W., Schulze, R.E., Lumsden, T.G., Hallowes, L.A. and Görgens, A.H.M., 2002: Estimation of streamflow reductions resulting from commercial afforestation in South Africa, WRC Report No. TT173/02, Pretoria, South Africa.

Gwate, O., Mantel, S.K., Palmer, A.R., Gibson, L.A., Munch, Z., 2018: Measuring and modelling evapotranspiration in a South African grassland: Comparison of two improved Penman-Monteith formulations, *Water SA*, 44, 482-494.

Gyamfi, C., Ndambuki, J.M. and Ramadhan, W.S., 2016: Hydrological responses to land use/cover changes in the Olifants Basin, South Africa, *Water*, 8, 588-604.

Harlow, J., 2018: *Assessing spatial and temporal patterns of groundwater recharge on Catalina Island, California, from soil water balance modelling*, Masters in Science (MSc) dissertation, California State University, Long Beach.

Hagemann, S., Arpe, K. and Roeckner, E., 2006: Evaluation of the hydrological cycle in the ECHAM5 model, *Journal of Climate*, 19, 3810-3827.

Hartemink, A.E., 2005: Plantation agriculture in the tropics: environmental issues, *Outlook on Agriculture*, 34(1), 11-21.

Hasenmueller, E.A. and Criss, R.E., 2013: Water balance estimates of evapotranspiration rates in areas with varying land use, in S.G. Alexandris (ed.), *Evapotranspiration - An overview*, Intech, 1-21.

Hendriks, M.R., 2010: *Introduction to physical hydrology*, Oxford University Press, Oxford, UK, 1-276.

Hillel, D., 2008: Soil-water dynamics, *Soil in the Environment*, 91-101, https://doi.org/10.1016/B978-0-12-348536-6.50012-5.

Hörmann, K. and Floater, M.S., 2006: Mean value coordinates for arbitrary planar polygons, *ACM Transactions on Graphics*, 25(4), 1424-1441.

Hughes, D.A., 2002: The development of an information modelling system for regional water resource assessments, Proceedings from the 4th International FRIEND Conference, IAHS Puplication 274, 43-49.

Hughes, D.A., 2005: SPATSIM, an integrating framework for ecological Reserve determination and implementation, WRC Report no. 245/04, Pretoria, South Africa.

Hughes, J.D. and Liu, J., 2008: MIKE SHE: Software for integrated surface water/ground water modeling, *Groundwater*, 46(6), 797-802.

Im, S., Kim, H., Kim, C. and Jang, C., 2009: Assessing the impacts of land use changes on watershed hydrology using MIKE SHE, *Environmental Geology*, 57, 231-239.

Inman-Bamber, N.G. and Smith, D.M., 2005: Water relations in sugarcane and response to water deficits, *Field Crops Research*, 92, 185-202.

Isik, S., Kalin, L., Schoonover, J.E., Srivastava, P. and Lockaby, B.G., 2013: Modeling effects of changing land use/cover on daily streamflow: an Artificial Neural Network and curve number based hybrid approach, *Journal of Hydrology*, 485, 103-112.

Jacobson, M.G., 2003: Wood versus water: Timber plantations in semiarid South Africa, *Journal of Forestry*, 101(5), 31-35.

James, A.L. and Roulet, N.T., 2009: Antecedent moisture conditions and catchment morphology as controls on spatial patterns of runoff generation in small forest catchments, *Journal of Hydrology*, 377, 351-366.

Jencso, K.G., McGlynn, B.L., Gooseff, M.N., Wondzell, S.M., Bencala, K.E. and Marshall, L.A., 2009: Hydrologic connectivity between landscapes and streams: transferring reach- and plot-scale understanding to the catchment scale, *Water Resources Research*, 45, W04428, doi:10.1029/2008WR007225.

Jewitt, G.P.W. and Schulze, R.E., 1999: Verification of the ACRU model for forest hydrology applications. *Water SA, 25*(4), 483-489.

Jewitt, G.P.W., Lorentz, S.A., Gush, M.B., Thornton-Dibb, S., Kongo, V., Wiles, L., Blight, J., Stuart-Hill, S.I., Versfeld, D. and Tomlinson, K., 2009: Methods and guidelines for the licensing of SFRAs with particular reference to low flows, WRC Report no. 1428/1/09, Pretoria, South Africa.

Johnston, H.T., Elsawy, E.M. and Cochrane, S.R., 1980: A study of the infiltration characteristics of undisturbed soil under simulated rainfall, *Earth Surface Processes*, 5, 159-174.

Jonckheere, I., Fleck, S., Nackaerts, K., Muysa, B., Coppin, P., Weiss, M. and Baret, F., 2004: Review of methods for *in situ* leaf area index determination Part I. Theories, sensors and hemispherical photography, *Agricultural and Forest Meteorology*, 121, 19-35.

Jorrat, M.D.M., Araujo, P.Z. and Mele, F.D., 2018: Sugarcane water footprint in the province of Tucumán, Argentina. Comparison between different management practices, *Journal of Cleaner Production*, 188, 521-529.

Jovanovic, N., Mu, Q., Bugan, R.D.H., Zhao, M., 2015: Dynamics of MODIS evapotranspiration in South Africa, *Water SA*, 41(1), 79-90.

Jyrkama, M.I. and Sykes, J.F., 2007: The impact of climate change on spatially varying groundwater recharge in the Grand River watershed (Ontario), *Journal of Hydrology*, 338, 237-250.

Kakembo, V., Rowntree, K. and Palmer, A.R., 2007: Topographic controls on the invasion of *Pteronia incana* (Blue bush) onto hill-slopes in Ngqushwa (formerly Peddie) District, Eastern Cape, *Catena*, 70, 185–199.

Khalil, R., 2017: Determination of potential runoff coefficient using GIS and remote sensing, *Journal of Geographic Information System*, 9, 752-762.

Kimber, P.C., 1974: The root system of Jarrah (*Eucalyptus marginata*), Research Paper No. 10, Forests Department of Western Australia, Perth, Australia.

King, J., Mitchell, S. and Pienaar, H., 2011: Water supply and demand, in King, J. and Pienaar, H. (eds.) *Sustainable use of South Africa's inland waters: A situation assessment of resource directed measures 12 years after the 1998 National Water Act*, WRC Report No. TT 491/11, Pretoria, South Africa, 1-16.

Kirkham, M. B., 2005: *Principles of Soil and Plant Water Relations*, Elsevier Academic Press, Burlington, 101–115.

Klamerus-Iwan, A., 2014: Different views on tree interception process and its determinants, *Forest Research Papers*, 75(3), 291-300.

Kok, TS, 1976. Die geohidrologie van die Bloemendalbasboompiaas, distrik Pietermantzburg, Natal. Internal report GH.2924, of the Geohydrology Directorate of the Department of Water Affairs and Forestry, South Africa.

Kozak, J.A., Ahuja, L.R., Green, T.R. and Ma, L., 2007: Modelling crop canopy and residue rainfall interception effects on soil hydrological components for semi-arid agriculture, *Hydrological Processes*, 21, 229-241.

Krishnaswamy, J., Bonell, M., Venkatesh, B., Purandara, B.K., Rakesh, K.N., Lele, S., Kiran, M.C., Reddy, V. and Badiger, S., 2013: The groundwater recharge response and hydrologic services of tropical humid forest ecosystems to use and reforestation: support for the "infiltration evapotranspiration trade-off" hypothesis, *Journal of Hydrology*, 498, 191-209.

Kristensen, K.J. and Jensen, S.E., 1975: A model for estimating actual evapotranspiration from potential evapotranspiration, *Nordic Hydrology*, 6, 170-188.

Kruger, F., Crafford, J. and Ginsburg, A., 2008: The regulation of water-use impacts of forestry in South Africa: Appraisal of the development of policy and governance, Workshop on Forest Governance and Decentralization in Africa, 8-11 April 2008, Durban, South Africa.

Kruger, F.J. and Bennett, B.M., 2013: Wood and water: An historical assessment of South Africa's past and present forestry policies as they relate to water conservation, *Transactions of the Royal Society of South Africa*, 68(3), 163-174.

Kuenene, B., 2013: *Hillslope hydropedology of the Two Streams catchment in KwaZulu-Natal*, Doctor of Philosophy (PhD) dissertation, University of the Free State, Bloemfontein.

Laclau, J.P., Bouillet, J.P., Goncalves, J.L.M., Silva, E.V., Jourdan, C., Cunha, M.C.S. and Moreira, M.R., 2008: Mixed-species plantations of *Acacia mangium* and *Eucalyptus grandis* in Brazil: Growth dynamics and aboveground net primary production, *Forest Ecology and Management*, 255, 3905-3917.

LAI-2000 Plant Canopy Analyser, 1989: *LAI-2000 Technical Information*, LICOR Inc., Lincoln, Nebraska, USA.

LAI-2200 Pant Canopy Analyser, 2012: *LAI-2200 Plant Canopy Analyser Instruction manual*, LICOR Inc., Lincoln, Nebraska, USA.

Lambin, E.F., Turner, B.L., Geisy, H.J., Agbola, S.B., Angelsen, A., Bruce, J.W., Coomes, O.T., Dirzo, R., Fischer, G., Folke, C., George, P.S., Homewood, K., Imbernon, J., Leemans, R., Li, X., Moran, E.F., Mortimore, M., R, P.S., Richards, J.F., Skanes, H., Steffen, W., Stone, G.D., Svedin, U., Veldkamp, T.A., Vogel, C. and Xu, J., 2001: The causes of land-use and land-cover change: moving beyond the myths, *Global Environmental Change*, 11, 261-269.

Lambin, E.F., Geist, H.J. and Lepers, E., 2003: Dynamics of land-use and land-cover change in tropical regions, *Annual Review of Environment and Resources*, 28, 205-241.

Lane, S.A. and Richards, K.S., 2001: The 'validation' of hydrodynamic models: Some critical perspectives, in: M.G. Anderson and P.D. Bates (eds.), *Model validation perspectives in hydrological science*, John Wiley and Sons, Ltd, Chichester, UK, 413-438.

Lawrence, D.M., Thornton, P.E., Oleson, K.W. and Bonan, G.B., 2005: The partitioning of evapotranspiration into transpiration, soil evaporation, and canopy evaporation in a GCM: Impacts on land–atmosphere interaction, *Journal of Hydrometeorology*, 8, 862-880.

Le Maire, G., Marsden, C., Verhoef, W., Ponzoni, F.J., Lo Seen, D., Begue, A., Stape, J. and Nouvellon, Y., 2011: Leaf area index estimation with MODIS reflectance time series and model inversion during full rotations of Eucalyptus plantations, *Remote Sensing of Environment*, 115, 589-599.

Le Maitre, D.C., Versfeld, D.B. and Chapman, R.A., 2000: The impact of invading alien plants on surface water resources in South Africa: A preliminary assessment, *Water SA*, 26(3), 397-408.

Le Maitre, D.C., van Wilgen, B.W., Gelderblom, C.M., Bailey, C., Chapman, R.A. and Nel, J.A., 2002: Invasive alien trees and water resources in South Africa: Case studies of the costs and benefits of management, *Forest Ecology and Management*, 160, 143-159.

Le Maitre, D.C., Forsyth, G.G., Dzikiti, S. and Gush, M.B., 2016: Estimates of the impacts of invasive alien plants on water flows in South Africa, *Water SA*, 42(4), 659-671.

Le Roux, J.J., Newby T.S. and Sumner, P.D., 2007: Monitoring soil erosion in South Africa at a regional scale: review and recommendations, *South African Journal of Science*, 103, 329-335.

Le Roux, J.J., 2012: *Water erosion risk assessment in South Africa: towards a methodological framework*, Doctor of Philosophy (PhD) dissertation, University of Pretoria, Pretoria.

Leij, F. J., Alves, W. J., van Genuchten, M. T. and Williams, J. R., 1996: The UNSODA unsaturated soil hydraulic database, user's manual version 1.0. EPA Report No. EPA/600R-96/095, National Risk Management Laboratory, Office of Research and Development, Cincinnati, Ohio.

Legesse, D., Vallet-Coulomb, C. and Gasse, F., 2003: Hydrological response of a catchment to climate and land use changes in Tropical Africa: case study South Central Ethiopia, *Journal of Hydrology*, 275, 67-85.

Licata, J.A., Gyenga, J.E., Fernandez, M.E., Schlichter, T.M. and Bond, B.J., 2007: Increased water use by ponderosa pine plantations in northwestern Patagonia, Argentina compared with native forest vegetation, *Forest Ecology and Management*, 255(3-4), 753-764.

Lindström, G., Johansson, B., Persson, Gardelin, M. and Bergström, S, 1997: Development and test of the distributed HBV-96 hydrological model, *Journal of Hydrology*, 201, 272-288.

Loucks, D.P. and van Beek, E., 2005: *Water resources systems planning and management: An introduction to methods, models and applications*, United Nations Educational, Scientific and Cultural Organization, Italy, 231-292.

Lin, H., Chen, J., Pei, Z., Zhang, S. and Hu, X., 2009: Monitoring sugarcane growth using ENVISAT ASAR data, *IEEE Transactions on Geoscience and Remote Sensing*, 47(8), 2572-2580.

Liu, Y., Xiao, J., Ju, W., Xu, K., Zhou, Y. and Zhao, Y., 2016: Recent trends in vegetation greenness in China significantly altered annual evapotranspiration and water yield, *Environmental Research Letters*, 11(9), 094010.

Ma, L., He, C., Bian, H. and Sheng, L., 2016: MIKE SHE modeling of ecohydrological processes: merits, applications, and challenges, *Ecological Engineering*, 96, 137-149.

McGuire, K.J., McDonnell, J.J., Weiler, M., Kendall, C. and McGlynn, B.L., 2005: The role of topography on catchment-scale water residence time, *Water Resources Research*, 41, W05002, doi:10.1029/2004WR00365.

Merritt, W.S., Letcher, R.A. and Jakeman, A.J., 2003: A review of erosion and sediment transport models, *Environmental Modelling and Software*, 18, 761-799.

Miao, C. and Ni, J., 2009: Variation of natural streamflow since 1470 in the middle Yellow River, China, *International Journal of Environmental Research and Public Health*, 6, 2849-2864.

Miller, S.N., Kepner, W.G., Mehaffey, M.H., Hernandez, M., Miller, R.C., Goodrich, D.C., Devonald, K.K., Heggem, D.T. and Miller, W.P., 2002: Integrating landscape assessment and hydrologic modelling for land cover change analysis, *Journal of the American Water Resources Association*, 38(4), 915-929.

Mimikou, M.A., Baltas, E.A. and Tsihrintzis, V.A., 2016: *Hydrology and water resource systems analysis*, Taylor and Francis, UK, 223-266.

Moradkhani, H. and Sorooshian, S., 2008: General review of rainfall-runoff modeling: model calibration, data assimilation, and uncertainty analysis, in S. Sorooshian, K. Hsu, E. Coppola, B. Tomassetti, M. Verdecchia, and G. Visconti (eds.), *Hydrological modelling and the water cycle: Coupling the atmospheric and hydrological models*, Springer, New York City, United State, 1-26.

Morbidelli, R., Saltalippi, C., Flammini, A. and Govindaraju, R.S., 2018: Role of slope on infiltration: A review, *Journal of Hydrology*, 557, 878-886.

Morgan, R.P.C., 2005: *Soil erosion and conservation*, 3rd edition, Blackwell Publishing, Oxford, UK, 45-66.

Mu, W., Yu, F., Li, C., Xie, Y., Tian, J., Liu, J and Zhao, N., 2015: Effects of rainfall intensity and slope gradient on runoff and soil moisture content on different growing stages of spring maize, *Water*, 7, 2990-3008.

Mucina, L. and Rutherford, M.C., 2006: *The vegetation of South Africa, Lesotho and Swaziland*, South African National Biodiversity Institute (SANBI), Pretoria, 348-437.

Mugabe, F.T., Chitata, T., Kashaigili, J., Chagonda, I., 2011: Modelling the effect of rainfall variability, land use change and increased reservoir abstraction on surface water resources in semi-arid southern Zimbabwe, *Physics and Chemistry of the Earth Journal*, 36(14-15), 1025-1032.

Music, B. and Caya, D., 2007: Evaluation of the hydrological cycle over the Mississippi River basin as simulated by the Canadian Regional Climate Model (CRCM), *Journal of Hydrometeorology*, 8, 969-988.

Muzylo, A., Llorens, P., Valente, F., Keizer, J.J., Domingo, F. and Gash, J.H.C., 2009: A review of rainfall interception modelling: *Journal of Hydrology*, 370, 191-206.

Nijssen, B., Schnur, R. and Lettenmaier, D.P., 2001: Global retrospective estimation of soil moisture using the Variable Infiltration Capacity land surface model, 1980-93, *Journal of Climate*, 14, 1790-1808.

Oeurng, C., Sauvage, S., Sánchez-Pérez, J., 2010: Assessment of hydrology, sediment and particulate organic carbon yield in a large agricultural catchment using the SWAT model, *Earth Surface Processes and Landforms*, 35, 1289-1301.

Ojima, D.S., Galvin, K.A. and Turner, B.L., 1994: The global impact of land-use change: To understand global change, natural scientists must consider the social context influencing human impact on environment, *Bioscience*, 44, 300-304.

Oyebode, O.K., 2014: Modelling streamflow response to hydro-climate variables in the upper Mkomazi River, South Africa, Master of Technology: Civil Engineering, Durban University of Technology, South Africa.

Payn, T., Carnus, J.M., Freer-Smith, P., Kimberley, M., Kollert, W., Liu, S., Orazio, C., Rodriguez, L., Silva, L.N. and Wingfield, M.J., 2015: Changes in planted forests and future global implications, *Forest Ecology and Management*, 352, 57-67.

Pimentel, D., 2006: Soil erosion: A food and environmental threat, *Environment, Development and Sustainability*, 8, 119-137.

Pohl, B., Macron, C. and Monerie, P.A., 2017: Fewer rainy days and more extreme rainfall by the end of the century in Southern Africa, *Scientific Reports*, 7, 46466.

Prucha, B., Graham, D., Watson, M., Avenant, M., Esterhuyse, S., Joubert, A., Kemp, M., King, J., le Roux, P., Redelinghuys, N., Rossouw, L., Rowntree, K., Seaman, M., Sokolic, F., van Rensburg, L., van der Waal, B., van Tol, J. and Vos, T., 2016: MIKE-SHE integrated groundwater and surface water model used to simulate scenario hydrology for input to DRIFT-ARID: the Mokolo River case study, *Water SA*, 42(3), 384-398.

Rajmánek, M. and Richardson, D.M., 2011: Eucalypts, in D. Simberloff, and M. Rajmánek (eds.), *Encyclopedia of Biological Invasions*, University of California Press, Berkeley and Los Angeles, 203-209.

Rangan, H., Kull, C.A. and Alexander, L., 2010: Forest plantations, water availability, and regional climate change: Controversies surrounding *Acacia mearnsii* plantations in the upper Palnis Hills, southern India, *Regional Environmental Change*, 10, 103-117.

Rangecroft, S., Birkinshaw, S., Rohse, M., Day, R., McEwen, L., Makaya, E. and van Loom, A.F., 2018: Hydrological modelling as a tool for interdisciplinary workshops on future drought, *Progress in Physical Geography*, 42(2), 237-256.

Raz-Yaseef, N., Rotenberg, E. and Yakir, D., 2010: Effects of spatial variations in soil evaporation caused by tree shading on water flux partitioning in a semi-arid pine forest, *Agricultural and Forest Meteorology*, 150, 454-462.

Raz-Yaseef, N., Yakir, D., Schiller, G. and Cohen, S., 2012: Dynamics of evapotranspiration partitioning in a semi-arid forest as affected by temporal rainfall patterns, *Agricultural and Forest Meteorology*, 157, 77-85.

Reichardt, K., Dourado-Neto, D., Schwantes, A.P. and Timm, L.C., 2013: Soil water storage as related to water balances, International Centre for Theoretical Physics Report 2444-17.

Renard, B., Kavetski, D., Kuczera, G., Thyer, M, and Franks, S.W., 2010: Understanding predictive uncertainty in hydrologic modeling: The challenge of identifying input and structural errors, *Water Resources Research*, 46, W05521, doi:10.1029/2009WR008328.

Richardson, J.S., Naiman, R.J. and Bisson, P.A., 2012: How did fixed-width buffers become standard practice for protecting freshwaters and their riparian areas from forest harvest practices? *Freshwater Science*, 31(1), 232-238.

Rosenquist, L., Hansen, K., Vesterdal, L. and van der Salm, C., 2010: Water balance in afforestation chronosequences of common oak and Norway spruce on former arable land in Denmark and southern Sweden, *Agriculture and Forest Meteorology*, 150, 196-207.

Sahin, V. and Hall, M.J., 1996: The effects of afforestation and deforestation on water yields, *Journal of Hydrology*, 178, 293-309.

Savenije, H.H.G., 2004: The importance of interception and why we should delete the term evapotranspiration from our vocabulary, *Hydrological Processes*, 18, 1507-1511.

Saxton, K.E. and Rawls, W.J., 2006: Soil water characteristic estimates by texture and organic matter for hydrologic solutions, *Soil Science Society of America Journal*, 70, 1569-1578.

Scheepers, H., Wang, J., Gan, T.Y. and Kuo, C.C., 2018: The impact of climate change on inland waterway transport: Effects of low water levels on the Mackenzie River, *Journal of Hydrology*, 566, 285-298.

Scholl, M., Eugster, W. and Burkard, R., 2010: Understanding the role of fog in forest hydrology: stable isotopes as tools for determining input and partitioning of cloud water in montane forests, *Hydrological Processes*, 25, 353-366.

Schulze, E.D., Mooney, H.A., Sala, O.E., Jobbagy, E., Buchmann, N., Bauer, G., Canadell, J., Jackson, R.B., Loreti, J., Oesterheld, M. and Ehleringer, J.R., 1996: Rooting depth, water

availability, and vegetation cover along an aridity gradient in Patagonia, *Oecologia*, 108, 503-511.

Schulze, R.E., 1995: Hydrology and agrohydrology: A text to accompany the ACRU 3.00 agrohydrological modelling system, WRC Report no. TT69/95, Pretoria, South Africa.

Scott, D.F. and Lesch, W., 1997: Streamflow responses to afforestation with Eucalyptus grandis and Pinus patula and to felling in the Mokobulaan experimental catchments, South Africa, *Journal of Hydrology*, 199, 360-377.

Scott, D.F. and Smith, R.E., 1997: Preliminary empirical models to predict reductions in total and low flows resulting from afforestation, *Water SA*, 23, 135-140.

Scott, D.F. and Le Maitre, D.C., 1998: The interaction between vegetation and groundwater: Research prioirties for South Africa, WRC Report no. 730/1/98, Pretoria, South Africa.

Scott, D.F., Le Maitre, D.C. and Fairbanks, D.H.K., 1998: Forestry and streamflow reductions in South Africa: A reference system for assessing extent and distribution, *Water SA*, 24(3), 187-199.

Scott, D.F., 1999: Managing riparian zone vegetation to sustain streamflow: Results of paired catchment experiments in South Africa, *Canadian Journal of Forest Research*, 29(7), 1149-1157.

Scott, D.F., Prinsloo, F.W., Moses, G., Mehlomakulu, M. and Simmers, A.D.A., 2000: A re-analysis of the South African catchment afforestation experimental data, WRC Report no. 810/1/00, Pretoria, South Africa.

Scott, D.F. and Gush, M.B., 2017: Forest management and water in the Republic of South Africa, in P.A. Garcia Chevesich, D.G Neary, D.F. Scott, R.G. Benyon and T. Reyna (eds.), *Forest management and the impact on water resources: A review of 13 countries*, Paris: International Hydrological Programme (IHP) -VIII / Technical Document No. 37, UNESCO.

Şen, Z., 2015: Chapter 2 – Basic porous medium concepts, *Practical and Applied Hydrogeology*, 43-97, https://doi.org/10.1016/B978-0-12-800075-5.00002-9.

Shi, P., Yuan, Y., Zheng, J., Wang, J., Ge, Y. and Qiu, G., 2007: The effect of land use/cover change on surface runoff in Shenzhen region, China, *Catena*, 69(1), 31-35.

Silalertruksa, T. and Gheewala, S.H., 2018: Land-water-energy nexus of sugarcane production in Thailand, *Journal of Cleaner Production*, 182, 521-528.

Silveira, L., Gamazo, P., Alonso, J. and Martínez, L., 2016: Effects of afforestation on groundwater recharge and water budgets in the western region of Uruguay, *Hydrological Processes*, 30, 3596-3608.

Singh, S.K., Ibbitt, R., Srinivasan, M.S. and Shankar, U., 2017: Inter-comparison of experimental catchment data and hydrological modelling, *Journal of Hydrology*, 550, 1-11.

Siriwardena, L., Finlayson, B.L. and McMahon, T.A., 2006: The impact of land use change on catchment hydrology in large catchments: The Comet River, Central Queensland, Australia, *Journal of Hydrology*, 326, 199-214.

Sivapalan, M., Viney, N.R. and Zammit, C., 2002: LASCAM: Large Scale Catchment Model, in: V.P., Singh and D.K., Frevert, *Mathematical models of large watershed hydrology*, Water Resources Publication, Colorado, USA, 577- 648.

Smithen, A.A. and Schulze, R.E., 1982: The spatial distribution in Southern Africa of rainfall erosivity for use in the Universal Soil Loss Equation, *Water SA*, 8, 74-78.

Smithers, J. and Schulze, R., 1995: ACRU Agrohydrological Modelling System, User Manual Version 3.00, WRC Report no. TT70/95, Pretoria, South Africa.

Snyman, H.A., 1999: Soil erosion and conservation, in N.M. Tainton (ed.), *Veld management in South Africa*, University of Natal Press, Pietermaritzburg, 355-380.

Soil Survey Division Staff, 1993: *Soil survey manual*, United States Department of Agriculture Handbook No. 18, Washington, USA.

Sonnenborg, T.O., Christiansen, J.R., Pand, B., Bruge, A., Stisen, S. and Gundersen, P., 2017: Analyzing the hydrological impact of afforestation and tree species in two catchments with contrasting soil properties using the spatially distributed model MIKE SHE SWET, *Agricultural and Forest Meteorology*, 239, 118-133.

Stockle, C.O., James, L.G., Bassett, D.L. and Saxton, K.E., 1991: Effect of evapotranspiration underprediction on irrigation scheduling and yield of corn: a simulation study, *Agricultural Water Management*, 19, 167-179.

Strauss, S., 2001: Benefits and risks of biotic exchange between *Eucalyptus* plantations and native Australian forests, *Austral Ecology*, 26, 447–457.

Sui, D.Z. and Maggio, R.C., 1999: Integrating GIS with hydrological modeling: practices, problems, and prospects, *Computers, Environment and Urban Systems*, 23, 33-51.

Teutschbein, C. and Seibert, J., 2010: Regional climate models for hydrological impact studies at the catchment scale: a review of recent modeling strategies, *Geography Compass*, 4(7), 834-860.

Teutschbein, C. and Seibert, J., 2012: Bias correction of regional climate model simulations for hydrological climate-change impact studies: Review and evaluation of different methods, *Journal of Hydrology*, 456-457, 12-29.

Tewari, D.D., 2009: A detailed analysis of evolution of water rights in South Africa: An account of three and a half centuries from 1652 AD to present, *Water SA*, 35(5), 693-710.

Thornthwaite, C.W. and Mather, J.R., 1957: Instructions and tables for computing potential evapotranspiration and the water balance, *Publications in Climatology*, 10(3), 185-311.

Toohey, R.C., Boll, J., Brooks, E.S. and Jones, J.R., 2018: Effects of land use on soil properties and hydrological processes at the point, plot, and catchment scale in volcanic soils near Turrialba, Costa Rica, *Geoderma*, 315, 138-148.

Trenberth, K.E., Dai, A., Rasmussen, R.M. and Parsons, D.B., 2003: The changing character of precipitation, *Bulletin of the American Meteorological Society*, 84, 1205-1217.

Trenberth, K.E., Smith, L., Qian, T., Dai, A. and Fasullo, J., 2006: Estimates of the global water budget and Its annual cycle using observational and model data, *Journal of Hydrometeorology*, 8, 758-769.

Troch, P.A., Martinez, G.F., Pauwels, V.R.N., Durcik, M., Sivapalan, M., Harman, C., Brooks, P.D., Gupta, H. and Huxman, T., 2009: Climate and vegetation water use efficiency at catchment scales, *Hydrological Processes*, 23, 2409-2414.

Turner, B.L., Meyer, W.B. and Skole, D.L., 1994: Global land-use/land-cover change: Towards an integrated study, *Royal Swedish Academy of Sciences*, 23(1), 91-95.

van Breda Weaver, A., 1991: The distribution of soil erosion as a function of slope aspect and parent material in Ciskei, Southern Africa, *GeoJournal*, 23(1), 29-34.

van der Walt, I.J., Struwig, A. and van Rensburg, J.R.J., 2004: Forestry as a streamflow reduction activity in South Africa: Discussion and evaluation of the proposed procedure for the assessment of afforestation permit applications in terms of water sustainability, *GeoJournal*, 61, 173-181.

van Dijk, A.I.J.M. and Keenan, R.J., 2008: Planted forests and water in perspective, *Forest Ecology and Management*, 251(1-2), 1-9.

van Genuchten, M.T., 1980: A closed-form equation predicting the hydraulic conductivity of unsaturated soils, *Soil Science Society of America Journal*, 44, 892-898.

van Wilgen, B.W., Richardson, D.M., Le Maitre, D.C., Marais, C. and Magadlela, D., 2001: The economic consequences of alien plant invasions: Examples of impacts and approaches to sustainable management in South Africa, *Environment, Development and Sustainability*, 3, 145-168.

van Wilgen, B.W., Forsyth, G.G., Le Maitre, D.C., Wannenburgh, A., Kotzé, J.D.F., van den Bergh, E. and Henderson, L., 2012. An assessment of the effectiveness of a large national-scale invasive alien plant control strategy in South Africa. *Biological Conservation*, 148, 28-38.

Van Wilgen, B.W., 2015: Plantation forestry and invasive pines in the Cape Floristic Region: Towards conflict resolution, *South African Journal of Science*, 111(7-8), 1-2.

Van Wyk, D.B., 1987: Some effects of afforestation on streamflow in the Western Cape Province, South Africa, *Water SA*, 13, 31-36.

van Wyk, E., van Tonder, G.J. and Vermeulen, D., 2012: Characteristics of local groundwater recharge cycles in South African semi-arid hard rock terrains: Rainfall–groundwater interaction, *Water SA*, 38(5), 747-754.

Vanclay, J.K., 2009: Managing water use from forest plantations, *Forest Ecology and Management*, 257, 385-389.

Versfeld, D.B., Le Maitre, D.C. and Chapman, R.A., 1998: Alien Invading Plants and Water Resources in South Africa: A preliminary assessment, WRC Report No. TT 99/98, Pretoria, South Africa.

Vertessy, R.A., 2001: Impacts of plantation forestry on catchment runoff, in E.K.S., Nambiar and A.G. Brown (eds.), *Plantations, farm forestry and water: Proceedings of a National Workshop, Melbourne, 21-22 July*, 2000, RIRDC Report No. 01.20, Rural Industries Research Development Corporation Report, Canberra, 9-19.

Vertessy, R.A., Zhang, L. and Dawes, W.R., 2003: Plantations, river flows and river salinity, *Australian Forestry*, 66(1), 55-61.

Vogel, R.M., Lall, U., Cai, X., Rajagopalan, B., Weiskel, P.K., Hooper, R.P. and Matalas, N.C., 2015: Hydrology: The interdisciplinary science of water, *Water Resources Research*, 51, 4409-4430.

Wallach, R., Grigorin, G. and Rivlin, J., 1997: The errors in surface runoff prediction by neglecting the relationship between infiltration rate and overland flow depth, *Journal of Hydrology*, 200, 243-259.

Warburton, M.L., Schulze, R.E. and Jewitt, G.P.W., 2012: Hydrological impacts of land use change in three diverse South African catchments, *Journal of Hydrology*, 414-415, 118-135.

Wang, X., Williams, J.R., Gassman, P.W., Baffaut, C., Izaurralde, R.C., Jeong, J. and Kiniry, J.R., 2012: EPIC and APEX: Model use, calibration and validation, *American Society of Agricultural and Biological Engineers*, 55(4), 1447-1462.

Westerhoff, R.S., 2015: Using uncertainty of Penman and Penman–Monteith methods in combined satellite and ground-based evapotranspiration estimates, *Remote Sensing of Environment*, 169, 102-112.

Wicks, J.M. and Bathurst, J.C., 1996: SHESED: a physically based, distributed erosion and sediment yield component for the SHE hydrological modelling system, *Journal of Hydrology*, 175, 213-238.

Williams, D. G., Cable, W.L., Hultine, K.R., Hoedjes, J., Yepez, E., Simonneaux, V., Er-Raki, S., Boulet, G., de Bruin, H. and Chehbouni, A., 2004: Evapotranspiration components determined by stable isotope, sap flow and eddy covariance techniques. *Agricultural and Forest Meteorology*, 125, 241-258.

Williams, J.R., Izaurralde, R.C., Williams, C. and Steglich, E.M., 2015: *Agricultural policy/environmental extender model: Theoretical documentation version 0806*, Agrilife Research, Texas.

Wösten, J.H.M. and van Genuchten, M.T.H., 1988: Using texture and other soil properties to predict the unsaturated soil hydraulic functions, *Soil Science Society of America Journal*, 52, 1762-1770.

WWF, IIASA, 2012: *Living Forests Report*, Gland, Switzerland.

Wyatt, C.J.W., O'Donnell, F.C. and Springer, A.E., 2015: Semi-arid aquifer responses to forest restoration treatments and climate change, *Groundwater*, 53, 207-216.

Xiang-Wei, H., Ming-An, S. and Horton, R., 2010: Estimating van Genuchten model parameters of undistributed soils using an integral method, *Pedosphere*, 20(1), 55-62.

Xu, C.Y. and Singh, V.P., 2004: Review on regional water resources assessment models under stationary and changing climate, *Water Resources Management* 18, 591-612.

Xu, Z.X., Ito, K., Schultz, G.A. and Li, J.Y., 2001: Integrated hydrologic modeling and GIS in water resources management, *Journal of Computing in Civil Engineering*, 15(3), 217-223.

Xu, Z.X., Pang, J.P., Liu, C.M. and Li, J.Y., 2009: Assessment of runoff and sediment yield in the Miyun Reservoir catchment by using SWAT model, *Hydrological Processes*, 23, 3619-3630.

Yates, S.R., van Genuchten, M.T. and Leij, F.J., 1989: Analysis of predicted hydraulic conductivities using RETC computer program, *Soil Science Society of America Journal*, 56, 347-354.

Yang, X. and You, X., 2013: Estimating parameters of Van Genuchten model for soil water retention curve by intelligent algorithms, *Applied Mathematics and Information Sciences*, 7(5), 1977-1983.

Yokoo, Y., Sivapalan, M. and Oki, T., 2008: Investigating the roles of climate seasonality and landscape characteristics on mean annual and monthly water balances, *Journal of Hydrology*, 357, 255-269.

Young, R.A., Onstad, C.A., Bosch, D.D. and Anderson, W.P., 1989: AGNPS: A nonpoint-source pollution model for evaluating agricultural watersheds. *Journal of Soil and Water Conservation*, 44(2), 168-173.

Zaimes, G., Nichols, M. and Green, D., 2007: Characterization of riparian areas, in G. Zaimes (ed.), *Understanding Arizona's riparian areas*, University of Arizona Extension Pub, University of Arizona Extension, Tucson, 15-29.

Zhang, L., Dawes, W.R. and Walker, G.R., 1999: Predicting the effect of vegetation changes on catchment average water balance, Cooperative research centre for catchment hydrology, Technical Report 99/12.

Zhang, L., Dawes, R. and Walker, G.R., 2001: Response of mean annual evapotranspiration to vegetation changes at catchment scale, *Water Resources Research*, 37(3), 701-708.

Zhang, L., Nan, Z., Yu, W., Zhao, Y. and Xu, Yi., 2018: Comparison of baseline period choices for separating climate and land use/land cover change impacts on watershed hydrology using distributed hydrological models, *Science of the Total Environment*, 622–623, 1016-1028.

Zhang, M., Liu, N., Harper, R., Li, Q., Liu, K., Wei, X., Ning, D., Hou, Y. and Liu, S., 2017: A global review on hydrological responses to forest change across multiple spatial scales: Importance of scale, climate, forest type and hydrological regime, *Journal of Hydrology*, 546, 44-59.

Zhang, Z., Wang, S., Sun, G., McNulty, S.G., Zhang, H., Li, J., Zhang, M., Klaghofer, E. and Strauss, P., 2008: Evaluation of the MIKE SHE model for application in the Loess Plateau, China, *Journal of the American Water Resources Association*, 44(5), 1108-1120.

Zhao, F., Zhang, L., Chiew, F.H.S., Vase, J. and Cheng, L., 2013: The effect of spatial rainfall variability on water balance modelling for south-eastern Australian catchments, *Journal of Hydrology*, 493, 16-29.

Zhu, Y., Ren, L., Horton, R., Lű, H., Wang, Z. and Yuan, F., 2018: Estimating the contribution of groundwater to the root zone of winter wheat using root density distribution functions, *Vadose Zone Journal*, doi:10.2136/vzj2017.04.0075.

Zotarelli, L., Dukes, M.D., Romero, C.C., Migliaccio, K.W. and Morgan, K.T., 2015: Step by step calculation of the Penman-Monteith evapotranspiration (FAO-56 method), Agricultural and Biological Engineering Department, Uf/IFAS Extension, University of Florida.

Zou, L., Zhan, C., Xia, J., Wang, T. and Gippel, J., 2017: Implementation of evapotranspiration data assimilation with catchment scale distributed hydrological model via an ensemble Kalman Filter, *Journal of Hydrology* 549, 685-702.

Appendices

Appendix A: MIKE SHE scenario (current and future) set-ups

Table A.1: MIKE SHE input data for the simulation specification module.

Simulation Specification module				
Input field		**MIKE SHE initial current scenario**	**MIKE SHE calibrated current scenario**	**MIKE SHE future scenario**
Simulation title		Current Scenario Two Streams 2007 – 2016	Current Scenario Two Streams 2007 – 2016	Future scenario Two Streams 2019 – 2028
Simulation period		14th February 2007 - 2nd October 2016	14th February 2007 - 2nd October 2016	14th February 2019 - 2nd October 2028
Time step control	**Time Steps**			
	Initial time step	6 hrs	2 hrs	2 hrs
	Max allowed OL time step	0.5 hrs	6 hrs	6 hrs
	Max allowed UZ time step	2 hrs	6 hrs	6 hrs
	Max allowed SZ time step	24 hrs	24 hrs	24 hrs
	Increment of reduced time step length			
	Increment rate	0.05	0.05	0.05
	Parameters for precipitation-dependent time step control			
	Max precipitation depth per time step	10 mm	10 mm	10 mm
	Max infiltration amount per time step	10 mm	10 mm	10 mm
	Input precipitation rate requiring its own time step	0.1 mm/hr	0.1 mm/hr	0.1 mm/hr
OL Computational Control Parameters	**Solver type and solver specific parameters (Successive Overrelaxation (SOR))**			
	Maximum number of iterations	200	200	200
	Maximum head change per iteration	0.0001 m	0.0001 m	0.0001 m
	Maximum residual error	0.0001 m/d	0.0001 m/d	0.0001 m/d
	Under-relaxation factor	0.9	0.9	0.9
	Common stability parameters			
	Threshold water depth for overland flow	0.0001 m	0.0001 m	0.0001 m

	Threshold gradient for applying low-gradient flow reduction	0.0001	0.0001	0.0001
	Overland-river exchange calculation			
		Manning equation (using OL flow Manning numbers)	Manning equation (using OL flow Manning numbers)	Manning equation (using OL flow Manning numbers)
UZ Computational Control Parameters	**UZ-SZ Coupling Control**			
	Max profile water balance error	0.001 m	0.001 m	0.001 m
	Richards equation parameters (Iteration Control)			
	Maximum number of iterations	50	50	50
	Iteration stop criteria (fraction of Psi)	0.002	0.002	0.002
	Richards equation parameters (Timestep Reduction Control (UZ Restart))			
	Max. Water balance error in one node (fraction)	0.03	0.03	0.03
SZ Computational Control Parameters	**Solver type**			
		Precautioned Congugate Gradient, Transient	Precautioned Congugate Gradient, Transient	Precautioned Congugate Gradient, Transient
	Iteration Control			
	Maximum number of iterations	50	51	52
	Maximum head change per iteration	0.005 m	0.005 m	0.005 m
	Maximum residual error	0.0005 m/d	0.0005 m/d	0.0005 m/d
	Sink de-activation in dying cells			
	Saturated thickness threshold	0.05 m	0.05 m	0.05 m
	Advanced settings			
		Gradual drain-activation	Gradual drain-activation	Gradual drain-activation
		Horizontal conductance averaging between iterations	Horizontal conductance averaging between iterations	Horizontal conductance averaging between iterations
	Under-relaxation	No under-relaxation	No under-relaxation	No under-relaxation
	Maximum exchange from river during one time step			
	Max. Fraction of H-point volume	0.9	0.9	0.9

*Default values highlighted.

Table A.2: MIKE SHE input data for the model domain and grid module.

Model Domain and Grid module

Input field		MIKE SHE initial current scenario	MIKE SHE calibrated current scenario	MIKE SHE future scenario
		Catchment defined by .Dfs File	Catchment defined by .Dfs File	Catchment defined by .Dfs File
Catchment size and orientation	NX	199	199	199
	NY	181	181	181
	Cell size	6	6	6
	Rotation	0	0	0
Catchment origin and map projection	X0	270837.69	270837.69	270837.69
	Y0	6766229.94	6766229.94	6766229.94
	Map Projection Type	WGS 1984 UTM 36S	WGS 1984 UTM 36S	WGS 1984 UTM 36S

Table A.3: MIKE SHE input data for the topography module.

Topography module			
Input field	**MIKE SHE initial current scenario**	**MIKE SHE calibrated current scenario**	**MIKE SHE future scenario**
Spatial distribution	Grid file (.dfs2)	Grid file (.dfs2)	Grid file (.dfs2)
File input	5m DEM	5m DEM	5m DEM

Table A.4: MIKE SHE input data for the climate module.

Climate module				
Input field		**MIKE SHE initial current scenario**	**MIKE SHE calibrated current scenario**	**MIKE SHE future scenario**
Precipitation rate	Spatial distribution	Uniform	Uniform	Uniform
	Temporal distribution	Time varying (.dfs0)	Time varying (.dfs0)	Time varying (.dfs0)
	File input	Daily rainfall from 14 February 2007 - 2 October 2016	Daily rainfall from 14 February 2007 - 2 October 2017	Daily rainfall from 14 February 2019 - 2 October 2028
Reference evapotranspiration	Spatial distribution	Uniform	Uniform	Uniform
	Data type	Time varying (.dfs0)	Time varying (.dfs0)	Time varying (.dfs0)
	File input	Daily reference evapotranspiration from 14 February 2007 - 2 October 2016	Daily reference evapotranspiration from 14 February 2007 - 2 October 2017	Daily reference evapotranspiration from 14 February 2019 - 2 October 2028

Table A.5: MIKE SHE input data for the land use module.

Land Use module				
Input field		**MIKE SHE initial current scenario**	**MIKE SHE calibrated current scenario**	**MIKE SHE future scenario**
Vegetation	Spatial	Station based	Station based	Station based
	Data type	Grid codes (.dfs2)	Grid codes (.dfs2)	Grid codes (.dfs2)
	Input file	Vegetation map	Vegetation map	Vegetation map
	Sugarcane (*S. officinarum*)			
	Temporal distribution	Vegetation property file	Vegetation property file	Vegetation property file
	Recycling mode	None	None	None
	Riparian vegetation			
	Temporal distribution	Constant	Constant	Constant
	LAI constant value	2.69	2.69	2.69
	RD constant value	1000 m	1000 m	1000 m
	Black wattle (*A. mearnsii*)			
	Temporal distribution	Vegetation property file	Vegetation property file	NA
	Recycling mode	None	None	NA
	E. dunnii			
	Temporal distribution	NA	NA	Timeseries file
	LAI timeseries file	NA	NA	LAI record extending from 14 February 2019 - 2 October 2028
	RD timeseries file	NA	NA	RD record extending from 14 February 2019 - 2 October 2028
Evapotranspiration Parameters	**General ET parameters**			
	Canopy interception	0.05 mm	0.05 mm	0.05 mm
	2-Layer Water Balance ET Parameters			
	Reduced ET from roots when UZ deficit fraction is below	1	1	1
	Gravity Flow and Richards ET Parameters			
	C1	0.3	0.3	0.3

	C2	0.2	0.2	0.2
	C3	20 mm/d	21 mm/d	22 mm/d
	Aroot	0.25 1/m	0.25 1/m	0.25 1/m

*Default values highlighted.

Table A.6: MIKE SHE input data for the vegetation development ,of the vegetation property file, for the sugarcane (*S. officinarum*) and black wattle (*A. mearnsii*) vegetation classes.

Vegetation development				
Sugarcane (*S. officinarum)*				
Development stage	**End day (days)**	**Leaf Area Index**	**Rooting depth (mm)**	**Kc**
Start	0	3.57	1000	0.96
	107	3.57	1000	0.96
	411	3.57	1000	0.96
First harvest	412	0.00	0	0.00
	534	3.57	1000	0.96
	1082	3.57	1000	0.96
Second harvest	1083	0.00	0	0.00
	1203	3.57	1000	0.96
	1751	3.57	1000	0.96
Third harvest	1752	0.00	0	0.00
	1873	3.57	1000	0.96
	2420	3.57	1000	0.96
Fourth harvest	2421	0.00	0	0.00
	2544	3.57	1000	0.96
	3089	3.57	1000	0.96
Fifth harvest	3090	0.00	0	0.00
	3212	3.57	1000	0.96
End	3519	3.57	1000	0.96
Black wattle (*A. mearnsii*)				
Development stage	**End day (days)**	**Leaf Area Index**	**Rooting depth (mm)**	**Kc**
Start	0	1.21	10000	0.60

27/02/2007	13	0.71	10000	0.60
04/04/2007	49	0.81	10000	0.40
11/05/2007	86	0.86	10000	0.55
21/06/2007	127	0.85	10000	0.30
26/07/2007	162	1.03	10000	0.30
28/08/2007	195	1.60	10000	0.30
10/10/2007	238	2.16	10000	0.45
12/11/2007	270	2.34	10000	0.60
29/04/2008	439	2.39	10000	0.65
05/08/2008	537	2.45	10000	0.70
12/11/2008	636	2.42	10000	0.85
13/02/2009	729	2.85	10000	0.90
05/11/2010	1359	2.88	10000	0.90
13/01/2011	1428	3.02	10000	0.90
31/03/2011	1505	3.04	10000	0.90
07/09/2011	1665	3.05	10000	0.90
27/09/2011	1685	3.16	10000	0.90
27/01/2012	1807	3.25	10000	0.90
31/07/2012	1993	3.31	10000	0.90
30/11/2012	2115	3.29	10000	0.90
31/01/2013	2177	3.42	10000	0.90
31/03/2013	2236	3.74	10000	0.90
17/07/2013	2344	3.61	10000	0.90
12/10/2013	2431	3.74	10000	0.90
End	3519	3.74	10000	0.90

Table A.7: MIKE SHE input data for the rivers and lakes module.

Rivers and Lakes module

Input field		MIKE SHE initial current scenario	MIKE SHE calibrated current scenario	MIKE SHE future scenario
Models	Models	Hydrodynamic	Hydrodynamic	Hydrodynamic
	Simulation mode	Unsteady	Unsteady	Unsteady
Input		Network file	Network file	Network file
		Cross-section file	Cross-section file	Cross-section file
		Boundary data file	Boundary data file	Boundary data file
		HD parameter file	HD parameter file	HD parameter file
Simulation	Time step type	Fixed time step	Fixed time step	Fixed time step
	Time step	1 sec	1 sec	1 sec
Network editor				
Branch properties	Branch name	Two streams stream	Two streams stream	Two streams stream
	Topo ID	Stream 1	Stream 1	Stream 1
	Upstream chainage	0	0	0
	Downstream chainage	748.93	748.93	748.93
	Flow direction	Positive	Positive	Positive
	Maximum dx	10000 mm	10000 mm	10000 mm
	Branch type	Regular	Regular	Regular
MIKE SHE links	Conductance	River bed only	River bed only	River bed only
	Leakage Coefficient	5 x 10-6	6 x 10-6	7 x 10-6
	Flood area	No flooding	No flooding	No flooding
	Bed topography	Use grid data	Use grid data	Use grid data
	Bed leakage	Use river data	Use river data	Use river data
	Weir coefficient	1.838	1.838	1.838
	Head exponent	1.5	1.5	1.5
	Minimum upstream height above bank for full weir width	0.1	0.1	0.1
	Minimum flow area for overbank spilling	1	1	1
	Linear reservoir exchange	Gaining reach	Gaining reach	Gaining reach
Cross-section editor				
	Section type	Open	Open	Open

	Radius type	Resistance radius	Resistance radius	Resistance radius
Resistance numbers	Transversal distribution	Uniform	Uniform	Uniform
	Uniform value	1	1	1
	Resistance type	Relative resistance	Relative resistance	Relative resistance
Boundary editor				
Upstream boundary	Boundary description	Open	Open	Open
	Boundary type	Inflow	Inflow	Inflow
	Data type	Discharge	Discharge	Discharge
Downstream boundary	Boundary description	Open	Open	Open
	Boundary type	Q-h	Q-h	Q-h
	Data type	Discharge and Water Level	Discharge and Water Level	Discharge and Water Level
Hydrodynamic Parameters				
Initial	Water level	0	0	0
	Discharge	0	0	0
Wind	Topographical factor	1	1	1
	Friction factor	0.0024	0.0024	0.0024
Bed resistance	Approach	Uniform Section	Uniform Section	Uniform Section
	Resistance formula	Manning (M)	Manning (M)	Manning (M)
	Global resistance number	30	30	30
Wave Approximation	Global wave approximation	Fully dynamic	Fully dynamic	Fully dynamic
Default values	Delta	0.5	0.5	0.5
	Delhs	0.01	0.01	0.01
	Delh	0.1	0.1	0.1
	Alpha	1	1	1
	Theta	1	1	1
	Eps	0.0001	0.0001	0.0001
	Dh Node	0.01	0.01	0.01
	Zeta Min	0.1	0.1	0.1
	Struc Fac	0	0	0

	Inter 1Max	10	10	10
	Nolter	1	1	1
	MaxIterSteady	100	100	100
	FroudeMax	-1	-1	-1
	FroudeExp	-1	-1	-1

*Default values highlighted.

Table A.8: MIKE SHE input data for the overland flow module.

Overland Flow module				
Input field		**MIKE SHE initial current scenario**	**MIKE SHE calibrated current scenario**	**MIKE SHE future scenario**
Manning Number	Spatial distribution	Grid file (.dfs2)	Grid file (.dfs2)	Grid file (.dfs2)
	Input file	Manning M input	Manning M input	Manning M input
Detention Storage	Spatial distribution	Uniform	Uniform	Uniform
	Value	2 mm	2 mm	2 mm
Initial Water Depth	Spatial distribution	Uniform	Uniform	Uniform
	Value	0 mm	0 mm	0 mm

*Default values highlighted.

Table A.9: MIKE SHE input data for the unsaturated flow module.

Unsaturated Flow module				
Input field		**MIKE SHE initial current scenario**	**MIKE SHE calibrated current scenario**	**MIKE SHE future scenario**
Calculation Column Classification Type		Calculated in all grid points	Calculated in all grid points	Calculated in all grid points
Initial Condition		Equilibrium pressure profile	Equilibrium pressure profile	Equilibrium pressure profile
Macropore Flow		None	None	None
Soil Profile Definitions	Spatial Distribution	Distributed	Distributed	Distributed
	Data Type	Grid codes (.dfs2)	Grid codes (.dfs2)	Grid codes (.dfs2)
	Soil Profile descriptions	See Table A.10	Remains unchanged (see Table A.10)	Remains unchanged (see Table A.10)

*Default values highlighted.

Table A.10: MIKE SHE input data for the soil profiles for the seven soil types considered.

Soil Profiles				
Kranskop				
Soil profile	**From depth (m)**	**To depth (m)**	**Soil names**	
	0	0.4	ah	
	0.4	0.8	ye	
	0.8	2.5	re	
	2.5	55	saphrolite	
Vertical Discretization	**From depth (m)**	**To depth (m)**	**Cell height**	**No. of cells**
	0	1	0.2	5
	1	2	0.5	2
	2	55	1	53
Inanda				
Soil profile	**From depth (m)**	**To depth (m)**	**Soil names**	
	0	0.4	ah	
	0.4	2	re	
	2	55	saphrolite	
Vertical Discretization	**From depth (m)**	**To depth (m)**	**Cell height**	**No. of cells**
	0	1	0.2	5
	1	2	0.5	2
	2	55	1	53
Magwa				
Soil profile	**From depth (m)**	**To depth (m)**	**Soil names**	
	0	0.4	ah	
	0.4	1	ye	
	1	2	on	
	2	55	saphrolite	
Vertical Discretization	**From depth (m)**	**To depth (m)**	**Cell height**	**No. of cells**
	0	1	0.2	5

	1	2	0.5	2
	2	55	1	53
Clovelly				
Soil profile	**From depth (m)**	**To depth (m)**	**Soil names**	
	0	0.4	ot	
	0.4	0.8	ye	
	0.8	55	saphrolite	
Vertical Discretization	**From depth (m)**	**To depth (m)**	**Cell height**	**No. of cells**
	0	1	0.2	5
	1	2	0.5	2
	2	55	1	53
Oakleaf				
Soil profile	**From depth (m)**	**To depth (m)**	**Soil names**	
	0	0.4	ot	
	0.4	1.75	ne	
	1.75	55	saphrolite	
Vertical Discretization	**From depth (m)**	**To depth (m)**	**Cell height**	**No. of cells**
	0	1	0.2	5
	1	2	0.5	2
	2	55	1	53
Katspruit				
Soil profile	**From depth (m)**	**To depth (m)**	**Soil names**	
	0	1	ot	
	1	1.2	G	
	1.2	55	saphrolite	
Vertical Discretization	**From depth (m)**	**To depth (m)**	**Cell height**	**No. of cells**
	0	1	0.2	5
	1	2	0.5	2
	2	55	1	53
Griffin				

Soil profile	**From depth (m)**	**To depth (m)**	**Soil names**	
	0	0.4	ot	
	0.4	0.8	ye	
	0.8	2.5	re	
	2.5	55	saphrolite	
Vertical Discretization	**From depth (m)**	**To depth (m)**	**Cell height**	**No. of cells**
	0	1	0.2	5
	1	2	0.5	2
	2	55	1	53

Table A.11: MIKE SHE input data for the saturated zone module.

Saturated Zone module				
Input field		**MIKE SHE initial current scenario**	**MIKE SHE calibrated current scenario**	**MIKE SHE future scenario**
	Hydrogeologic parameter distribution	Assign parameters via geological layers	Assign parameters via geological layers	Assign parameters via geological layers
Geological layer -Natal Sandstone				
Horizontal hydraulic conductivity	Spatial distribution	Uniform	Uniform	Uniform
	Value	3.2 x 10-5	3.2 x 10-5	3.2 x 10-5
Vertical hydraulic conductivity	Spatial distribution	Uniform	Uniform	Uniform
	Value	3.2 x 10-5	3.2 x 10-5	3.2 x 10-5
Specific yield	Spatial distribution	Uniform	Uniform	Uniform
	Value	0.2	0.2	0.2
Specific storage	Spatial distribution	Uniform	Uniform	Uniform
	Value	0.0019	0.0019	0.0019
Computational layer - Natal Sandstone				
Initial potential head	Spatial distribution	Grid file (.dfs2)	Grid file (.dfs2)	Grid file (.dfs2)
	Input file	Water table level at the start of the simulation	Water table level at the start of the simulation	Water table level at the start of the simulation
Outer Boundary Conditions	Type	Zero-flux	Zero-flux	Zero-flux

	Extent	Total domain	Total domain	Total domain
Internal Boundary Conditions	Boundary condition distribution type	None	None	None

*Default values highlighted.

Table A.12: MIKE SHE input data for the storing of results module.

Storing of results module				
Input field		**MIKE SHE initial current scenario**	**MIKE SHE calibrated current scenario**	**MIKE SHE future scenario**
Result output units		Internal MIKE SHE units	Internal MIKE SHE units	Internal MIKE SHE units
Water Movement Output	Overland	24 hrs	24 hrs	24 hrs
	Precipitations, Evapotranspiration, Unsaturated zone	24 hrs	24 hrs	24 hrs
	Saturated zone Heads	24 hrs	24 hrs	24 hrs
	Saturated zone Fluxes	24 hrs	24 hrs	24 hrs
Detailed timeseries output	Minimum output timestep	24 hrs	24 hrs	24 hrs
	Input file	Observed evapotranspiration record 1 October 2011 - 25 October 2013	Observed evapotranspiration record 1 October 2011 - 25 October 2014	Observed evapotranspiration record 1 October 2011 - 25 October 2015
Detailed M11 timeseries output	Minimum output timestep	24 hrs	25 hrs	26 hrs
	Input file	Observed streamflow record 14 February 2007 - 9 December 2013	Observed streamflow record 14 February 2007 - 9 December 2014	Observed streamflow record 14 February 2007 - 9 December 2015
Grid series output	Water balance components	All selected	All selected	All selected

Appendix B: Catchment delineation

The Two Streams catchment and sub-catchments were previously delineated and used in past research projects on the Two Streams site (Figure B.1; Everson *et al*., 2006, 2014; Clulow *et al*., 2011). However, given the sharp, straight boundary lines of the catchment and sub-catchment the researcher was concerned with the accuracy of the boundaries and thus generated new boundaries for this study.



Figure B.1: The original Two Streams catchment delineated for previous WRC reports (Everson *et al*., 2006, 2014; Clulow *et al*., 2011).

The catchment delineation process was undertaken using Arc Hydro tools in ArcGIS 10.3 software. The only input needed was a DEM – the DEM used is described under *Chapter 4 Methodology* section 4.3.3 *Topography module*. To delineate the catchment and sub-catchment a step-by-step series of sequential processes was followed, whereby the output of the first step becomes the input of the second step and so on. Within ArcHydro the DEM had to undergo a number of *Terrain Preprocessing* steps followed by a number of *Watershed Processing* steps (Figure B.2).

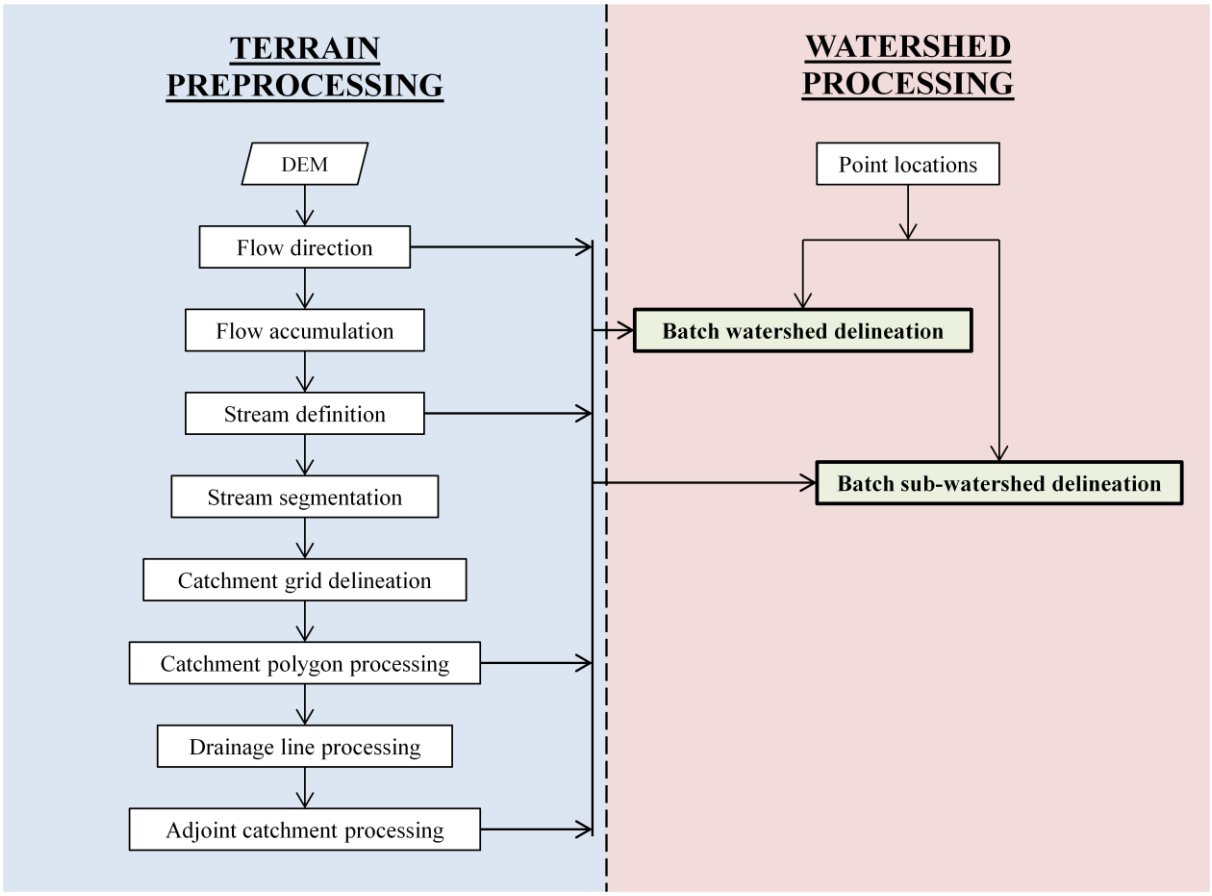

Figure B.2: Steps taken in delineating the Two Streams catchment and sub-catchments using ArcHydro in ArcGIS 10.3.

B.1 Terrain preprocessing tools

Terrain preprocessing was undertaken to identify the surface drainage pattern. The steps in the *Terrain preprocessing* menu were performed in sequential order, from top to bottom. The functions considered were: *Flow direction, Flow accumulation, Stream definition, Stream segmentation, Catchment grid delineation, Catchment polygon processing, Drainage line processing and Adjoint catchment processing* (Figure B.2).

B.1.1 Flow direction

This function calculates the flow direction based on the input DEM (Figure B.3). It gives an indication of the direction of the steepest decline from each cell within the DEM.

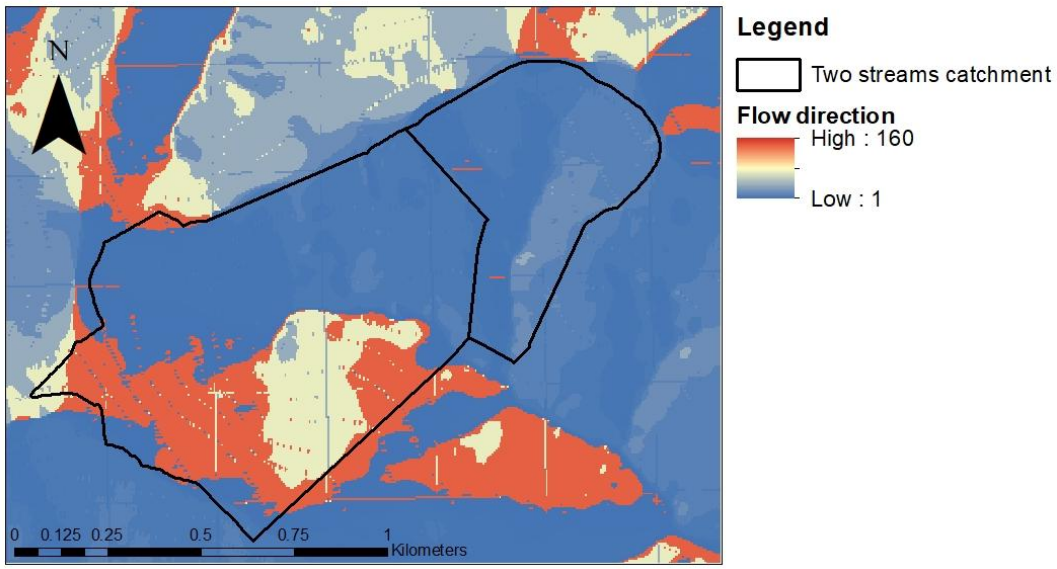

Figure B.3: Flow direction output from the Arc Hydro Terrain preprocessing step.

B.1.2 Flow accumulation

This function calculates the accumulated 'weight' of all cells flowing into each down slope cell in the output raster (Figure B.4). The flow accumulation output is calculated using the flow direction output (Figure B.3).

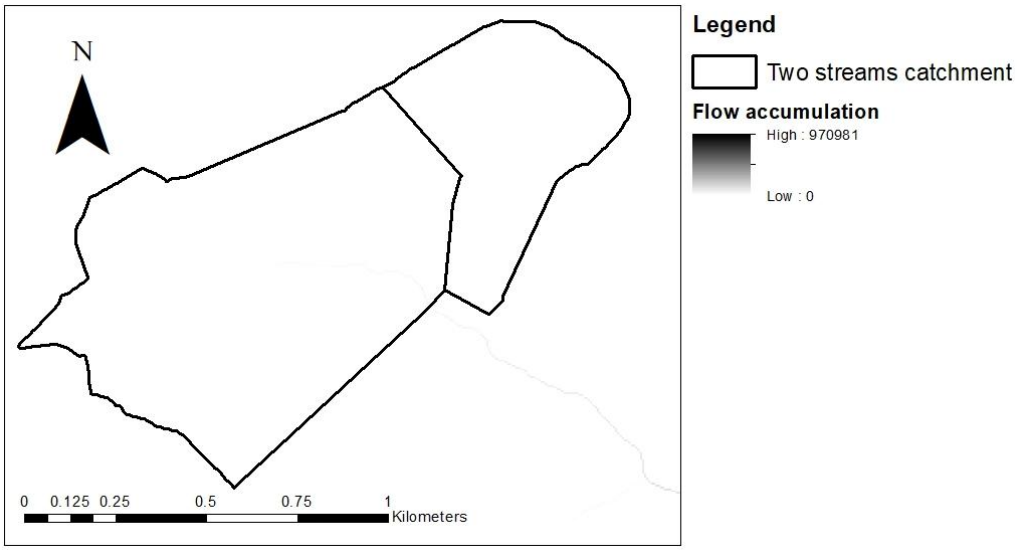

Figure B.4: Flow accumulation output from the Arc Hydro Terrain preprocessing step.

B.1.3 Stream definition

This function defines the streams within the DEM defined area (Figure B.5). It is based on the Flow accumulation output (Figure B.4) and a user specified threshold. The threshold value is used to determine which

cells fall within a stream and which do not. A cell with a value equal to or greater than the threshold is assigned a value of one indicating it to be part of the stream, whilst a cell with a value lower than the threshold is assigned a no data value. The smaller the threshold used the denser the stream network considered and usually the greater the number of delineated catchments, which may hinder delineation performance. To try and prevent the generation of a too dense stream network the default value of 9710 was used for this study.

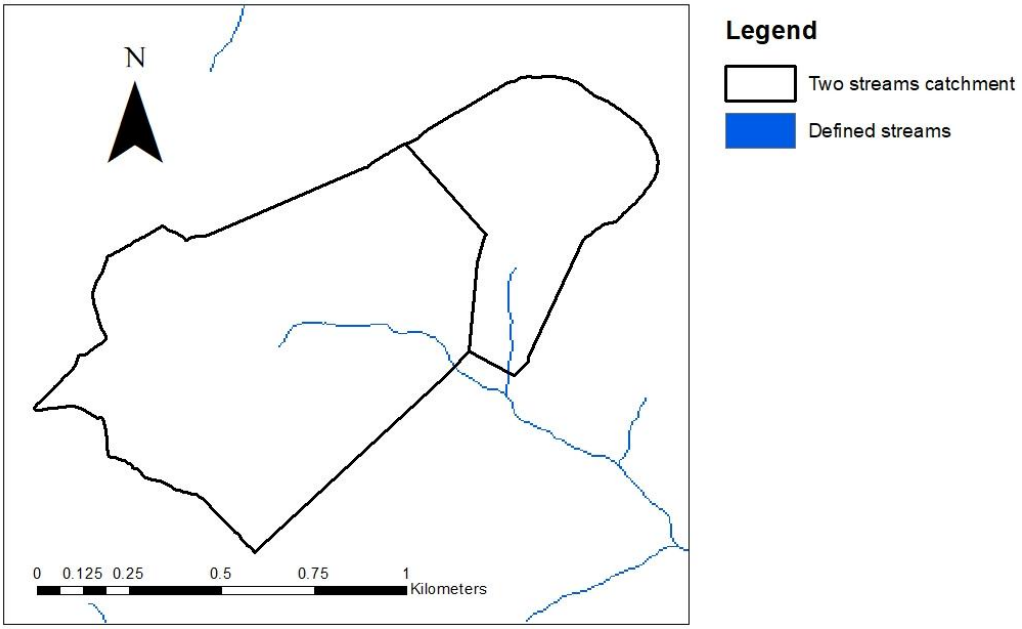

Figure B.5: Stream definition output from the Arc Hydro Terrain preprocessing step.

B.1.4 Stream Segmentation

This function is used to segment streams (Figure B.6). A segment may either be a head segment, or it may be a segment between two segment junctions. All the cells in a segment have the same assigned value that is specific to that segment. The input requirements for the stream segmentation output are the flow direction output (Figure B.3), the defined stream output (Figure B.5), a sink watershed grid and a sink link grid. Both the sink watershed and sink link grids are optional inputs that can be added to cover the input stream grid so that no stream links are created in those areas. For this study, these optional inputs were not included.

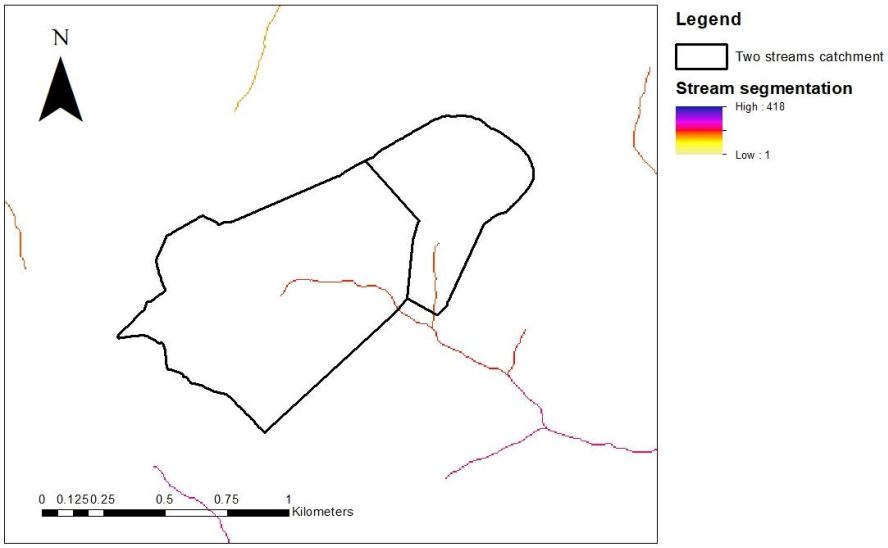

Figure B.6: Stream segmentation output from the Arc Hydro Terrain preprocessing step.

B.1.5 Catchment grid delineation

This function is used to delineate catchments by assigning a value to each cell indicating what catchment that cell belongs to (Figure B.7). The value assigned corresponds to the value carried by the Stream Segment that drains that area (Figure B.6).

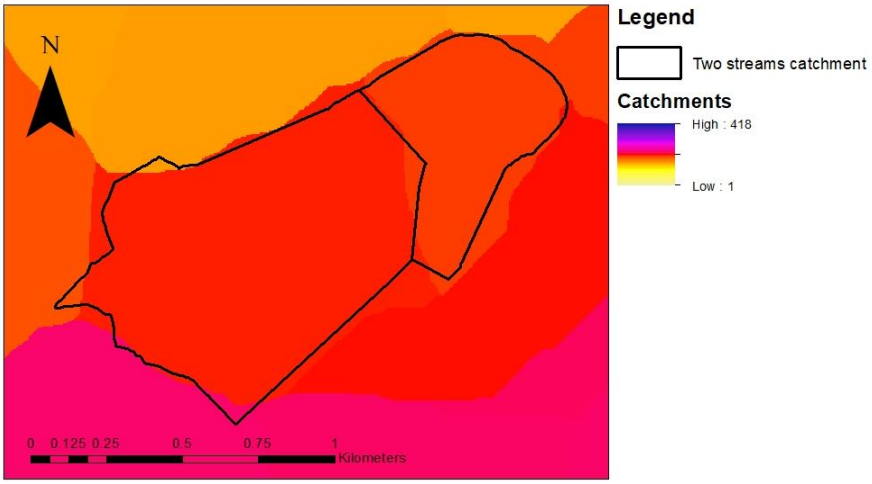

Figure B.7: Catchment grid delineation output from the Arc Hydro Terrain preprocessing step.

B.1.6 Catchment polygon processing

This function uses the Catchment grid (Figure B.7) as an input in generating a catchment polygon feature class (Figure B.8).

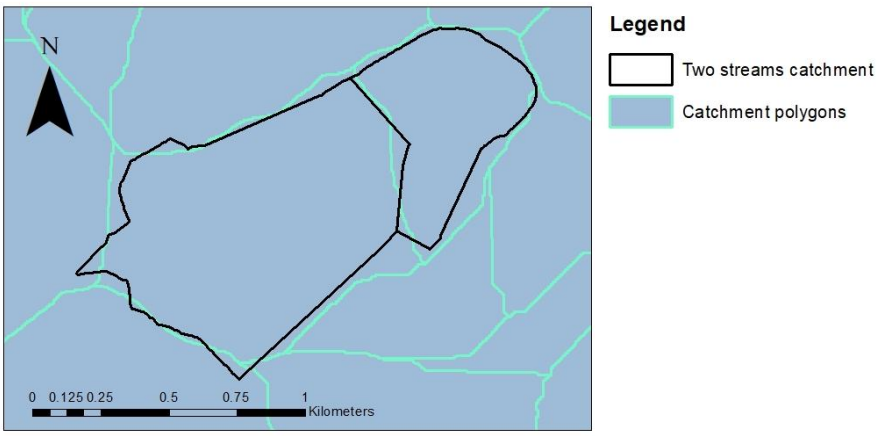

Figure B.8: Catchment polygon processing output from the Arc Hydro Terrain preprocessing step.

B.1.7 Drainage line processing

This function is used to convert the stream segmentation output (Figure B.6) into a drainage line feature class (Figure B.9).

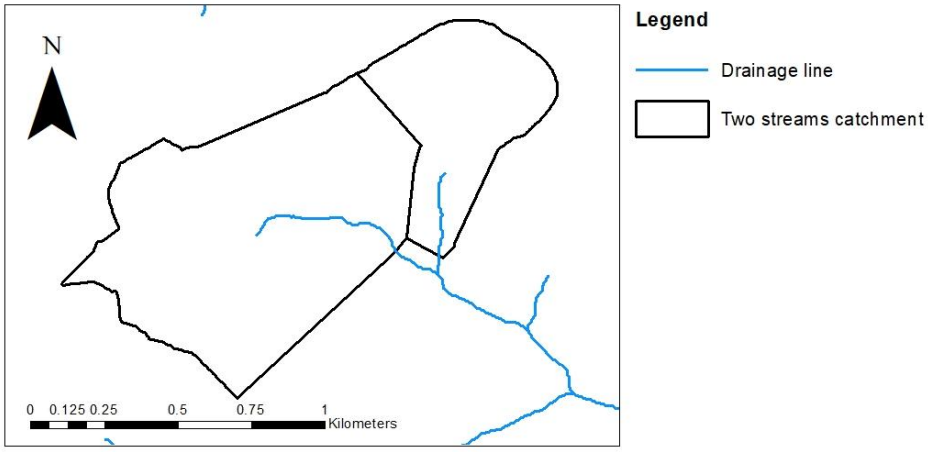

Figure B.9: Drainage line processing output from the Arc Hydro Terrain preprocessing step.

B.1.8 Adjoint Catchment Processing

This function is used to generate the combined upstream catchments from the catchment polygon output (Figure B.8) feature class. For each catchment that is not a head catchment, a polygon representing the whole upstream area draining to its inlet point is constructed and an overall feature class is produced (Figure B.10).

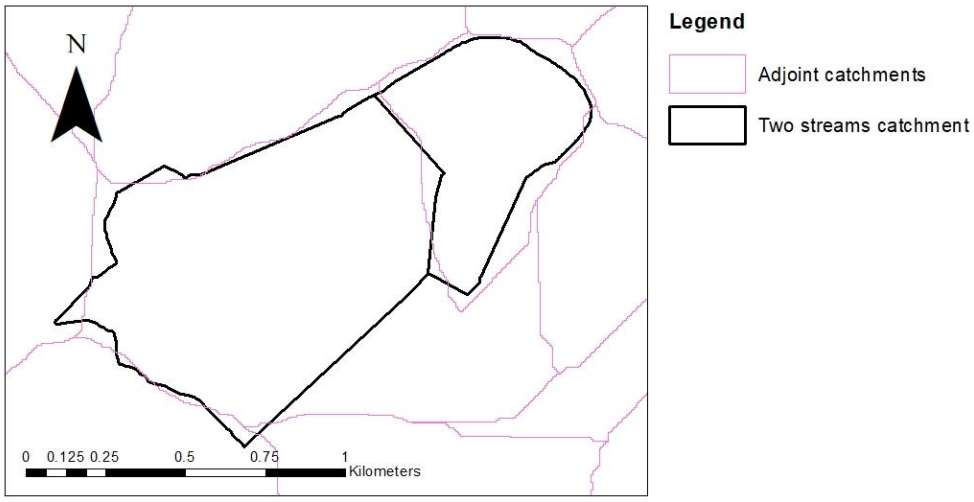

Figure B.10: Adjoint catchment processing output from the Arc Hydro Terrain preprocessing step.

B.2 Watershed Processing

Following the terrain preprocessing steps, the watershed delineation functions can be followed as the preprocessing steps partition the terrain into manageable units to allow for fast delineation operations.

B.2.1 Delineation functions

B.2.1.1 Batch Watershed Delineation

This function is used to delineate a catchment based on a point location selected by the user (Figure B.11). The input requirements for the delineation process include: the flow direction output (Figure B.3), the defined streams output (Figure B.5), snap stream grid, the catchment feature class output (Figure B.8) and the adjoint feature class output (Figure B.10). The snap stream grid input is optional and was not included for this project.

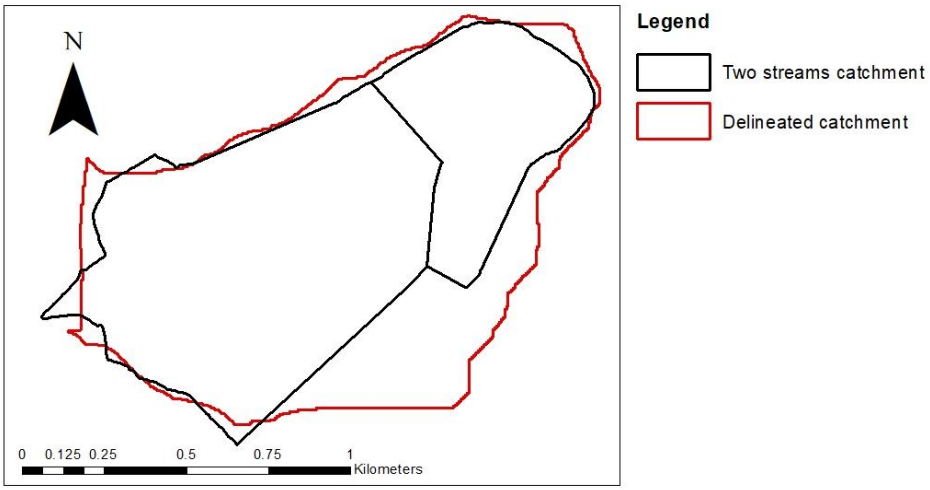

Figure B.11: Batch watershed delineation output from the Arc Hydro Terrain preprocessing step.

B.2.1.2 Batch Sub-watershed delineation

This function delineates sub-watersheds (Figure B.12). The input requirements are the same as the fore-mentioned *Batch watershed delineation* inputs, the difference between the two are the user defined point locations to define the outlet points of the sub-catchments of interest.

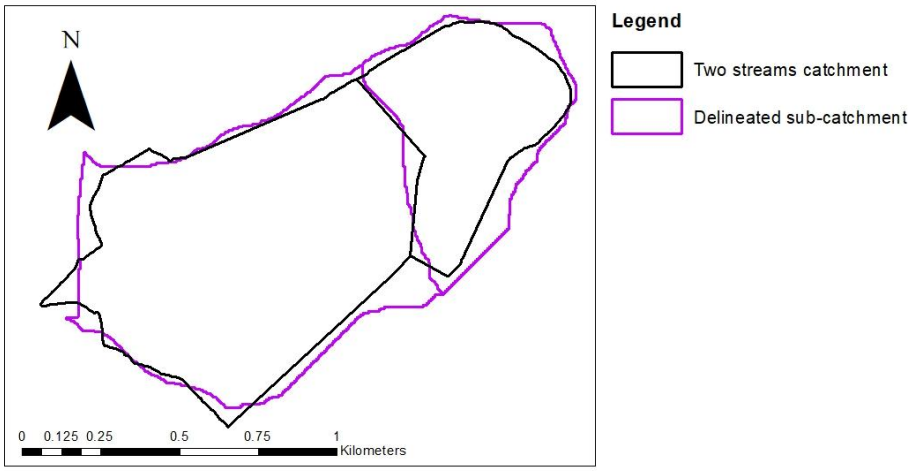

Figure B.12: Batch sub-watershed delineation output from the Arc Hydro Terrain preprocessing step.

Appendix C: Penman-Monteith equation

The FAO Penman-Monteith equation requires three climatic data inputs: air temperature, air humidity and solar radiation (Zotarelli *et al*., 2015). All climatic data were taken from the three AWS described in *Chapter 3 Methodology* under section 3.3.4 *Climate module*.

C.1 Air temperature

Temperature input requirements included maximum, minimum and mean temperature (°C). All temperature records extended from the 14th of February 2007 to the 2nd of October 2016 and were daily recordings (a total of 3519 days considered).

C.1.1 Maximum temperature

Majority of the Maximum temperature record was taken from the FAO AWS record (3239 days – approximately 92.1%). 110 days (approximately 3.1%) were taken from the mast AWS and 170 days (approximately 4.8%) from the SAWS weather station record. The FAO AWS and mast AWS record had an extremely significant ($P < 0.0001$) very strong Pearson's correlation coefficient of 0.91 and a strong coefficient of determination (R^2) of 0.83 (Figure C.1) and was deemed sufficient to patch the gaps in the FAO AWS record.

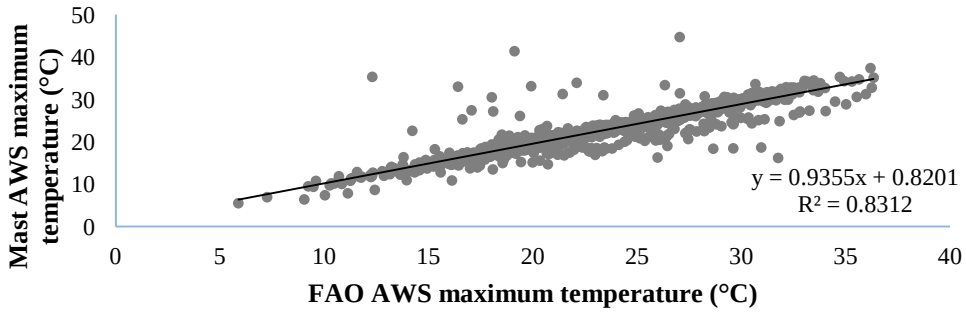

Figure C.1: Correlation between the FAO Automatic Weather Station daily maximum temperature (°C) record and the mast Automatic Weather station daily maximum temperature (°C) record.

Once gaps were patched using the mast AWS record there were still 170 days missing. These missing days were patched using the SAWS maximum temperature record. The combined AWS record and the SAWS record were found to have an extremely significant ($P < 0.0001$) very strong Pearson's correlation coefficient of 0.9 and a

strong coefficient of determination (R^2) of 0.81 (Figure C.2) and was deemed sufficient to patch the remaining missing days.

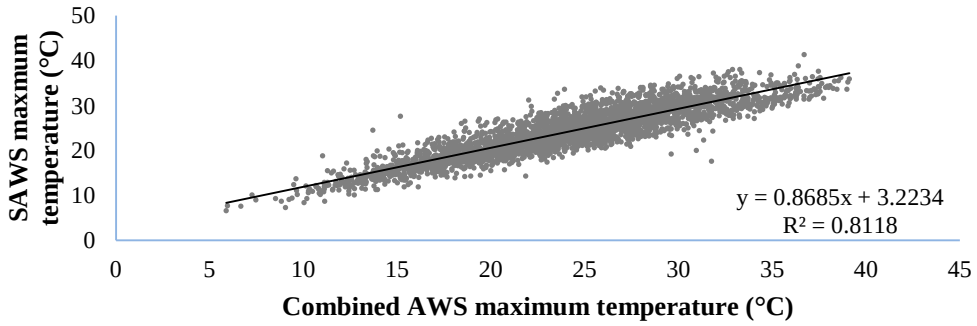

Figure C.2: Correlation between the combined Automatic Weather Station daily maximum temperature (°C) record for the Two Streams site and the South African Weather Services' Greytown weather stations daily maximum temperature (°C) record.

Following patching of the FAO AWS record the daily maximum temperature for the site was obtained for the study period (Figure C.3). The average maximum temperature over the study period was 24.4˚C with a standard deviation of 5.85.

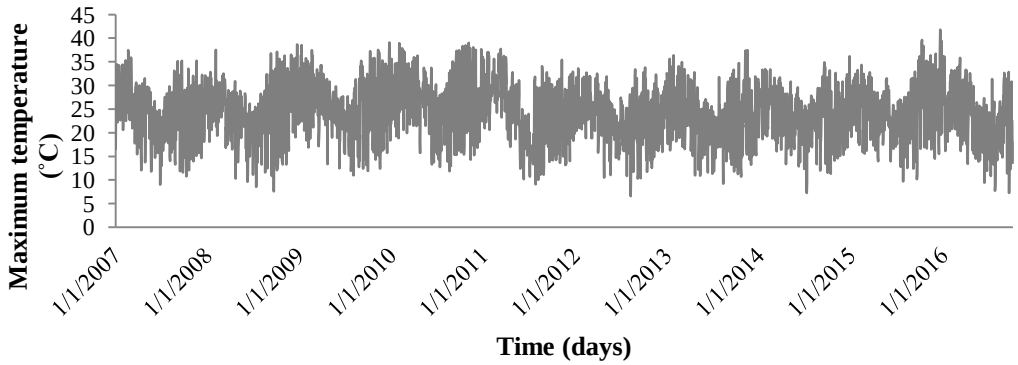

Figure C.3: Daily maximum temperature (˚C) record extending from 14 February 2007 – 02 October 2016 for the Two Streams study site.

C.1.2 Minimum temperature

The daily minimum temperature (˚C) record comprises 3240 days taken from the FAO AWS, 105 days from the mast AWS and 174 days from the SAWS weather record. The Two Streams site AWSs had an extremely

significant ($P < 0.0001$), strong Pearson's correlation coefficient of 0.91 and a strong coefficient of determination (R^2) value of 0.84 (Figure C.4). This correlation value was deemed sufficient to use to patch the FAO AWS record.

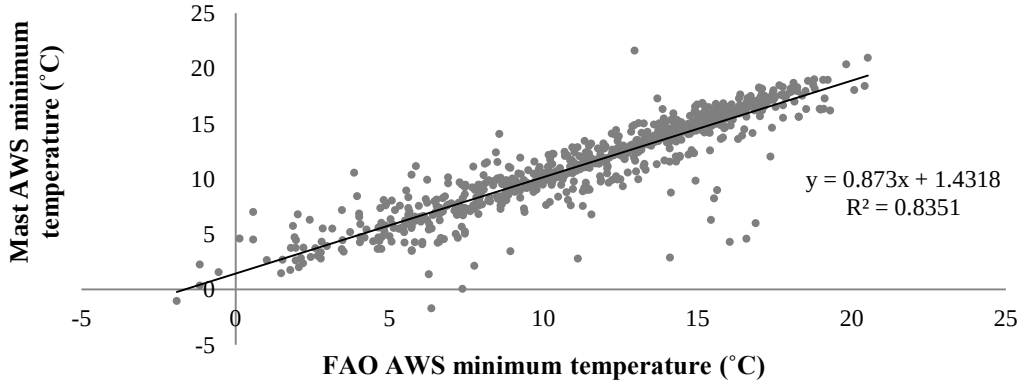

Figure C.4: Correlation between the FAO Automatic Weather Station daily minimum temperature (°C) record and the mast Automatic Weather station daily minimum temperature (°C) record.

Once the FAO AWS record was patched using the mast AWS record there were still 174 missing days in the record that needed to be patched. To do so the SAWS weather record was used. The combined AWS record and the SAWS record were found to have an extremely significant ($P < 0.0001$), strong Pearson's correlation coefficient of 0.89 and a strong coefficient of determination (R^2) of 0.79 (Figure C.5).

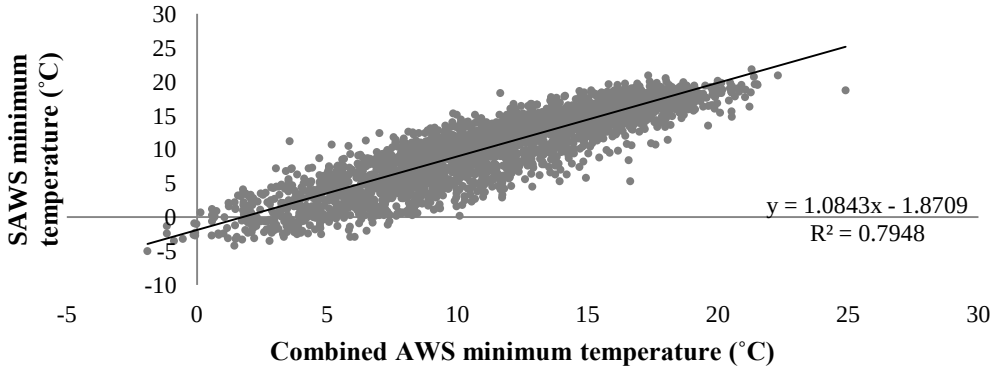

Figure C.5: Correlation between the combined Automatic Weather Station daily minimum temperature (°C) record for the Two Streams site and the South African Weather Services' Greytown weather stations daily minimum temperature (°C) record.

Following patching the daily minimum temperature record for the site was obtained (Figure C.6). The average minimum temperature over the period of the 14th of February 2007 – 2nd of October 2016 was 11.52˚C with a standard deviation of 4.39.

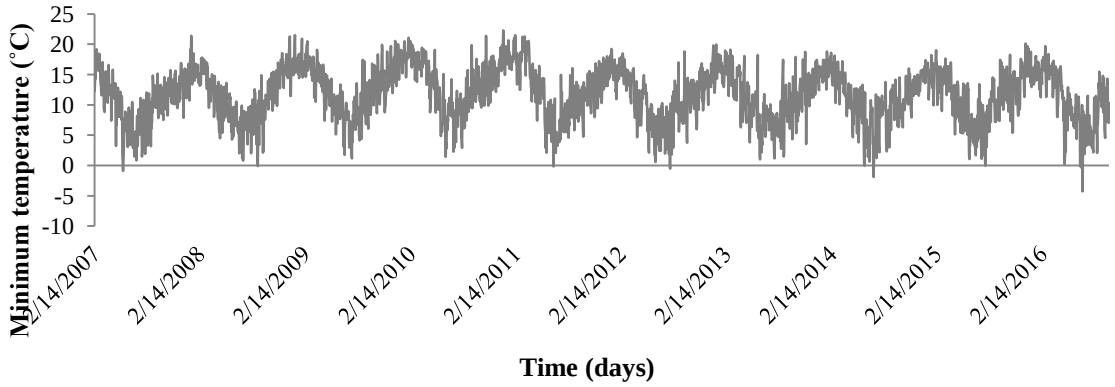

Figure C.6: Daily minimum temperature (˚C) record extending from 14 February 2007 – 02 October 2016 for the Two Streams study site.

C.1.3 Mean temperature

The mean temperature record, extending from the 14th of February 2007 to the 2nd of October 2016, was taken mostly from the FAO AWS record with 3268 days. 15 days were taken from the Mast AWS and 235 days from the SAWS weather record. The two AWS records for the site were compared and found to have an extremely significant ($P < 0.0001$), strong positive Pearson's correlation coefficient of 0.91 (Figure C.7).

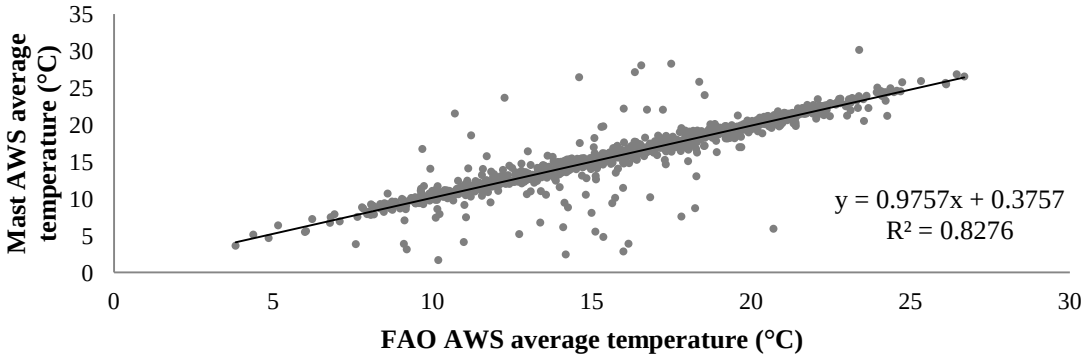

Figure C.7: Correlation between the FAO Automatic Weather Station daily average temperature (°C) record and the mast Automatic Weather station daily average temperature (°C) record.

Comparing the combined AWS record taken from the two site AWSs with the SAWS weather station record it was found that they had an extremely significant ($P < 0.0001$), strong positive Pearson's correlation coefficient of 0.89 and a strong coefficient of determination (R^2) of 0.79 (Figure C.8).

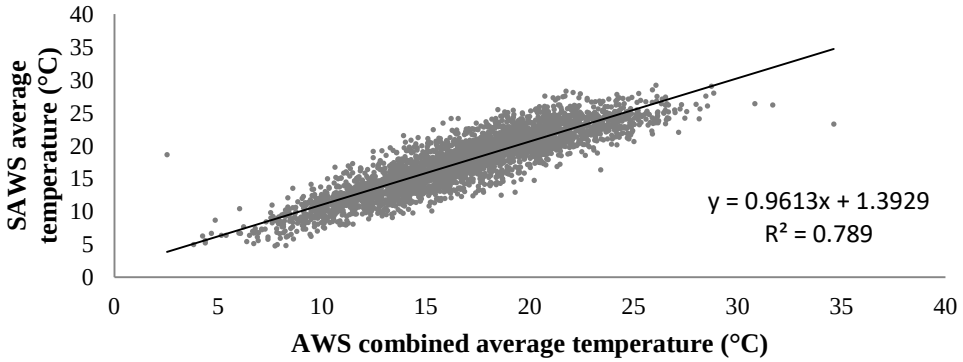

Figure C.8: Correlation between the combined Automatic Weather Station daily average temperature (°C) record for the Two Streams site and the South African Weather Services' Greytown weather stations daily average temperature (°C) record.

Following patching the daily average temperature (˚C) record for the 14th of February 2007 to the 2nd of October 2016 was obtained (Figure C.9). The average temperature over the study period was 16.84˚C with a standard deviation of 4.43.

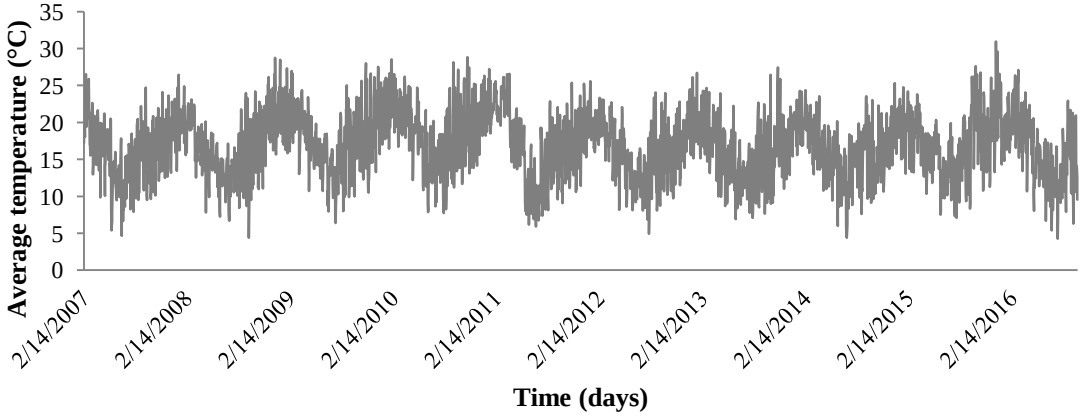

Figure C.9: Daily average temperature (˚C) record extending from 14 February 2007 – 02 October 2016 for the Two Streams study site.

C.2 Wind speed

The wind speed record extended for the same length of time as the temperature records from the 14th of February 2007 to the 2nd of October 2016. Wind speed was recorded daily with a total of 3519 days recorded. Prior to the wind speed record being patched all wind speed records were adjusted for height to 2 m above ground level (required for the Penman-Monteith method (Zotarelli *et al*., 2015); Equation C.1). The FAO AWS wind speed record was recorded at 2 m and thus did not need to be adjusted. The mast AWS record records wind speed at 24 m above ground level and thus needed to be adjusted. The SAWS record also needed to be adjusted as this record was taken at 10 m above ground level.

$$u_2 = u_h \frac{4.87}{\ln(67.8h - 5.42)}$$

Equation C.1: Average daily wind speed ($m.s^{-1}$) measured at 2 m above ground level (Zotarelli *et al*., 2015).

Where: u_2 = wind speed 2m above the ground surface (m/s); u_h= wind speed at height of the measurement above the ground surface (m/s); and h = height of the measurement above the ground surface (m).

On comparison of the FAO AWS wind speed record and the adjusted mast AWS wind speed record they were found to have a extremely significant ($P < 0.0001$) positive Pearson's correlation coefficient of 0.71 and a coefficient of determination (R^2) of 0.5 (Figure C.10).

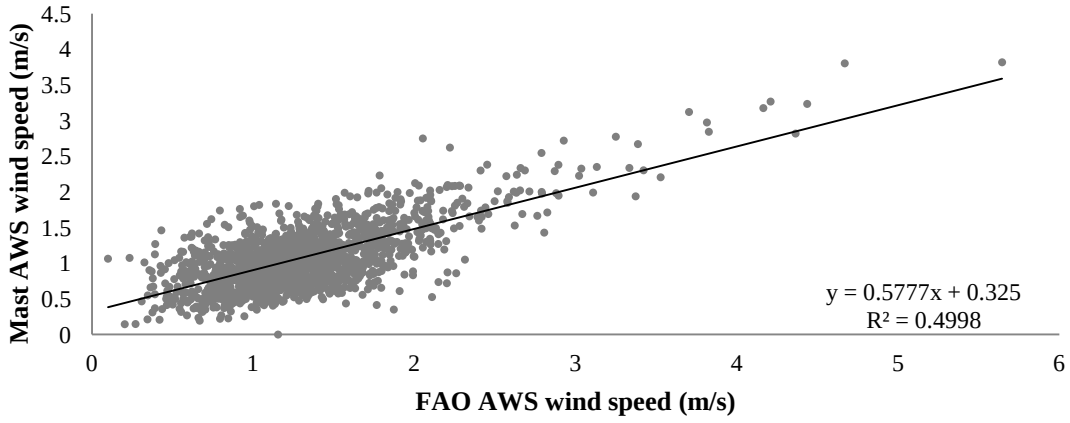

Figure C.10: Correlation between the FAO Automatic Weather Station daily wind speed ($m.s^{-1}$) record and the mast Automatic Weather Station daily wind speed ($m.s^{-1}$) record.

The combined AWS record compared to the SAWS wind speed record was found to have an extremely significant ($P < 0.0001$) Pearson's correlation coefficient of 0.56 and a coefficient of determination (R^2) of 0.31 (Figure C.11). This value was deemed sufficient to patch the missing gaps in the combined AWS record (89 days).

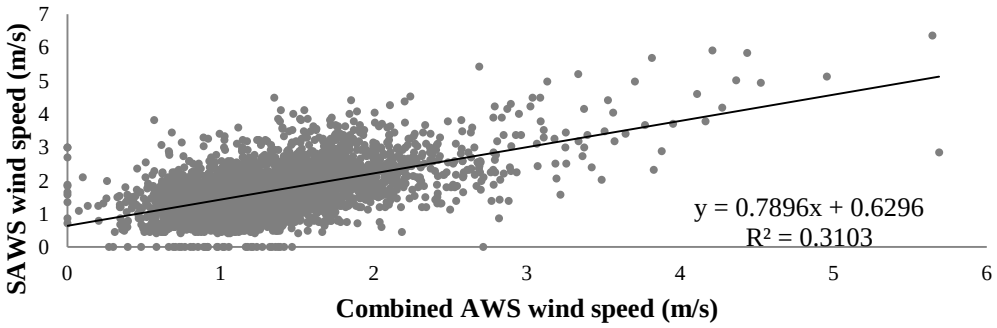

Figure C.11: Correlation between the combined Automatic Weather Station daily wind speed ($m.s^{-1}$) record for the Two Streams site and the South African Weather Services' Greytown weather stations daily wind speed ($m.s^{-1}$) record.

Following patching the daily wind speed record for the period 14 February 2007 – 02 October 2016 was obtained (Figure C.12). Majority of the data was taken from the FAO AWS record (3239 days – approximately 92%) and 191 days were taken from the mast AWS (approximately 5.43%).

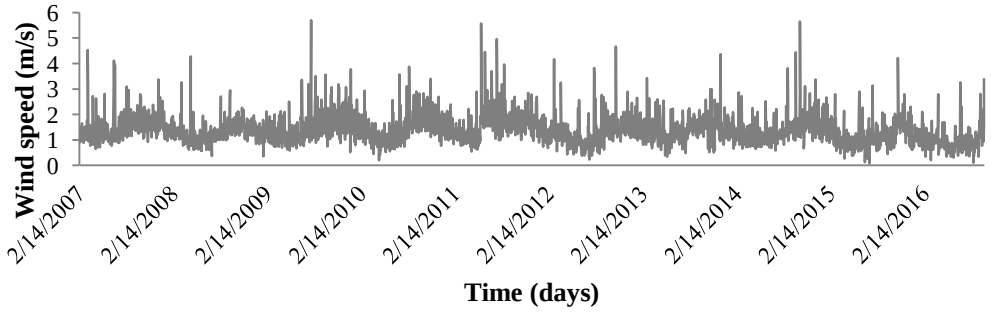

Figure C.12: Daily wind speed (m/s) record extending from 14 February 2007 – 02 October 2016 for the Two Streams study site.

C.3 Relative humidity

Unlike the other weather variables discussed this far the relative humidity record was taken primarily from the SAWS weather record, this was because the FAO AWS record only has a maximum and minimum relative

humidity record and not an average record, as is the case with the mast AWS record. There were 36 days (approximately 1.02%) missing from the SAWS average relative humidity record over the period of the 14th of February 2007 – 2nd of October 2016. These days were patched using an average of the FAO AWS maximum and minimum relative humidity record. The SAWS and FAO AWS relative humidity (%) records had an extremely significant ($P < 0.0001$) Pearson's correlation coefficient of 0.58 and a coefficient of determination (R^2) of 0.34 (Figure C.13).

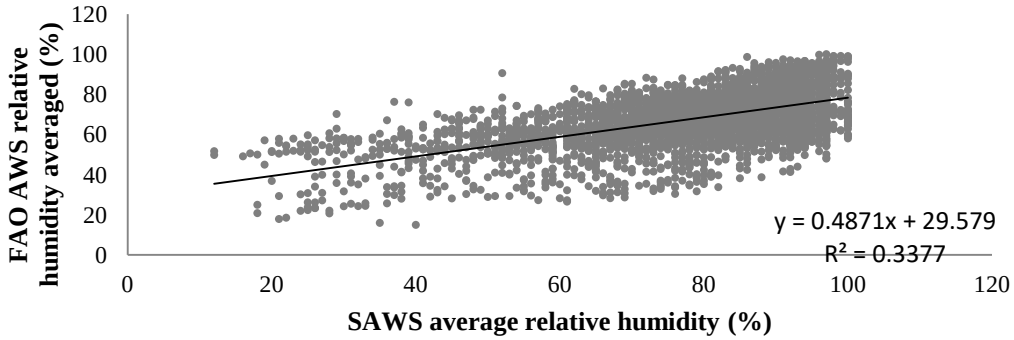

Figure C.13: Correlation between the South African Weather Services' Greytown weather stations daily average relative humidity (%) record and the FAO Automatic Weather Station daily relative humidity (%) record averaged for the Two Streams site.

Following patching the daily average relative humidity record for the site was obtained for the period 14 February 2007 – 02 October 2016 (Figure C.14).

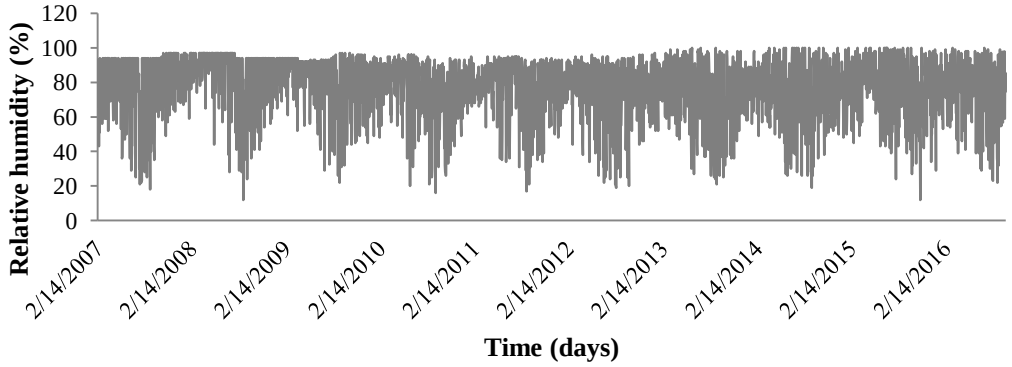

Figure C.14: Daily average relative humidity (%) record extending from 14 February 2007 – 02 October 2016 for the Two Streams study site.

C.4 Solar radiation

Solar radiation (MJ/m²/day) data was only captured by the FAO AWS record. The mast AWS however captured net radiation (MJ/m²/day) data. The SAWS did not have a record of solar radiation for Greytown. There were 3236 days of solar radiation data captured for the period of the 14th of February 2007 – 2nd of October 2016. In order to patch the missing 233 days the relationship between the solar radiation and net radiation was determined by comparing the datasets using a scatter plot and deriving a relationship from the linear trend-line fitted to the scatter plot (Figure C.15).

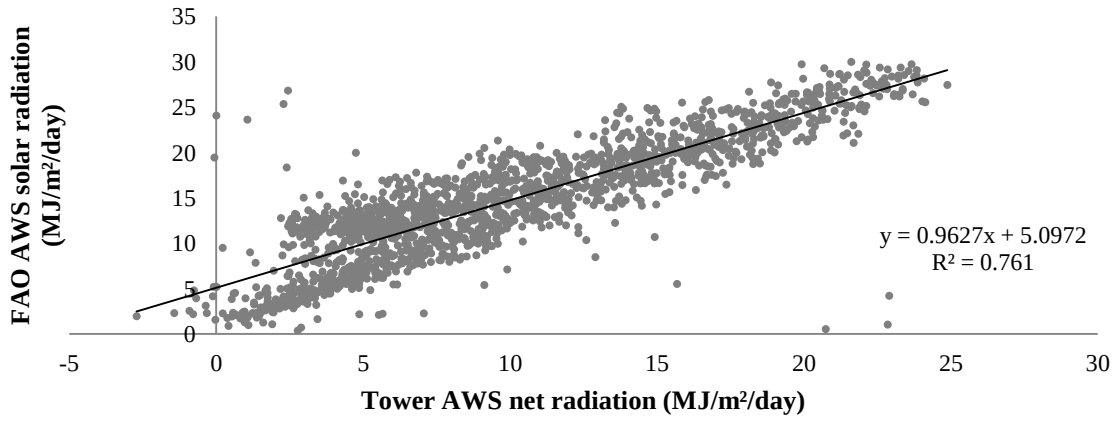

Figure C.15: Correlation between the FAO Automatic Weather Station solar radiation ($MJ.m^{-2}.day^{-1}$) record and the mast Automatic Weather station daily net radiation ($MJ.m^{-2}.day^{-1}$) record.

Based on the correlation scatter plot linear regression an equation was derived to define the relationship between the solar radiation record and the net radiation record (Equation C.2).

$$y = 0.9627x + 5.0972$$

Equation C.2: The relationship determined between the FAO Automatic Weather Station's solar radiation (MJ/m²/day) record and the mast Automatic Weather Station's daily net radiation (MJ/m²/day) record.

Where: y = solar radiation (MJ/m²/day); and x = net radiation (MJ/m²/day).

This relationship was applied to the net radiation record to derive a solar radiation record based on their extremely significant ($P < 0.0001$), strong Pearson's correlation coefficient of 0.87 and a strong coefficient of determination (R^2) of 0.76 (Figure C.15). Following patching the solar radiation record for the period of the 14th

of February 2007 – 2nd of October 2016 was obtained (Figure C.16). There are however still some gaps that cannot be patched by alternate data sources (22 days) – shown by the orange lines in Figure C.16). These gaps fall on the 2nd of November 2013 to the 11th of November 2013 and on the 25th of June 2016 to the 6th of July 2016.

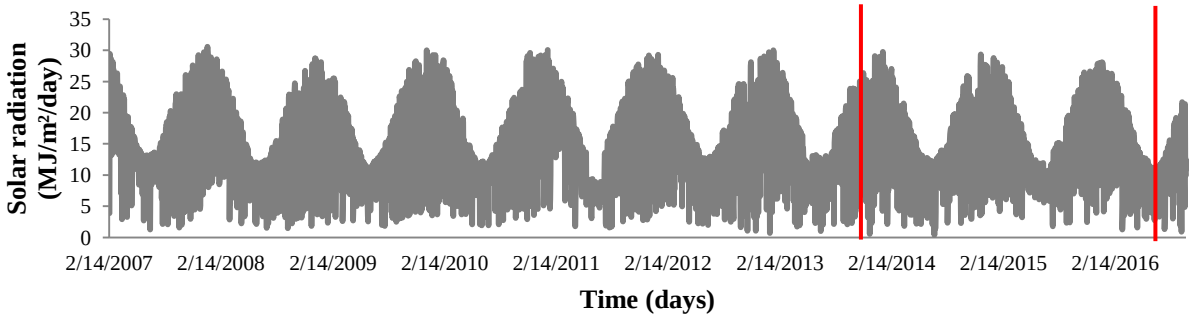

Figure C.16: Daily solar radiation ($MJ.m^{-2}.day^{-1}$) record extending from 14 February 2007 – 02 October 2016 for the Two Streams study site, with gaps identified in red.

In order to patch these gaps, the monthly averages for June, July and November for the entire temporal period considered were averaged and used as the missing values accordingly. June was found to have an average solar radiation of 9.91 $MJ.m^{-2}.day^{-1}$, July 10.74 $MJ.m^{-2}.day^{-1}$ and November 15.78 $MJ.m^{-2}.day^{-1}$. These values were in-filled for their respective months. Following the in-filling process the daily solar radiation ($MJ.m^{-2}.day^{-1}$) record for the Two Streams site was obtained (Figure C.17).

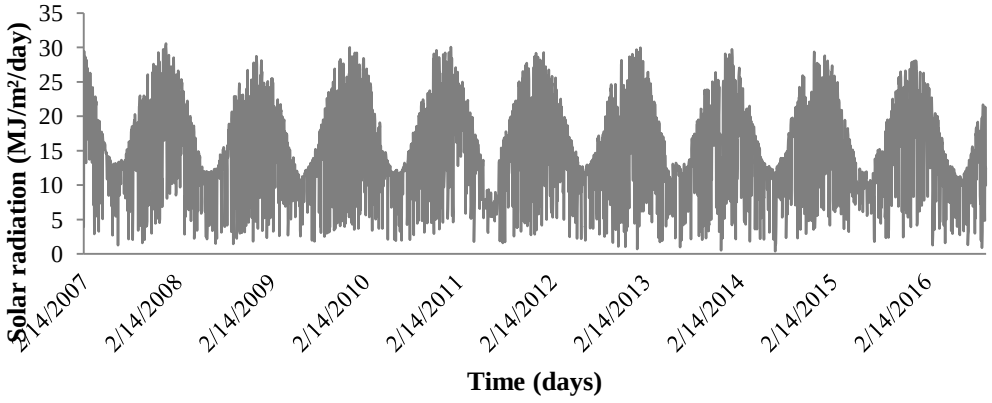

Figure C.17: Daily solar radiation ($MJ.m^{-2}.day$) record extending from 14 February 2007 – 02 October 2016 for the Two Streams study site.

C.5 Penman-Monteith Equation

Once all input weather variables were prepared (as described above) a number of calculations were undertaken to determine the ET_{Ref} based on the Penman-Monteith Equation (Equation 4.1). All step by step calculations used are described in Zotarelli *et al.* (2015). Following the multiple calculation steps the daily ET_{Ref} record for the period of the 14th of February 2007 – 2nd of October 2016 for the study site was obtained (Figure 5.2).

Appendix D: Vegetation inputs for the land use module in MIKE SHE

D.1 Black wattle (*A. mearnsii*) vegetation property file

The black wattle vegetation property file comprises 2431 days of varied LAI and K_c value reading and had a constant RD of 10 m (Table D.1).

Table D.1: Black wattle vegetation property file (.etv) input data for the period 14 February 2007 – 12 October 2013.

End day (start: 14/2/2007)	**LAI** (unitless)	**K_c** (unitless)
0	1.2	0.6
13	0.7	0.6
49	0.9	0.6
86	0.8	0.4
127	0.9	0.3
162	1.0	0.3
195	1.6	0.3
238	2.2	0.5
270	2.3	0.6
439	2.4	0.7
537	2.5	0.7
636	2.4	0.9
729	2.5	0.9
1359	2.5	0.9
1428	2.6	0.9
1505	2.6	0.9
1665	2.7	0.9
1685	2.8	0.9
1807	2.9	0.9
1993	2.9	0.9
2115	2.9	0.9
2177	3.0	0.9
2236	3.2	0.9
2344	3.3	0.9
2431	3.7	0.9

D.2 Riparian vegetation LAI estimation

Normalized difference vegetation index (NDVI) images were generated in ArcGIS 10.3 software using the *Image Analysis* toolbar. Within the *Image Analysis* toolbar, the bands appropriate for analysis, in this case the red and NIR bands were selected (separately for each image). For all five images considered the red band was band 3 and the NIR band was band 4. Once the above was completed the NDVI icon under *Properties* in the *Image Analysis* toolbar was selected to generate an NDVI.

Once the NDVIs were created, random point values from the riparian vegetation class of the study site were identified. To generate random points the *Create random points* tool was used. This tool is located under

Feature Class in the *Data Management Tools* in the ArcToolbox. Fifteen random points were generated and considered for each NDVI. To extract the NDVI values of each point from the NDVI images the *Spatial Analyst* tool, *Extract Values to Points*, was used. The outcome was fifteen NDVI point values for each of the five SPOT images considered (Table D.2).

Table D.2: Normalized Difference Vegetation Index (NDVI) values extracted at fifteen random point locations within the riparian vegetation class of five NDVI images generated from SPOT imagery.

Point No.	**Coordinates**		**Satellite images NDVI values**				
	Latitude	**Longitude**	**01/02/2007**	**17/07/2007**	**19/01/2011**	**31/07/2012**	**04/10/2015**
1	S 29° 12' 31.36"	E 30° 39' 10.85"	-0.0395	-0.0065	-0.1795	0.1818	0.4874
2	S 29° 12' 27.75"	E 30° 39' 10.39"	-0.0323	-0.1333	-0.3023	0.2442	0.6942
3	S 29° 12' 25.77"	E 30° 39' 5.2"	-0.0390	-0.0986	-0.2263	0.1523	0.1813
4	S 29° 12' 30.21"	E 30° 39' 11.6"	-0.0390	-0.2477	-0.1837	0.1928	0.7337
5	S 29° 12' 24.88"	E 30° 38' 56.43"	-0.0065	0.1086	-0.2097	0.1977	0.8250
6	S 29° 12' 26.31"	E 30° 39' 2"	-0.0446	0.1528	-0.2000	0.1408	0.9465
7	S 29° 12' 31.34"	E 30° 39' 13.92"	-0.0253	-0.3010	-0.1935	0.1871	0.4774
8	S 29° 12' 26.29"	E 30° 38' 59.37"	0.0173	0.0690	-0.1783	0.1656	0.5601
9	S 29° 12' 30.38"	E 30° 39' 12.02"	-0.0260	-0.2364	-0.1919	0.1899	1.0000
10	S 29° 12' 29.86"	E 30° 39' 16.55"	-0.1275	-0.1864	-0.1852	0.2125	0.6786
11	S 29° 12' 29.14"	E 30° 39' 11.33"	-0.0327	-0.1667	-0.1702	0.1329	0.6000
12	S 29° 12' 25.33"	E 30° 38' 55.91"	-0.0127	0.0889	-0.1783	0.1868	0.7341
13	S 29° 12' 25.51"	E 30° 39' 3.2"	-0.0327	0.1100	-0.1756	0.1370	0.4752
14	S 29° 12' 28"	E 30° 38' 56.48"	-0.0058	0.0957	-0.1908	0.0551	0.3188
15	S 29° 12' 28.21"	E 30° 39' 12.5"	-0.0588	-0.1405	-0.1837	0.2147	0.5385

Leaf area index (LAI) values were derived, using Equation 4.3, based on each NDVI value (Table D.3).

Table D.3: Leaf Area Index (LAI) values calculated for each Normalized Difference Vegetation Index (NDVI) value extracted from the NDVI images generated from SPOT imagery.

Point No.	**Coordinates**		**Satellite images LAI value**				
	Latitude	**Longitude**	**01/02/2007**	**17/07/2007**	**19/01/2011**	**31/07/2012**	**04/10/2015**
1	S 29° 12' 31.36"	E 30° 39' 10.85"	2.300	2.103	3.443	1.235	0.318
2	S 29° 12' 27.75"	E 30° 39' 10.39"	2.255	2.994	5.580	1.012	-0.132
3	S 29° 12' 25.77"	E 30° 39' 5.20"	2.297	2.709	4.027	1.349	1.237
4	S 29° 12' 30.21"	E 30° 39' 11.60"	2.297	4.361	3.489	1.194	-0.207
5	S 29° 12' 24.88"	E 30° 38' 56.43"	2.102	1.531	3.801	1.176	-0.373
6	S 29° 12' 26.31"	E 30° 39' 2.00"	2.332	1.347	3.679	1.395	-0.574
7	S 29° 12' 31.34"	E 30° 39' 13.92"	2.213	5.539	3.602	1.215	0.342
8	S 29° 12' 26.29"	E 30° 38' 59.37"	1.971	1.711	3.430	1.297	0.149
9	S 29° 12' 30.38"	E 30° 39' 12.02"	2.217	4.177	3.583	1.205	-0.657
10	S 29° 12' 29.86"	E 30° 39' 16.55"	2.943	3.520	3.506	1.122	-0.101
11	S 29° 12' 29.14"	E 30° 39' 11.33"	2.258	3.308	3.345	1.428	0.061
12	S 29° 12' 25.33"	E 30° 38' 55.91"	2.138	1.618	3.430	1.216	-0.208
13	S 29° 12' 25.51"	E 30° 39' 3.20"	2.258	1.525	3.401	1.411	0.348
14	S 29° 12' 28.00"	E 30° 38' 56.48"	2.098	1.587	3.571	1.777	0.774
15	S 29° 12' 28.21"	E 30° 39' 12.50"	2.425	3.057	3.489	1.114	0.198
Average LAI							**2.012**

Appendix E: MIKE SHE rivers and lakes module and related software connections.

In order to model river flow and determine river discharge in MIKE SHE, the MIKE SHE model needs to link to external MIKE 11 software, as MIKE SHE is incapable of modeling river flow itself. MIKE 11 software has a number of input requirements that make-up a simulation file which is then linked to the MIKE SHE model (Figure E.1). To generate the MIKE 11 input requirements MIKE Hydro software was used. MIKE Hydro has two modules: *Basin module* and *river module*. For this study, the *river module* of MIKE Hydro was used to generate the MIKE 11 inputs.

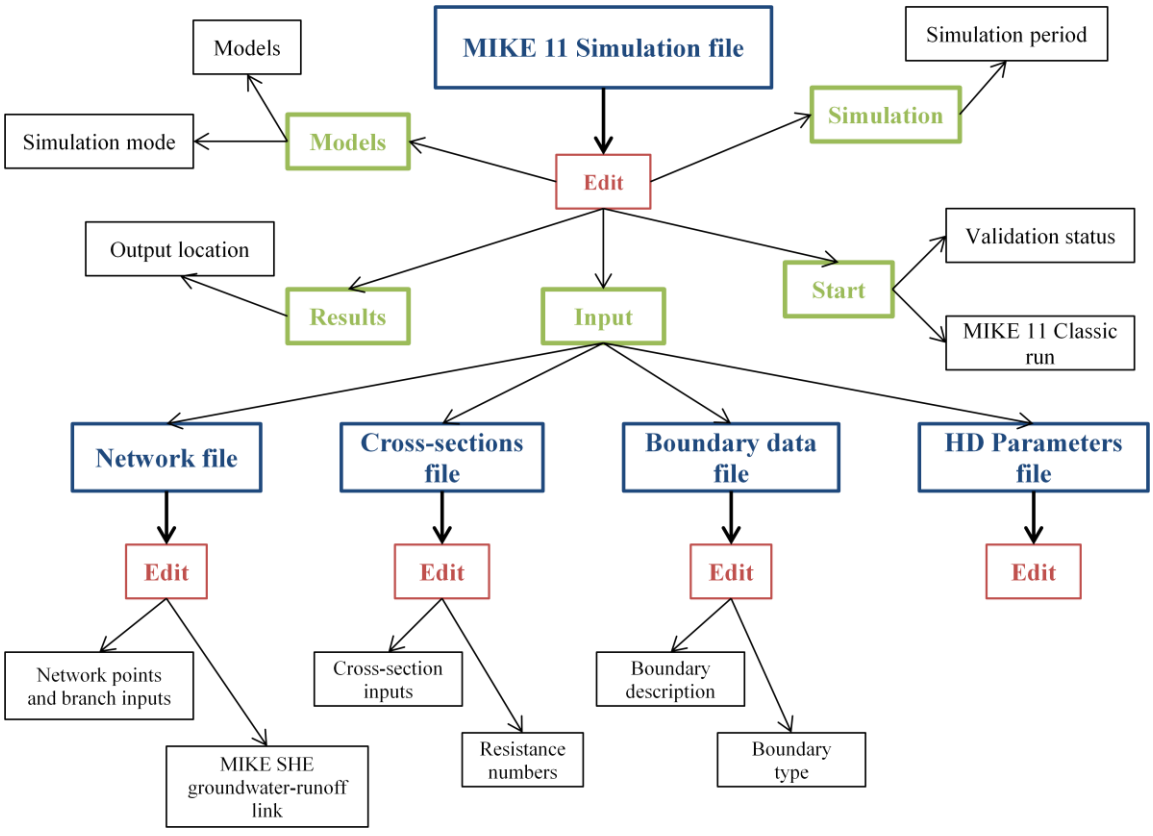

Figure E.1: Flow chart for MIKE 11 model set-up.

To run the *river module* in MIKE Hydro, two sub-modules were considered: *river network* and *map configuration*. The *river network* sub-module is used to input information on river branches and to generate river cross-sections. The river branch information required is: the branch name, topo ID, start and end chainage, flow direction, and branch type (Table E.1). The *map configurations* sub-module was used to define the river cross-

sections. Under the map configurations sub-module the DEM for the site was input and the option to *Use DEM for cross section digitization* was selected. To generate the cross-sections the *Auto generate cross section* option under the tools tab was selected, the input requirements included the cross-section interval and cross-section width. For this study, an interval of 200 m and a width of 100 m were used, once input cross sections for the site were generated.

Table E.1: The branch properties defined in the river network section of a MIKE Hydro research (DHI software, 2012).

Branch Property	**Description**	**Available Options**
Branch name	Any name assigned to the branch	User defined
Topo ID	The Topographical Identifier is used to allow simulations of numerous scenarios.	User defined
Start chainage	The chainage of the first point in the branch.	User defined Model default set to 0 m
End chainage	The chainage of the last point in the branch (the difference in chainage from the start to the end point indicate the length of the river (m)).	User defined
Flow direction	Determines how chainage is interpreted in terms of flow direction.	Positive – flow direction from low to high chainage; or Negative – flow direction from high to low chainage
Branch type	The type of branch selected.	Regular – normal branch with several calculation points defined from cross-sections; Link channel – a short branch used to connect a flood plain to the main river branch; or Routing – No cross-sections are required and flow is calculated using a simplified hydraulic calculation.

Once the river network and river cross-sections were generated, in MIKE Hydro, all data were exported as MIKE 11 files using *export* under the *File* tab. Once the MIKE Hydro files were exported into MIKE 11 files they were then inputted into the MIKE SHE rivers and lakes module. The MIKE SHE rivers and lakes module is used to link the MIKE SHE model to the MIKE 11 simulation file. Within the MIKE SHE Rivers and lakes module (Figure E.1) the MIKE 11 simulation file (containing all information on river network and cross-sections) can be edited allowing for improved simulation specifications of the MIKE Hydro outputs.

E.1. MIKE 11 simulation editor

The MIKE 11 simulation file (Figure E.1) contained the simulation and computational parameters for modeling the Two Streams sub-catchment river. To access the input files within the MIKE 11 simulation file, the MIKE 11 simulation editor was used. The simulation editor has five tabs. In the first tab one selected which *Models* to

be included in the MIKE 11 simulation. For this study, the *Hydrodynamic* model was selected. Also under the *Models* tab, the simulation mode must be selected. For this study, the *Unsteady* simulation mode was chosen over the *Quasi steady* mode, to allow for the hydrodynamic calculations to be based on the hydrodynamic flow conditions. The second tab allows for the MIKE 11 Input files to be included in the simulation. For this study, the following *Inputs* were included: *Network*, *Cross-sections*, *Boundary data* and *HD Parameter* (each of these input files were outputs from the MIKE Hydro model previously described). These inputs were accessed using their respective editors. The third tab is the *Simulation* tab, where one sets the simulation parameters. For this study, the simulation period was set to a fixed time step type over one (1) second intervals for the length of the simulation. The fourth tab – the *Results* tab – is used to specify the output location for the MIKE 11 simulation results. The final tab is the *Start* tab which provides the validation status of the MIKE 11 set-up based on the provision of all input requirements and where one selects to start the MIKE 11 simulation.

E.2. MIKE 11 Network editor

The network editor was used to input and edit the river network (Figure E.1). The river network editor allows the river branch properties to be inputted; these properties were included in MIKE Hydro and were automatically transferred to the river network editor when exported from MIKE Hydro. The MIKE 11 Network editor is used to link the MIKE 11 simulation file to the MIKE SHE model. To do so the *Tabular view* option was selected under the *View* tab – this changed the layout from a graphical to a tabular view. In the *Tabular view* the *Runoff/groundwater links* option was selected. To link the two models the user inputs the*:* Branch name, upstream chainage, downstream chainage, conductance, leakage coefficient, flooding area, bed topography, bed leakage, weir coefficient, head exponent, minimum upstream height above bank for full weir width, overbank spilling and linear reservoir exchange. For this study, most of these parameters were left as their default values (Appendix A). The values input were: Branch name - Two streams river, upstream chainage – 0 m and downstream chainage – 748.93 m. The input values are the same as those input in the branch properties section of the MIKE Hydro set-up (Table 4.6).

E.3. MIKE 11 Cross-sections editor

The cross-sections editor was used to manage, store and display the cross-section information for the model (Figure E.1). There are two types of cross-section data; the *raw survey data* and the *derived processed data*. The raw data describes the shape of the cross section whilst the processed data are derived from the raw data and

contains all information used by the model (e.g. level, cross section area, flow width, hydraulic/resistance radius; DHI software, 2012). Each cross section is uniquely identified by the following three keys: *River name* – the name given to the river branch; *Topo ID* – topographical identification name; and *Chainage* - river chainage at the cross-section location (DHI software, 2012). All cross-sections generated in MIKE Hydro were imported into the cross-sections editor. The river name and topo ID were the same for each cross section and were kept the same as the branch properties generated in MIKE Hydro (Table 4.6). The chainage was defined in MIKE Hydro where it was specified that cross-sections will be generated at 200 m intervals along the length of the stream. The stream is 748.93 m in length and there were five cross-sections generated (Figure E.2). In addition to the above, resistance number properties needed to be defined for each cross-section, as described in the paragraph below.

The resistance numbers section defined bed resistance. Under the resistance numbers section (part of the *raw survey data* tab) the user defines the *transversal distribution* and the *resistance type* of each cross-section included (DHI software, 2012). The *transversal distribution* is the resistance across the cross-section. There are three possible options to choose from under transversal distribution: *Uniform, high/low flow zones* or *distributed*. Uniform transversal distribution is used when a single resistance number is applied throughout the cross-section. For the high/low flow zones option three resistance numbers need to be defined for the left high flow resistance, right high flow resistance and the low flow resistance. The distributed transversal distribution is selected to define a resistance number for each X, Z dataset in the cross-sections raw dataset (DHI software, 2012). For this study, the *Uniform transversal distribution* option was selected and a uniform value of 1 was used as this was the default setting in the cross-sections editor. The resistance type is used to define the resistance method for the cross section. There are five options to choose from: *Relative resistance, Manning's n, Manning's m, Chezy number, Darcy-Weisbach (k;* DHI software, 2012). For this study, the default *Relative resistance* option was chosen (Appendix A).

E.4. MIKE 11 boundary editor

The boundary editor is used to specify the boundary conditions of the MIKE 11 model (Figure E.1). For the Two Streams stream, two boundaries were identified: One at the starting point of the river (29°12′26.45″S; 30°38′49.55″E) with a chainage of 0 m and one at the end-point of the river (29°12′32.19″S; 30°39′18.25″E)

with a chainage of 748.93 m. The weir is located at approximately 591.2 m along the stream. For each boundary a boundary description and boundary type was specified.

The boundary description describes the nature of the boundary. There are six boundary description options to choose from: *Open; point source; distributed source; global; structures*; and *closed* (DHI software, 2012). An *open* boundary is specified at the free upstream and/or downstream ends of the model domain. A *point source* boundary is used where time-varying or constant lateral inflows and/or outflows occur within the model domain. A *distributed source* boundary is used where time-varying or constant lateral distributed inflows and/or outflows occur along river reaches within the model domain. A *global* boundary is used when particular boundary conditions are applicable over the entire model domain. A *structures* boundary can be used in combination with three different structure types: dam, dam break and regulating structure. The closed boundary is used at the free upstream and/or downstream ends of the model domain where a zero-flux condition across the boundary is applicable (DHI software, 2012). For this study, the upstream point (starting point) and the downstream point (end-point) of the stream were both set as *open* boundaries.

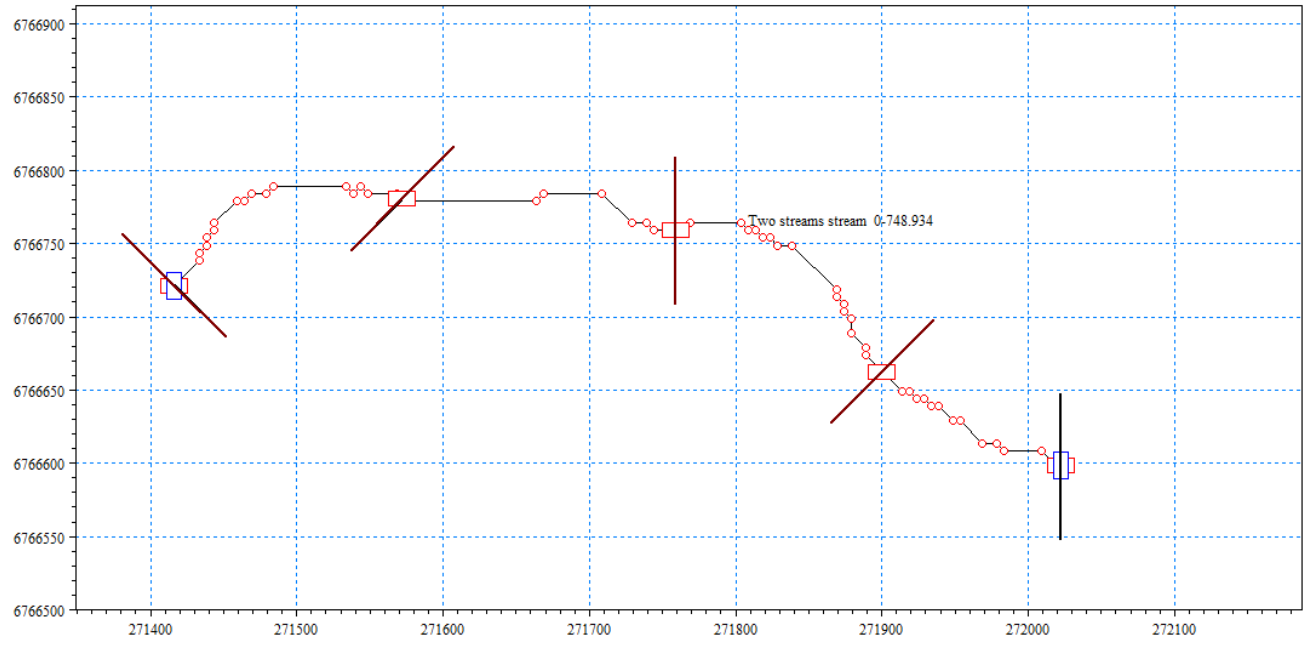

Figure E.2: Model screenshot showing the locations of cross-sections generated along the length of the Two Streams stream.

The boundary type is dependent on the boundary description as only certain boundary types can be selected depending on the boundary description provided. In total, there are twenty-six possible combinations of boundary description and boundary type in MIKE SHE (DHI software, 2012). Given that the open boundary option was chosen there were six valid boundary types to choose from: *Inflow, water level, Q-h, bottom level, sediment transport* and *sediment supply*. The *inflow* boundary type is used when the user requires a time-varying hydrograph condition. The *water level* boundary type is used when a time-varying water level condition is required. The *Q-h* boundary type is used when the relationship between the water level and discharge is known. The *bottom level* boundary type is used when there is a variation in the bottom level. The *sediment transport* type is used to show the variation of the inflow of the sediment. The *sediment supply* boundary type is used when the bottom level or the sediment transport is known (DHI software, 2012). For this study, the *inflow* boundary type was used for the upstream point and the *Q-h* boundary type was used for the downstream point. The inflow boundary was set at a constant value of 0 $m^3.s^{-1}$, for the start of the simulation. For the Q-h boundary discharge ($m^3.s^{-1}$) or 'Q' values and water level (m) or 'h' values were input for the start of the simulation. These values were generated in MIKE 11 using the *Auto calculation of Q/h table* tool under the *tools* tab in the MIKE 11 boundary editor.

Appendix F: van Genuchten soil water retention curves (SWRC)

This Appendix compares the SWRC of the Kuenene (2013) soil properties to those of the generic database of unsaturated hydraulic properties (UNSODA) soils (Leij *et al.*, 1996; Table F.1). The UNSODA soils database is made up of soil hydraulic data from approximately 800 soil profiles collected worldwide and from which a collection of pedotransfer functions have been derived, and based on soil texture (Feddes *et al.*, 2001). Soil water retention curves (SWRCs) are used to relate soil moisture suction (pf) and soil moisture content ($cm^3.cm^{-3}$). Soil water retention curves (SWRCs) show how much water a particular soil is capable of retaining (Wösten and van Genuchten, 1988).

By determining field capacity (green line) and wilting point (red line) of the particular soil a SWRC can be used to determine plant available moisture (moisture content at field capacity – moisture content at wilting point), i.e. the amount of water available to be taken up by plants through the roots (Kirkham, 2005; Ghanbarian-Alavijeh *et al*., 2010). Field capacity is amount of soil moisture in the soil a few days following soil wetting, once excess water has drained away and the rate of downward water movement has decreased (Kirkham, 2005). Wilting point is the smallest amount of soil moisture present in the soil for plant use, required for plants not to wilt if the soil moisture decreases below this point vegetation will wilt as they are unable to recover turgidity (Kirkham, 2005).

Comparison of the SWRCs of the two datasets (Table F.1) found the Kuenene (2013) soils to have greater water retention than the UNSODA soils (Leij *et al*., 1996), for every soil horizon except for Clovelly ot (loam texture), Inanda re (clay loam texture) and Magwa ye (clay loam texture), as summarised in section 5.6.1 (Table 5.11).

Table F.1: Soil water retention curves (SWRC) for the Kuenene (2013) soil (used in this study) and the generic UNSODA soils (Leij *et al*., 1996) based on the soil textural classes and soil horizons defined by Kuenene (2013). The SWRCs indicate field capacity (green line), wilting point (red line) and plant available water (moisture content at field capacity minus moisture content at wilting point).

(Kuenene, 2013)	**UNSODA (Leij et al., 1996)**
Clovelly	

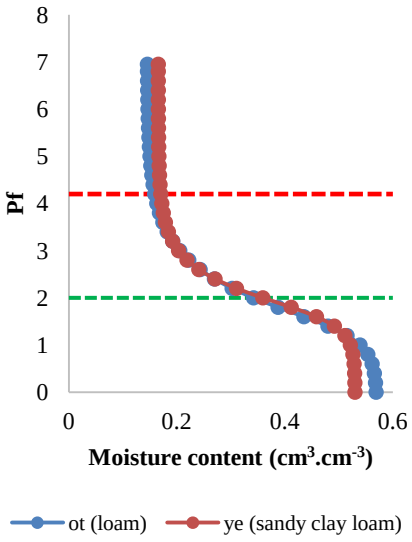

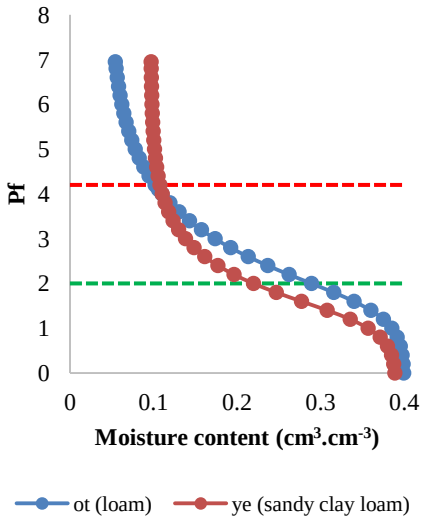

Griffin

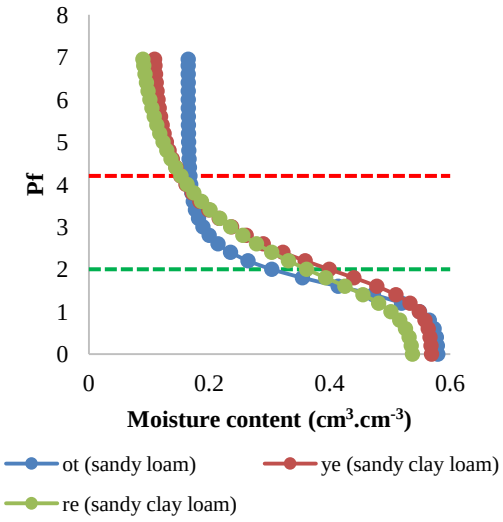

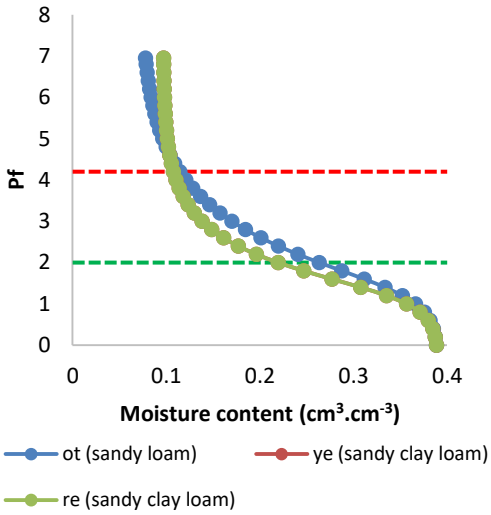

Inanda

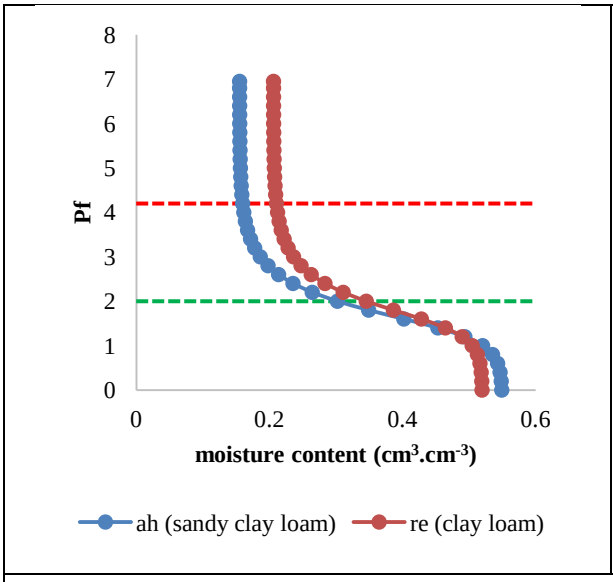

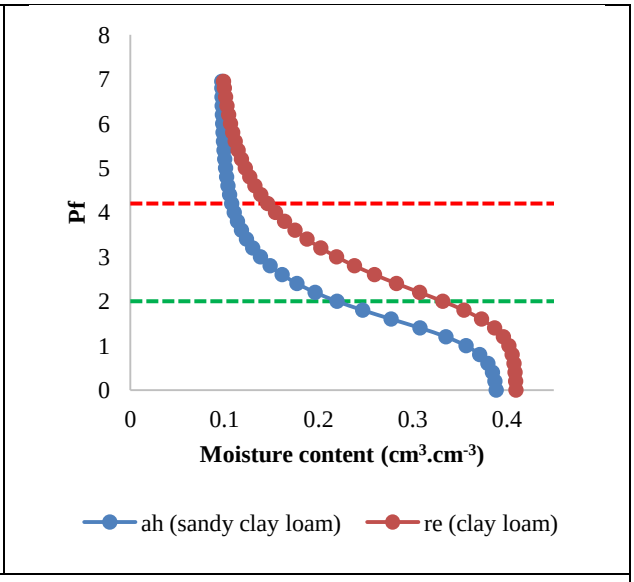

Katspruit

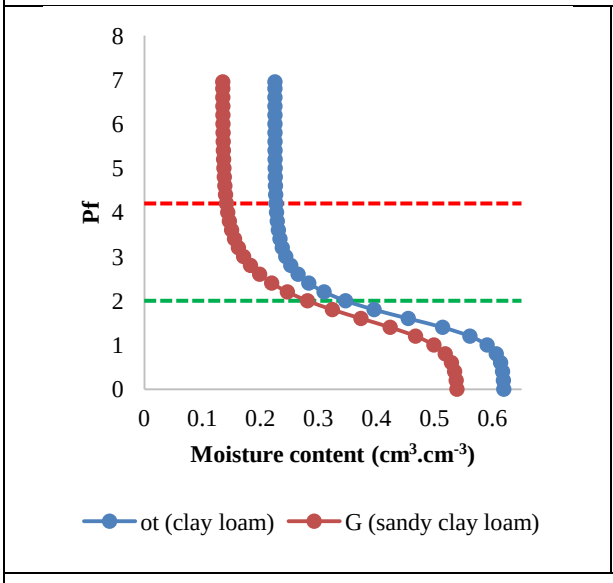

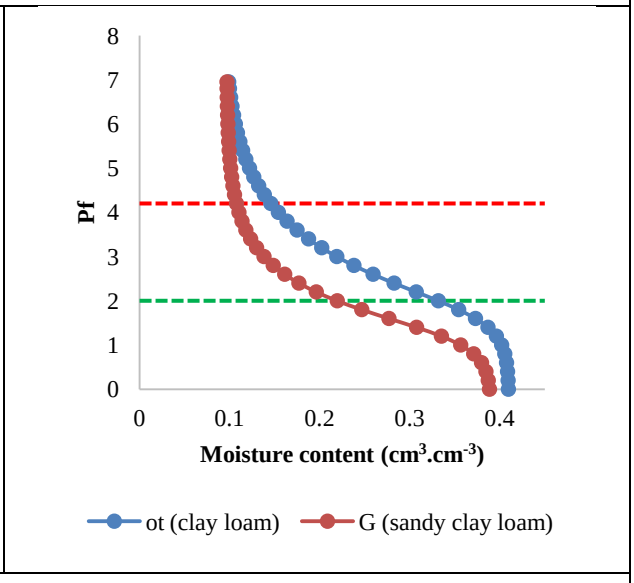

Kranskop

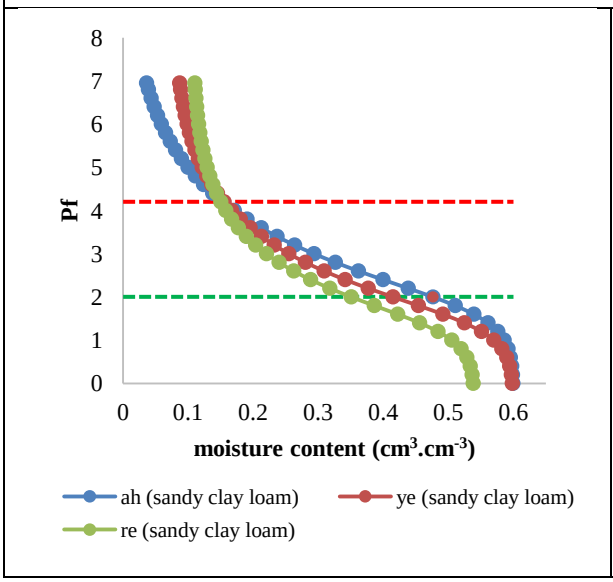

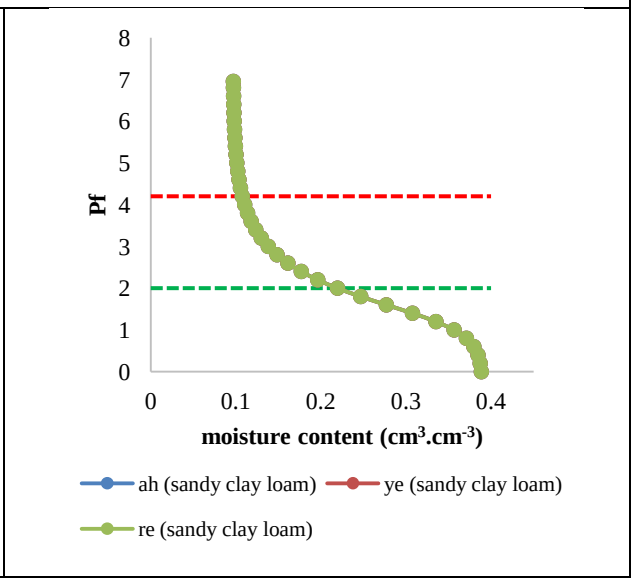

Magwa

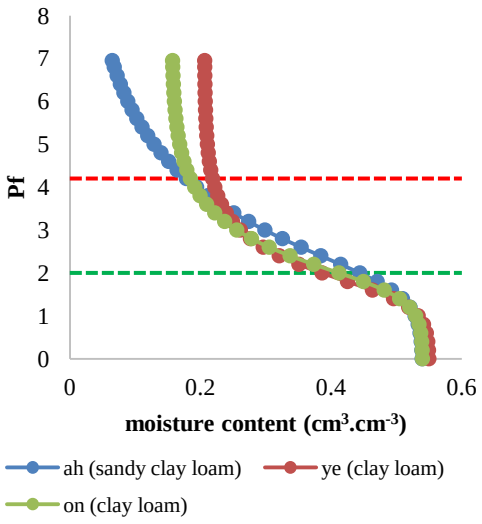

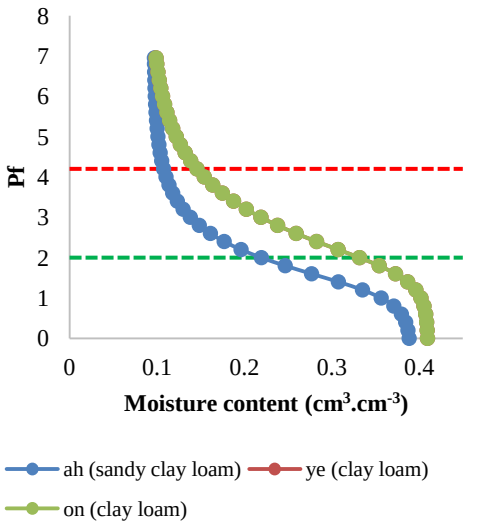

Oakleaf

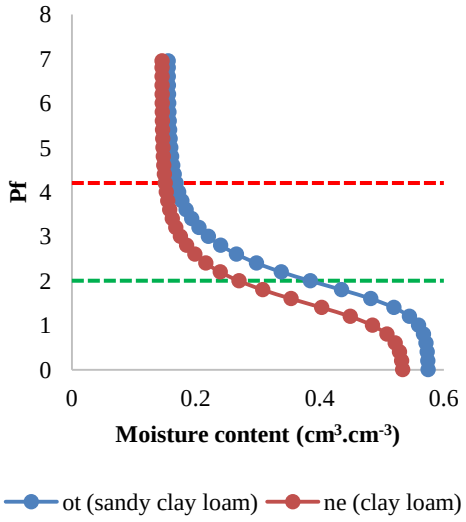

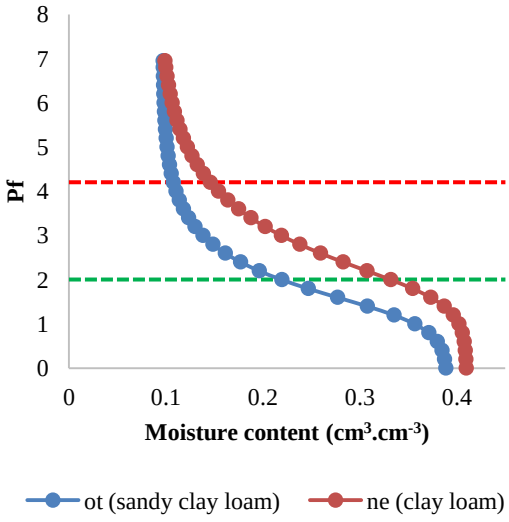

Appendix G: Determining MIKE SHE model error specific to model component

To determine where model error is specifically concentrated, within the hydrological components modeled within MIKE SHE, the water balance error is calculated per model component, using the *water balance* utility. There are five model components specified in the *water balance* utility: precipitation and snowmelt, CIS, OL, UZ, and SZ. Each component has a range of inflow and outflow processes that allows for the calculation of the water balance error per component (Table G.1), the snowmelt component was not considered for this study as no snow was modeled. The inflow and outflow processes included in the water balance calculations, per component, overlap between components that feed into each other, for example canopy throughfall is included as an outflow process of the CIS component, but as an inflow process into the OL component (Table G.1). The total model error is the accumulation of all component error in the model.

Table G.1: Water balance components and processes involved in the calculation of water balance error (DHI software, 2012).

Component	**Item**	**Description**	**Sign in the water balance error calculation**
CI	Precipitation	Total precipitation reaching the canopy	Inflow = negative
	Canopy throughfall	Water moving as canopy throughfall to ponded water	Outflow = positive
	Evaporation	Evaporation from intercepted storage	Outflow = positive
	CIS	The change in CIS	Positive with increasing storage
	Error	**CIS water balance error**	**Positive = water surplus**
OL	Canopy throughfall	Water moving as canopy throughfall to ponded water	Inflow = negative
	Evaporation	Evaporation from ponded water	Outflow = positive
	I_{UZ}	I_{UZ} from ponded water into the unsaturated zone	Outflow = positive
	SZ to OL	Direct flow up from the saturated zone to OL	Inflow = negative
	OL to SZ	Direct flow down from OL to the SZ	Outflow = positive
	OL boundary inflow	Inflow to overland storage across the boundary of the model/water balance sub-area.	Inflow = negative
	OL boundary outflow	Outflow to overland storage across the boundary of the model/water balance sub-area.	Outflow = positive
	Overland storage	The change in overland water storage	Positive if storage increases
	Error	**Error in OL**	**Positive = water surplus**
UZ	I_{UZ}	I_{UZ} from ponded water into the UZ	Inflow = negative
	Evaporation	Evaporation from the UZ	Outflow = positive
	E_t	E_t from the root zone	Outflow = positive
	SZ recharge	Recharge out of the bottom of the soil into the SZ	Outflow = positive
	UZ storage	Change in the UZ storage	Positive for increasing storage
	Error	**UZ water balance error**	**Positive = water surplus**
SZ	SZ recharge	Recharge out of the bottom of the soil into the SZ	Inflow = negative

	Evapotranspiration	Evapotranspiration directly from the SZ	Outflow = positive
	SZ boundary inflow	Inflow to the SZ across the model boundary of the model/water balance sub-area	Inflow = negative
	SZ boundary outflow	Outflow to the SZ across the model boundary of the model/water balance sub-area	Outflow = positive
	Flow from SZ to OL	Upward flow directly from the SZ to ponded water	Outflow = positive
	Flow from OL to SZ	Downward flow directly from ponded water to the SZ	Inflow = negative
	SZ storage	Change in the SZ storage	Positive when storage increases
	Baseflow	Baseflow from the SZ to MIKE 11 river	Outflow = positive
	I_{UZ}	I_{UZ} from MIKE 11 river to the SZ	Inflow = negative
	Error	**SZ water balance error**	**Positive = water surplus**

Appendix H: Determination of time series data distribution

All MIKE SHE current scenario hydrological time series components of the sugarcane, riparian and black wattle vegetation classes and the MIKE SHE future scenario *E. dunnii* time series components were tested for normality to determine whether parametric or non-parametric statistics would need to be used as part of the analysis. Testing for normality provides an indication of whether the dataset tested is normally distributed and thus displays a bell-shaped frequency histogram.

To test for normality a chi-squared goodness-of-fit test was employed (as described in section 4.6.2). The chi-squared goodness-of-fit test yielded the same results for every hydrological component for all three vegetation classes considered, $P < 2.20 \times 10^{-16}$ indicating that each dataset tested was not normally distributed ($P < 0.05$). To further assess the distributions of the different time series results of the hydrological components frequency histograms were generated. Based on the test for normality and inspection of frequency histograms, is was determined that non-parametric tests would be used for statistical analysis carried out, namely the Kruskal Wallis test by ranks and the Wilcoxon's signed rank test (described further under section 4.6.2)

The evapotranspiration records of the current scenario vegetation classes and the future scenario *E. dunnii* vegetation class were all right skewed (Figure H.1).

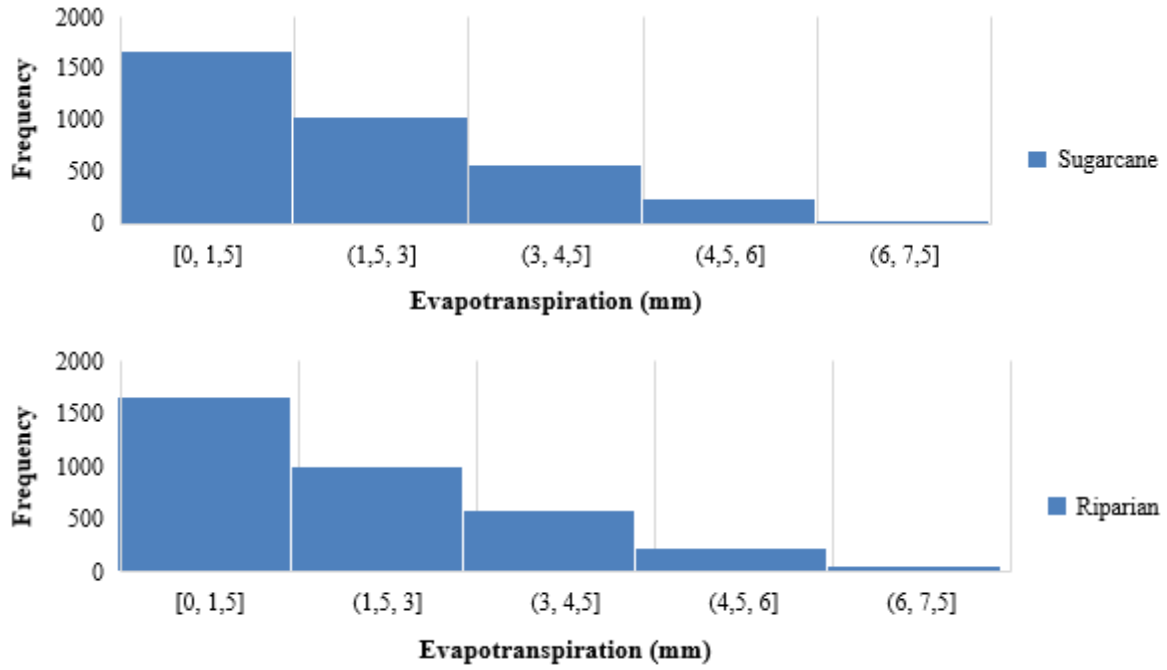

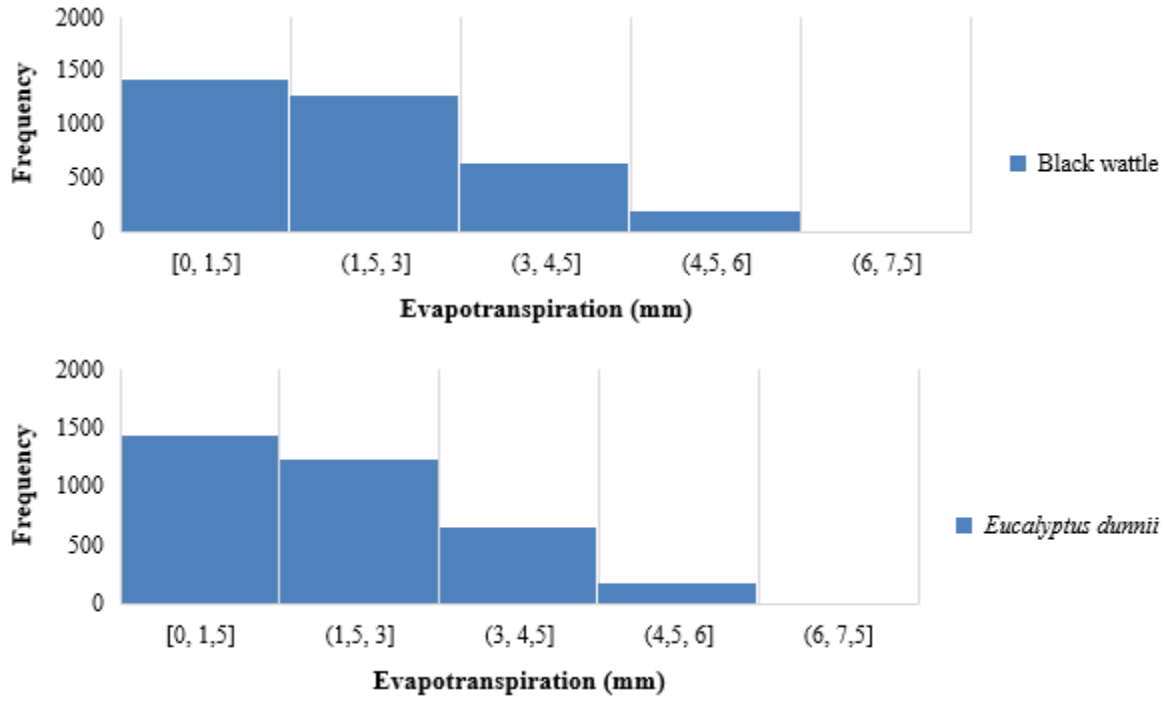

Figure H.1: Frequency histograms of the evapotranspiration records of the three current scenario vegetation classes and the future scenario *E. dunnii* vegetation class.

The canopy interception storage records of the current scenario vegetation classes and the future scenario *E. dunnii* vegetation class were all right skewed (Figure H.2). This was evident given that over 85 % of each of the canopy interception storage records of each vegetation class considered was equal to 0 mm.

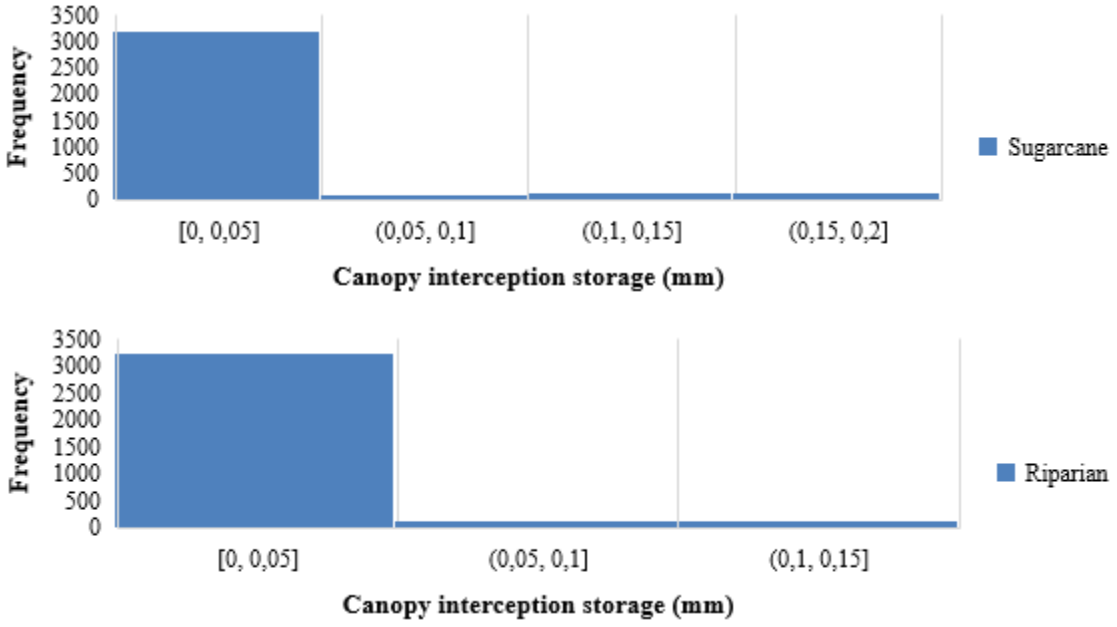

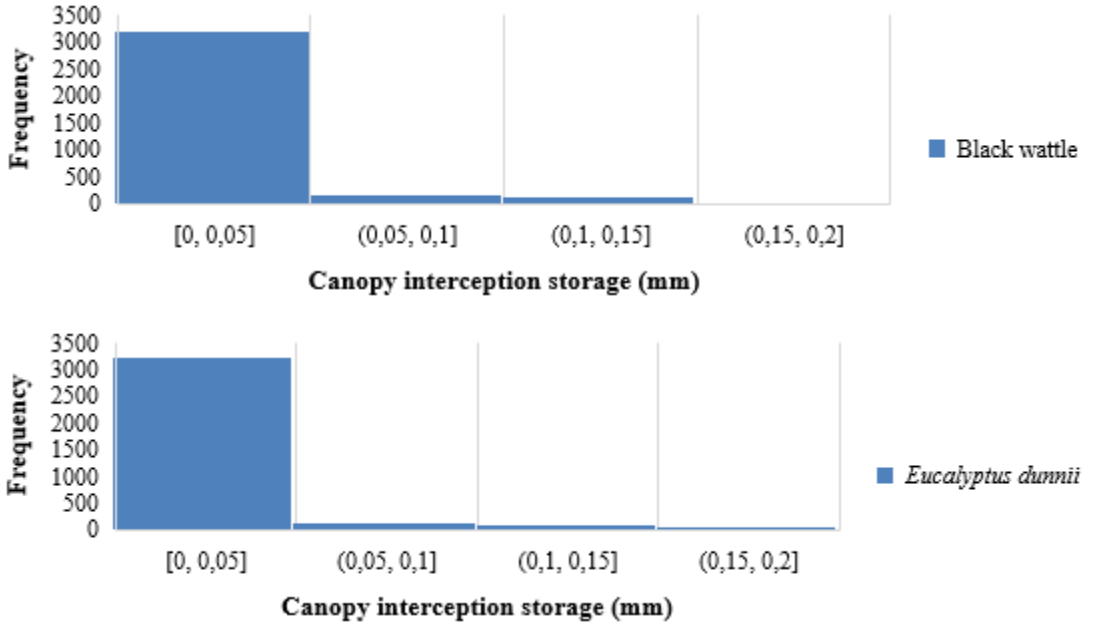

Figure H.2: Frequency histograms of the canopy interception storage records of the three current scenario vegetation classes and the future scenario *E. dunnii* vegetation class.

Considering the depth of overland flow records of all four vegetation classes, they were also all found to be right skewed (H.3).

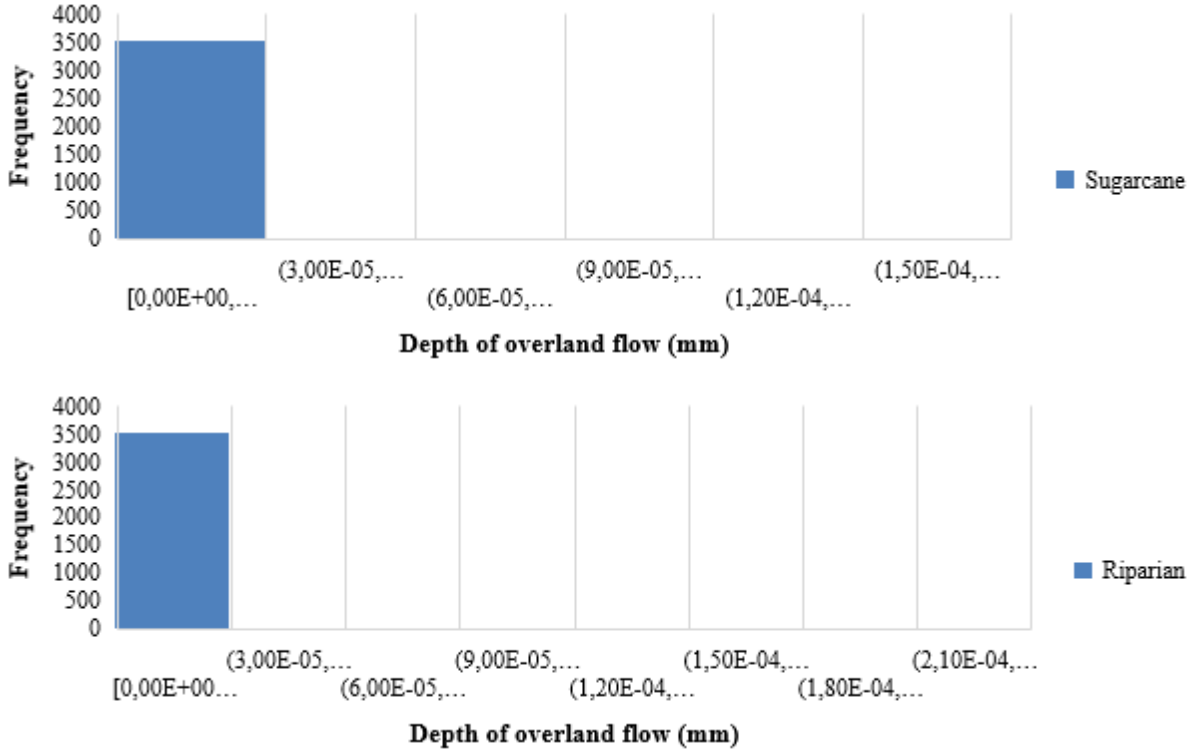

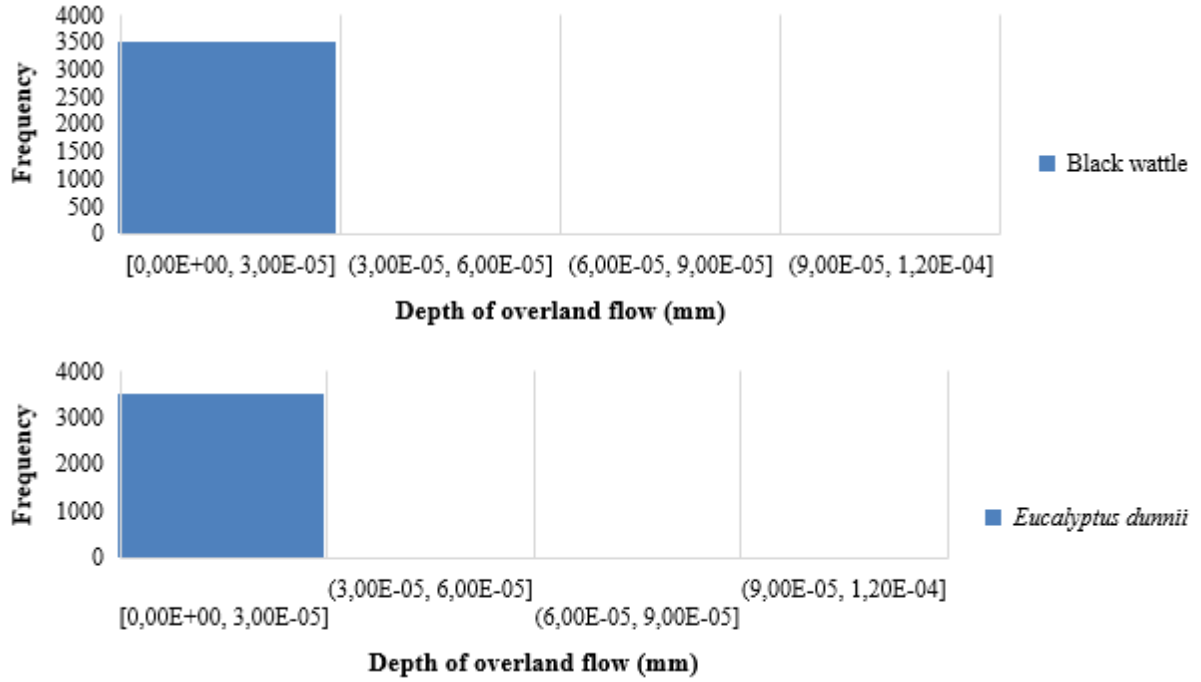

Figure H.3: Frequency histograms of the depth of overland flow records of the three current scenario vegetation classes and the future scenario *E. dunnii* vegetation class.

Considering the infiltration to the unsaturated zone records of all three vegetation classes of concern, they were all found to be right skewed (Figure H.4).

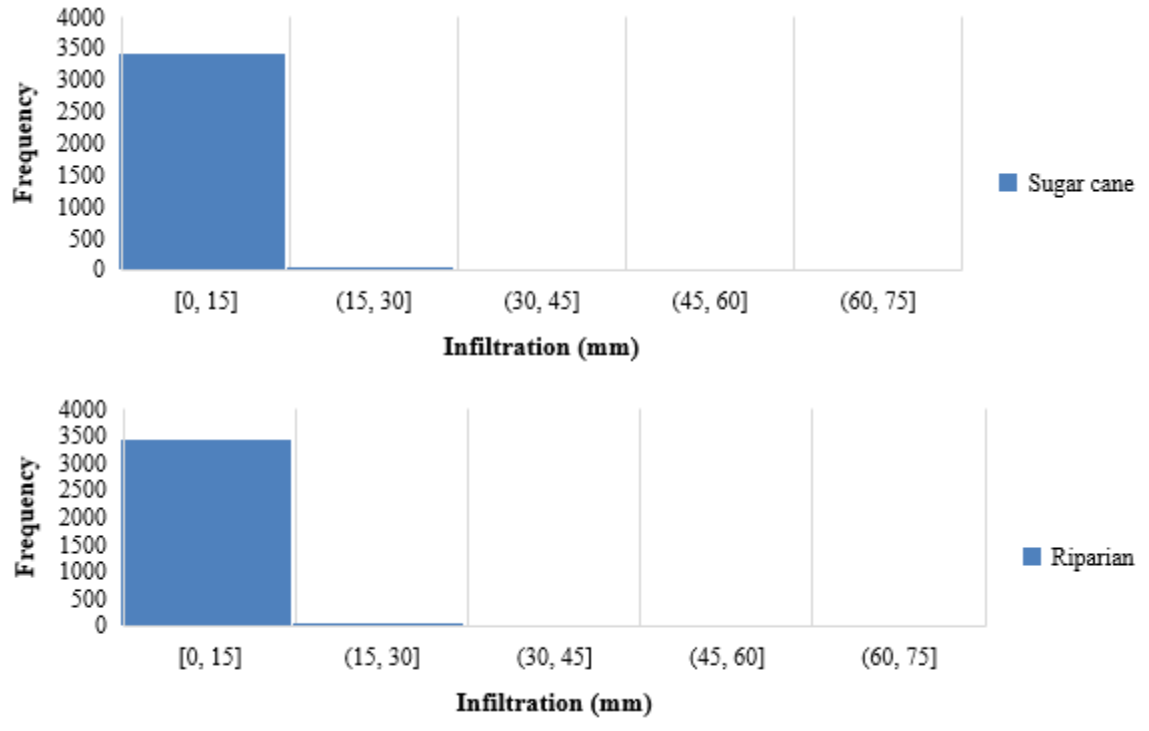

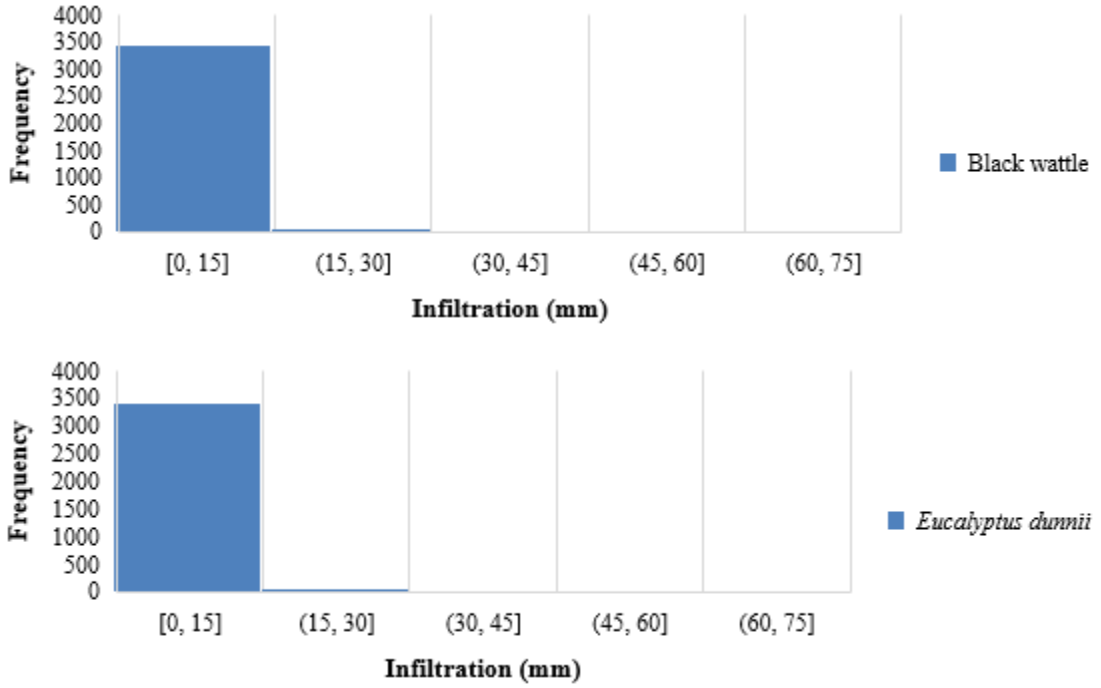

Figure H.4: Frequency histograms of the infiltration records of the three current scenario vegetation classes and the future scenario *E. dunnii* vegetation class.

Similar to the above, the groundwater recharge records of the current scenario vegetation classes and the future scenario *E. dunnii* vegetation class were all found to be right skewed, and thus not normally distributed (Figure H.5).

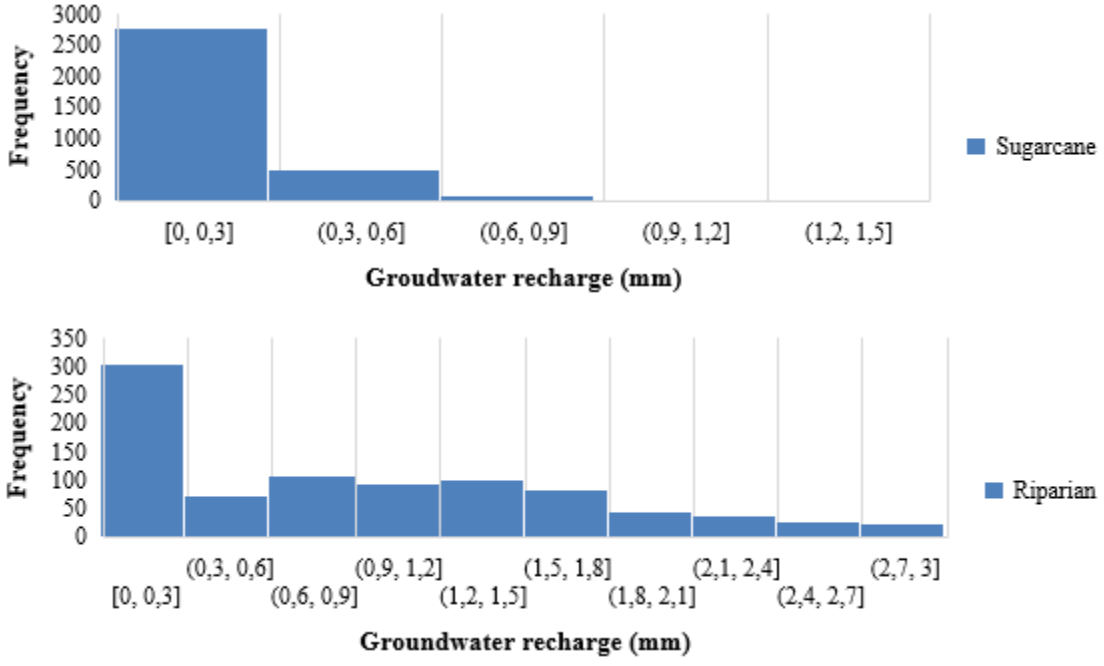

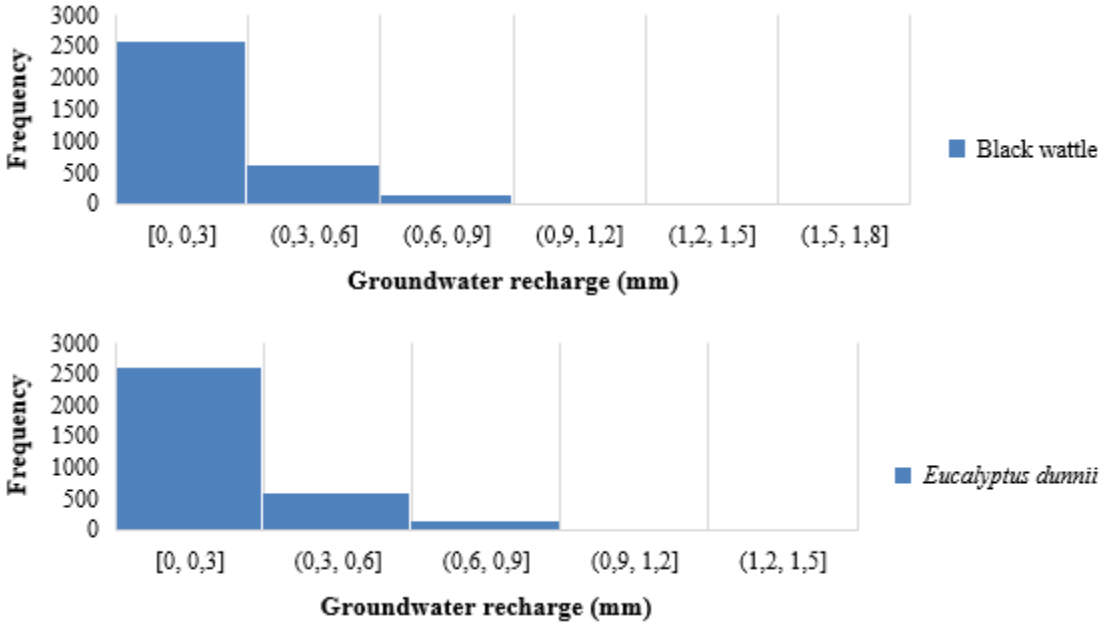

Figure H.5: Frequency histograms of the groundwater recharge records of the three current scenario vegetation classes and the future scenario *E. dunnii* vegetation class.